Université de Montréal

Rôle du système ubiquitine protéasome dans les séparations de phase nucléaires

Présentée par : **Nadine Sen Nkwe Dibondo**

Programmes de biologie moléculaire, Faculté de médecine

Thèse présentée à la Faculté de médecine en vue de
l'obtention du grade de Ph.D. en Biologie Moléculaire option générale

Avril, 2020

RÉSUMÉ

Le système ubiquitine-protéasome représente une plateforme de signalisation cellulaire chez les eucaryotes et joue un rôle majeur dans la coordination des processus cellulaires. Des progrès récents suggèrent que l'ubiquitination joue un rôle important dans les phénomènes de séparation de phase liquide-liquide (LLPS), un processus permettant la localisation d'une quantité accrue de protéines dans un compartiment subcellulaire, afin de réaliser une fonction biologique. En effet, il a été démontré que l'ubiquitination joue un rôle central dans les mécanismes qui gouvernent la LLPS durant la formation des granules de stress dans le cytoplasme ou les foci de réparation de l'ADN dans le noyau. D'autre part, chez la levure, des travaux ont montré que le protéasome est capable de s'assembler sous forme de granules dans le cytoplasme suite à un stress métabolique. Toutefois, les mécanismes par lesquels le système ubiquitine-protéasome ainsi que ses régulateurs contrôlent les processus de LLPS restent à déterminer.

Dans la première étude de cette thèse, nous avons investigué le mécanisme d'action de la déubiquitinase USP16, qui a été suggérée comme un régulateur négatif de la LLPS, empêchant la formation des foci de réparations de dommages à l'ADN. Cependant, nos résultats démontrent que USP16 est majoritairement cytoplasmique et que seulement une entrée forcée de USP16 dans le noyau empêche la formation des foci de réparation des cassures double brin induites par des radiations ionisagntes et ce en favorisant la déubiquitination de l'histone H2A. De plus, aucune translocation nucléaire de USP16 n'a été observée durant le cycle cellulaire ou suite à des dommages à l'ADN. Nos travaux montrent que USP16 est activement exclue du noyau via son signal d'export nucléaire et régulerait indirectement la LLPS menant à la formation des foci de réparation de l'ADN.

Dans la deuxième étude, nous décrivons le comportement dynamique des protéines du protéasome lors d'une LLPS induite par un stress métabolique. Nos résultats indiquent que le protéasome forme des foci distincts dans le noyau des cellules humaines en réponse à une privation de nutriments. Nous avons constaté que ces foci sont enrichis en ubiquitine conjuguée et nous avons démontré que le récepteur d'ubiquitine Rad23B ainsi que l'absence des acides aminés non essentiels sont des éléments clés nécessaires à l'assemblage de ces foci du

protéasome. De plus, des expériences de survie cellulaire montrent que la présence de ces foci est associée à la mort des cellules par apoptose.

En conclusion, nos travaux mettent en lumière l'importance du système ubiquitine-protéasome dans la formation et la régulation des foci cellulaires suite à une LLPS. De même, cette étude aidera également à approfondir notre compréhension sur les mécanismes qui gouvernent l'homéostasie des protéines, la survie cellulaire et le développement du cancer.

Mots-clés : Séparation de phase liquide-liquide, LLPS, USP16, réparation des cassures double brin, export nucléaire, protéasome, Rad23B, acides aminés.

ABSTRACT

The ubiquitin-proteasome system represents a major cell-signaling platform in eukaryotes and plays a pivotal role in the coordination of cellular processes. Recent studies provided evidence that ubiquitination plays a role in liquid-liquid phase separation (LLPS), a process that results in the localization of highly increased levels of a protein in a defined subcellular compartment, in order to achieve a biological function. Indeed, ubiquitination has been shown to play a central role in the mechanisms that govern LLPS and subsequent formation of stress granules in the cytoplasm or the DNA repair foci in the nucleus. On the other hand, several studies have shown that the proteasome itself is able to form granules in the cytoplasm following metabolic stress in yeasts. However, the mechanisms by which the ubiquitin-proteasome system and its regulators control LLPS processes remain to be determined.

In the first study of this thesis, we investigated the mechanism of action of USP16 deubiquitinase, which has been suggested as a negative regulator of LLPS preventing the formation of DNA damage repair foci. However, our results demonstrate that USP16 is predominantly cytoplasmic and that only enforced nuclear entry of USP16 prevents the formation of repair foci after double strand breaks induced by ionizing radiation, and this by promoting the deubiquitination of histone H2A. In addition, no nuclear translocation of USP16 was observed during cell cycle or following DNA damage. Our study shows that USP16 is actively excluded from the nucleus via its nuclear export signal and would indirectly regulate LLPS that lead to DNA repair foci.

In the second study, we describe the dynamic behavior of proteasome proteins during metabolic stress, a process that involves LLPS. Our results indicate that the proteasome forms distinct foci in the nucleus of human cells in response to nutrients deprivation. We found that these foci are enriched with conjugated ubiquitin and demonstrated that the ubiquitin receptor Rad23B as well as the absence of nonessential amino acids are the key elements necessary for the assembly of these proteasome foci. In addition, cell survival experiments show that the presence of these foci is associated with cell death by apoptosis.

In conclusion, our work has shed new light on the importance of the ubiquitin-proteasome system in the formation and regulation of cell foci following LLPS. Likewise, this

study will also help deepen our understanding of the mechanisms leading to protein homeostasis, cell survival and cancer development.

Keywords: Liquid-liquid phase separation, LLPS, USP16, double strand break repair, nuclear export, proteasome, Rad23B, amino acids.

.

TABLE DES MATIERES

LISTE DES TABLEAUX

CHAPITRE 2

CHAPITRE 3

LISTE DES FIGURES

CHAPITRE 1

CHAPITRE 2

CHAPITRE 3

CHAPITRE 4

LISTE DES ABBREVIATIONS

53BP1 : p53-Binding Protein 1

AND : Acide DésoxyriboNucléique

ADRM1 : ADhesion Regulating Molecule 1

APC/C : Anaphase-Promoting Complex/Cyclosome

APF : ATP-dependent Proteolysis Factor

ARN : Acide RiboNucléique

ASXL : Additional Sex Comb-Like

ATM : Ataxia Telangiectasia Mutated

ATP : Adénosine-5′-TriPhosphate

ATR : Ataxia Telangiectasia and Rad3 related

BAP1 : BRCA1-Associated Protein 1

BER : Réparation par excision de base, « Base Excision Repair »

BMI1 : B lymphoma Mo-MLV Insertion region 1

BRCA1 : Breast Cancer-Associated 1

CBXs : Chromobox proteins

CMML : Leucémie Myélomonocytaire Chronique, « Chronic Myelomonocytic Leukaemia »

CUBI : Composite Ubiquitin Binding Interface

CUE : Coupling of Ubiquitin conjugation to ER degradation

DDR : Réponse aux dommages à l'ADN, « DNA Damage Response »

DEUBAD : DEUBiquitinase ADaptor

DNA-PK : DNA-dependent Protein Kinase

DSB : Cassure d'ADN double brin, « DNA Double Strand Break »

DUB : Déubiquitinase

EED : Embryonic Ectoderm Development

EZH2 : Enhancer of Zeste Homologue 2

FFS : Fluorescence Fluctuation Spectroscopy

FUS : FUsed in Sarcoma

H2AK119ub : Monoubiquitination de H2A sur la lysine K119

H2AK13/15ub : Monoubiquitination de H2A sur les lysines K13 et K15

HCF-1 : Host Cell Factor 1

HECT : Homologous to the E6AP Carboxyl Terminus

HERC2 : HECT and RLD Domain Containing E3 Ubiquitin Protein Ligase 2

HR : Recombinaison Homologue, « Homologous Recombination »

IR : Radiation ionisante, « Ionizing Radiation »

JAMM : JAB1/MPN+/MOV34

K : Lysine

LLPS : Séparation de phase liquide-liquide, « Liquid-Liquid Phase Separation »

MCPIP1 : Monocyte Chemotactic Protein-Induced Protein 1

MDC : Mediator Of DNA Damage Checkpoint 1

MINDY : Motif Interacting with Ubiquitin (MIU)-containing novel DUB family

MJD : Machado-Josephin Domain proteases

MMR : Réparation des mésappariements de base, « MisMatch Repair »):

Mps1 : Monopolar Spindle 1

MRN : Complexe protéique constitué des protéines Mre11, Rad50 et Nbs1

mTOR : Mammalian Target Of Rapamycin

NER : Réparation par excision de nucléotide, « Nucléotide Excision Repair »

NES : Signal d'export nucléaire, « Nuclear Export Signal »

NFAT : Nuclear Factor of Activated T cells

NF-κB : Nuclear Factor Kappa B

NHEJ : Jonction d'extrémités non-homologues, « Non-Homologous End Joining »

NLS : Signal de localisation nucléaire, « Nuclear Localisation Signal »

OUT : Ovarian Tumor Domain proteases

PARP1 : Poly-(ADP-ribose) polymérase1

PcG : Polycomb-Group

PcGF : PcG RING Fingers

PH : Polyhomeotic

PLK : Polo-Like Kinase

PML : Leucémie Promyélocytaire « ProMyelocytic Leukemia »

PRC : Polycomb Repressive Complexe

PRU : Pleckstrin-like Receptor for Ubiquitin

PSC : Posterior Sex Combs

PTM : Modification post-traductionnelle, « Post Translational Modification »

RBR : Ring Between Ring

RING : Really Interesting New Gene

RIP : Receptor Interacting Protein

ROS : Espèces réactives de l'oxygène, « Reactive Oxygen Species »

SCE : Sex Comb Extra

SCF : SKP1–CUL1–F-box-protein

SCM : Sex Comb on Midleg

SIPAN : Starvation Induced Proteasome Assemblies in the Nucleus

SSB : Cassure simple brin, « Single Strand Break »

SUZ12 : SUppressor of Zeste 12

TRAF : TNF Receptor Associated Factor

UBA : UBiquitin Associated domain

UBD : UBiquitin Binding Domain

UBL : UBiquitin-Like domain

UCH : Ubiquitin C-terminal Hydrolase

UEV : Ubiquitin binding site of the ubiquitin E2 Variant

UIM : Ubiquitin Interacting Motifs

UPS : Système Ubiquitine-Protéasome, « Ubiquitin Proteasome System »

USP : Ubiquitin Specific Protease

UV : Ultraviolet

Znf UBP : Zinc-Finger Ubiquitin Binding Domain

γH2AX : Histone H2AX phosphorylée sur la sérine S139

➢ ***À mon époux Ulrich et à mes enfants***

La richesse et les liens qui nous unissent sont un trésor qui n'a pas de prix. Merci pour vos sacrifices.

Vous êtes ma bonne étoile et je vous aime tellement.

➢ ***À mon Papa***

Qui ne pourra jamais lire ce mémoire.

Merci de m'avoir toujours guidé tout au long de ma vie.

Tu me manques.

REMERCIEMENTS

Je tiens tout d'abord à exprimer toute ma gratitude à mon superviseur le Dr El Bachir Affar, pour m'avoir accueilli dans son laboratoire, pour m'avoir formé, m'avoir conseillé bien au-delà de la recherche et m'avoir donné l'opportunité de réaliser ces travaux de recherche aussi intéressants que passionnants. Un merci spécial pour ta franchise, ta rigueur et ton soutien dans les moments de doute et de difficultés personnelles. « *Yes, you are the best* ».

Un merci particulier à mes collègues, amis et membres d'équipe (passé et présent), pour leur aide, leur soutien, leurs conseils, leur disponibilité, ainsi que pour leur sympathie. Un clin d'œil spécial à Diana Adjaoud pour ses conseils, son aide dans toutes les tracasseries administratives et pour ses services de garde gratuits.

Je voudrais également remercier le personnel administratif des programmes de biologie moléculaire et du CRHMR pour leur aide précieuse. Ainsi que les différentes équipes du CRHMR avec qui j'ai eu l'occasion de partager des projets excitants. Leurs suggestions et commentaires ont contribué à la réalisation mes différents projets.

Un grand merci aux membres du « *Nadine Comédie Club », Saad et Damehan,* pour ces moments de délire et de fous rires. Merci d'avoir été des amis si formidables et d'avoir remplacé des moments difficiles en des moments magiques. Nos après-midi de détente et nos discussions quotidiennes me manquent.

Je tiens également à remercier tous les membres de mon comité de suivi et comité pré-doctoral. Nos discussions, vos suggestions et vos conseils m'ont aidé à mener à bien mes différents projets.

Un énorme merci aux organismes subventionnaires : la Fondation Cole, les Fonds de recherche du Québec - Santé (FRQS), la fondation Cherbaka, la fondation de l'hôpital Maisonneuve-Rosemont et les programmes de biologie moléculaire de l'Université de Montréal qui m'ont appuyé financièrement durant mon doctorat.

Je voudrais remercier tous les membres de mon jury pour l'effort et le temps qu'ils ont consacré à la lecture et à la correction de mon travail malgré leur programme chargé. C'est tout un honneur de vous avoir comme membre du jury.

Je remercie du fond du cœur ma famille, ma belle-famille et tous mes amis pour leur soutien moral, leur encouragement, leur amour inconditionnel et tous les moments de décompression. Cela m'a donné de l'énergie pour mieux avancer.

Il n'y a pas assez de mots pour remercier mon cher et tendre époux Ulrich. Cette thèse est aussi la tienne. Merci pour toutes les nuits passées à relire mon mémoire, à corriger mes manuscrits et mes demandes de bourses. Merci pour tes conseils, ta générosité, ta patience, tes encouragements et ton soutien. Surtout merci pour ton amour. Je t'aime très fort.

Finalement, je remercie tous ceux qui ont contribué de près ou de loin à la réussite de ce travail.

CHAPITRE 1

1 INTRODUCTION

L'homéostasie des protéines fait intervenir des systèmes d'adressage complexes permettant leurs repliements ou dégradations afin d'éviter l'accumulation de protéines défectueuses et d'assurer le recyclage des acides aminés. Il existe plusieurs voies de protéolyse cellulaire.

(a) Le système endosomale, responsable de la dégradation des protéines via des enzymes hydrolytiques (hydrolases) provenant de l'appareil de Golgi. Il joue un rôle important dans le tri de molécules incorporées dans les cellules [1].

(b) Le système lysosomale dont le principal acteur est un organite cytosolique appelé lysosome contient une variété d'enzymes hydrolytiques permettant de digérer par autophagie de nombreuses molécules et organites cellulaires [2].

(c) Le système ubiquitine protéasome (UPS), qui est une machinerie assurant la dégradation des protéines marquées par l'ubiquitine. Il est impliqué dans la plupart des fonctions cellulaires. Dans ce qui suit, nous allons présenter le fonctionnement de l'UPS, sa spécificité ainsi que son mode de régulation [3].

1.1 Le système ubiquitine-protéasome

Chez les eucaryotes, l'UPS est l'un des acteurs majeurs dans la protéolyse intracellulaire. Il a été découvert pour la première fois en 1977 par Aaron Ciechanover, Avram Hershko et Irwin Rose [4]. Contrairement aux voies de dégradation par les hydrolases citées précédemment, ce mode de protéolyse non lysosomale nécessite la présence d'énergie sous forme d'Adenosine Triphosphate (ATP), ainsi qu'une étape d'ubiquitination qui consiste à la fixation d'au moins 4 molécules d'ubiquitines (autrefois appelé APF pour « ATP-dépendent Proteolysis Factor ») sur la protéine substrat destinée à la dégradation par le protéasome [5].

1.1.1 L'ubiquitination

L'ubiquitination est une modification post-traductionnelle (PTM) à trois étapes qui consiste en l'attachement d'une ou de plusieurs molécules d'ubiquitine (76 acides aminés) sur la protéine substrat. La première étape nécessite la présence de l'ATP et permet l'activation de l'ubiquitine par l'enzyme activatrice E1. Par la suite, l'ubiquitine activée est transférée au groupement thiol de la cystéine active de l'enzyme de conjugaison E2. Enfin, l'enzyme E3 ligase va assurer le transfert de l'ubiquitine sur le substrat via une liaison covalente

isopeptidique entre la glycine terminale de l'ubiquitine (G76) et une lysine (K) interne ou encore un groupement amine N-terminal du substrat [6] (**Figure 1-1**).

Il existe 2 enzymes E1 chez l'humain : la plus connue est l'enzyme UBE1 ou UBA1 et la seconde enzyme UBE1L2 ou UBA6 est majoritairement exprimée dans les testicules [7, 8]. Environ 40 enzymes E2 ont été répertoriées chez les mammifères et près de 700 enzymes E3 sont responsables de la reconnaissance du substrat et de la spécificité de la réaction d'ubiquitination [8]. Les études récentes ont démontré que les enzymes E2 peuvent aussi induire l'ubiquitination en ciblant directement le substrat sans passer par les enzymes E3 ligases [8, 9].

Il existe quatre groupes d'enzymes E3 ligases dont les deux derniers ont été récemment découverts. Le premier contient un domaine RING (Really Interesting New Gene) et catalyse l'attachement de l'ubiquitine au substrat simultanément avec l'enzyme E2 liée à l'ubiquitine [10]. Le second possède un domaine HECT (Homologous to the E6AP Carboxyl Terminus), qui d'abord reçoit l'ubiquitine de l'E2 et ensuite, favorise la liaison de l'ubiquitine au substrat [11]. Le troisième regroupe les E3 ligases U-box dont le mécanisme est similaire à celle des E3 à domaine RING, mais ne contiennent pas les résidus chélateurs de métaux strictement conservés chez ces dernières [12, 13]. Il existe enfin des E3 ligases appelées RBR (RING Between RING) qui sont une combinaison entre les mécanismes des E3 ligases RING et HECT [14, 15]. En effet, les enzymes RBR contiennent deux domaines RING (RING 1 et 2) séparés par un domaine IBR. Tandis que le domaine RING1 est chargé de recruter l'enzyme E2 portant l'ubiquitine activée, le domaine RING2 contient une cystéine catalytique qui permet la liaison à l'ubiquitine. C'est au niveau C-terminal du E3 ligase RBR que se fera la reconnaissance et la fixation de l'ubiquitine sur le substrat [14, 15] (**Figure 1-1**).

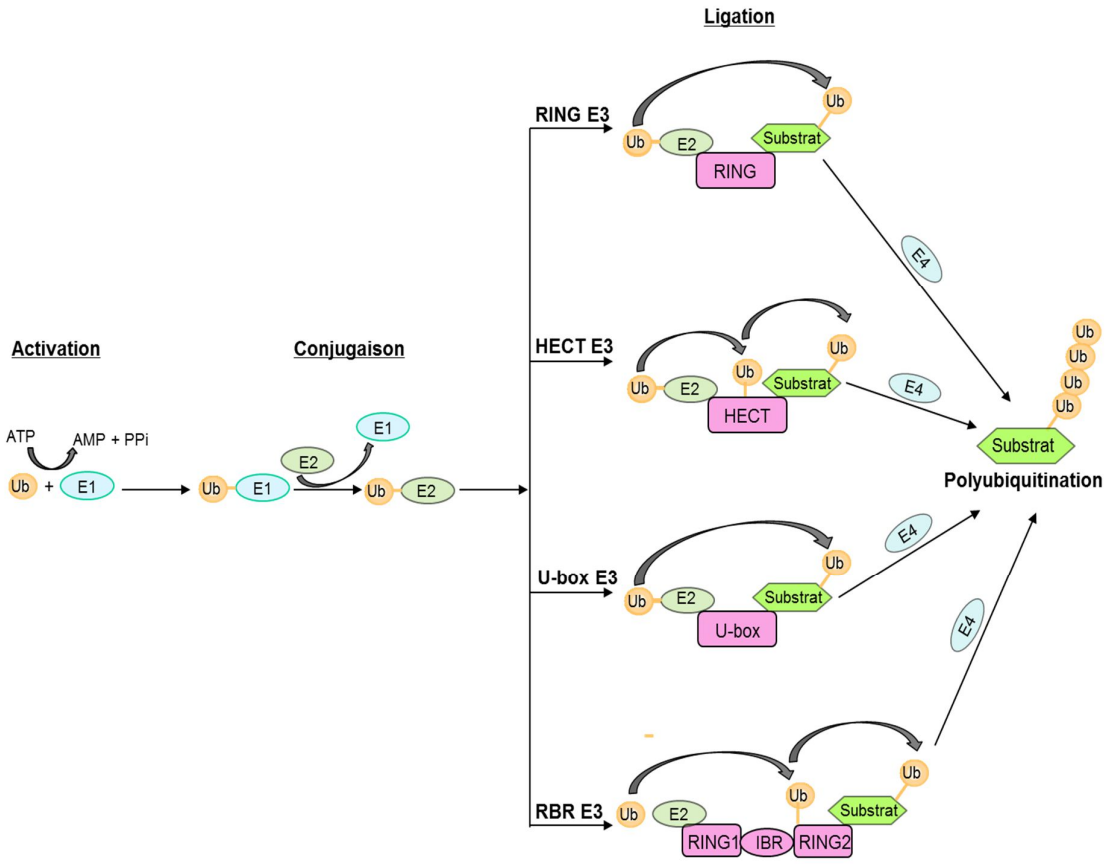

Figure 1-1 : Le mécanisme d'ubiquitination.

Illustration des différentes étapes de l'ubiquitination impliquant les enzymes E1, E2, E3 et E4.

1.1.1.1 Les différents types d'ubiquitination

La diversité des enzymes citées ci-dessus illustre la complexité des mécanismes d'ubiquitination. Pour ajouter un autre niveau de complexité, l'ubiquitine elle-même contient 7 lysines (K6, K11, K27, K29, K33, K48 et K63) et une méthionine (M1) à son extrémité N-terminal qui peuvent être utilisées pour former des chaînes d'ubiquitine variées [16, 17] (**Figure 1-2**).

Lorsqu'une seule molécule d'ubiquitine se fixe sur le substrat, on parle de monoubiquitination. Cette modification a longtemps été considérée comme un événement non-protéolytique impliqué dans les interactions entre les protéines et les diverses activités du substrat. Cependant, des études récentes ont démontré l'implication de la monoubiquitination dans la dégradation des protéines par le protéasome [18-21]. Lorsque la protéine est monoubiquitinée sur plusieurs lysines du même substrat, on parle de multi-monoubiquitination. La lysine monoubiquitinée peut également servir de cible pour la formation de polymères

d'ubiquitine [22]. On parle dans ce cas de polyubiquitination homotypique (la conjugaison des chaînes d'ubiquitine se fait sur la même lysine) ou polyubiquitination hétérotypique (la conjugaison des chaînes d'ubiquitine se fait sur des lysines différentes) [22]. Il est possible d'avoir des branchements ou ramifications où plusieurs polymères se forment sur une même molécule d'ubiquitine [23]. Cependant, les fonctions des chaînes d'ubiquitine ramifiées sont très peu étudiées (**Figure 1-2**). Bien que les E3 ligases soient responsables de la reconnaissance et de la fixation de l'ubiquitine sur le substrat, il a été montré que l'allongement des chaînes d'ubiquitine peut impliquer la présence d'une quatrième enzyme (E4) qui favoriserait la processivité de la réaction [24, 25] (**Figure 1-1**).

L'ubiquitination fait partie des PTMs régulant de nombreux processus cellulaires. Plusieurs études ont été réalisées dans le but de comprendre la fonction liée à ces différentes configurations de chaînes d'ubiquitine. Il a été montré que la polyubiquitination sur la lysine K48 conduit à la dégradation de la protéine cible par le protéasome [26]. Ce processus joue un rôle important dans l'élimination des protéines endommagées et la régulation de la demi-vie des protéines. C'est le cas par exemple de la protéine p53, dont l'activité est régulée par l'ubiquitine ligase MDM2. En effet, MDM2 catalyse la polyubiquitination K48 de p53 sur six lysines situées à son extrémité C-terminal afin d'induire sa dégradation par le protéasome [27, 28]. Cette modification de p53 a une influence majeure sur sa stabilité, sa localisation et ses activités transcriptionnelles [28]. Un autre exemple est celui de la dégradation des cyclines par l'UPS. Des études récentes ont montré que la régulation du cycle cellulaire se fait par la destruction des complexes cyclines/CDKs via la polyubiquitination K48 médiée par les ubiquitines ligases SCF (SKP1-CUL1-F-box-protein) et APC/C (Anaphase-Promoting Complex/Cyclosome) [29-31].

D'autre part, la polyubiquitination du substrat sur la lysine K63 de l'ubiquitine est connue pour jouer un rôle dans la signalisation cellulaire de manière indépendante de la dégradation [26]. Cette dernière modification est impliquée dans divers processus cellulaires tels que la réparation de l'ADN, l'endocytose, et d'autres mécanismes de signalisation intracellulaire [26, 32]. On peut citer comme exemple la polyubiquitination K63 du facteur de transcription NF-κB (Nuclear Factor Kappa B) médiée par l'ubiquitine E3 ligase TRAF (TNF receptor associated factor). Cette modification permet l'activation de la voie de signalisation NF-κB, impliquée dans les fonctions immunitaires et l'oncogenèse [33]. Les chaînes de polyubiquitines liées à la lysine K63 jouent un rôle important dans la réparation des dommages à l'ADN. Notamment, l'action combinée des ubiquitines E3 ligases RNF8 et RNF168 induit la

polyubiquitination de l'histone H1 et la monoubiquitination de l'histone H2A [34, 35]. Ces PTMs servent de marques importantes pour la reconnaissance des facteurs impliqués dans la réparation du dommage à l'ADN et permettent le maintien de la stabilité du génome.

De manière intéressante, il y a quelques années, le Dr Kanata et son équipe ont montré qu'il existe des chaînes hybrides K63-K48. Cette coopération entre ces chaînes dont les fonctions sont opposées génère un signal unique permettant spécifiquement la régulation positive de la signalisation de la protéine NF-κB [36-38].

La fonction des autres lysines de l'ubiquitine a été moins étudiée. Néanmoins, certains travaux ont montré que l'ubiquitination sur les lysines K6 et K27 semble générer des signaux non protéolytiques qui sont généralement impliqués dans les voies de réparation des dommages à l'ADN [26]. Tandis que l'ubiquitination liée à K11 et K29 semble favoriser la dégradation des protéines cibles, les liaisons K33 sont impliquées dans le trafic intracellulaire médié par l'appareil de Golgi. [16, 26, 39, 40]. Quant aux chaînes formées sur la méthionine M1, elles joueraient un rôle important dans la régulation de la voie NF-κB [26].

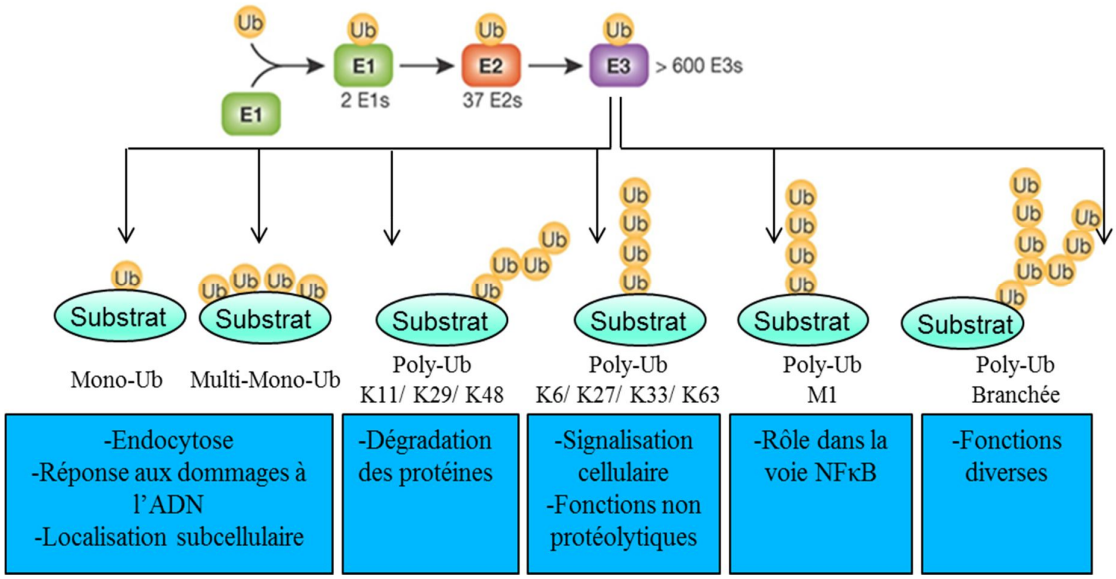

Figure 1-2 : Les différents types d'ubiquitination.

Représentation schématique des différents types d'ubiquitination, ainsi que leurs voies de signalisation. Modifiée de [41].

1.1.1.2 La monoubiquitination de l'histone H2A sur sa lysine 119 (H2AK119ub)

Plusieurs études ont démontré que les PTMs des histones jouent un rôle crucial dans la régulation de la structure de la chromatine et de l'activité des gènes. Chez l'humain, la drosophile et les plantes, les protéines des groupes Polycomb (PcG) ont été identifiés à travers leurs rôles dans le maintien épigénétique de l'expression des gènes impliqués dans le développement [42, 43]. Des analyses biochimiques ont révélé que les PcG sont regroupées en deux complexes répresseurs principaux nommés Polycomb repressive complexe 1 (PRC1) et Polycomb repressive complexe 2 (PRC2) [44, 45]. Ces complexes ont été initialement découverts chez la drosophile [46]. Les principales protéines composant le complexe PRC2 sont au nombre de trois : EZH2 (Enhancer of Zeste Homologue 2), EED (Embryonic Ectoderm Development) et SUZ12 (Suppressor of Zeste 12) [47, 48]. Les protéines EED et SUZ12 sont nécessaires à l'activité catalytique de EZH2 qui est responsable de la mono-, di- ou triméthylation de la lysine 27 de l'histone H3 (H3K27me1, 2 ou 3) [47, 48].

Les complexes PRC1 sont une famille diversifiée de complexes contenant de multiples composants. Chez la drosophile, le complexe PRC1 est constitué des protéines Polycomb (Pc), Sex Comb Extra (Sce), Posterior Sex Combs (PSC), Polyhomeotic (Ph) et Sex Comb on Midleg (Scm) [46, 49]. Chez les mammifères, chacune de ses protéines a plusieurs homologues. Il existe une donc une diversité de complexes PRC1 formés à partir de ces protéines alternatives. Ainsi, on y trouve trois homologues de la protéine Ph (PH1, PH2 et PH3) ; deux homologues de Sce (Really Interesting New Gene 1 (RING1A et RING1B)) ; six homologues de PSC (PcG RING fingers 1-6 (PcGFs)) ; deux homologues de Scm (SCMH1 et 2) ; la protéine Pc est représentée par de multiples homologues nommés CBXs (Chromobox proteins). Les protéines PcGFs incluent la protéine BMI1 (B lymphoma Mo-MLV Insertion region 1) qui est le cofacteur le plus caractérisé [50]. Chez les mammifères c'est le complexe BMI1-RING1B qui forme le noyau central du complexe PRC1 [50-52]. L'unité catalytique de ce complexe est portée par la protéine RING1B qui catalyse la monoubiquitination de l'histone H2A sur la lysine 119 (H2AK119ub).

Des travaux antérieurs ont proposé un modèle selon lequel PRC2 serait recruté à la chromatine pour catalyser la triméthylation H3K27me3, une marque reconnue par PRC1. Ce dernier à son tour, est recruté sur la chromatine pour induire H2AK119ub, ce qui a pour effet la compaction et l'inactivation de la chromatine [53, 54]. Contrairement à ce modèle, d'autres groupes de recherche suggèrent que les complexes PRC1 sont d'abord recrutés à la chromatine,

ce qui induit la monoubiquitination H2AK119ub suivi du recrutement de PRC2 [55, 56]. Bien qu'une équipe ait révélé que l'histone H2A pourrait être polyubiquitinée [57], la monoubiquitination de H2A est majoritaire et représente près de 10 % de H2A totale dans la cellule [58].

Plusieurs travaux ont rapporté l'implication de H2AK119ub médiée par PRC1 dans la répression génique. L'inactivation du chromosome X (Xi) par exemple est un excellent modèle pour la compréhension de la répression des gènes. En effet, les travaux réalisés par Fang et al. indiquent que les protéines RING1B et H2AK119ub sont spécifiquement enrichies sur le chromosome Xi des cellules souches trophoblastiques et des cellules souches embryonnaires [59]. Aussi, par diverses analyses, ces auteurs ont suggéré que RING1B et H2AK119ub sont probablement impliquées dans le stade d'initiation de l'inactivation du chromosome X [59]. D'autre part, la régulation épigénétique via l'ubiquitination de H2A a été impliquée dans le développement embryonnaire. En effet, les études montrent que les protéines RING1B et H2AK119ub sont recrutées sur les sites spécifiques des gènes Hox, qui sont les gènes impliqués dans le développement embryonnaire [60]. Ainsi, la déplétion de RING1B conduisant à une diminution des niveaux de H2AK119ub entraîne une dé-répression des gènes Hox et une prolifération des cellules souches embryonnaire [61].

Plusieurs analyses ont défini l'importance de H2AK119ub dans le cycle cellulaire des cellules de mammifère. D'abord, H2AK119ub a initialement été signalée comme étant réduite dans les cellules au repos (phase G0) et dans les cellules différenciées [62]. Dans les cellules en prolifération, H2AK119ub est présente tout au long du cycle cellulaire, mais disparaît pendant la transition G2/M et tout au long de la mitose pour ensuite être restauré après la formation de l'enveloppe nucléaire [63, 64]. Il est possible que les marques d'histone répressives médiées par les complexes PcG doivent être supprimées pour permettre la décondensation de la chromatine, nécessaires pendant la mitose et la division cellulaire [65].

1.1.2 Le protéasome

Le protéasome 26S est un complexe multi-protéique de très gros poids moléculaire (2500 kDa) impliqué dans la protéolyse ATP-dépendante des protéines polyubiquitinées [66]. Il joue un rôle majeur dans de nombreux événements cellulaires tels que : la réplication, la transcription, le cycle cellulaire, l'apoptose et la réparation des dommages à l'ADN [67, 68]. Il est composé d'une soixantaine de protéines qui sont regroupées sous la forme d'un corps catalytique 20S et d'une sous-unité régulatrice 19S [69, 70]. La structure tridimensionnelle du

protéasome 26S montre que le corps catalytique 20S, sous forme de baril, est séquestré au niveau de ses extrémités par une chambre en forme d'anneau constituant la sous-unité régulatrice 19S [66] (**Figure 1-3**). Le protéasome se retrouve dans les compartiments cytoplasmiques et nucléaires de toutes les cellules eucaryotes. Toutefois, seule la sous unité catalytique est représentée chez les espèces primitives telles que les procaryotes [71].

1.1.2.1 Le protéasome 20S

La structure du corps catalytique est très conservée durant l'évolution. Il a une forme cylindrique constituée de quatre anneaux creux à l'intérieur duquel pénètre la protéine pour être dégradée. Chacun de ces anneaux est formé de sept sous-unités α et β et sont disposés de façon αββα où les sous-unités de l'anneau central β1 (PSMB6), β2 (PSMB7) et β5 (PSMB5) portent respectivement l'activité catalytique de type caspase (clive de préférence après les résidus acides), trypsine (clive de préférence après les résidus basiques) et chymotrypsine (clive de préférence après les résidus hydrophobes) [72, 73]. La partie externe α permet l'interaction avec la sous-unité régulatrice 19S et assure le rôle de portier en contrôlant l'accès à la chambre catalytique. Des données ont montré que lors d'un stress oxydatif, le corps catalytique 20S peut se désassembler de la particule 19S et trouver libre dans la cellule. Suite à cette dissociation, le protéasome 20S va être activé et va induire la dégradation des protéines oxydées de façon indépendante de l'ATP et de l'ubiquitine [74, 75].

Il existe des variations dans la composition des sous-unités du protéasome qui se traduisent par différents types ou associations des complexes du protéasome (**Figure 1-3**).

- Le corps catalytique 20S associé au corps régulateur 19S : il est le plus étudié et constitue le protéasome 26S (**Figure 1-3**).
- Le corps catalytique 20S associé au corps régulateur ATP-indépendant 11S aussi appelé PA28. Ce dernier est constitué de 3 membres : PA28α, PA28β, and PA28γ. Tandis que PA28γ (PSME3) forme un homoheptamère dans le noyau, PA28α et PA28β se retrouvent principalement dans le cytoplasme où ils forment un hétéroheptamère [70, 76, 77].
- Le corps catalytique 20S associé au corps régulateur PA200 ATP-indépendant localisé dans le noyau. Ce complexe est généralement impliqué dans la spermatogenèse et dans la réponse aux dommages à l'ADN [78-80].
- L'immunoprotéasome, une forme alternative du protéasome 20S où les sous-unités catalytiques PSMB6 (β1), PSMB7 (β2) et PSMB5 (β5) sont remplacées par les sous-

unités appelées PSMB9 (β1i), PSMB10 (β2i) et PSMB8 (β5i) [3]. Cette forme du protéasome est majoritairement exprimée dans les cellules du système immunitaire et est importante pour la présentation de l'antigène [3]. Il a été montré que l'immunoprotéasome peut s'associer soit avec le complexe 19S soit avec le complexe 11S.

Ces différents complexes régulateurs sont capables de modifier la fonction du corps catalytique. Ainsi, la signalisation du protéasome peut changer selon sa composition.

1.1.2.2 Le protéasome 19S

Le complexe 19S est formé d'environ vingt protéines et se lie aux extrémités du corps catalytique 20S. Il est divisé en deux compartiments :

(a) La base : elle se lie à l'anneau α du corps catalytique et est constituée de six sous-unités de type AAA+ ATPase appelé PSMC1-7 (ou Rpt1-7 chez la levure S. cerevisiae) permettant l'ouverture du protéasome 20S et de trois sous-unités non ATPases appelé PSMD (ou Rpn chez S. Cerevisiae) [3]. PSMD1 et 2 (Rpn2 et 1 respectivement) ont une activité de type structurale et servent d'échafaudage pour l'assemblage des sous-unités de la particule régulatrice [66, 81]. Elles sont capables de se lier aux récepteurs d'ubiquitine transportant la protéine ubiquitinée destinée à la dégradation. Ce qui facilite la translocation du substrat vers l'anneau α [66]. La troisième sous-unité ADRM1 (Rpn13) est un récepteur d'ubiquitine important pour la reconnaissance du substrat ubiquitiné. Elle interagit avec les chaînes d'ubiquitine au niveau des boucles de son domaine PRU (Pleckstrin-like Receptor for Ubiquitin) [81, 82]. Des expériences de cryo-microscopie électronique et de résonnance magnétique nucléaire ont montré que ADRM1 se lie à la sous-unité PSMD1 [83, 84]. De manière intéressante, des études ont prouvé que PSMD2 serait aussi capable de lier l'ubiquitine et pourrait donc être considérée comme un récepteur de l'ubiquitine [66, 85].

(b) Le couvercle : il est formé de six sous-unités non ATPases PSMD3, PSMD6, PSMD8, PSMD11, PSMD12 et PSMD13 (Rpn3, Rpn7, Rpn12, Rpn6, Rpn5 et Rpn9 respectivement) organisées en un module caractéristique appelé « protéasome-COP9-initiation factor 3 » (PCI) [86-89]. Il contient aussi une sous-unité DSS1 (Rpn15/Sem1), qui fonctionne comme un stabilisateur moléculaire de l'hétérodimère PSMD3/PSMD6

[90] et un complexe hétérodimère PSMD7/PSMD14 (Rnp8/Rpn11) qui permet le clivage des chaînes d'ubiquitine avant la dégradation du substrat [91].

Les études ont montré qu'il existe un récepteur d'ubiquitine PSMD4 (Rpn10), intégré au sein du couvercle via des interactions entre son domaine N-terminal appelé Von Willenbrand et les sous-unités PSMD7, PSMD14 et PSMD13 [92, 93]. Ce récepteur fait le lien entre la base et le couvercle et est capable de reconnaître le substrat et de se lier aux chaînes d'ubiquitine via son motif d'interaction avec l'ubiquitine.

Le complexe 19S a une structure dynamique. Il assure la reconnaissance du substrat, le clivage et le recyclage des chaînes d'ubiquitine, l'activation du complexe 20S ainsi que la translocation du substrat vers le corps catalytique [94]. Il existe des protéines plus ou moins capables de s'associer à la sous-unité régulatrice du protéasome et de jouer un rôle dans son activité. Ce sont notamment les déubiquitinases tels que USP14 et UCH37, les ubiquitines ligases comme la protéine Hul5 et les récepteurs d'ubiquitine extrinsèques tels que les protéines Rad23 A et B [70, 95, 96].

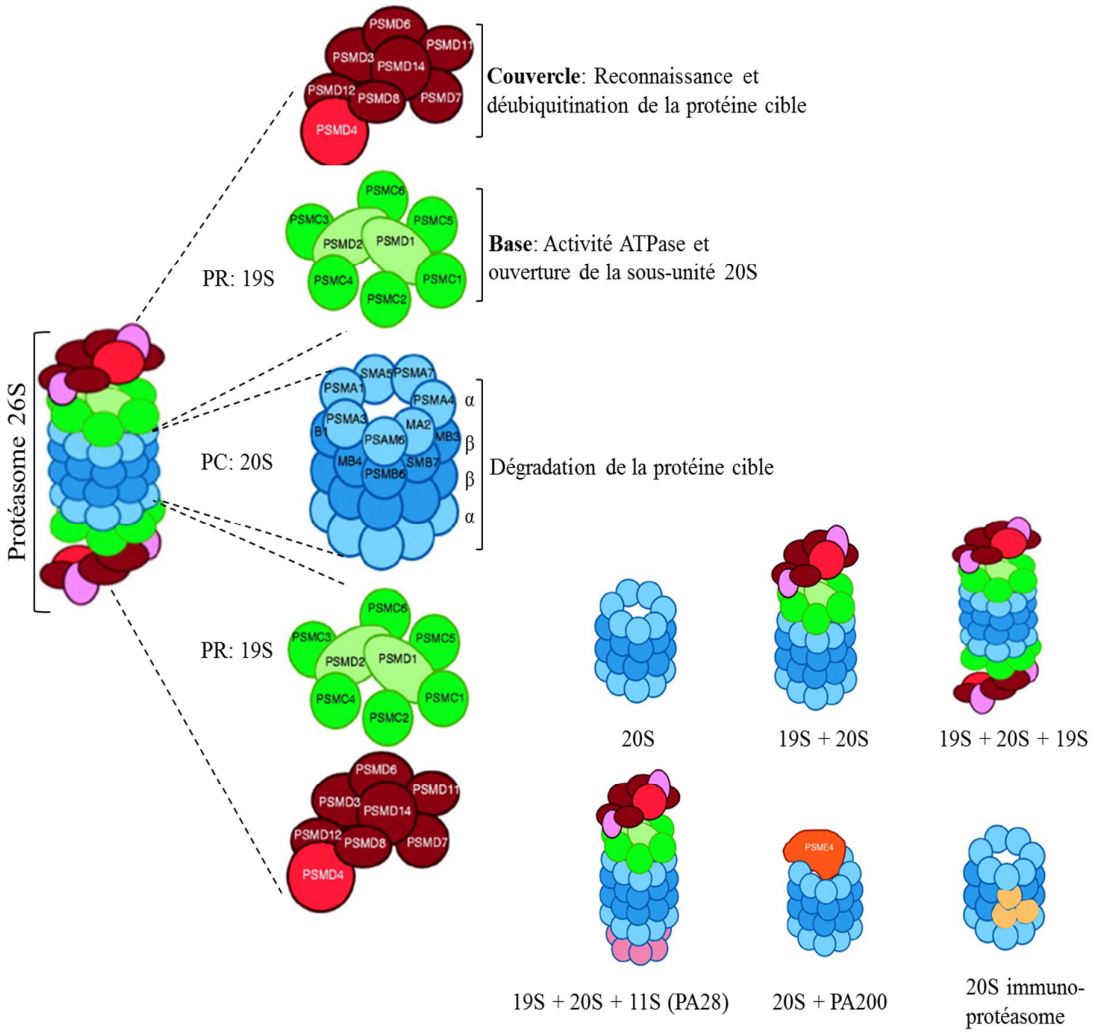

Figure 1-3 : Le protéasome.

Représentation schématique des sous-unités du protéasome 26S et des différents types de protéasome. La partie catalytique (PC) est constituée de deux anneaux α et β nécessaires à la dégradation protéolytique. La partie régulatrice (PR), composée d'une base et d'un couvercle est responsable de la reconnaissance et de la déubiquitination de la protéine cible. Modifiée de [86].

1.1.2.3 Les récepteurs de l'ubiquitine

Il existe de nombreux récepteurs d'ubiquitine. Leur principal rôle est de discriminer quel type d'ubiquitination est associé au substrat et de permettre leur orientation vers différentes voies cellulaires [97]. Certains récepteurs sont associés à la fonction du protéasome et aident les protéines polyubiquitinées à atteindre le protéasome [98]. Six récepteurs d'ubiquitine associés au protéasome sont actuellement connus. Trois font partie des sous-unités régulatrices

intrinsèques du protéasome, PSMD2, PSMD4 et ADRM1 (Rpn1, Rpn10 et 13 respectivement). Chez les eucaryotes, PSMD4 contient deux ou trois séquences hélicoïdales appelées UIM (Ubiquitin-Interacting Motif) permettant sa liaison avec l'ubiquitine ou avec d'autres récepteurs liés au protéasome [99]. ADRM1 reconnaît l'ubiquitine à travers un domaine globulaire PRU. De plus, elle contient une séquence appelée DEUBAD (DEUBiquitinase ADaptor), impliquée dans la liaison avec la déubiquitinase UCH37 [99, 100]. PSMD2 contient deux régions de liaison aux ligands T1 et T2. T1 est responsable de la liaison entre PSMD2 et l'ubiquitine ou entre PSMD2 et les autres récepteurs d'ubiquitine associés au protéasome. Quant à T2, il permet l'interaction avec les déubiquitinases USP14 [99]. Bien que les sous-unités, PSMD4 et ADRM1 soient généralement considérées comme les principaux récepteurs d'ubiquitine du protéasome, la question sur la spécificité de ces récepteurs vis-à-vis du substrat n'a pas encore clairement été établie.

Les trois autres récepteurs, Rad23, Dsk2 et Ddi1, s'associent de façon réversible et transitoire avec le protéasome via leur domaine UBL (Ubiquitin-Like domain) et sont considérés comme des récepteurs d'ubiquitine extrinsèques [101]. Ces dernières possèdent des motifs d'interaction avec l'ubiquitine ou UBD (Ubiquitin Binding Domain) et peuvent interagir de manière autonome avec l'ubiquitine. De ce fait, elles sont capables de reconnaître les protéines ubiquitinées et de les escorter vers le protéasome. La reconnaissance du substrat par le protéasome semble être un mécanisme complexe, dans le sens où un seul substrat ubiquitiné peut être lié par plusieurs récepteurs d'ubiquitine [82].

Il a été signalé que suite à des stress induits par une privation en acides aminés ou en raison d'une inhibition du protéasome, ces récepteurs sont polyubiquitinés, ce qui interfère avec la liaison et la dégradation du substrat [101]. D'autre part, des recherches ont rapporté que le récepteur Rad23B permettrait la localisation d'une quantité accrue de protéines dans un compartiment subcellulaire via un mécanisme de séparation de phase liquide-liquide (LLPS) [102]. La pertinence de Rad23B dans les phénomènes de LLPS sera discutée dans le chapitre 3 de cette thèse.

1.1.2.4 Le récepteur d'ubiquitine Rad23

La protéine Rad23 chez la levure et ses homologues humains Rad23A et Rad23B sont des récepteurs de l'ubiquitine contenant un domaine UBL et deux domaines UBA (Ubiquitin-Associated domain) (**Figure 1-4**). Elles sont impliquées dans la dégradation protéasomale et sont capables de reconnaître préférentiellement les chaînes d'ubiquitine K48 et de se lier aux

protéines polyubiquitinées grâce à leurs domaines UBA [103]. Cette liaison va permettre l'adressage des substrats jusqu'au protéasome où les différents Rad23 se lient via leur domaine UBL [104]. L'enzyme Rad23 peut aussi recruter une ubiquitine ligase spécifique pour l'élongation de la chaîne d'ubiquitine sur le substrat. C'est le cas par exemple de la protéine Ufd2, une enzyme E4, responsable de l'allongement des chaînes, qui se lie à Rad23 pour induire la polyubiquitination et la dégradation du substrat [105]. Outre leur interaction avec le protéasome, ces récepteurs peuvent aussi se retrouver libres et exercer des activités indépendantes du complexe protéasomale.

Paradoxalement à leur rôle dans la protéolyse, Rad23A et B ont été initialement identifiées à travers leur fonction dans la réparation des dommages à l'ADN par excision de nucléotides (NER : Nuclear Excision Repair) [106, 107]. Des travaux indiquent que Rad23 stabilise et protège la protéine Rad4 de la dégradation [106]. En effet, le complexe Rad23/Rad4 reconnaît et se lie à l'ADN endommagé et prépare la lésion aux étapes successives entraînant l'excision de l'ADN endommagé [108].

Des études structurales ont apporté quelques éléments de réponses quant à la complexité de la fonction de Rad23. En effet, ce récepteur peut adopter une conformation ouverte ou fermée importante pour la régulation de ses fonctions [109]. Cependant, comment l'équilibre entre l'engagement de Rad23 dans la dégradation protéasomale et son implication dans le NER est-il coordonné ? Des études sur sa dynamique et sa cinétique d'interaction avec ses partenaires nous donneront des indices sur son mode de fonctionnement.

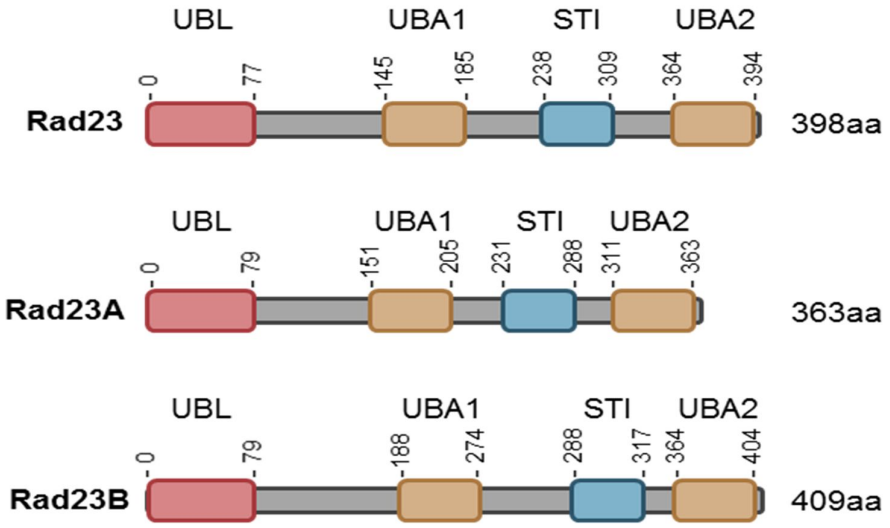

Figure 1-4 : Représentation schématique des récepteurs Rad23, Rad23A et Rad23B.

Adaptée de [110]

1.1.2.5 Régulation métabolique du protéasome

Le protéasome est un complexe multiprotéique responsable de la dégradation des protéines et d'assurer le recyclage des acides aminés. À travers cette fonction, le protéasome est impliqué dans une variété de processus cellulaires tels que le contrôle de la qualité des protéines, le cycle cellulaire, la présentation de l'antigène, l'apoptose et la signalisation cellulaire. Cependant, le mécanisme de régulation du protéasome est peu connu. Les études ont suggéré que le protéasome pourrait être modifié et régulé par des facteurs métaboliques. En effet, il y a une vingtaine d'années environ, les travaux de Sumegi et al. ont rapporté que chez la drosophile, le protéasome 26S pourrait être modifié par O-GlcNAcylation, une PTM impliquée dans le métabolisme du glucose [111]. Par la suite, les études menées par Zhang et son équipe ont révélé que le protéasome serait également modifié par O-GlcNAcylation dans les cellules de mammifère et que cette modification pourrait inhiber la fonction du protéasome [112]. Quelques années plus tard, Zhang et son équipe ont proposé que la protéine PSMC6 (Rpt6 chez la levure), serait la cible de la phosphorylation de la kinase PKA, ce qui entraînerait une stimulation du protéasome. De plus, étant donné que PKA stimule la gluconéogenèse, ces auteurs mentionnent que la régulation par PKA pourrait se produire à travers le métabolisme du glucose [113].

Des études récentes ont montré que, suite à une privation de carbone chez la levure et chez les plantes, le protéasome subit une LLPS et s'accumule dans le cytoplasme sous forme de granules, favorisant ainsi la viabilité des cellules [114]. Cependant, chez les mammifères, il existe des mécanismes qui coordonnent à la fois la synthèse et la dégradation protéiques. Ceci est le cas par exemple de la kinase mTOR (Mammalian Target Of Rapamycin), qui favorise l'anabolisme et la synthèse des protéines, ainsi que les voies de signalisation qui coordonnent la protéolyse par le système UPS [115]. Des études récentes ont révélé que suite à une privation en acides aminés, le protéasome peut être dégradé par autophagie et cette dégradation est médiée par la kinase mTOR [116, 117].

Pris ensemble, ces différents travaux dévoilent que la fonction du protéasome est régulée par le métabolisme cellulaire (glucose, acides aminés, nutriments). Ceci pourrait être nécessaire pour le contrôle de la disponibilité des acides aminés dans la cellule.

1.2 La régulation des réactions d'ubiquitination

L'ubiquitination est un processus réversible. En effet, toutes les étapes de modification conduisant à la fixation de l'ubiquitine sur le substrat sont finement contrôlées. Cette régulation peut se faire d'une part via d'autres PTMs qui peuvent induire ou inhiber le processus d'ubiquitination (Plus de détails dans l'annexe) et d'autre part via la déubiquitination qui est un processus capable d'enlever l'ubiquitine sur la protéine substrat [118].

1.2.1 La déubiquitination

La réaction de déubiquitination est assurée par des enzymes appelées déubiquitinases (DUBs) [119]. Il existe environ 100 DUBs capables de cliver les liaisons peptidiques ou isopeptidiques entre la glycine G76 de l'ubiquitine et le substrat ou de cliver les liaisons entre les ubiquitines [119]. Les DUBs font partie de la superfamille des protéases et ont été classées en 7 familles selon leurs structures et leurs activités catalytiques. Les DUBs les plus connues sont les protéases (a) UCH (Ubiquitin C-terminal hydrolase), (b) USP (Ubiquitin Specific Protease), (c) OTU (Ovarian Tumor Domain protease), (d) MJD (Machado-Josephin Domain protéases), (e) JAMMs (JAB1/MPN/MOV34 metalloenzymes) [120, 121]. Deux autres familles de DUBs ont récemment été caractérisées, ce sont les MCPIP1 (Monocyte Chemotactic Protein-Induced Protein 1) [122] et les MINDY (Motif Interacting with Ub-containing Novel DUB family) [119, 123]. La plupart des enzymes de ces familles sont des cystéines protéases, dont l'activité enzymatique réside sur le groupe thiol d'une cystéine centrale, à l'exception de la famille des JAMMs qui sont considérées comme des métalloprotéases dont l'activité catalytique est coordonnée par le Zinc.

1.2.1.1 Étude fonctionnelle des déubiquitinases

Les DUBs jouent un rôle crucial dans la majorité des régulations qui impliquent l'ubiquitine. L'implication de ces protéases dans la maturation ou le blocage de l'action des ligases E3 a été démontrée à plusieurs niveaux, notamment :

- **La production de l'ubiquitine mature**

L'ubiquitine est synthétisée sous forme de précurseurs qui sont soit des chaînes linéaires de polyubiquitine, soit de l'ubiquitine associée aux protéines ribosomales [124, 125]. Certaines DUBs comme les protéines UCHL3, USP9X, USP7, USP5 et Otulin ont été impliquées dans le

clivage des chaînes précurseurs d'ubiquitine et dans la maturation de nouvelles molécules d'ubiquitine [124].

- **Recyclage des chaînes d'ubiquitine**

Afin de permettre l'homéostasie de l'ubiquitine, il existe un système de recyclage des molécules d'ubiquitine via les DUBs associées au protéasome. En effet, les DUBs PSMD14, UCH37 et USP14 de la sous-unité régulatrice 19S du protéasome seraient responsables d'enlever et de recycler les chaînes d'ubiquitine avant que le substrat ne s'engage vers le complexe catalytique pour être dégradé [126]. Il a été proposé que USP14 agit préférentiellement sur les substrats qui portent des chaînes d'ubiquitine multiples [127]. Dans cette étude, les auteurs montrent que les chaînes libres de longueurs et de types de liaison divers sont toutes clivées par USP14. Aussi, en utilisant la technique de spectrométrie de masse, ils ont confirmé que seules les liaisons K48, importantes pour la dégradation protéasomale, n'étaient pas clivées dans cette réaction [127]. Contrairement à leur implication dans la dégradation des protéines, USP14 et UCH37 peuvent aussi sauver les substrats de la dégradation en déubiquitinant et en favorisant la dissociation entre le substrat et le protéasome avant l'étape d'engagement [128]. Ceci permet d'épargner les substrats qui ne sont pas destinés à la destruction. Cependant, une fois engagé, le substrat ne peut plus être sauvé. Par la suite, PSMD14 permet de cliver les ubiquitines restantes avant que le substrat rentre dans la chambre catalytique [129].

- **Changement du signal**

Il existe des déubiquitinases portant une activité E3 ligase et qui sont capables de changer la signalisation du substrat. C'est le cas de la protéine A20, qui possède un domaine N-terminal à activité déubiquitinase de type OTU. Ce domaine permet la suppression des chaînes K63 sur la protéine RIP (Receptor Interacting Protein). En parallèle, le côté C-terminal de A20 fonctionne comme une ubiquitine ligase et permet la polyubiquitination K48 de RIP, la conduisant vers une dégradation protéasomale [130].

- **Stabilité et localisation du substrat**

Le rôle des DUBs est de s'opposer à la signalisation induite par l'ubiquitination et ainsi de renverser le signal de destruction de la protéine cible [131]. Aussi, les DUBs ont la capacité de réguler la localisation subcellulaire des protéines. Par exemple, la protéase USP10 est capable

de déubiquitiner la protéine p53, d'empêcher son exportation nucléaire et ainsi de stabiliser la protéine. Ce qui antagonise l'action de l'ubiquitine ligase MDM2 [132].

1.2.1.2 Spécificité des déubiquitinases

Alors qu'il existe environ 600-700 E3 ligases capables d'effectuer l'ubiquitination de plus de 5000 protéines, seulement 100 DUBs sont des régulateurs de ces événements [8, 64, 119, 133]. Cela mène à la question sur la spécificité des DUBs pour leurs substrats. En effet, les DUBs possèdent une structure modulaire contenant différents domaines leur permettant d'interagir avec le substrat. Par exemple, les DUBs possèdent des domaines UBDs (Ubiquitin Binding Domain) idéaux pour reconnaître une conformation ou un branchement de chaînes d'ubiquitine [134, 135]. Plusieurs types d'UBD ont été caractérisés : ce sont les UIM (Ubiquitin Interacting Motif), les domaines UBA (Ubiquitin Associated domain), les motifs CUE (Coupling of Ubiquitin conjugation to ER degradation), les motifs UEV (Ubiquitin binding site of the ubiquitin E2 variant), les domaines Znf UBP (Zinc-Finger Ubiquitin Binding domain). Ces différents domaines ont une structure et des séquences consensus qui divergent, ce qui explique leur capacité à reconnaître plusieurs types de chaînes [131, 136, 137].

D'autre part, la reconnaissance du substrat par les DUBs peut être indirecte et médiée par l'association de complexes multi-protéiques. Par exemple, des études récentes ont montré que la déubiquitinase BAP1 (BRCA1-Associated Protein 1) de la famille des UCH doit interagir avec le domaine DEUBAD de la famille des ASXLs ce qui crée une interface de liaison à l'ubiquitine appelé CUBI (Composite Ubiquitin Binding Interface). La formation de ce complexe va donc induire l'activation de la protéine BAP1 responsable de la déubiquitination de l'histone H2A sur la lysine K119 permettant ainsi la régulation de la progression du cycle cellulaire et la réparation des dommages à l'ADN [138, 139]. De manière intéressante, BAP1 est aussi capable de cibler plusieurs substrats pour permettre de nombreux processus cellulaire. Des études antérieures ont suggéré que la protéine HCF-1 (Host Cell Factor-1) est un substrat de BAP1. En effet, BAP1 serait capable de reverser la polyubiquitination K48 de HCF-1 au niveau de son domaine Kelch [140]. Ainsi, la régulation de HCF-1 via son interaction avec BAP1 est importante pour le contrôle de la progression du cycle cellulaire à la transition G1/S [141]. D'autre part, Ruan et son équipe ont proposé que BAP1 régule la gluconéogenèse par son interaction avec la O-linked N-acétylglucosamine transférase (OGT). Ces auteurs rapportent que suite à des variations en glucose, le complexe BAP1/OGT/HCF-1 se lie et stabilise le coactivateur transcriptionnel PGC-1α, important pour la gluconéogenèse hépatique,

ceci via l'induction de sa O-GlcNAcylation et sa déubiquitination [142]. Un autre rôle de BAP1 a été attribué dans la réparation des dommages à l'ADN par recombinaison homologue via la régulation de H2AK119ub [138]. Récemment, notre équipe a montré que BAP1 est capable d'être sa propre cible et de s'auto-déubiquitiner. Ceci permet à cette DUB de se protéger d'une éventuelle séquestration cytoplasmique médiée par la ligase atypique UBE2O [143]. Tous ces exemples démontrent que les mécanismes conduisant à la spécificité de cette DUB pour ses différents substrats sont d'une grande complexité.

Mise à part la reconnaissance des substrats par leurs domaines UBD, certaines familles de DUBs tels que les JAMMs ont la capacité d'hydrolyser spécifiquement les chaînes K63 [144], tandis que celles de la famille des MINDY ont une préférence pour couper les chaînes longues K48 [123].

- **De nombreuses DUBs ciblant un même substrat**

Bien que de nombreuses études aient abordé l'importance de la forte spécificité des DUBs, la plupart des substrats ubiquitinés sont régulés par plus d'une déubiquitinase. Cette situation est bien illustrée dans le cas de la protéine substrat p53. En effet, la DUB USP7 (aussi connu sous le nom de HAUSP) possède des extensions N-terminales et C-terminales qui sont importantes pour sa spécificité de liaison avec le complexe p53-MDM2. Ainsi, USP7 se lie à MDM2 et celui-ci lui sert de pont pour la déubiquitination et la stabilisé p53 par USP7 [145, 146]. D'autres études ont montré que les protéases USP10, USP49 ou encore USP29 ont aussi la capacité de déubiquitiner et induire l'activation et la stabilité du suppresseur de tumeur p53 [132, 147]. Un autre exemple est l'ubiquitination de l'histone H2AK119 qui est contrôlée par plusieurs DUBs telles que les protéines USP16/UBP-M, USP3, MYSM1 ou BAP1 [143, 148]. Pourquoi faut-il plusieurs deubiquitinases pour réguler une même protéine ? La façon dont ces enzymes coordonnent leurs actions pour réguler l'ubiquitination de H2A dans un environnement cellulaire spécifique reste mal connue. Par conséquent, des études plus approfondies pour clarifier le mécanisme moléculaire conduisant à la reconnaissance des substrats par leurs DUBs devraient être réalisées.

1.2.2 La déubiquitinase USP16 (Ubiquitin Specific Protease 16)

L'ubiquitination de l'histone H2AK119 est une modification post-traductionnelle essentielle au remodelage de la chromatine, nécessaire à la LLPS, à la réparation de l'ADN et la progression du cycle cellulaire [138, 139]. Elle est réversible et est hautement contrôlée par

plusieurs DUBs tels que BAP1, MYSM1, USP3 ou encore USP16 [143, 148]. Contrairement aux autres DUBs localisées au sein du noyau, il a été montré que USP16 se retrouve principalement dans le cytoplasme [149]. Il est donc pertinent de comprendre pourquoi et comment cette protéase cytoplasmique est transloquée dans le noyau pour réguler H2AK119ub alors qu'il existe déjà plusieurs DUBs nucléaires capables de reverser cette modification.

1.2.2.1 Structure, localisation et expression de USP16

USP16 est une protéine qui contient 823 acides aminés et est codée par un gène situé sur le chromosome 21 chez l'humain [150, 151]. Les informations recueillies dans les bases de données « CbioPortal for cancer genomics », « GeneCards », et « PhosphoSitePlus » ont révélé que USP16 semble être exprimée de façon ubiquitaire dans tous les types cellulaires et dans tous les tissus y compris le cerveau, les poumons, le foie, les reins, le cœur, le cerveau, le placenta, les muscles squelettiques, et le pancréas. Il a été indiqué que le gène USP16 peut subir un épissage alternatif au niveau de l'ARN aboutissant à la génération de cinq isoformes distinctes de cette protéine. Cependant, la fonction de ces isoformes n'a pas encore été caractérisée.

Comme la plupart des DUBs de la famille des USPs, USP16 contient un domaine de liaison à l'ubiquitine (Znf-UBP) capable de reconnaître et de se lier à la molécule d'ubiquitine (**Figure 1-5**). La structure cristalline de ce domaine en forme de doigt de zinc a été établie. Contrairement à d'autres domaines de liaison à l'ubiquitine, ce domaine Znf-UBP contient une poche hydrophobe permettant la liaison avec le motif de diglycine C-terminal libre de l'ubiquitine [152-155]. En plus de son domaine Znf-UBP, USP16 possède un domaine catalytique réparti sur 2 régions [156] (**Figure 1-5**). Comme la plupart des DUBs de la famille USP, ce domaine catalytique contient deux boîtes de cystéine et d'histidine hautement conservées qui lui confèrent une activité catalytique [156, 157]. C'est la cystéine active située en position 205 du domaine catalytique de USP16 qui contrôle son activité déubiquitinase [149].

Notre intérêt principal résidait dans la compréhension des mécanismes de transport de USP16 pouvant moduler la LLPS au cours des réponses aux dommages à l'ADN (discuté ultérieurement). Bien que la structure cristallographique de USP16 n'a pas encore été caractérisée, un groupe de chercheurs a rapporté que USP16 pourrait posséder plusieurs signaux de localisation nucléaire (NLS) qui seraient requis pour son transport dans le noyau [158] (**Figure 1-5**). Ces motifs sont de courtes séquences riches en acides aminés basiques chargés

positivement. Il existe des NLS classiques qui peuvent être soit de type monopartite, soit de type bipartite. Le type monopartite consiste en une seule séquence d'acides aminés basiques. L'exemple le plus connu est la séquence NLS de l'antigène T Large du virus SV40 : PKKKRKV [159, 160]. Les NLS classiques de type bipartite sont composés de deux motifs d'acides aminés basiques séparés par une séquence d'espacement d'environ 10 acides aminés (par exemple, la séquence NLS de la nucléoplasmine : KR [PAATKKAGQA] KKKK) [159, 160]. Il existe aussi des NLS non classiques ou atypiques dont les séquences sont variables et peuvent atteindre jusqu'à 20 acides aminés [159, 160]. Les NLS s'associent à des protéines de la famille des importines ou transportines et le complexe importine/NLS-protéine est ensuite transporté dans le noyau à travers les pores nucléaires [161-163].

Il a été suggéré que la localisation cytoplasmique de USP16 pouvait être médiée par l'intermédiaire d'un signal d'export nucléaire (NES) [158] (**Figure 1-5**). En général, les NES sont de courtes séquences d'acides aminés hydrophobes reconnues par un transporteur appelé exportine. Ce dernier va reconnaître la séquence consensus $Lx_{2,3}Lx_{2,3}LxL$ du NES (où L est la leucine ou un résidu hydrophobe et x peut être n'importe quel acide aminé) et par la suite, va se lier et transporter la protéine cargo vers le cytoplasme à travers les pores nucléaires [164]. L'exportine 1 ou CRMI est la principale exportine cellulaire et facilite l'exportation des protéines qui ont un motif de type NES vers le cytoplasme [165, 166]. Néanmoins, bien que ces NLS et NES potentiels ont été proposés, il serait important de vérifier la fonctionnalité de ces motifs afin d'établir le mécanisme de transport de USP16 dans la cellule.

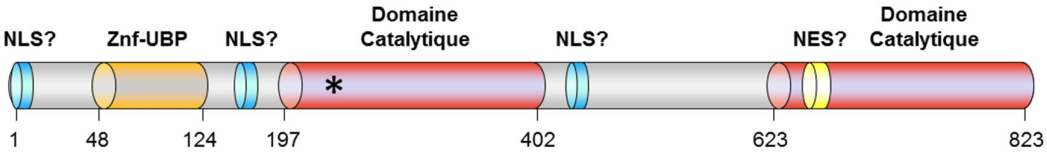

Figure 1-5 : Illustration graphique des domaines de USP16 (humain).

La protéine USP16 serait constituée d'un domaine catalytique reparti sur deux régions, d'un domaine de liaison à l'ubiquitine (Znf-UBP), des signaux de localisation nucléaires (NLS) potentiels et d'un signal d'export nucléaire potentiel. L'Astérix indique la cystéine catalytique. Modifiée de [158].

1.2.2.2 Implication fonctionnelle de USP16

- **Rôle de USP16 dans le cycle cellulaire**

La protéase USP16/Ubp-M est une déubiquitinase à cystéine de la famille des USPs [167]. Elle a été découverte il y a une vingtaine d'années par Vincent T. Marchesi et son équipe [149]. Ces auteurs ont montré par différentes expériences que USP16 se localise préférentiellement dans le cytoplasme et pourrait être impliquée dans la déubiquitination de H2AK119ub, un événement nécessaire à la répression de l'expression génique, la condensation/décondensation de la chromatine et la progression du cycle cellulaire [149] (**Figure 1-6**).

Comme mentionné précédemment dans la section 1.1.1.2, il a été suggéré que les niveaux de H2AK119ub commencent à diminuer lorsque les cellules entrent en phase mitotique (M), atteignent des niveaux très bas au milieu de la phase M (métaphase), puis commencent à se rétablir lorsque les cellules sortent de la mitose [63, 64]. D'autre part, certaines investigations suggèrent que lors de la transition G2/M du cycle cellulaire, l'histone H3 serait phosphorylée sur sa sérine 10 (H3S10P) par la kinase AuroraB et cette modification serait nécessaire pour le déclenchement de la mitose [168-170].

Les travaux menés par Joo et son équipe proposent que la déubiquitination de H2A par USP16 induise le relâchement de la chromatine, donnant ainsi accès à Aurora B pour permettre la phosphorylation de H3 et le déclenchement de la mitose [171]. Dans cette investigation, ces auteurs ont rapporté que la déplétion de USP16 entraîne un retard de la phase G2/M, une diminution de la prolifération cellulaire et une augmentation des niveaux de H2AK119ub [171] (**Figure 1-6**).

Il est important de noter que contrairement au modèle selon lequel déubiquitination de H2AK119ub par USP16 est une condition préalable à H3S10P [171], Frangini et son équipe proposent un mécanisme de régulation transcriptionnelle selon lequel Aurora B phosphoryle l'histone H3 sur la sérine 28 (H3S28P) au niveau des promoteurs actifs des cellules quiescentes [172, 173]. H3S28P va alors faciliter l'activité déubiquitinase de USP16 au niveau des gènes transcrits ainsi que l'inhibition de l'ubiquitination médiée par Ring1B sur l'histone H2A [172]. Il serait donc important d'investiguer le mécanisme de régulation de USP16 et de comprendre davantage comment ces différentes PTMs sont coordonnées.

Lors de la mitose, plusieurs protéines telles que la cycline B, la polo-like kinase 1 (PLK1) et Aurora-B vont s'accumuler pour permettre l'assemblage des kinétochores au niveau

des régions centromériques des chromosomes et la ségrégation des chromosomes [174]. La PLK1 est essentielle à la division cellulaire et à la cytocinèse [175]. Elle est localisée à la fois au niveau des centrosomes et au niveau des kinétochores [176-178] et elle est impliquée dans la maturation des centrosomes, la cohésion des chromatides sœurs et l'attachement adéquat des fuseaux mitotiques aux kinétochores [179, 180].

Des travaux ont révélé qu'il existe des PTMs susceptibles d'avoir un impact sur la localisation de PLK1. C'est le cas par exemple de la monoubiquitination de PLK1 sur sa lysine 492 par l'ubiquitine ligase CUL3-KLHL22, qui conduit à sa dissociation des kinétochores [181, 182]. Il a été rapporté que USP16 pourrait contrecarrer l'action menée par CUL3-KLHL22 en interagissant et en déubiquitinant la PLK1 [183]. Cette action permettrait d'assurer la rétention de PLK1 sur les kinétochores, ce qui est nécessaire pour la ségrégation chromosomique et l'alignement optimal des chromosomes lors de la mitose [183, 184] (**Figure 1-6**).

- **Rôle de USP16 dans la réponse aux dommages à l'ADN**

L'ADN subit en permanence plusieurs altérations par de nombreux agents physiques et chimiques. Ces agressions peuvent causer des dommages ou des mutations au sein de l'ADN, provoquant ainsi une instabilité génomique qui pourrait être à l'origine de l'apparition de cancers. Afin de se défendre contre ces altérations génomiques, les cellules sont dotées de mécanismes de réparation, qui forment collectivement la réponse aux dommages à l'ADN (DDR).

Bien que l'ubiquitination de H2A soit connue pour son implication dans les mécanismes de répression transcriptionnelle [185, 186], plusieurs études ont révélé qu'elle pourrait avoir un rôle actif dans la régulation directe de la chromatine au site des dommages à l'ADN en réponse aux stress génotoxiques [187] et dans la formation et la résolution de la LLPS [188-190]. Ainsi, la déubiquitination de H2A menée par USP16 pourrait avoir un rôle majeur dans la régulation de la DDR. Dans la section 1.3.3.5 de ce manuscrit, nous aborderons de manière beaucoup plus détaillée l'implication de USP16 dans la séparation de phase au cours de la réparation des cassures double brin de l'ADN.

- **Autres rôles de USP16**

(a) - Hors mis son rôle dans la régulation du cycle cellulaire et dans la DDR, il s'avère que chez les embryons de xénope, USP16 module la structuration embryonnaire antéro-postérieure par la régulation de l'expression des gènes Hox [171]. En effet, les gènes Hox sont impliqués

dans différents aspects du développement embryonnaire [191]. Des travaux ont montré que l'activation des gènes Hox pendant l'embryogenèse est médiée par le remodelage de la chromatine permettant le passage d'un état répressif à un état permissif [192]. Chez la drosophile par exemple, les gènes Hox sont considérés comme des facteurs de transcription nécessaires à la formation des organes au niveau des axes antéro-postérieurs et dorso-ventraux [193].

Il existe cependant des indices montrant que l'ubiquitination pourrait réguler plusieurs gènes Hox. C'est le cas de la protéine Ring1B du complexe PRC1 qui régule la fonction des gènes Hox en ubiquitinant l'histone H2AK119 [194]. Ceci a pour conséquence la restructuration de la chromatine et l'inactivation de l'expression de certains gènes [195-197]. De manière intéressante, les analyses d'hybridation in situ ont révélé que l'inhibition de USP16 réduit considérablement l'expression de la protéine Hoxd10 dans la région postérieure des embryons du xénope. Il semblerait donc que USP16 joue un rôle dans la régulation de l'expression des gènes Hox, via la déubiquitination H2AK119ub [171].

(b) – Au cours de ces dernières années, plusieurs autres fonctions ont été attribuées à USP16. Il a été proposé que USP16 régule l'expression de nombreux gènes impliqués dans l'hématopoïèse. En effet, USP16 semble maintenir un état normal du cycle cellulaire des cellules souches hématopoïétiques et embryonnaires en réprimant l'expression de la protéine Cdkn1a (p21cip1), un inhibiteur de l'entrée du cycle cellulaire [198, 199].

(c) – D'autres investigations ont rapporté plusieurs fonctions de USP16 au sein du cytoplasme. Tout d'abord, les travaux menés par Zhang et son équipe ont suggéré que USP16 régule l'activation des lymphocytes T à travers la déubiquitination de la calcineurine sur la lysine K327 dans le cytoplasme [200]. La calcineurine est une phosphatase constitutivement polyubiquitinée sur sa lysine K327. Elle constitue un médiateur important dans la transmission du signal dépendant du calcium à une grande variété de réponses cellulaires [201]. En réponse à une stimulation intracellulaire qui augmente les niveaux de calcium intracellulaire, USP16 pourrait rapidement déubiquitiner la calcineurine. Cette déubiquitination va permettre l'activation de la calcineurine, qui, à son tour, va induire la déphosphorylation et la translocation nucléaire des membres de la famille du facteur nucléaire des cellules T activées (NFAT), impliqués dans l'expression de nombreux gènes et dans la prolifération cellulaire [200, 202].

(d) – Par la suite, d'autres travaux menés par Montellese et son équipe ont révélé que USP16 pourrait jouer un rôle dans le mécanisme de maturation des ribosomes [203]. Le

ribosome mature est un complexe moléculaire constitué de deux sous-unités (40S et 60S). Leur assemblage débute par des particules pré-ribosomiques qui subissent un processus de maturation du noyau vers le cytoplasme où les particules ribosomiques matures sont libérées [204, 205]. Pour permettre cette biogenèse du ribosome, l'étude de Montellesse et al. a suggéré que USP16 pourrait être associée à la sous-unité pré-40S du ribosome au niveau du cytoplasme [203]. Cette interaction va conduire à la déubiquitination de la protéine ribosomale RPS27a sur sa lysine interne K113 [203] (**Figure 1-6**). Cependant, le mécanisme sous-jacent reste peu défini.

Bien que le rôle de USP16 dans la régulation de H2AK119ub soit déjà rapporté, cette diversité dans sa fonction et dans sa localisation subcellulaire suggère un mécanisme de régulation complexe. Nos travaux actuels abordent plus en détail les mécanismes de régulation de USP16 importants pour exercer ses fonctions (voir le chapitre 2 de cette thèse).

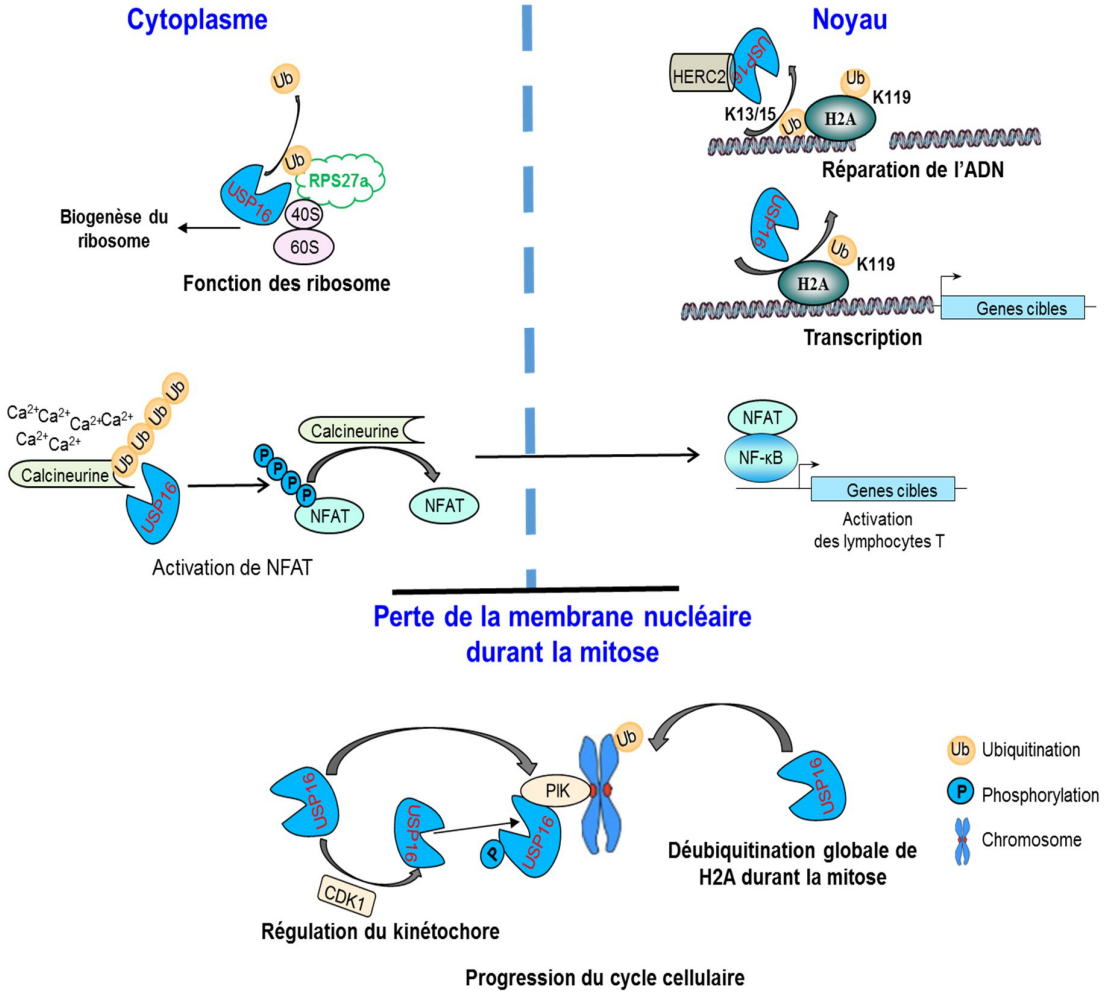

Figure 1-6 : Différentes voies de signalisation impliquant la déubiquitinase USP16.

Représentation schématique des voies de signalisation montrant le rôle de USP16 dans la progression du cycle cellulaire, la transcription, la réponse aux dommages à l'ADN, la biogenèse des ribosomes et l'activation des lymphocytes T. Voir texte pour plus de détails.

1.2.2.3 Implication clinique de USP16

Au cours de la dernière décennie, plusieurs recherches ont rapporté l'implication de USP16 dans de nombreuses maladies. Tout d'abord, en 2008, Dr Chaffanet et son équipe ont identifié une mutation du gène USP16 codant pour des fusions anormales de protéines chez des patients atteints de leucémie myélomonocytaire chronique (CMML) [150]. Dans cette étude, les auteurs montrent que suite à des anomalies d'épissage de la protéine USP16, suivi d'une délétion d'un des domaines fonctionnels du facteur de transcription RUNX1, il se crée un réarrangement chromosomique conduisant à une protéine de fusion USP16-RUNX1. Il est intéressant de noter que bien que l'implication de RUNX1 dans les cancers et plus spécifiquement dans les leucémies a bien été établie [206-208], le rôle de USP16 dans cette maladie reste à clarifier.

D'autre part, plusieurs études publiées récemment ont révélé l'implication de USP16 dans le syndrome de Down [151, 209, 210]. En effet, la plupart des personnes atteintes du syndrome de Down ont trois copies du chromosome 21. Le gène USP16 situé sur le chromosome 21 est donc présent en trois copies chez ces patients. En tant que régulateur épigénétique via la déubiquitination de H2AK119ub, la triplication du gène USP16 pourrait accélérer la vitesse à laquelle les cellules souches sont utilisées au début du développement. Ce qui aurait pour conséquence, une diminution du renouvellement des cellules souches hématopoïétiques, des progéniteurs neuronaux ou encore des fibroblastes et une augmentation de la différenciation des cellules [199, 209]. Cette dérégulation du comportement cellulaire pourrait conduire à des troubles neurodégénératifs chez des personnes trisomiques.

De manière intéressante, les études effectuées par Qian et al. ont attribué à USP16 la fonction de suppresseur de tumeur [211]. Ces auteurs ont dévoilé par des données cliniques que le taux de protéine USP16 est diminué dans les cellules cancéreuses du foie par rapport au taux dans les cellules normales. Aussi, la suppression de USP16 promeut la diminution du suppresseur de tumeur p21 et augmente l'expression des protéines antiapoptotiques Bcl-XL/Bcl-2 dans les cellules tumorales du foie [211]. Toutefois, le lien direct entre USP16 et le

contrôle transcriptionnel de gènes qui régulent la croissance et la prolifération cellulaire n'a pas été clairement établi.

Collectivement, ces données suggèrent que USP16 serait un élément clé de plusieurs processus biologiques et pourrait être un facteur déterminant dans l'apparition des maladies.

1.3 La séparation de phase liquide-liquide (LLPS)

1.3.1 Définition de la LLPS

La LLPS est un mécanisme moléculaire au cours duquel des protéines qui existent à l'état non agrégé ou soluble dans la cellule s'accumulent en un endroit précis, sous forme de corps dépourvus de membranes et forment une structure active dans le but de promouvoir ou d'inhiber un processus [212]. Cet assemblage résulte d'une concentration rapide de plusieurs molécules de protéines qui interagissent les unes avec les autres via des interactions intermoléculaires. Ainsi, la LLPS pourrait permettre une séquestration des protéines en un compartiment distinct. [213] (**Figure 1-7**).

Selon la littérature, il existe plusieurs appellations différentes de ces compartiments formés suite à la LLPS. Ils sont souvent appelés des granules, des condensats, des foci, des corps, des complexes ou des assemblages [214]. De plus, étant donné la plénitude de complexes protéiques que l'on peut trouver dans la cellule, différents critères de consensus ont été établis dans le but de définir qu'un compartiment cellulaire se forme via le LLPS [214-216]. Ces compartiments devraient :

- Maintenir une forme sphérique
- Être dépourvus de membrane
- Fusionner après un contact
- Contenir des molécules mobiles qui peuvent subir un réarrangement
- Avoir une taille de bonne dimension
- Avoir une taille dépendante de la concentration en protéine

Les résultats de plusieurs études ont montré que l'assemblage des protéines via la LLPS est médié par des domaines protéiques contenant des séquences désordonnées de faible complexité. C'est le cas par exemple de la protéine TDP-43 qui subit une LLPS médiée par sa région hélicoïdale unique contenant des séquences de faible complexité [217]. Cette protéine

peut se séparer de façon réversible et peut présenter des propriétés de séparation de phase en formant des gouttelettes dans les cellules [217]. La manipulation de cette séquence entraîne une perturbation de la croissance des gouttelettes. Néanmoins, la composition et l'organisation de ces domaines à faible complexité restent peu connues. Aussi, les recherches sur les interactions qui favorisent la formation de compartiments sans membranes contenant différentes protéines ont montré que les liaisons entre les macromolécules au sein des différentes phases liquides sont basées sur des forces faibles telles que les interactions électrostatiques, hydrophobes ou les ponts d'hydrogènes [218, 219]. D'autres études indiquent que la LLPS peut être facilitée par des interactions impliquant différents domaines liant des protéines ou des polymères d'acide nucléique [220].

Les agrégations de macromolécules qui résultent de la LLPS peuvent être dynamiques, réversibles et modulées en fonction de différents stimuli [221, 222]. Parmi les différentes structures formées par la LLPS on y retrouve :

- Les corps de cajal, « Cajal Bodies » : Site de biogenèse et la maturation des snRNPs (small nuclear RiboNucleoProtein) du spliceosome [223].
- Les corps PML, « ProMyelocytic Leukaemia bodies » : Structures nucléaires intercalées entre la chromatine. Ils sont impliqués dans la régulation de diverses fonctions cellulaires [223, 224].
- Les granules de stress : Agrégations cytoplasmiques contenant des protéines et des ARNm qui s'assemblent en réponse à l'exposition à un stress [225].
- Les granules P : Agrégation d'ARN et de protéines associés au métabolisme de l'ARN [226].
- Les nucléoles : Sites de biogenèse des ribosomes à l'intérieur du noyau [227].
- Les corps P, « P-Bodies » : Lieu de stockage d'ARNm non traduits [228]
- Les foci de dommage à l'ADN : Structures formées à la suite de la relocalisation des protéines impliquées dans le système de réponse aux dommages de l'ADN [229, 230]
- Speckles : Compartiment de stockage/assemblage/modification/recyclage des facteurs d'épissage afin d'approvisionner les sites de transcription [231].

De nos jours, des progrès importants ont été réalisés dans la caractérisation du comportement de ces agrégations et la séparation de phase est apparue comme un mécanisme important gouvernant de nombreux processus cellulaires. Cependant, le mode de régulation et le rôle de ces compartiments restent mal compris.

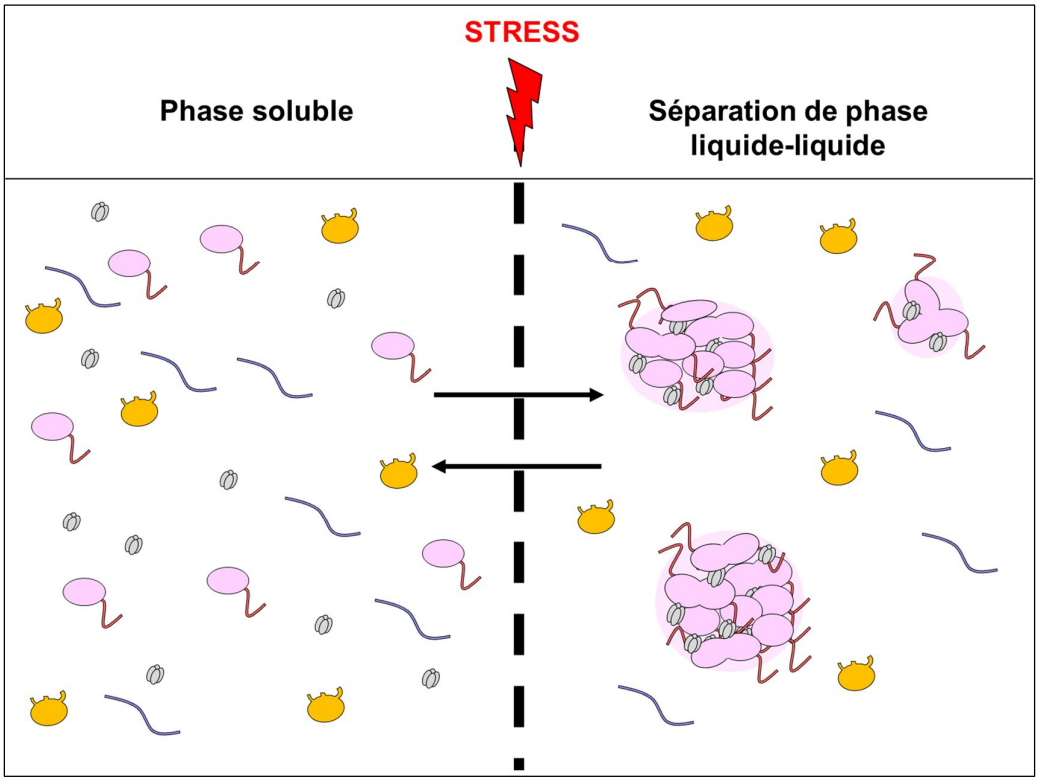

Figure 1-7 : Représentation schématique de la séparation de phase liquide-liquide.

Suite à divers stress, les protéines contenant des domaines de faible complexité qui se trouvaient à l'état soluble dans la cellule subissent une LLPS et fusionnent librement via des interactions intermoléculaires transitoires permettant la formation d'une structure dynamique.

1.3.2 Dérèglement de la LLPS dans l'apparition des maladies

La LLPS définit des compartiments distincts pour organiser efficacement les processus cellulaires. Cependant, quel pourront être les conséquences d'une perturbation dans la LLPS et des structures formées ? Des travaux récents ont décrit comment les organites sans membranes se forment via la LLPS. Par exemple, le groupe de Patel et al., a révélé que la protéine de liaison à l'ARN FUS (Fused in Sarcoma), impliquée dans la transcription, la biogenèse de l'ARN et dans la réparation des dommages à l'ADN, subit une LLPS suite à des stress [232]. En effet, suite à des cassures double brin de l'ADN, FUS subit une LLPS et est recrutée au site du dommage pour participer à la réparation de la lésion [233]. Cependant, des expériences de cryo-microscopie électronique ont dévoilé que suite à des mutations survenues sur la protéine FUS, les gouttelettes liquides de FUS passent à un état solide, agrégé et plus stable avec le temps [232]. Par conséquent, ces auteurs suggèrent que les altérations dans la séparation de phase de

la protéine FUS peuvent être au cœur des maladies liées à l'âge telles que la sclérose latérale amyotrophique (ALS) [232, 233].

D'autres études ont montré qu'à la suite de stress cellulaires, les protéines TDP-43 et FUS subissent une LLPS et co-localisent avec les marqueurs de granule de stress classiques. [234, 235]. Toutefois, en réponse à un stress oxydatif, les mutations de TDP-43 et de FUS causant des maladies sont significativement enrichies dans les granules de stress par rapport aux formes sauvages des protéines [234, 235]. Ces différentes variations peuvent être pertinentes pour l'homéostasie des motoneurones altérés dans la ALS.

L'étude de ces structures sans membranes ainsi que la compréhension de leur formation serait primordiale pour empêcher le développement de pathologies liées à la LLPS.

1.3.3 Rôle de l'ubiquitination dans la LLPS au cours de la réponse aux dommages à l'ADN

1.3.3.1 Les dommages à l'ADN

Notre ADN est susceptible de subir différents dommages au cours de la vie de la cellule. Ces altérations de l'ADN peuvent se produire de façon spontanée ou être induites par différents stress ou agents génotoxiques. Pour maintenir l'intégrité du génome, les cellules utilisent un réseau complexe de cascades de signalisations qui constituent la réponse aux dommages à l'ADN (**Figure 1-8**). Parmi les agents capables d'endommager l'ADN, on peut citer :

(a) Certains produits issus du métabolisme cellulaire comme les espèces réactives de l'oxygène (ROS), qui oxydent les bases et induisent des cassures simple brin (SSB) de l'ADN [236, 237].

(b) Les mésappariements de bases issus d'erreurs lors de la réplication de l'ADN, causant des insertions, des délétions et des décalages de base [238].

(c) Les stress induits par des radiations ultraviolettes (UV) qui provoquent la distorsion de l'hélice d'ADN [239].

(d) Les radiations ionisantes (IR) pouvant causer des cassures simple brin ou double brin de l'ADN [240].

(e) Les agents chimiothérapeutiques tels que le cisplatin et la mitomycine C qui génèrent des pontages intercaténaires empêchant la séparation des brins d'ADN [241].

(f) Le méthyle méthanesulfonate qui permet l'alkylation de l'ADN, formant des adduits sur les atomes N et O [242].

Pour contrer ces menaces, les cellules ont développé un système de surveillance complexe capable de détecter et corriger les lésions de l'ADN. Les mécanismes moléculaires mis en place pour réparer l'ADN dépendent du type de dommage (**Figure 1-8**). On peut citer :

- La réparation par excision de base (BER, « Base Excision Repair ») : Cette voie de réparation est applicable à plusieurs types de dommages, y compris les cassures simple brin (SSB), les sites abasiques, les lésions de base d'alkylation et les lésions de base oxydantes. Cette voie de réparation est initiée par une glycosylase qui va reconnaître et vexciser les lésions ou les bases incorrectes. L'excision de la lésion de base va laisser un site apurinique/apyrimidinique (AP). Le site AP est ensuite clivé par l'endonucléase APE1 afin de générer une extrémité 3'hydroxyle et une extrémité 5'deoxyribosephosphate. Par la suite, la poly-(ADP-ribose) polymérase-1 (PARP1) est recrutée pour protéger les extrémités du brin et coordonner le recrutement des enzymes de réparation (XRCC1, ADN polymérase β et la ligase 3) au site du dommage. En effet, les résidus manquants sont re-synthétisés par l'ADN polymérase β et le complexe Ligase3/XRCC1 va sceller définitivement la cassure [243].
- La réparation par excision de nucléotide (NER, « Nucléotide Excision Repair ») : C'est la voie principalement utilisée pour réparer les dommages à l'ADN induits par les UV ou par des agents chimiques tels que le cisplatin. Ces agents de dommages induisent des lésions provoquant la distorsion de la double hélice d'ADN. Il existe deux voies de NER, la GG-NER (global génome NER) qui agit sur la totalité du génome, et la TC-NER (transcription coupled NER) qui répare les lésions présentes dans les régions transcriptionnellement actives. La première étape de la réparation consiste en la reconnaissance de la lésion. En effet, la distorsion de l'ADN est reconnue par le complexe XPC/Rad23B/Centrin2 (GG-NER) ou par l'arrêt de l'ARN polymérase II en cours d'élongation (TC-NER). Une fois la lésion reconnue, une panoplie de facteurs protéiques (TFIIH, XPB, XPD) sont recrutés pour permettre l'ouverture de l'ADN endommagée. Une fois l'ADN ouvert, les protéines XPA, RPA, XPG et XPF/ERCC1 vont déclencher l'excision du fragment endommagé. La partie excisée va ensuite être synthétisée par les ADN polymérases δ, suivi d'une ligation par le complexe Ligase3/XRCC1 [243].

- La réparation des mésappariements de base (MMR, « Mismatch Repair ») : Cette voie de réparation est impliquée dans les mutations de bases (insertions, délétions) et dans les mésappariements des bases générés au cours de la réplication et de la recombinaison de l'ADN. La MMR débute par une reconnaissance des mésappariements ou de mutations médiées par les hétérodimères MSH2-MSH6 (MutSα) ou MSH2-MSH3 (MutSβ). Ces complexes s'associent aux hétérodimères MutL (MLH1-PMS2, MLHL1-PMS1 et MLH1-MLH3) qui sont essentiels à la réparation [244]. Ce dernier dimère permet le recrutement de l'endonucléase (EXO1), impliquée dans la dégradation de l'ADN mésapparié. Enfin, les protéines de la réplication sont recrutées pour synthétiser l'ADN manquant, qui sera par la suite scellé par la ligase1 [243].
- Les mécanismes de réparation de l'ADN suites aux cassures double brin seront traités en détail dans la section suivante, car directement pertinent au sujet de cette thèse.

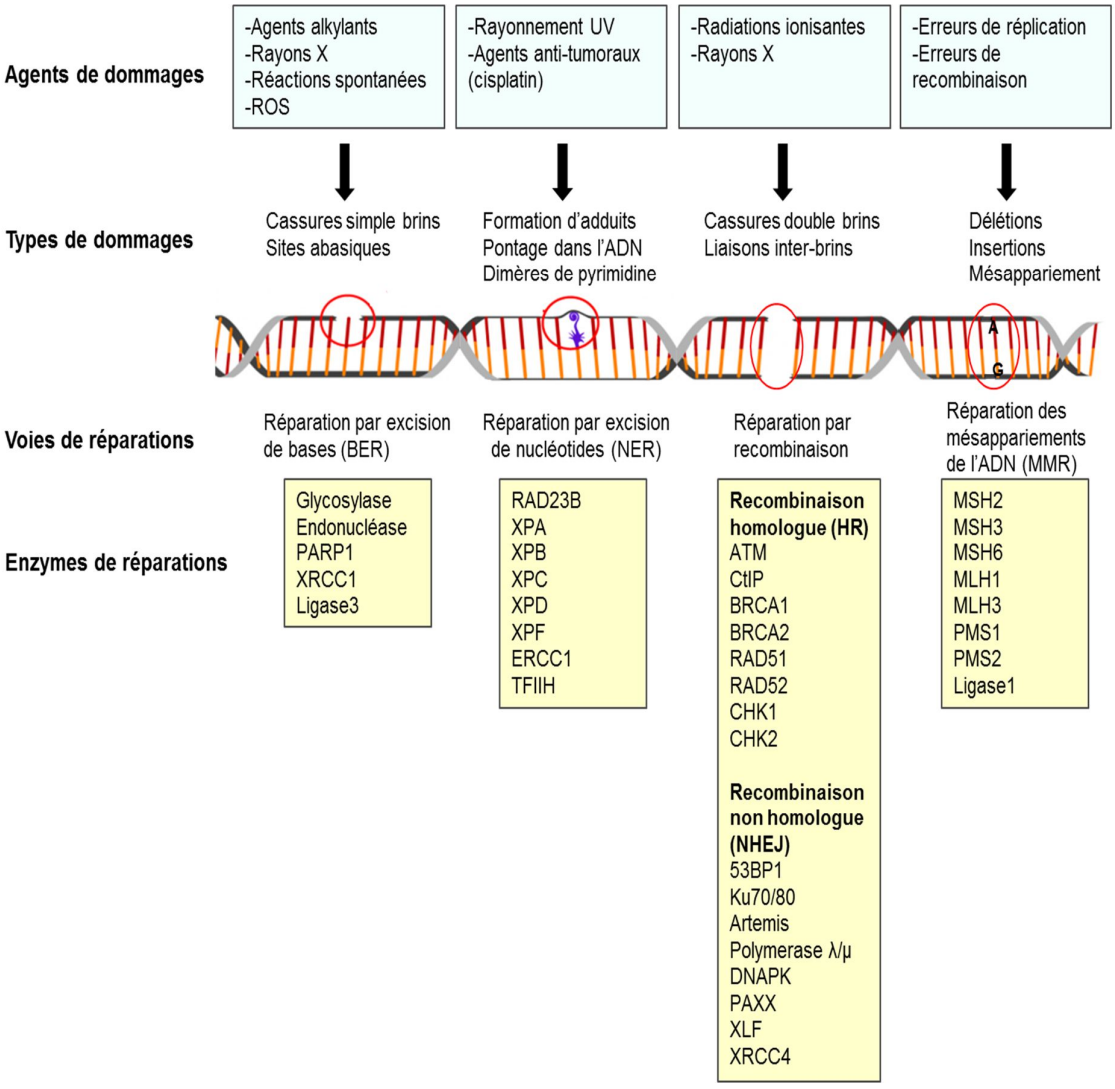

Figure 1-8 : Schéma récapitulant les causes de dommages à l'ADN et leurs voies de réparation.

Suite à un dommage survenu au niveau de l'ADN, différentes voies de réparation peuvent être activées selon le type de dommage. Quatre voies de réparation ont été citées : la réparation par excision de base (BER), la réparation par excision de nucléotide (NER), la réparation des mésappariements de base (MMR), et la réparation par recombinaison homologue (HR), ou par recombinaison des extrémités non homologue (NHEJ). Suite à la détection du dommage, diverses protéines spécifiques sont recrutées au niveau du site de dommage pour effectuer la réparation de l'ADN.

1.3.3.2 Réponse à la suite des cassures double brin (DSB)

Les cassures d'ADN double brin de l'ADN sont réparées par différents mécanismes, y compris la recombinaison homologue (HR, « Homologous Recombinaison ») et la jonction d'extrémités non-homologues (NHEJ, « Non Homologous End Joining »).

La HR s'effectue généralement au cours des phases S et G2 du cycle cellulaire, car elle utilise la séquence homologue de la chromatide sœur comme matrice afin de recopier l'information génétique pour effectuer la réparation. Ce mécanisme repose sur l'activité recombinase de la protéine RAD51 qui forme un filament de nucléoprotéine, capable d'envahir la chromatide sœur pour chercher de l'homologie de séquence [245, 246]. Cette voie de réparation est généralement lente et permet une réparation fidèle, sans perte de l'information génétique. Contrairement à la HR, la NHEJ se produit tout au long du cycle cellulaire et consiste en un rattachement direct des deux extrémités de la cassure. Dans le cas où les extrémités du bris sont non compatibles, il existe des exonucléases (Artemis) qui dégradent les extrémités afin d'établir la liaison entre les nucléotides. Les polymérases λ et μ peuvent également intervenir en ajoutant les acides nucléiques manquants pour permettre d'établir la liaison [247, 248]. Cette voie de réparation est connue pour être moins fiable et peut causer des insertions ou délétions au niveau du dommage [249, 250]. Toutefois, il a récemment été démontré qu'il existe des voies de réparations NHEJ alternatives qui servent de voie de secours dans les cellules déficientes en NHEJ [251-253].

Afin de réparer les lésions de l'ADN, plusieurs protéines peuvent s'assembler les unes avec les autres au niveau du site du dommage, où elles forment une structure cellulaire particulière appelée foci de dommage à l'ADN. Cependant, la structure et l'organisation de ces foci ne sont pas clairement établies. Des études récentes suggèrent que les foci de dommage à l'ADN ont des propriétés liquides et pourraient coexister au sein de la cellule en tant que compartiments sans membrane formés suite à une LLPS [229].

1.3.3.3 Mécanismes de signalisation menant à la LLPS à la suite des DSB

Les différentes voies de signalisation impliquées lors d'un DSB ont longtemps été caractérisées (**Figure 1-9**). Brièvement, lors d'une DSB, le complexe Mre11/Rad50/Nbs1 (MRN) se lie aux extrémités de la cassure pour initier l'assemblage d'un complexe macromoléculaire. Des données suggèrent que recrutement du complexe de réparation MRN requiert une région intrinsèque désordonnée [254, 255]. De plus, cette région est connue pour

sa capacité de s'agréger et à se séparer en phase de gouttelettes liquides (LLPS), ce qui génère des organites ou foci nucléaires sans membrane [256, 257].

En effet, le complexe MRN va déclencher le recrutement et l'activation de la kinase ATM. Celle-ci à son tour recrute et phosphoryle tous les membres du complexe MRN [258]. Cette étape est cruciale pour le processus de réponse aux dommages. Des expériences ont montré que la mutation des sites de phosphorylation de la protéine Mre11 bloque le processus de réparation [258]. Parallèlement, ATM catalyse la phosphorylation de l'histone variant H2AX sur la sérine 139 (γH2AX). Cette phosphorylation de H2AX peut aussi être médiée par les protéines kinases Ataxia Telangiectasia and Rad3-related (ATR) et DNA-dependent Protein Kinase (DNA-PK). En effet, DNA-PK est activée lors de la réparation NHEJ alors que l'activation de ATR se produit au niveau des dommages associés à la réplication de l'ADN [259]. Des études ont révélé que la protéine FUS qui est un substrat de ATM et de DNA-PK [260, 261], est capable de subir une LLPS *in vivo* et *in vitro* [262, 263]. Aussi, la déplétion de FUS conduit à une altération de la réparation DSB par HR et par NHEJ [264].

Ensuite, la protéine médiatrice MDC1 (Mediator Of DNA Damage Checkpoint 1) va lier γH2AX et assurer un recrutement supplémentaire de ATM entraînant une amplification du signal γH2AX qui peut se propager de 1 à 2 mégabases environ du site DNA et sert de plateforme pour recruter diverses protéines de réparation [35]. MDC1 activée va permettre la mise en place d'une cascade de signaux d'ubiquitination en recrutant les ubiquitines ligases RNF8 et RNF168 [35]. RNF8 interagit avec MDC1 via son domaine de liaison à phosphoserine FHA [35], puis s'assemble en complexe avec les protéines UBC13 et HERC2 pour induire la polyubiquitination K63 sur l'histone H1 [265]. C'est alors que RNF168 reconnaît la chaîne d'ubiquitine K63 conjuguée sur H1 et catalyse l'ubiquitination de l'histone H2A sur les lysines K13 et K15 (H2AK13/15ub) [35, 266]. Cette signalisation dépendante de l'ubiquitination médiée par RNF8-RNF168 va faciliter le recrutement des effecteurs 53BP1 (NHEJ) ou BRCA1 (HR) au niveau du DSB afin de réparer le dommage [259] (**Figure 1-9**). Des études récentes ont indiqué que 53BP1 subit une séparation de phase liquide-liquide induite par les dommages à l'ADN. En effet, les auteurs montrent que 53BP1 présente un comportement semblable à des gouttelettes liquides. Elle est capable de fusionner avec les structures de réparation de l'ADN et de s'auto-assembler de façon dynamique [230].

Les différentes protéines impliquées dans la réparation des dommages à l'ADN sont capables de former des foci visibles au microscope. Conformément aux données actuelles, la LLPS favoriserait le recrutement et l'interaction de ces protéines au niveau du site de dommage.

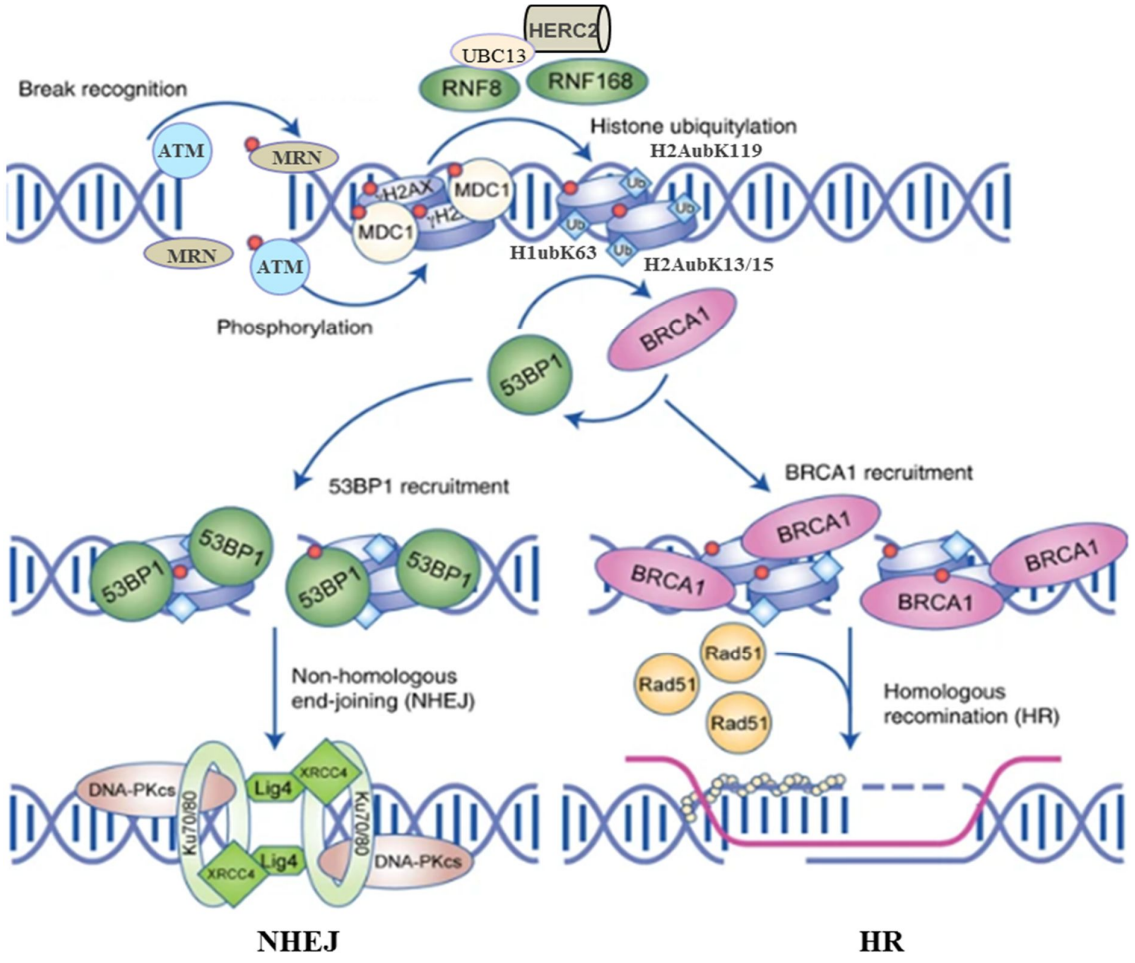

Figure 1-9 : Cascade de signalisations impliquées dans la réparation des DSB.

NHEJ, la jonction d'extrémités non-homologues. HR, recombinaison homologue. Voir le texte pour plus de détails. Modifiée de [267].

1.3.3.4 Rôle des DUBs dans la régulation de la LLPS suite aux DSB

Plusieurs études montrent que les foci de dommage induit par la LLPS peuvent être régulés par les DUBs. C'est le cas par exemple des DUBs de la famille de OTU, OTUB1 et OTUB2 qui abolissent l'apparition des foci 53BP1 au niveau du site du dommage. Tandis que OTUB1 s'oppose à l'action de l'ubiquitine ligase RNF168 de façon non dépendante de son activité catalytique en interagissant et en inhibant l'activité de l'enzyme de conjugaison UBC13 [268, 269], OTUB2 quant à lui utilise son activité catalytique pour empêcher le recrutement de RNF168 [270]. Par divers mécanisme, OTUB1 et OTUB2 vont altérer la LLPS importante pour la formation des foci 53BP1. Les déubiquitinases de la famille des USPs peuvent aussi réguler la LLPS. On peut citer comme exemple les DUBs USP3 et USP44 qui peuvent altérer le

recrutement de RNF168 [268, 271, 272]. Ou encore la protéase, USP34 qui stabilise la E3 ligase RNF168 en supprimant ses chaînes dégradantes d'ubiquitine, ce qui favorise la réaction d'ubiquitination lors des bris double brin de l'ADN [273].

Plusieurs travaux sont apparus au cours des dernières années, impliquant le complexe polycomb comme un compartiment capable de subir une LLPS. Robert Kingston et son équipe ont dévoilé par des expériences *in vitro* que la sous-unité CBX2 du complexe PRC1 provoque la séparation de phase en gouttelette de PRC1 [274]. Par ailleurs, l'étude de Tatavosian et al. révèle que le complexe CBX2-PRC1 possède des propriétés de type liquide et s'assemble sous forme de condensat dans le noyau. Leurs analyses suggèrent que le complexe polycomb s'assemble par LLPS pour réorganiser la chromatine [190]. Étant donné que le complexe PRC1 stimule la compaction et la répression de la chromatine via la catalyse de H2AK119ub [51, 52], il est possible que les DUBs agissent en tant que modulateur du mécanisme de la LLPS en régulant le signal induit par PRC1.

1.3.3.5 Implication de USP16 dans la régulation de la LLPS suite aux DSB

Récemment, un concept selon lequel la formation de l'hétérochromatine est induite par la LLPS a émergé [190, 275]. Par ailleurs, Shakya et son équipe ont proposé que l'histone H2A forme des gouttelettes en présence de l'ADN et les nucléosomes *in vitro* [276]. Ces données soulèvent de nouvelles questions sur le lien entre l'organisation de la chromatine médiée par la LLPS suite à des DSB et la régulation de H2AK119ub catalysée par les DUBs.

Diverses analyses soulignent l'importance de USP16 dans la régulation de l'ubiquitination de H2A lors d'un dommage à l'ADN. En effet, des études suggèrent que USP16 jouerait un rôle actif dans la régulation de la chromatine aux sites des dommages à l'ADN en réponse aux stress génotoxiques [187]. Aussi, des analyses récentes ont spécifié que USP16 reverse l'inhibition de la transcription médiée par ATM sur les sites de cassures double brin de l'ADN, très probablement via sa capacité à déubiquitiner H2A [277]. Par la suite, Zhang et son équipe ont rapporté que USP16 pourrait interagir avec l'ubiquitine ligase HERC2 dont le rôle est bien connu dans la DDR [278, 279]. En effet, HERC2 forme un complexe avec les E3 ligases RNF8 et RNF168 responsables de H2AK13/15ub [278, 280]. Cette ubiquitination médiée par RNF8-RNF168 va faciliter la LLPS de 53BP1 et permettre son recrutement au niveau de la lésion [230, 259]. En cas de dommage, la liaison de USP16-HERC2 permettrait l'augmentation rapide des niveaux protéiques de USP16. Cette surexpression de USP16 régulerait négativement H2AK119ub, H2AK13/15ub et les foci d'ubiquitine induits par les

dommages à l'ADN. Ce processus serait nécessaire pour la terminaison du signal d'ubiquitine [279] (**Figure 1-9**).

Suite à toutes ces recherches, USP16 apparaît comme un régulateur clé de la réponse aux dommages à l'ADN. Il est possible que USP16 module LLPS via la perturbation des protéines impliquées dans cette séparation. Cependant, les mécanismes moléculaires par lesquels USP16 impacte la réparation des DSB ne sont pas bien caractérisés et en particulier comment USP16 est acheminée dans le noyau pour réguler la LLPS et la réponse dommages a l'ADN. Les travaux présentés dans le chapitre 2 de ce manuscrit porteront sur la caractérisation moléculaire et fonctionnelle de USP16 et son rôle dans la régulation des LLPS lors d'un dommage induit par IR.

1.3.4 Rôle de l'UPS dans la LLPS suite à des stress

Au cours des dernières années, de nouveaux corps cellulaires formés suite à une LLPS ont été découverts. Les données actuelles montrent qu'ils sont nombreux, de tailles et de morphologies différentes, possèdent différentes fonctions spécifiques et sont assemblés à la suite de diverses contraintes de la cellule. On peut ainsi citer :

– Les corps nucléaires SAM68 formés suite à des trafics d'ARN messagers dans le noyau [281].

– Les granules de périchromatine formées suite à un choc thermique [282].

– Les corps isolants de la chromatine formés en réponse à un stress osmotique [283].

– Les corps nucléaires PML (Leucémie Promyélocytaire) associés à divers stress cellulaire comme la mort cellulaire par apoptose ou par sénescence [284, 285].

– Les granules de protéasome formées en réponse à un stress salin, un stress oxydatif ou une privation de carbone [286].

Le protéasome est une machine protéolytique majeure qui régule l'homéostasie de nombreuses protéines et est essentiel pour la survie de la cellule. Les données récentes ont montré que le protéasome serait capable de subir une LLPS afin de générer une structure dynamique appelée granule de protéasome [114].

Plusieurs travaux ont tenté de comprendre les principales caractéristiques de ces granules du protéasome, telles leurs fonctions, leurs localisations subcellulaires ou encore leurs compositions moléculaires. En effet des études ont révélé que chez la levure *S. Cerevisiae*, le protéasome 26S est déplacé du noyau vers le cytoplasme pendant la quiescence [287]. Le

protéasome cytoplasmique s'assemble en une structure appelée granule de stockage de protéasome, et ces structures sont rapidement dissipées lorsque les cellules reprennent la prolifération [287].

D'autres équipes ont rapporté que chez la levure *S. Cerevisiae* et chez la plante *Arabidopsis thaliana*, le protéasome s'accumule sous forme de granules dans le cytoplasme suite à une privation en carbone, ce qui le protège contre toute éventuelle dégradation par autophagie [114]. Il est donc clair que la formation de ces granules du protéasome est un facteur clé dans la réponse suite à un stress chez la levure. Il devient donc nécessaire et important de caractériser ces corps protéasomales dans les cellules humaines.

Le chapitre 3 de cette thèse sera consacré à l'identification des mécanismes sous-jacents à l'assemblage et au désassemblage des granules du protéasome formés suite à une LLPS dans le noyau de la cellule humaine.

1.4 Hypothèses et Objectifs

La séparation de phase liquide-liquide (LLPS) est un processus dynamique et rapide permettant la formation de structures distinctes dans la cellule. Ce mode de régulation unique a suscité beaucoup d'intérêt au cours de ces dernières années. Les avancées dans la compréhension de ce mécanisme de séparation de phase ont permis d'identifier des systèmes particuliers comme le système ubiquitine protéasome (UPS) et la chromatine, capables d'être régulés suite à des LLPS.

L'ubiquitination de l'histone H2A (H2AK119ub) est une modification post-traductionnelle impliquée dans la compaction de la chromatine nécessaire à la répression de la transcription des gènes, à la réparation des dommages à l'ADN et à la progression du cycle cellulaire. Afin de permettre le dynamisme de la chromatine, il a été proposé que la protéine USP16 est capable de déubiquitiner l'histone H2A et permettre la régulation de nombreux processus cellulaire.

Dans le chapitre 2 de cette thèse, nous nous intéressons particulièrement à la régulation de H2AK119ub médiée par la déubiquitinase USP16 au cours des dommages à l'ADN. En effet, H2AK119ub servirait de tremplin pour permettre la LLPS importante pour le recrutement des foci de réparation de la protéine 53BP1 au site du dommage. Ainsi, la déubiquitination de H2A catalysée par USP16 influencerait la LLPS, nécessaire à la réparation de l'ADN et au remodelage de la chromatine. Cependant, USP16 est une protéine cytoplasmique et son mécanisme moléculaire est mal connu. En nous basant sur les données de la littérature, nous

postulons l'hypothèse qu'un transport passif ou actif de USP16 serait nécessaire pour la déubiquitination de H2A et la régulation de la LLPS au cours de la réparation des dommages à l'ADN. Comme objectifs, nous allons :

- Investiguer la contribution de USP16 dans la déubiquitination de H2A durant les différentes phases du cycle cellulaire.
- Investiguer le mécanisme de transport de USP16.
- Caractériser la façon dont USP16 régule la LLPS à travers l'assemblage et le désassemblage des foci de réparation

Par la suite, dans le chapitre 3 de cette thèse, nous avons voulu investiguer l'implication de l'UPS lors de la LLPS. En effet, les études précédentes effectuées chez la levure ont mentionné que suite à divers stress métaboliques, le protéasome serait capable de subir une LLPS pour former des granules dans le cytoplasme. Ces granules semblent être nécessaires pour protéger le protéasome de la dégradation par autophagie et favorisent la viabilité des cellules.

Plusieurs stimuli externes ou stress métaboliques peuvent induire la déstabilisation des voies de signalisation de l'UPS ou de l'homéostasie du protéasome conduisant à diverses maladies telles que le cancer ou la dégénérescence neuronale. La biogenèse du protéasome et sa fonction dans le cytoplasme des cellules humaines sont bien connues. Cependant, son mécanisme de régulation suite à un stress induit par une privation de nutriments n'est toujours pas clair. En relation avec la littérature, nous émettons l'hypothèse que la privation de nutriments induit une relocalisation des composants du protéasome dans le noyau et/ou dans le cytoplasme sous forme de foci pour réguler la dégradation des protéines et/ou pour protéger le protéasome de sa dégradation par autophagie. Nous avons, en effet, découvert la présence de foci du protéasome dans le noyau suite à un stress métabolique. Comme objectifs de cette deuxième partie, nous allons :

- Caractériser la structure et la composition des foci de protéasome nucléaire
- Étudier les voies de signalisation responsables de la formation de ces foci
- Comprendre la fonction précise de ces foci dans la régulation des processus cellulaires.

CHAPITRE 2

2 ARTICLE: A potent nuclear export mechanism imposes USP16 cytoplasmic localization during interphase

---

Article publié à Journal of Cell Science
J Cell Sci. 2020 Feb 24;133(4)

Nadine Sen Nkwe[1], Salima Daou[1,2], Maxime Uriarte[1], Jessica Gagnon[1,3], Nicholas Victor Iannantuono[1,3], Haithem Barbour[1], Helen Yu[1,4], Louis Masclef[1], Erlinda Fernández[1], Natalia Zamorano Cuervo[1,5], Nazar Mashtalir[1,6,7], Loïc Binan[1,8], Mikhail Sergeev[1], François Bélanger[1], Elliot Drobetsky[1,9], Eric Milot[1,9], Hugo Wurtele[1,9], Santiago Costantino[1,8] and El Bachir Affar[1,9,10]

[1]Maisonneuve-Rosemont Hospital Research Center, Montréal, QC H1T 2M4, Canada.
[2]Lunenfeld-Tanenbaum Research Institute, Sinai Health System, Toronto, ON M5G 1X5, Canada.
[3]Institute for Research in Immunology and Cancer, University of Montréal, Montréal, QC H3T 1J4, Canada.
[4]Developmental and Stem Cell Biology Program and Arthur and Sonia Labatt Brain Tumor Research Centre, Hospital for Sick Children, Toronto, ON M5G 0A4, Canada.
[5]CRCHUM-Centre Hospitalier de l'Université de Montréal, 900 rue Saint Denis, Montréal, QC H2X 0A9, Canada.
[6]Department of Pediatric Oncology, Dana-Farber Cancer Institute and Harvard Medical School, Boston, MA 02215, USA.
[7]Broad Institute of MIT and Harvard, Cambridge, MA 02142, USA.
[8]Department of Ophthalmology, University of Montréal, Montréal, Québec, Canada.
[9]Department of Medicine, University of Montréal, Montréal H3C 3J7, Québec, Canada.

[10]Correspondence: el.bachir.affar@umontreal.ca

Keywords: Deubiquitinase; Ubiquitin; USP16; UBP-M; H2AK119; Nuclear export; Cell proliferation; Mitosis; DNA double stand break repair.

Introduction de l'article

Le chapitre 2 de cette étude est relié à la première hypothèse de la thèse.

L'ubiquitination de l'histone H2A est une modification post-traductionnelle essentielle à la transcription, la réparation des dommages à l'ADN et la progression du cycle cellulaire. Des études suggèrent que les modifications de H2A pourraient être importantes pour la régulation de la séparation de phase liquide-liquide nécessaire à la réparation des cassures double brin et au remodelage de la chromatine. Il a été rapporté que la protéine USP16 est une déubiquitinase cytoplasmique capable de déubiquitiner l'histone H2A dans le noyau. Cependant, le mécanisme d'import-export effectué par USP16 pour exercer sa fonction reste méconnu.

Les résultats développés dans cet article indiquent que USP16 possède un signal d'export nucléaire qui permet son accumulation dans le cytoplasme. De manière intéressante, nous avons pu montrer que USP16 n'est pas retenue dans le noyau suite à des dommages à l'ADN induits par les radiations ionisantes. Par ailleurs, cette déubiquitinase est capable de diffuser passivement dans le noyau après la rupture de la membrane nucléaire lors de la mitose pour déubiquitiner l'histone H2A. Pris ensemble, nos données suggèrent que USP16 régulerait de façon indirecte la réparation des dommages à l'ADN.

Contribution

En tant que première auteure de cet article, ma contribution est de 75 %. J'ai participé à la conception, la préparation des protocoles et à la réalisation de la grande majorité des expériences. J'ai assemblé toutes les figures et j'ai rédigé le manuscrit avec la collaboration du Dr El Bachir Affar.

2.1 Abstract

USP16 (also known as UBP-M) has emerged as a histone H2AK119 deubiquitylase [192] implicated in the regulation of chromatin-associated processes and cell cycle progression. Despite this, available evidence suggests that this DUB is also present in the cytoplasm. How the nucleo-cytoplasmic transport of USP16, and hence its function, is regulated has remained elusive. Here, we show that USP16 is predominantly cytoplasmic in all cell cycle phases. We identified the nuclear export signal (NES) responsible for maintaining USP16 in the cytoplasm. We found that USP16 is only transiently retained in the nucleus following mitosis and then rapidly exported from this compartment. We also defined a non-canonical nuclear localization signal (NLS) sequence that plays a minimal role in directing USP16 into the nucleus. We further established that this DUB does not accumulate in the nucleus following DNA damage. Instead, only enforced nuclear localization of USP16 abolishes DNA double-strand break (DSB) repair, possibly due to unrestrained DUB activity. Thus, in contrast to the prevailing view, our data indicate that USP16 is actively excluded from the nucleus and that this DUB might indirectly regulate DSB repair.

2.2 Introduction

Ubiquitylation is a critical post-translational modification that regulates a myriad of signaling events and cellular processes (Gomez-Diaz and Ikeda, 2018; Grumati and Dikic, 2018; Hammond-Martel et al., 2012; Harper et al., 2018; Hu and Sun, 2016; Schwertman et al., 2016; Uckelmann and Sixma, 2017; Vucic et al., 2011; Werner et al., 2017; Wertz and Dixit, 2010). This modification is catalyzed by the concerted action of E3 ubiquitin ligases and E2 ubiquitin-conjugating enzymes, which play central roles in substrate recruitment, and in dictating the mode of ubiquitin molecule attachment, respectively (Yau and Rape, 2016; Zheng and Shabek, 2017). E3 (about 600 genes) and E2 (about 40 genes) enzyme pairs target a wide spectrum of cellular proteins, consistent with the pervasive role of the ubiquitin system in cell function and homeostasis (Clague et al., 2015). Indeed, deregulation of ubiquitin conjugation underlies numerous human pathologies, including cancer and neurodegenerative diseases (Heaton et al., 2016; Mendler et al., 2016; Popovic et al., 2014; Rubinsztein, 2006; Senft et al., 2018; Tanaka and Matsuda, 2014).

Deubiquitylation is responsible for the timely removal of ubiquitin from substrates, and as such can regulate protein function in a proteasome-dependent or -independent manner. A

large superfamily of more than 100 deubiquitylases (DUBs), which are either cysteine- or metallo-proteases, are primary determinants in mediating or terminating ubiquitin signaling processes (Clague et al., 2019; Eletr and Wilkinson, 2014; Nijman et al., 2005; Reyes-Turcu et al., 2009). DUBs are critical for diverse cellular processes, including cell cycle control, membrane signaling, transcription and DNA damage/repair processes (Bonacci et al., 2018; Daou et al., 2018; Hammond-Martel et al., 2012; Hu and Sun, 2016; Jackson and Durocher, 2013; Nishi et al., 2014; Perrody et al., 2016). Moreover, DUBs are regulated at the levels of multi-protein complex assembly, enzymatic activity and subcellular localization, although their mechanisms of action are not fully understood (Clague et al., 2019; Fraile et al., 2012; Komander et al., 2009; Mevissen and Komander, 2017; Sahtoe and Sixma, 2015).

USP16 (also known as UBP-M), a widely-expressed cysteine protease of the USP family, has been implicated in the control of chromatin-associated processes, cell proliferation and differentiation (Cai et al., 1999; Joo et al., 2007; Mimnaugh et al., 2001; Yang et al., 2014). Increased dosage of *USP16* (located on chromosome 21), as a consequence of gene triplication, has been shown to inhibit stem cell renewal and to promote cellular senescence, mechanisms that in turn might contribute to the pathogenesis of Down's syndrome (Adorno et al., 2013). The *USP16* gene locus is targeted by oncogenic translocations with the transcription factor RUNX1 during leukemia, suggesting that USP16 might play important roles in the hematopoietic system (Gelsi-Boyer et al., 2008). Indeed, while *Usp16* gene ablation causes embryonic lethality in mice, conditional inactivation in the bone marrow has demonstrated that this DUB is required for proper hematopoiesis and lineage commitment of hematopoietic stem cells (HSCs) (Gu et al., 2016; Yang et al., 2014). On the other hand, USP16 is not required for renewal of embryonic stem cells, but rather regulates their differentiation (Gu et al., 2016; Yang et al., 2014).

While the importance of USP16 in pathophysiology is becoming increasingly recognized, the relationship between its subcellular localization and function remains largely unclear. Initial observations have revealed that USP16 is primarily in the cytoplasm (Cai et al., 1999; Urbé et al., 2012). Interestingly, a catalytic dead mutant of USP16 was found to be nuclear, suggesting a potential role of enzymatic activity in coordinating the subcellular localization of this DUB (Cai et al., 1999), but the significance of this event remained unexplained. Importantly, the main roles attributed to USP16 are related to nuclear processes, such as transcription and DNA repair (Frangini et al., 2013; Joo et al., 2007; Shanbhag et al.,

2010; Yang et al., 2014; Zhang et al., 2014). It has been reported that USP16 deubiquitylates histone H2AK119 (hereafter H2Aub), a polycomb repressive complex 1 (PRC1)-catalyzed chromatin modification that regulates gene expression and DNA repair (Cai et al., 1999; Joo et al., 2007). Several studies have reported that USP16 depletion leads to deregulation of gene expression and that this DUB could be detected at gene regulatory regions (Gu et al., 2016; Joo et al., 2007; Yang et al., 2014). Other studies suggest that USP16 might directly regulate chromatin remodeling at sites of DNA damage (Shanbhag et al., 2010; Zhang et al., 2014). USP16 also appears to influence mitosis, as its knockdown induces G2/M delay and decreases cell proliferation (Joo et al., 2007). In addition, it has been proposed that deubiquitylation of histone H2Aub by USP16 is prerequisite for histone H3S10 phosphorylation, a chromatin modification mark associated with mitosis (Joo et al., 2007). More recently, USP16 has been shown to regulate the stability of PLK1 at kinetochores by promoting kinetochore–microtubule attachments and proper chromosome alignment (Zhuo et al., 2015).

Despite the above studies reporting that USP16 exerts important functions in DNA-associated processes, it remained largely unclear (1) how the potential import of USP16 into the nucleus regulates such processes and (2) whether the observed changes on DNA repair and gene expression are direct effects of USP16 recruitment to chromatin or an indirect consequence of its depletion or overexpression. Moreover, the molecular determinants that might regulate USP16 nuclear import or export have not been identified. For instance, systematic identification of nuclear export signals (NES) in DUBs, using multiple prediction tools, failed to reveal such motifs in USP16 (Garcia-Santisteban et al., 2012). However, preliminary results of domain mapping suggested that USP16 contains potential NLS and NES sequences (Xu et al., 2013), but the identity of genuine and transferable nuclear import and export signals in this DUB has remained elusive.

In this study, we rigorously established the subcellular localization of USP16 during cell cycle progression and identified the molecular determinants that coordinate USP16 nucleo-cytoplasmic trafficking. Our data challenge the current conclusions on USP16 function and support a model whereby cytoplasmic USP16 might indirectly regulate chromatin function in the absence of active translocation into the nucleus.

2.3 Results

- **USP16 is predominantly cytoplasmic during interphase.**

To determine the relationship between USP16 localization and function, we first generated an anti-USP16 antibody and used RNAi to validate the specific detection of endogenous USP16 by immunoblotting (**Figure 2-S1A**). Next, we conducted a hypotonic lysis-based subcellular fractionation of HEK293T and U2OS cells, and then purified nuclei through a sucrose cushion. Immunodetection of poly(ADP-ribose) polymerase 1 (PARP-1) and lactate dehydrogenase (LDH), nuclear and cytoplasmic enzymes, respectively, was conducted to control for cross-contamination of fractions. We observed that while LDH was almost completely absent from the nuclear fraction, a minor pool of USP16 remained associated with nuclei (**Figure 2-1A**). We reasoned that either a pool of USP16 could be associated with cellular membranes and organelles that co-fractionate with the nucleus or a small fraction of USP16 might be localized inside the nucleus. To distinguish between these possibilities, we conducted immunostaining of USP16 on asynchronous cell populations. With several commercial anti-USP16 antibodies as well as one made in-house, we did not detect a specific endogenous USP16 signal in the nucleus, as the fluorescence signal in this compartment remained unchanged following USP16 depletion by siRNA (**Figure 2-S1B,C**). However, the cytoplasmic signal, detected with two commercial antibodies, significantly decreased following USP16 depletion, indicating the presence of this DUB in the cytoplasm (**Figure 2-S1B,C**). We then expressed Myc-tagged USP16 in U2OS cells through lentiviral transduction and conducted confocal microscopy, which revealed that this DUB is localized in the cytoplasm (**Figure 2-1B**). Relative quantification indicated that the immunofluorescence signal detected in the nucleus is indistinguishable from the background (**Figure 2-1B**). To exclude potential cell fixation artifacts, we expressed a GFP–USP16 fusion construct and monitored its subcellular localization on live cells. GFP signal quantification confirmed that GFP–USP16 is cytoplasmic with nearly undetectable levels inside the nucleus of transfected cells (**Figure 2-1C**). We also did not detect USP16 in the nucleus using 3D image deconvolution (**Figure 2-S1D**). The cytoplasmic localization of USP16 is not affected by the levels of DUB expression (**Figure 2-S1E**). USP16 is also cytoplasmic in IMR90 fibroblasts transduced with GFP–USP16 (**Figure 2-S1F**). Interestingly, we occasionally observed cells with a nucleocytoplasmic staining of GFP-USP16, generally in pairs of adjacent cells (**Figure 2-1D**). These cells have strongly reduced

H2Aub signal, consistent with the ability of USP16 to deubiquitylate this histone, and are extremely rare (representing less than 1% of counted cells).

Since USP16 has been associated with cell cycle progression (Joo et al., 2007), we sought to determine whether USP16 enters the nucleus at a specific cell cycle phase. U2OS cells transfected with a Myc–USP16 expression construct were synchronized at various cell cycle phases (**Figure 2-1E**) (Hammond-Martel et al., 2010; Vassilev et al., 2006). Flow cytometry analysis indicated that indeed cells were synchronized in the expected cell cycle phases (**Figure 2-1F, bottom panels**). Immunofluorescence staining showed that USP16 remains cytoplasmic in the G1, G1/S, S and G2 phases (**Figure 2-1F, top panels**). No noticeable changes in the levels of histone H2Aub were observed in the majority of USP16-transfected cells. Mitotic cells within the G2/M population (indicated by arrows) are typically round with condensed chromosomes and have low H2Aub levels. The staining of USP16 is diffuse in M phase cells, as their nuclear membranes are presumably disassembled. Interestingly, we found that the occasional presence of USP16 in both the cytoplasm and the nucleus of two adjacent cells is mostly associated with the G1 cell population (**Figure 2-1G**). The detection of a cytoplasmic bridge, which is indicative of incomplete cytokinesis, could be occasionally detected in the two daughter cells, suggesting that these cells are in early G1. These cells have reduced H2Aub levels and their number never exceeds 1–3% of the G1 cell population. These results together show that USP16 is cytoplasmic in all cell cycle phases, but exhibits nuclear accumulation in a very small proportion of G1 cells.

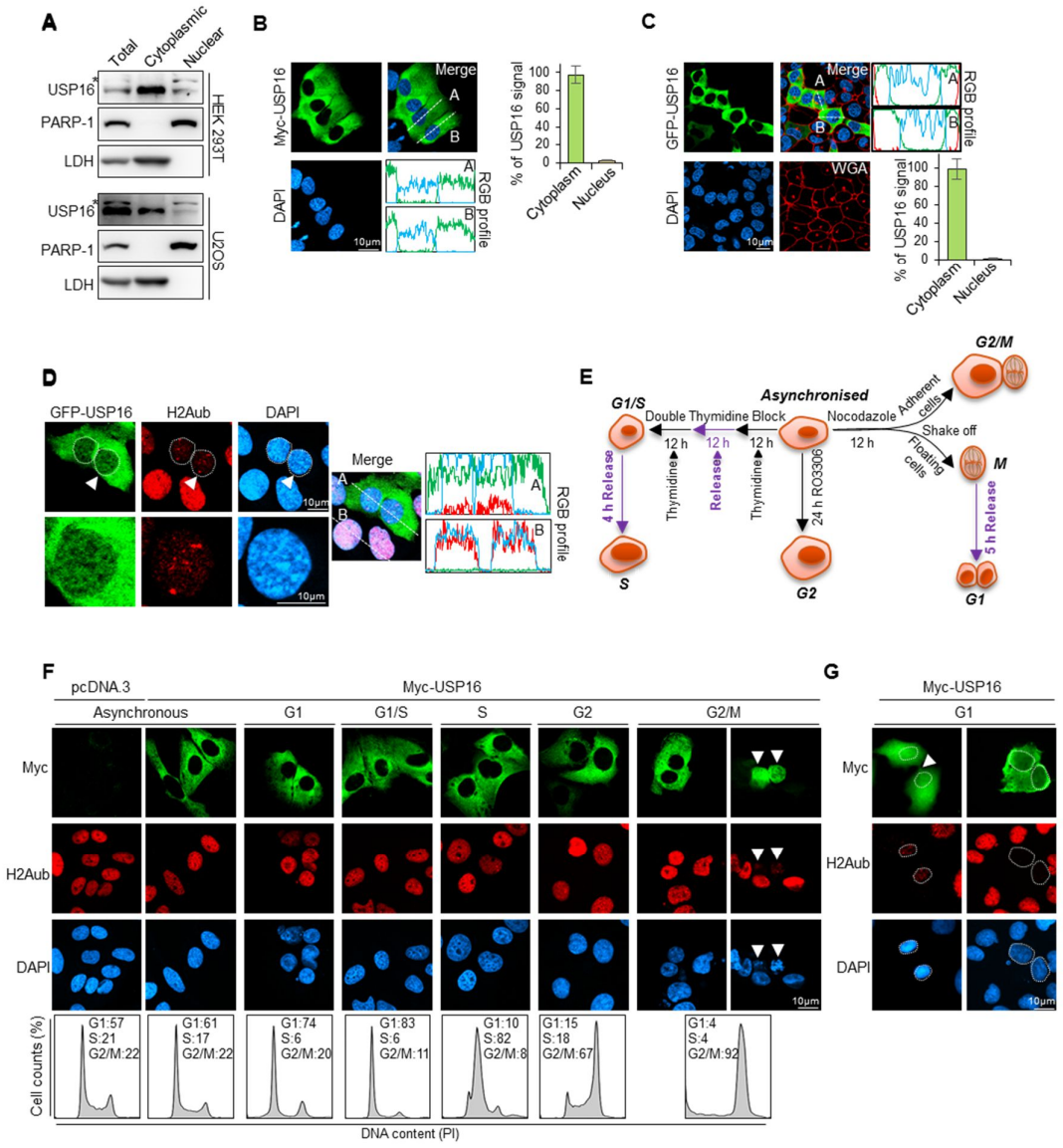

Figure 2-1 : USP16 is predominantly cytoplasmic during interphase.

(A) Subcellular fractionation and analysis of USP16 protein levels. Nuclear and cytoplasmic fractions were analyzed by immunoblotting. The asterisk indicates an upper band, occasionally observed, that might correspond to a non-specific protein or a modified form of USP16. LDH and PARP-1 were used as controls for the cytoplasmic and nuclear fractions, respectively. Representative of *n*=4 biological replicates. (B) Determination of USP16 localization by immunostaining. U2OS cells stably expressing Myc–USP16 were used for paraformaldehyde fixation and immunofluorescence. RGB profiles for the indicated linescans for anti-Myc or DAPI staining were generated using ImageJ, and relative quantification of USP16 protein signal in the nucleus versus cytoplasm was conducted. Data are presented as the mean±s.d. percentage

of USP16 signal in each compartment versus total signal and corresponds to an average quantification on 10 cells; *n*=5 biological replicates. (C) Determination of USP16 localization in live cells. U2OS cells stably expressing GFP–USP16 were used for the direct detection of GFP fluorescence. Alexa Fluor™ 594-conjugated wheat germ agglutinin (WGA) was used to stain plasma membrane. Relative quantification of USP16 protein was conducted as shown in B; *n*=3 biological replicates. (D) U2OS cells stably expressing GFP–USP16 were used for immunofluorescence analysis. The occasional presence of USP16 in nuclei is often observed in two adjacent cells. The nucleus highlighted with the arrowhead is shown magnified in the lower row. Relative intensity of USP16, H2Aub and DAPI signals was assessed; *n*=3 biological replicates. (E) Schematic representation of the procedures used to synchronize cells at different cell cycle phases. (F) U2OS cells were transfected with pcDNA.3 or GFP–USP16 constructs and following cell cycle synchronization (as indicated in E), subcellular localization of USP16 was determined. The cell cycle profile of each cell population was analyzed by propidium iodide staining and FACS (bottom panels). *n*=3 biological replicates. Arrowheads highlight cells with nuclear USP16. (G) The presence of USP16 in the nuclei of two adjacent cells is observed in G1 (1–3% of the total cell population). Two representative images are shown. The arrowhead indicates a cytoplasmic bridge between two daughter cells. Nuclei are encircled to indicate cells with nuclear USP16 and reduced levels of histone H2Aub. *n*=3 biological replicates.

- **USP16 is rapidly exported to the cytoplasm by the CRM1 system following M phase completion.**

It was previously observed that treatment of cells with leptomycin B (LMB), an inhibitor of CRM1 (also known as exportin 1)-mediated protein export, resulted in the accumulation of USP16 in the nucleus (Xu et al., 2013). However, (1) whether USP16 is actively imported into the nucleus through an NLS, (2) what are the kinetics and extent of USP16 entry into the nucleus, and (3) what are the molecular determinants responsible for USP16 nucleo-cytoplasmic transport, all remained unaddressed. Hence, we sought to rigorously study USP16 localization following inhibition of CRM1. Treatment of U2OS cells expressing Myc–USP16 with LMB caused an accumulation of this DUB in the nucleus with up to 35% of cells harboring both nuclear and cytoplasmic staining at 24 h post treatment (**Figure 2-2A,B**). (As control, the C2TA transcription factor, known to be regulated by nuclear export (Cressman et al., 2001), readily and rapidly accumulated in the nucleus in a majority of cells following 6 h of LMB

treatment. We also observed that, upon accumulation of USP16 in the nucleus, histone H2Aub levels were considerably reduced. Of note, most CRM1-exported proteins accumulate relatively quickly (within few hours) in the nucleus following LMB treatment and often with a predominant nuclear localization (Cressman et al., 2001; Esmaili et al., 2010; Julien et al., 2003; Liu and DeFranco, 2000; Murai et al., 2003; Rodier et al., 2001). In contrast, we observed an unusually protracted accumulation of USP16 in the nucleus after LMB treatment. In addition, USP16 was either equally distributed between the cytoplasm and the nucleus, or remained predominantly cytoplasmic, following LMB treatment (**Figure 2-2A,B**).

The observed nuclear localization of USP16 in G1 cells raised the possibility that USP16 might transiently reside in the nucleus after mitosis (**Figure 2-1G**), which would explain the occasional presence of nuclear USP16 in two adjacent cells in early G1. If this is the case, blocking cell cycle progression through mitosis would be expected to reduce the number of cells containing USP16 in the nucleus. Accordingly, treatment with RO3366, a CDK1 inhibitor that induces G2 cell cycle arrest, results in a strong decrease in the proportion of cells with nuclear USP16 following LMB treatment (**Figure 2-2C,D**). FACS analysis showed that RO3366 treatment results in nearly a 3-fold increase of G2 cells (**Figure 2-2C, bottom panels**). We also observed an increase of histone H3S10 phosphorylation following CDK1 inhibition, confirming the accumulation of pre-mitotic cells (**Figure 2-2C**). Interestingly, when cells are released from RO3366 to enter mitosis, no distinct nuclear accumulation of USP16 could be observed (**Figure 2-S2A**). When chromosome condensation could be readily detected, USP16 was still observed in the cytoplasm (**Figure 2-S2B**). However, when chromosomes became clearly distinct (**Figure 2-S2A, see 90 min time point**), USP16 generally showed a homogenous cellular distribution, likely due to nuclear membrane breakdown. Overall, the above results suggest that USP16 does not enter the nucleus prior to the onset of mitosis. We also note that while phosphorylation of histone H3S10 is strongly increased at this stage, no deubiquitylation of H2Aub could be observed (**Figure 2-S2C**). Moreover, when considering the condition of LMB treatment alone, cells with nuclear USP16 always manifested low levels of histone H2Aub (**Figure 2-2C**). However, no correlation could be made between the presence of USP16 in the nucleus and the levels of histone H3S10P. These results therefore indicate that H2Aub deubiquitylation is not a prerequisite for phosphorylation of H3S10.

To further determine whether USP16 transiently resides in the nucleus after mitosis, we synchronized cells in M phase with nocodazole followed by release into G1 in the presence or

absence of LMB. FACS analysis confirmed the enrichment of G1 cells following mitotic exit (**Figure 2-2E**). We observed that USP16 is retained in the nucleus following mitosis in the large majority of LMB-treated G1 cells (**Figure 2-2F,G**). Nevertheless, USP16 was either evenly distributed between the cytoplasm and the nucleus or was primarily observed in the cytoplasm. Interestingly, this effect appeared to be specific to USP16, as two other cytoplasmic proteins, UBE2O and RPS6, are not retained in the nucleus following LMB treatment of nocodazole-released M phase cells (**Figure 2-S2D,E**). These results, taken together suggest that, during mitosis, USP16 is transiently retained in the nucleus following nuclear membrane breakdown and exported to the cytoplasm after nuclear membrane assembly. Alternatively, USP16 might be transiently imported and localized in the nucleus of early G1 cells. Under both scenarios, our data suggest that specific molecular determinants are responsible for transient retention of USP16 in the nucleus.

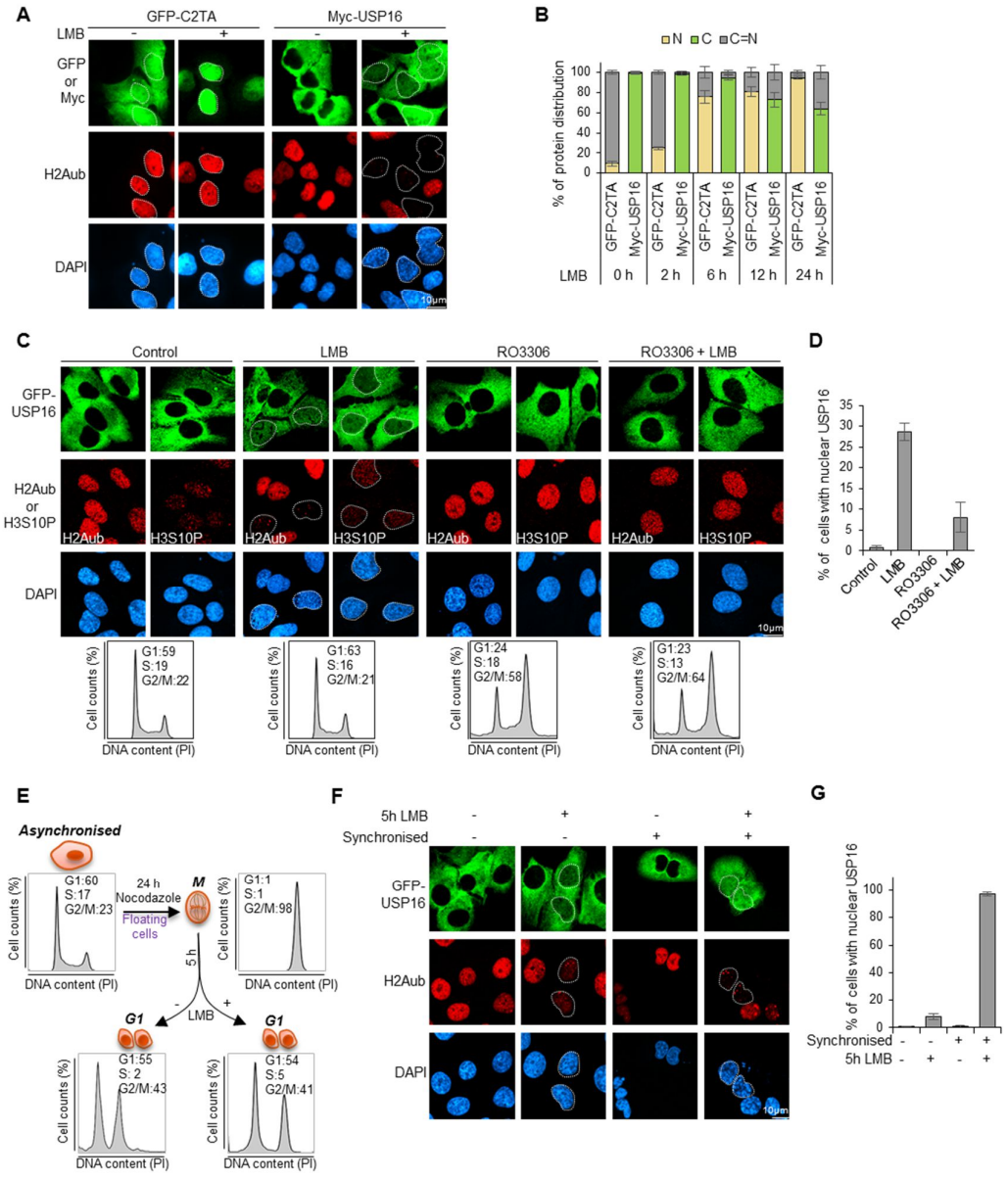

Figure 2-2 : USP16 is rapidly exported to the cytoplasm by a CRM1-mediated system following M phase completion.

(A) USP16 localization following inhibition of CRM1. U2OS cells were transfected with pDEST Myc-USP16 WT or GFP-C2TA and treated with LMB for 24 h. The USP16 subcellular localization was then determined. The localization of GFP-C2TA was monitored as a positive control for LMB treatment. Representative of *n*=3 biological replicates. **(B)** Cell counts of USP16 nuclear localization was conducted (as in A). C, predominant in the cytoplasm; N, predominant in the nucleus, C=N, equal distribution between cytoplasm and nucleus. More than 100 cells were counted in three independent experiments and values are presented as mean±s.d. **(C)** Localization of USP16 following CDK1 inhibition. U2OS cells stably expressing GFP–

USP16 were treated with RO3306 and/or LMB for 24 h. The USP16 subcellular localization and the levels of histone H2Aub and histone H3S10P were determined by direct GFP fluorescence or immunofluorescence. The cell populations were analyzed by FACS (bottom panels). *n*=3 biological replicates. **(D)** Cell counts for the nuclear localization of USP16 was conducted after RO3306 and/or LMB treatment (as shown in C). More than 100 cells were counted in three independent experiments and values are presented as mean±s.d. **(E)** Cell cycle profiles following release from mitotic block. U2OS cells stably expressing GFP–USP16 were blocked in metaphase following treatment with nocodazole. Partially adherent cells (mitotic population) were obtained by shake-off and released in the presence or absence of LMB for 5 h. Cell cycle profiles were determined by FACS analysis. **(F)** The USP16 subcellular localization and the levels of histone H2Aub were determined in cells treated as indicated in E and analyzed by direct fluorescence or immunofluorescence, respectively. **(G)** Cell counts for nuclear localization of USP16 was conducted after RO3306 and/or LMB treatment (as shown in E,F). More than 100 cells were counted in three independent experiments and values are presented as mean±s.d.

- **A non-canonical NLS moderately contributes to the nuclear localization of USP16.**

We sought to test the hypothesis that molecular determinants could be responsible for the transient nuclear localization of USP16. Using an NLS prediction algorithm (Nguyen Ba et al., 2009), we noticed several lysine/arginine-rich sequences that might act as nuclear targeting motifs (**Figure 2-S3A**). In particular, it has been reported that a lysine-rich region located within amino acids 124–197 could be responsible for USP16 nuclear localization (Xu et al., 2013). Within this region, amino acids 150–185 were identified by the NLS prediction algorithm, but with a low confidence score (**Figure 2-S3A**). We found that fusion of this sequence to the N-terminus of GFP [GFP150-185(USP16)] resulted in a chimeric protein that did not actively accumulate in the nucleus when compared to GFP alone (**Figure 2-S3B**). GFP fused to the NLS sequence from SV40T large antigen [GFPNLS(TAg)] and GFP alone were used as a positive and negative controls, respectively. Moreover, deletion of the 150–185 amino acid sequence in the context of the full-length protein (USP16Δ150-185) had no impact on the localization of USP16 following treatment with LMB (**Figure 2-S3C,D**).

Two other lysine/arginine-rich stretches along USP16, namely, amino acids 1–9 (MGKKRTKGK) and 437–459 (KHLQKKAKKQAKKQAKNQRRQQK), were also identified as potential nuclear-targeting sequences (**Figure 2-S3A**). The former sequence might

act as a monopartite NLS, which usually comprises a small stretch of basic amino acid residues (Kosugi et al., 2009; Lange et al., 2007). The 437–459 amino acid region exhibited the highest probability score, but does not conform to either typical monopartite or bipartite NLS sequences, the latter being characterized by two small clusters of basic amino acids separated by 10 to 12 amino acids (Kosugi et al., 2009). Instead, the 437–459 region contains a stretch of lysine residues intercalated with multiple polar glutamine residues and is longer than a classical monopartite NLS. To determine the potential contribution of each of the two motifs to USP16 localization, we first fused each sequence to the C-terminus of GFP. Our results show that 437–459 amino acid region [GFP437-457(USP16)], but not the 1–9 amino acid region [GFP1-9(USP16)], is sufficient to target GFP to the nucleus (**Figure 2-3A**). We therefore considered this sequence as the potential USP16 NLS [NLS(USP16)]. This putative NLS resides between the first catalytic region and the linker domain, and is highly conserved from human to *Drosophila* (**Figure 2-S3E**).

We analyzed the importance of this potential NLS in the context of the full-length protein, and observed an ~2-fold reduction in nuclear accumulation of USP16ΔNLS following 24 h of LMB treatment, with ~17% of cells showing nuclear USP16 (**Figure 2-3B,C**). Thus, the lysine rich 437–457 amino acid region of USP16 acts as an NLS in its natural context. However, the USP16 NLS might not be completely exposed within its natural location in the context of the full-length protein. Indeed, when USP16 NLS is fused to the N-terminus of USP16 [USP16NLS(USP16)], we observed a predominant cytoplasmic localization in untreated cells, whereas ~80% of cells exhibited USP16 in both cytoplasm and nucleus following 24 h of LMB treatment (**Figure 2-3B,C**). Nonetheless, this NLS remains less potent than the T antigen NLS, which led to the import of ~80% of USP16 [USP16NLS(TAg)] into the nucleus after only 6 h of LMB treatment (**Figure 2-3B,C**). Of note, as USP16 might form homo-tetramers *in vivo* (Joo et al., 2007), we wanted to test the possibility of endogenous USP16 self-interaction, which could impact the localization of USP16ΔNLS. We used a combination of CRISPR/Cas9-mediated knockout with siRNA to increase the efficacy of USP16 protein depletion, as subsets of cells remain refractory to either approach (**Figure 2-S4A,B**). We did not observe noticeable differences in localization of Cas9/siRNA-resistant USP16WT or USP16ΔNLS between controls and the corresponding conditions following depletion of endogenous USP16 (**Figure 2-S4C,D**). Taken together, our data indicate that USP16 contains a functional NLS that partially contributes to its nuclear localization.

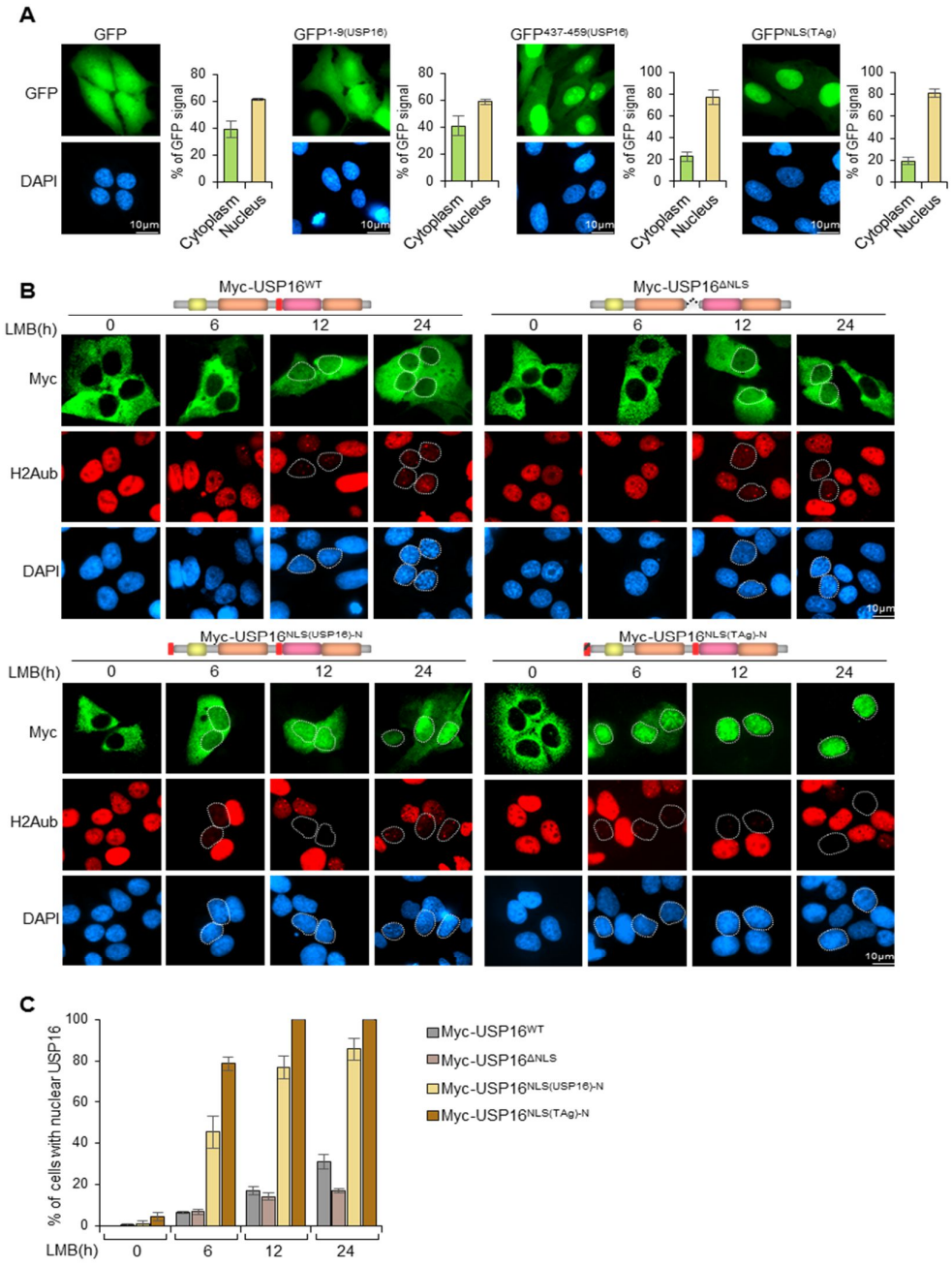

Figure 2-3 : Identification of a nuclear localization signal of USP16.

(A) Examination of several potential NLS sequences of USP16 for targeting GFP into the nucleus. U2OS cells were transfected with pOD35 GFP, pOD35 GFP 1-9 (USP16), pOD35 GFP 437-459 (USP16) or pOD35 GFP NLS (TAg) expression constructs. The subcellular localization of the GFP fusion proteins was detected by fluorescence microscopy. Quantification of GFP signal in the nucleus versus cytoplasm was conducted. Data is presented as the mean±s.d. percentage of GFP signal in each compartment versus total signal and corresponds to an average quantification on 10 cells; *n*=5 biological replicates. (**B)** Evidence

for a functional USP16 NLS. U2OS stably expressing Myc–USP16^{WT}, Myc–USP16$^{\Delta NLS}$, Myc–USP16$^{NLS(USP16)\text{-}N}$ or Myc–USP16$^{NLS(TAg)\text{-}N}$ were treated with LMB and used for immunofluorescence analysis. Schematic representation of the different USP16 mutants are shown at the top of each panel. **(C)** Cell counts from experiments performed as indicated in B represent the percentage of cells with nuclear USP16. More than 100 cells were counted and the values are presented as mean±s.d.; *n*=3 biological replicates.

- **Catalytic dead USP16 remains trapped by PRC1 substrates in the nucleus.**

As the USP16 NLS is located between the two regions of the catalytic domain, we hypothesized that USP16 catalytic activity might impact its nucleocytoplasmic transport. To address this, we took advantage of our set-up whereby release from nocodazole in combination with LMB treatment results in a highly enriched cell population with nuclear USP16. FACS analysis confirmed the expected cell cycle profiles following mitotic exit (**Figure 2-S4E**). We found that mutating the catalytic cysteine residue to a serine residue (USP16C205S) increased its nuclear retention, even in the absence of LMB (**Figure 2-S4A,B**). This was readily noticeable at 5 h post-release from mitotic block. It is interesting to note that USP16C205S is either equally distributed between the nucleus and the cytoplasm, or even predominantly localized in the nucleus. However, the nuclear localization of this variant is not maintained after 24 h of release from mitotic block. Deletion of USP16 NLS (USP16ΔNLS-C205S) only partially reduced nuclear localization of the catalytic dead mutant (**Figure 2-4A,B**). These results suggest that USP16 catalytic activity influences USP16 cytoplasmic localization after mitotic exit. However, since USP16C205S is predicted not to lose its ability to bind ubiquitin, we reasoned that this mutant might remain tightly associated with H2Aub, which is highly abundant in the nucleus, thus underpinning the apparent nuclear localization of this mutant. Alternatively, self-deubiquitylation might also regulate USP16 localization, as we previously demonstrated for the DUB BAP1, whose nucleocytoplasmic localization is regulated by the E2 conjugating enzyme and E3 ligase hybrid denoted UBE2O (Mashtalir et al., 2014). To distinguish these possibilities, we first depleted Ring1A and Ring1B (also known as RNF1 and RNF2, respectively), the two major E3 ligases that act on H2A K119, and observed relocalization of USP16C205S to the cytoplasm (**Figure 2-5A–C**). To further demonstrate that ubiquitin binding is essential for USP16 nuclear localization, we modeled the structure of the catalytic domain for this DUB using the available crystal structures of USP2 and USP7, both in complex with ubiquitin, and inferred the amino acids necessary for ubiquitin binding by

USP16 (**Figure 2-5D**). The structural modeling of USP16 catalytic domain (the linker region between the CD1 and CD2 was removed) complies with the known features of the classical USP catalytic domain. Notably, we observed the three parts of a USP catalytic domain: the Fingers, Palm and Thumb. Importantly, the ubiquitin-binding pocket aligns very well with both the USP2 and USP7 ubiquitin-binding interfaces. Therefore, we generated two mutants within two portions of the catalytic domain, CD1-M or CD2-M. First, we validated, using two DUB activity probes, that a distinct upper band shift is observed for wild-type USP16, indicating that nearly all of the USP16 pool is labeled with the ubiquitin probe (**Figure 2-5E**). In contrast, no band shift was observed for the CD1-M and CD2-M mutants indicating their inability to bind ubiquitin (**Figure 2-5E**). Next, we transduced U2OS with wild-type USP16 and corresponding mutants, and found that ablation of ubiquitin binding completely prevents nuclear accumulation of USP16 (**Figure 2-5F,G**). We conclude that catalytic inactive USP16 remains artificially trapped in the nucleus, that is, it cannot be released from PRC1 substrates and, notably, the highly abundant ubiquitylated H2AK119.

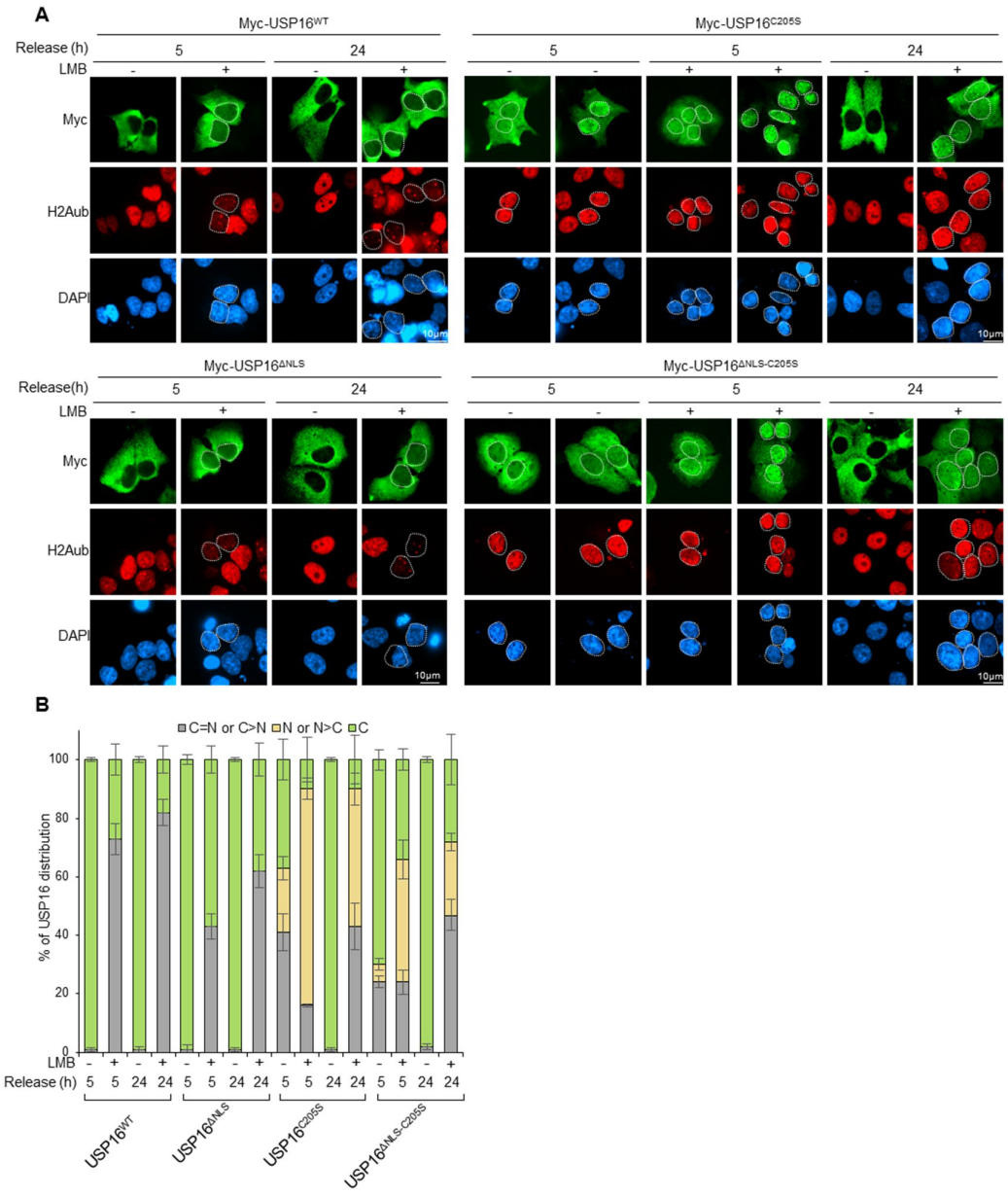

Figure 2-4 : Inhibition of DUB activity results in USP16 cytoplasmic localization.

(A) Mutation of the catalytic cysteine residue results in USP16 nuclear retention. U2OS stably expressing Myc–USP16^{WT} and its catalytically inactive mutant Myc–USP16^{C205S}, or Myc-USP16$^{\Delta NLS}$ or Myc-USP16$^{\Delta NLS\text{-}C205S}$ were treated with nocodazole for 24 h. Mitotic cells were harvested by shake-off and then released for 5 h or 24 h in the presence or absence of LMB. The subcellular localization of USP16 was detected by immunofluorescence. **(B)** Cell counts from experiments shown in A representing the percentage of cells with nuclear and/or cytoplasmic USP16. N, predominantly nuclear; N>C, mainly in the nucleus rather than the cytoplasm; C=N, equal distribution between cytoplasm and nucleus; C>N, mainly in the

cytoplasm rather than the nucleus; C, predominantly cytoplasmic. More than 100 cells were counted in three independent experiments and values are presented as mean±s.d.; *n*=3 biological replicates.

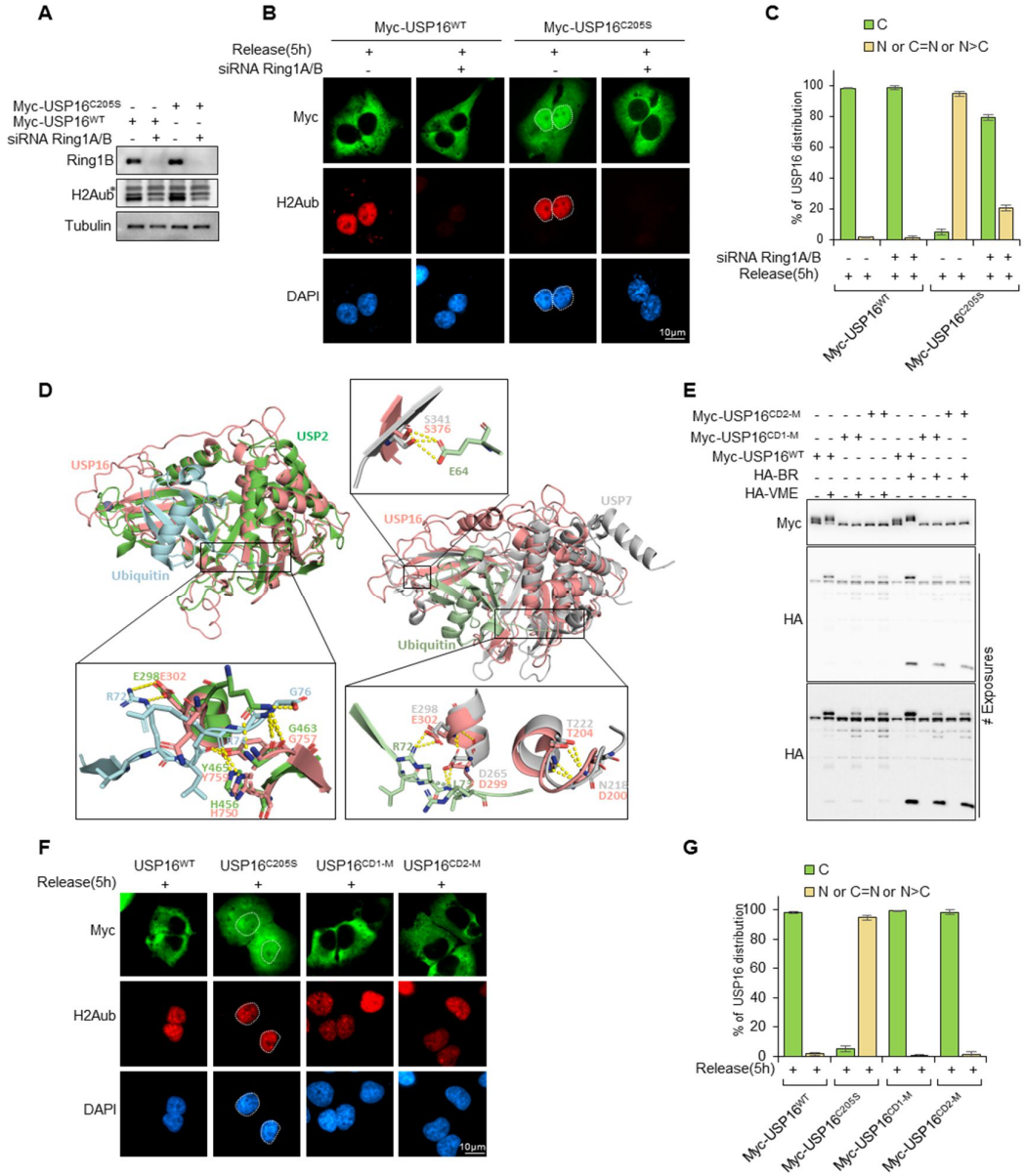

Figure 2-5 : Catalytic dead USP16 remains trapped by Ring1A and Ring1B substrates.

(A) U2OS stably expressing Myc–USP16^{WT} or Myc–USP16^{C205S} were transfected twice with control (NT) or Ring1A and Ring1B siRNAs for 72 h and used for immunoblotting. Tubulin was a loading control. The asterisk indicates a non-specific band. Representative of *n*=3 biological replicates. **(B)** U2OS stably expressing Myc–USP16^{WT} or Myc–USP16^{C205S} were transfected twice with control (NT) or Ring1A and Ring1B siRNAs and treated with

nocodazole for 24 h. Mitotic cells were isolated by shake-off, released for 5 h and then used for immunostaining. **(C)** Cell counts from the experiment shown in B representing the percentage of cells with nuclear and/or cytoplasmic USP16. N, predominantly nuclear; N>C, mainly in the nucleus; C=N, equal distribution between cytoplasm and nucleus; C, predominantly cytoplasmic. More than 100 cells were counted in three independent experiments and values are presented as mean±s.d.; *n*=3 biological replicates. **(D)** Overall view of the structural modeling of USP16 catalytic domain. The structure resembles catalytic core domain of USP7/HAUSP. Structural alignment of USP16 with USP2 (left panel) and with USP7 (right panel) catalytic domains are presented. Both models show the alignment of USP16 catalytic domain for ubiquitin binding. Hydrogen bounds between the C-terminus of ubiquitin and USP16 residues are shown by the yellow dashes in the magnified image of the USP16–ubiquitin binding interface. USP16 catalytic domain (CD) is in salmon, USP2 CD in green, USP7 CD in gray, ubiquitin in aquamarine (left panel) or green (right panel). **(E)** Lysates from cells stably expressing $USP16^{CD1\text{-}M}$ or $USP16^{CD2\text{-}M}$ were labeled with HA-tagged ubiquitin-VME or ubiquitin-Br DUB activity probes and analyzed by immunoblotting. *n*=2 biological replicates. **(F)** U2OS stably expressing Myc–$USP16^{WT}$, Myc–$USP16^{C205S}$ or its ubiquitin-binding mutant forms Myc–$USP16^{CD1\text{-}M}$ and Myc-–$USP16^{CD2\text{-}M}$ were treated with nocodazole and mitotic cells were harvested and released for 5 h before immunostaining. Representative of *n*=3 biological replicates. **(G)** Cell counts from experiments shown in D representing the percentage of cells with nuclear and/or cytoplasmic USP16. N, predominantly nuclear; N>C, mainly in the nucleus rather than the cytoplasm; C=N, equal distribution between cytoplasm and nucleus; C, predominantly cytoplasmic. More than 100 cells were analyzed and values are presented as mean±s.d.; *n*=3 biological replicates.

- **Mapping of domains regulating USP16 nucleocytoplasmic trafficking.**

We sought to identify the molecular determinants responsible for USP16 exclusion from the nucleus. First, we fused the T antigen NLS (NLSTAg) to either the N- or C-terminus of USP16, and found that the resulting proteins, USP16NLS(TAg)-N and USP16NLS(TAg)-C are localized in the cytoplasm, but become predominantly or partially nuclear following LMB treatment, respectively. (**Figure 2-S5A,B**). Of note, fusing T antigen NLS to the N-terminus of USP16 promoted its nuclear entry more efficiently than the C-terminal fusion, suggesting that an additional molecular determinant at the C-terminus of USP16 is involved in coordinating its nuclear localization. However, the T antigen NLS might not be similarly exposed when fused

to N-terminus versus C-terminus of USP16. Thus, GFP was fused between T antigen NLS and USP16 at both N- and C-termini. Interestingly, the effect of T antigen NLS is still more important when fused to USP16 N-terminus (**Figure 2-S5A,B**). This suggests that a free C-terminus of USP16 might be involved in coordinating its subcellular localization. Nonetheless, in all cases, USP16 is excluded from the nucleus, and its nuclear accumulation is observed only after LMB treatment. Notably, a previous study suggested that the sequence near leucine 685 at the C-terminus of USP16, within the second region of the catalytic domain, might act as a CRM1-dependent NES (Xu et al., 2013) (**Figure 2-S5C**). When we fused this peptide sequence to the N-terminus of GFP [GFP685-708 (USP16)], we did not observe exclusion of the chimeric protein from the nucleus (**Figure 2-S5D**). In addition, deletion of this sequence from USP16 (USP16Δ685-708) does not perturb its retention in the cytoplasm nor its accumulation in the nucleus following LMB treatment (**Figure 2-S5E,F**). We also tested other leucine-rich regions of USP16 (301–313 and 374–392 amino acid sequences) as GFP fusions, and observed no effect on GFP localization (**Figure 2-S5C,D**). The NES from the HIV-1 REV protein was included as a positive control, which significantly excluded GFP from the nucleus to the cytoplasm. We then generated several deletion mutants of USP16 and tested their localization with and without LMB treatment. Deletion of either the C- or N- terminus of USP16, USP16ΔC-term or USP16ΔN-term, respectively, did not have a major effect on USP16 localization in untreated cells (**Figure 2- 6A,B**). However, treatment with LMB resulted in nuclear retention of USP16ΔN-term, but not USP16ΔC-term. Next, we deleted each of the two regions of the catalytic domain (CD1 and CD2) without removing the linker region and observed that, while deletion of CD1 did not impact USP16 localization, deletion of CD2 strongly reduced USP16 nuclear retention following LMB treatment (**Figure 2-6A,B**). These results further support our initial observations that a molecular determinant promoting USP16 nuclear localization is located in the C-terminal region. Importantly, in the absence of LMB treatment, we found that only the deletion of the linker region (460–618 amino acid sequence) resulted in partial nuclear retention of USP16. About 40% of cells showed USP16 either evenly distributed between the cytoplasm and nucleus or mostly localized in the cytoplasm, but with a distinct nuclear signal, and this was associated with a strong reduction of H2Aub levels (**Figure 2-6A,B**). Moreover, no major change was observed in the localization of USP16Δlinker upon LMB treatment. Interestingly this linker region separates the USP16 catalytic domain into two regions (amino acids 191–402 and 617–777) and its deletion does not impact DUB activity. Mutation of the catalytic cysteine residue resulted in increased nuclear localization of USP16 lacking the linker region USP16Δlinker-C205S. By contrast, unlike for wild-type USP16 (**Figure 2-S5A,B**),

addition of TAg-NLS to the N-terminus of USP16 lacking the linker domain [USP16Δlinker-NLS(TAg)-N] caused dramatic nuclear accumulation of this DUB, and this correlated with an increased proportion of cells with reduced levels of H2Aub (**Figure 2-6A,B**). Next, we transduced U2OS cells with lentiviral vectors for USP16 expression with or without the linker region (USP16ΔLinker) and conducted fractionation of nuclear and cytoplasmic proteins. This confirmed that a substantial fraction of USP16ΔLinker-C205S remained associated with the nucleus compared to the fraction for the cytoplasmic enzyme LDH (**Figure 2-6C**). We conclude that the linker sequence between the two regions of the catalytic domain must contain a determinant that ensures the cytoplasmic localization of USP16.

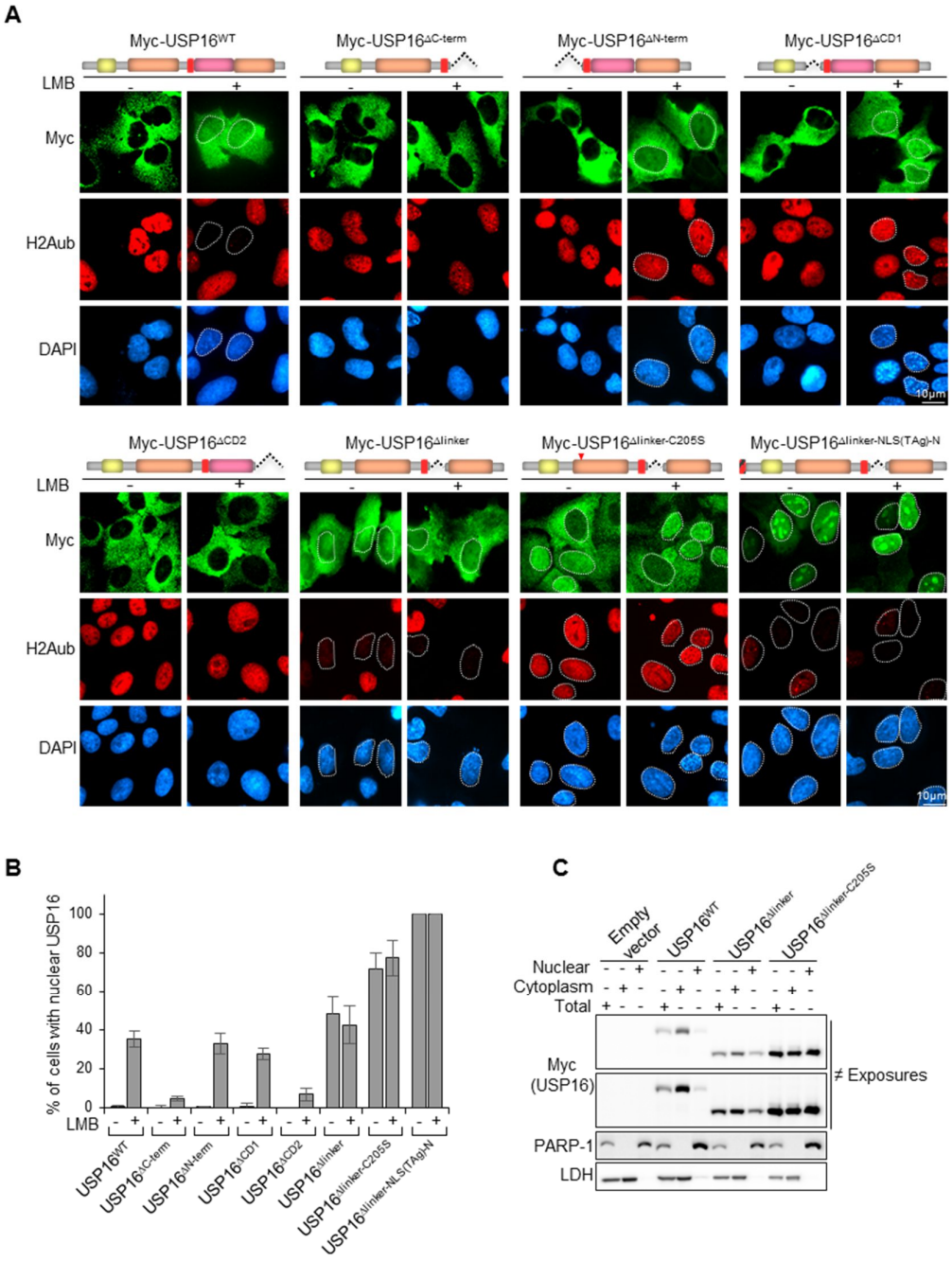

Figure 2-6 : The linker region within the catalytic domain is responsible for USP16 cytoplasmic retention.

(A) Mapping of USP16 domains responsible for its nuclear export. U2OS cells were transduced with lentiviruses to express various mutants of USP16. Cells were then treated with LMB for 24 h, and the subcellular localization of USP16 mutants was determined by immunofluorescence. Schematic views of the mutants are presented at the top of each panel.

Representative of *n*=3 biological replicates. **(B)** Cell counts from experiments shown in A representing the percentage of cells with nuclear USP16. For each condition, more than 100 cells were counted and values are presented as mean±s.d.; *n*=4 biological replicates. **(C)** The linker domain is responsible for USP16 cytoplasmic localization. U2OS cells stably expressing empty vector, Myc–USP16^{WT}, Myc-–USP16$^{\Delta linker}$ or Myc–USP16$^{\Delta linker\text{-}C205S}$ were harvested, and the nuclear and cytoplasmic fractions were obtained by fractionation and used for immunoblotting. LDH and PARP-1 were used as loading control for the cytoplasmic and nuclear fractions, respectively. Representative of *n*=3 biological replicates.

- **Identification of the authentic NES in USP16.**

We sought to further characterize the USP16 linker domain (amino acids 460–618) (**Figure 2-7A**), and found that this sequence was sufficient to retain GFP fusion protein in the cytoplasm, and to confer LMB responsiveness (**Figure 2-7B,C**). A similar result was obtained when we incorporated the TAg-NLS into the GFP–Linker construct [GFP–LinkerNLS(Tag)-N] (**Figure 2-7B,C**). These data suggest that the linker region of USP16 contains an NES that is sufficient to exclude USP16 from the nucleus. Therefore, we divided the linker into multiple overlapping amino acid sequences (**Figure 2-7A**). Remarkably the P2 and P5 fragments, which share a common sequence, were able to retain GFP in the cytoplasm as demonstrated by nuclear accumulation upon LMB treatment (**Figure 2-7B,C**). We further divided the P5 fragment into regions, P6, P7 and P8, and found that P6 was mostly in the cytoplasm and is responsive to LMB (**Figure 2-7B,C**). Indeed, comparing P6 to other known NES sequences revealed a hydrophobic (Φ) residue-rich region (ISNGFKNLNL) that is different from the previously proposed USP16 export motif (Xu et al., 2013), but fulfills the criteria that define a NES motif [Φ-X-(2,3)-Φ-X(2,3)-Φ-X-Φ; Fu et al., 2011; Fung et al., 2017]. This region of USP16 is highly conserved through evolution (**Figure 2-S6A**) and aligns with other known NES sequences (**Figure 2-S6B**), Next, we used the identified USP16 NES sequence to conduct molecular modeling, using a known crystal structure of PKI NES bound to the CRM1–Ran–RanBP1 complex and found that the identified USP16 NES matches the CRM1 NES-binding pocket (**Figure 2-7D**). Finally, we generated a U2OS cell line stably expressing a USP16 construct lacking the export motif (USP16ΔNES) and validated that USP16 accumulates in the nucleus without LMB treatment (**Figure 2-7E,F**). We also depleted endogenous USP16 using a combination of CRISPR/Cas9 and siRNA, and did not observe changes in the localization USP16ΔNES with or without LMB treatment (**Figure 2-S6C,D**). Finally, we tested the

interaction of the USP16 linker or its NES, and observed a strong interaction with CRM1 *in vitro* (**Figure 2-S6E**). We conclude that USP16 is maintained in the cytoplasm due to the presence of a potent NES located between the two regions of the catalytic domain.

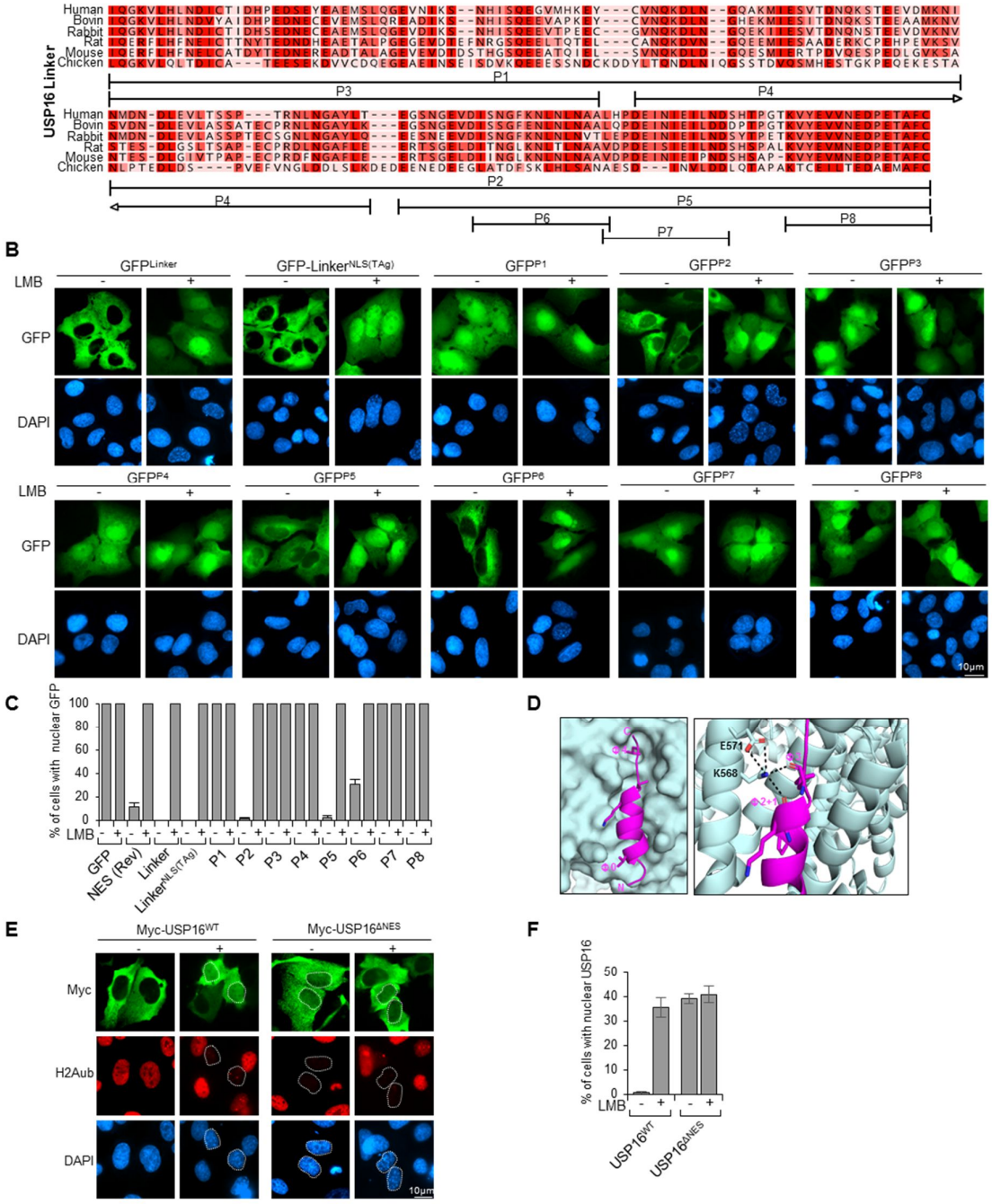

Figure 2-7 : Identification of the USP16 NES.

(A) Sequence conservation of the linker region of USP16. Sequences were obtained from UniProt and aligned using Geneious R8. A representation of the various regions of USP16

linker (P1 to P8) fused to the N-terminus of GFP as used in this study are shown underneath. **(B)** The USP16 NES is sufficient to retain GFP in the cytoplasm. U2OS cells were transfected with either pEGFP N3, GFP NES (HIV1 REV), GFP–linker, GFP–linker–NLS (T Large Antigen) or the various GFP fusion constructs shown in A (P1 to P8). Cells were treated with LMB for 24 h and the subcellular localization of these GFP fusions was determined. **(C)** Cell counts from experiments performed as indicated in B showing nuclear localization of GFP fusions in transfected cells before and after LMB treatment. For each condition, more than 100 cells were counted and values are presented as mean±s.d.; *n*=3 biological replicates. **(D)** Cartoon representation of the homology model of USP16 NES in complex with CRM1. The left panel shows the NES binding to the CRM1 groove. The Φ0 and Φ4 amino acids represent the start and the end of the NES consensus. Side chain representation of amino acids is shown. The right panel shows the amino acids that make contacts between USP16 NES (Φ2+1 and Φ3) and CRM1 groove (K568 and E571). The hydrogen bounds are shown by the black dashes. Φ denotes hydrophobic amino acid. **(E)** U2OS stably expressing Myc–USP16^{WT} or Myc–USP16$^{\Delta NES}$ were treated with LMB for 24 h. The subcellular localization was determined by immunofluorescence. Representative of *n*=3 biological replicates. **(F)** Cell counts from experiments performed as shown in E indicating nuclear localization of USP16. For each condition, more than 100 cells were counted and values are presented as mean±s.d.; *n*=3 biological replicates.

- **USP16 is not imported in the nucleus during genotoxic stress, but its enforced nuclear localization inhibits the assembly of DNA repair foci**

Following induction of DNA double-strand breaks (DSBs), several proteins are rapidly recruited to DNA damage sites to form repair foci including phosphorylated H2AX (γH2AX), as well as 53BP1 and BRCA1, two factors that promote DSB repair via non-homologous end joining (NHEJ) and homologous recombination (HR), respectively (Panier and Boulton, 2014; Zimmermann and de Lange, 2014). A previous finding showed that both overexpression and knockdown of USP16 perturbs DSB repair (Zhang et al., 2014), although a recent study reported that USP16 overexpression does not impact DSB repair foci (Wang et al., 2016). Thus, it remained unclear whether and, eventually, how USP16 could directly impact DSB repair. These conflicting results prompted us to determine whether USP16 undergoes translocation to the nucleus to directly regulate histone ubiquitylation during DNA damage repair. However, we did not observe any detectable accumulation of USP16 in the nucleus following ionizing

radiation (IR) treatment of U2OS or IMR90 lung fibroblasts (**Figure 2-S7A,B**). Moreover, we conducted cell fractionation of U2OS stably expressing Myc–USP16, and again did not observe any increase in nuclear USP16 post IR (**Figure 2-S7C**). Next, we expressed USP16 and its mutants (USP16C205S, USP16Δlinker and USP16Δlinker-C205S) to determine their impact on DNA repair foci. U2OS cells were treated or not for 24 h with LMB, exposed to IR and then analyzed 4 h later. In the absence of IR, no spontaneous 53BP1 foci were observed following USP16 transfection, even when this DUB localizes to the nucleus following either LMB treatment or deletion of the linker domain (**Figure 2-8A,B**). Strikingly, the presence of USP16Δlinker in the nucleus post IR was associated with a strong decrease in 53BP1 foci formation, which was dependent on the catalytic activity of USP16 (**Figure 2-8A,B**). Upon LMB treatment, USP16 nuclear retention also prevented IR-induced foci formation in a DUB activity-dependent manner (**Figure 2-8A,B**). Under all conditions, treatment with IR did not induce noticeable changes in the localization of USP16 or its mutants (**Figure 2-8C**). Taken together these results suggest that unscheduled accumulation of USP16 in the nucleus abrogates DSB repair.

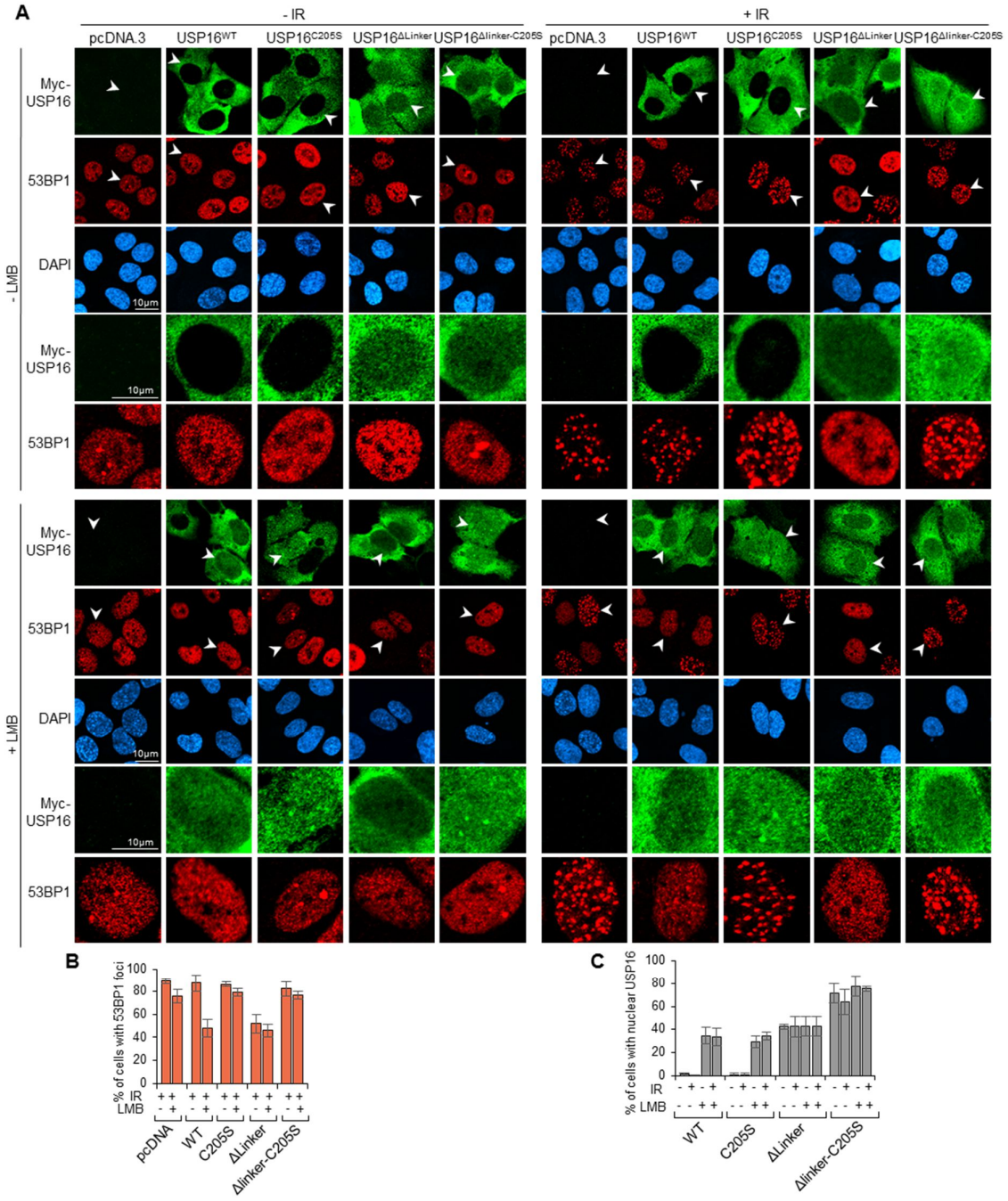

Figure 2-8 : Enforced nuclear accumulation of USP16 abolishes the assembly of DNA repair foci.

(A) U2OS cells were transfected with either pcDNA, Myc–USP16 WT, Myc–USP16 C205S, Myc–USP16 Δlinker or Myc–USP16 Δlinker C205S expression vectors and subjected to different treatments (10 nM LMB and/or 7.5 Gy ionizing radiation). The subcellular localization of USP16 and the presence of 53BP1 foci were detected with the indicated

antibodies. Arrowheads indicate the position of selected nuclei. **(B)** Cell counts from experiments performed as indicated in A showing the percentage of cells harboring 53BP1 foci in presence of Myc–USP16 or the corresponding mutants. Note that 53BP1 foci were counted automatically based on the whole-cell population of transfected and non-transfected cells. The results are presented as mean±s.d.; *n*=4 biological replicates. **(C)** Cell counts from experiments performed as indicated in A showing the nuclear localization of USP16 in transfected cells following LMB and/or ionizing radiation treatments. More than 100 cells were counted in four independent experiments and values are presented as mean±s.d.

2.4 Discussion

In this study, we provide novel insight into the function of USP16, and clarify the mechanisms that coordinate its trafficking between the cytoplasm and nucleus. First, our data indicate that USP16 is essentially cytoplasmic in all phases of the cell cycle including late G2, and is retained transiently in the nucleus during a brief period post mitosis. We identified a strong NES signal within the linker domain, which constitutes the major determinant of USP16 cytoplasmic localization. Moreover the hydrophobic amino acids that define the functionality of this motif, and which are critical for NES interaction with CRM1, are invariably found in most vertebrates, suggesting the biological importance of USP16 nuclear export. Second, we found that a catalytic dead USP16 mutant is retained in the nucleus through its ability to bind ubiquitylated proteins. Third, USP16 contains a functional, but weak, NLS that operates, in the context of the full-length protein, to influence USP16 subcellular localization. Fourth, while depletion of USP16 results in a DNA repair delay, this DUB is not actively translocated into the nucleus in response to genotoxic stress. Instead, only enforced expression of USP16 lacking its nuclear export signal inhibits DNA repair. Finally, we found that USP16 depletion results in the accumulation of conjugated ubiquitin species, likely reflecting a global perturbation of ubiquitin pools. This would be consistent with the presence of a ZNF UBP domain in USP16, which is known to bind the C-terminal di-glycine motif of unconjugated ubiquitin (Reyes-Turcu et al., 2006).

Cell fractionation experiments showed that a small pool of USP16 remains associated with nuclei even following their purification on a sucrose cushion. We initially hypothesized that this pool of USP16 is in the nucleus and might correspond to a subpopulation of cells at a specific phase of the cell cycle or that a small portion of USP16 could be uniformly present in the nucleus across all cell populations. Immunostaining studies indicated that only background

signals could be observed in the nucleus for the majority of cells, arguing against USP16 nuclear localization in interphase. Moreover, it is unlikely that the pool of USP16 that co-fractionates with nuclei corresponds to the early G1 cells with nuclear USP16, as the proportion of the cells is extremely low within an unsynchronized cell population. Instead, this pool of USP16 might be associated with the fraction of organelles that inherently co-sediments with nuclei. Thus, while we cannot definitely exclude the presence of minute levels of USP16 in the nucleus that are below the detection limit, our results suggest that the main roles of USP16 are exerted within the cytoplasm during interphase. As such, it would be interesting to further determine the subcellular distribution of USP16 within the cytoplasm, as well, as the precise function of USP16 in this compartment.

We provided evidence indicating that, under normal growth conditions, USP16 nuclear import does not occur before M phase. First, cell cycle arrest at the G2/M border following CDK1 inhibition is not accompanied by an enrichment in the percentage of cells with nuclear USP16. By contrast, a strong reduction of nuclear USP16, which is otherwise promoted by LMB treatment, could be observed following CDK1 inhibition. Importantly, even after cell cycle release from CDK1 inhibition, no enrichment of USP16 in the nucleus was apparent prior to the onset of mitosis. This result is in contrast with previous findings suggesting that phosphorylation of USP16 by CDK1 inhibits its export and promotes its nuclear localization (Xu et al., 2013). On the other hand, we also found that, in the absence of LMB treatment, no global deubiquitylation of H2AK119 could be detected in CDK1-inhibited G2 cells, while a strong increase of histone H3S10 phosphorylation was observed. Thus, H3S10 phosphorylation precedes mitotic H2Aub deubiquitylation, in contrast to previous results reporting the reverse relationship (Joo et al., 2007). Our results also argue against a direct role of USP16 in chromosome condensation, but whether there is a relationship between phosphorylation of histone H3S10 and subsequent deubiquitylation of histone H2Aub will require further investigation.

We established that USP16 resides in the nucleus for only a very short period of time after mitosis. This conclusion is based on several observations: (1) in an asynchronous cell population, only a very small proportion of cells (less than 1%) could be captured with nuclear USP16; (2) only after LMB treatment in combination of mitotic block release could nuclear USP16 be observed in a heterogeneous population of cells; (3) when USP16 is observed in the nucleus, this often corresponds to two adjacent cells, likely corresponding to daughter cells;

and (4) USP16 nuclear localization partially depends on its atypical, but functional, NLS. The function of USP16 in the nucleus in early G1 remains unknown, but could be required for post-mitotic deubiquitylation of residual H2Aub. Alternatively, a yet-to-be-discovered function of USP16 could take place in early G1 cells during chromosome decondensation and chromatin reorganization. Of note, the NLS of USP16, although lysine rich, is quite unusual and does not correspond to previously known nuclear import sequences (Lange et al., 2007; Soniat and Chook, 2015).

We also found that abolition of USP16 catalytic activity leads to enhanced nuclear retention of USP16 in G1 cells. This effect is only partially reduced following deletion of the USP16 NLS. Our data strongly suggest that catalytic dead USP16 remains strongly bound to ubiquitylated nuclear proteins through its catalytic domain, preventing its release and export to the cytoplasm. Consistent with this, deletions or mutations of the catalytic domain (CD1 or CD2), which would be expected to destroy the ubiquitin-binding interface of USP16, did not result in increased nuclear accumulation of USP16. Finally, depletion of Ring1A and Ring1B E3 ligase of H2AK119 strongly reduced nuclear localization of the catalytic dead USP16 mutant. Whether changes in the localization of catalytically inactive USP16 might reflect a physiological regulation remains to be investigated. In addition, it will be interesting to determine whether disease-associated mutations inactivate USP16 without altering its ability to bind ubiquitin, which in turn might have potential deleterious effects on H2Aub functions.

Our studies raise an important question regarding the roles of USP16 in the cytoplasm versus the nucleus. Since USP16 is predominantly cytoplasmic and, only following mitosis is rapidly exported to the nucleus where it remains for only a brief period, the function of USP16 NES appears to predominate over that of its NLS. Even when fused to the T antigen NLS, USP16 remains predominantly localized in the cytoplasm. These results suggest that USP16 activity might be deleterious in the nucleus under normal conditions, except at the end of mitosis, when this DUB might be needed to complete deubiquitylation of H2Aub before its exit to the cytoplasm. It is possible that USP16 is a promiscuous DUB that must be actively excluded from the nucleus to prevent undesirable deubiquitylation of nuclear proteins, events that can profoundly impact DNA repair mechanisms and epigenetic information. Of note, inhibition of USP16 export by LMB or deletion of its NES results in nuclear retention of this DUB in only a third of the total cell population, although these cells still do not show a predominant nuclear accumulation. Thus, we postulate that USP16, which resides in the cytoplasm during almost

the entire cell cycle, might exert heretofore unknown critical functions in this compartment. Another interesting point regards the phylogenetic co-evolution of NLS and NES sequences of USP16. It seems that the NLS appeared before the NES (Figures 3-S3E, 3-S6A), suggesting that USP16 might have preserved an ancestral function in the nucleus, and that its nuclear export with the potential acquisition of important cytoplasmic functions appeared later during evolution. Clearly, our study highlights the need of investigating the potential activity of this DUB in the cytoplasm and how its enzymatic activity is regulated to prevent potential promiscuous deubiquitylation.

2.5 Materials and methods

- **Antibodies**

Mouse monoclonal Anti-Flag (M2) (cat. #F3165) and anti-Myc (cat. #9E10) antibodies were obtained from Sigma-Aldrich and Covance, respectively. A rabbit polyclonal anti-USP16 antibody was generated in-house using a bacteria-purified N-terminal fragment of the human protein (service provided by EZ Biolabs). Rabbit monoclonal anti-H2Aub (D27C4) (cat. #8240) was obtained from Cell Signaling Technology. Mouse monoclonal anti RPS6 (C8) (cat. #sc-74459), mouse monoclonal anti-α-Tubulin (B-5-1-2) (cat. #sc-23948), mouse monoclonal anti-LDH (H-10)(cat. #133123), mouse monoclonal anti-PARP-1 (F-2) (cat. #sc-8007), mouse monoclonal anti-BRCA1 (D-9) (cat. #sc-6954), mouse monoclonal anti-Ring1B (N-32) (cat. #sc-101109), mouse monoclonal anti-ubiquitin (P4D1) (cat. #sc-8017), rabbit polyclonal anti-YY1 (H414) (cat. #sc-1703) and rabbit polyclonal anti-53BP1 (H300) (cat. #sc-22760) were purchased from Santa Cruz Biotechnology. Rabbit polyclonal anti-USP16 (cat. #14055-1-AP) was obtained from Proteintech. Mouse monoclonal anti-phospho-H3 (Ser10) (3H10) (cat. #05-806), mouse monoclonal anti-phospho-H2AX (Ser139) (JBW301) (cat. #05-636) and rabbit polyclonal anti-phospho-H3 (Ser10) (cat. #06-570) were obtained from Millipore. Rabbit polyclonal anti-USP16 (cat. #ab189838) was purchased from Abcam. Mouse monoclonal anti-HA hybridoma supernatant was used as previously described (Mashtalir et al., 2014). Additional information is described in (Table 3-S1).

- **Molecular cloning and plasmids**

siRNA-resistant human USP16 was generated by gene synthesis (BioBasic) and subcloned into pENTR D-Topo (Life Technologies), to generate pENTR USP16. All USP16 cDNA sequences were manually modified using codon degeneracy (Table 3-S2). The USP16

C205S construct was generated by DNA synthesis of a fragment containing a mutation in pBluescript plasmid (Biobasic) and then subcloned into the pENTR D-Topo plasmid containing USP16. The mutant cDNA constructs USP16 ΔNLS, USP16 Δ150-185, USP16 Δ685-708, USP16 ΔLinker, USP16 ΔLinker-C205S, USP16 ΔNLS-C205S, USP16 NLS (TAg)-N, USP16 NLS (TAg)-C, USP16 NLS (USP16)-N, USP16–GFP NLS (TAg)-C, GFP–USP16 NLS (TAg)-N and GFP–USP16 were all generated by PCR-based subcloning into either the pENTR D-Topo plasmid or modified Myc-pENTR D-Topo plasmid. USP16 ΔCD1, USP16 ΔCD2, USP16 ΔN-term, USP16 ΔC-term and USP16 ΔNES were generated by subcloning with annealed short adaptors into pENTR D-Topo USP16 plasmid or modified Myc-pENTR D-Topo plasmid. USP16 CD1-M and USP16 CD2-M ubiquitin-binding mutants were generated by subcloning synthetic fragments containing N200A/D299A/E302A/S376A/E380A or E644A/L646A/K682AR699A/F700A/K709A/H750A/Y759A, respectively. Both mutants were inserted into pENTR D-Topo USP16 plasmid or modified Myc-pENTR D-Topo plasmid. USP16 ΔLinker NLS (TAg) was generated by subcloning annealed NLS of SV40 large T antigen (TAg) sequence adaptors into the pENTR D-Topo USP16 ΔLinker plasmid. All USP16 expression constructs were generated using the USP16 siRNA-resistant plasmid. The pENTR D-Topo plasmids or modified Myc-pENTR D-Topo plasmids were recombined using LR clonase kit (Life Technologies) into pDEST-Myc plasmid or pLenti-CMV vector (17452, Addgene), respectively. pOD35 GFP 1-9 (USP16), pOD35 GFP NLS (USP16) and pOD35 GFP NLS (TAg) were generated by subcloning annealed oligonucleotides into the pOD35 plasmid (provided by Dr. Paul Maddox (Institute for Research in Immunology and Cancer, Canada). GFP-Linker, GFP-Linker-NLS (TAg), GFP 685-708, GFP 150-185, GFP-P1 (460-540), GFP-P2 (541-618), GFP-P3 (460-508), GFP-P4 (509-563) and GFP-P5 (564-618) were generated by PCR-based subcloning fragments of USP16 into the pEGFP-N3 plasmid. GFP-NES (HIV1 Rev), and additional USP16 fragments, GFP-P6 (572-586), GFP-P7 (585-597), GFP-P8 (604-618), GFP-301-313 and GFP-374-392 were generated by subcloning of the corresponding annealed short adaptors into the pEGFP-N3 plasmid. All constructs were verified by sequencing.

- **Cell culture, transient transfections and treatments**

U2OS osteosarcoma (ATCC, HTB-96) and HEK293T human embryonic kidney cells (ATCC, CRL-3216) were grown in Dulbecco's modified Eagle's medium (DMEM, Life Technologies) containing 5% new born calf serum (NBS), 1% L-glutamine and 1% penicillin/streptomycin. Normal human lung IMR90 fibroblasts (ATCC, CCL-186) were grown

in DMEM containing 10% fetal bovine serum (FBS), 1% L-glutamine and 1% penicillin/streptomycin. DNA plasmids were transfected into U2OS cells using Lipofectamine 2000 (Life Technologies). HEK293T cells were transfected using polyethylenimine [154] (Sigma-Aldrich). At 3 days post transfection, cells were treated with 10 nM leptomycin B (LMB) (cat. #9676S, Cell Signaling Technology), 200 ng/ml nocodazole (cat. #487928, Millipore-Sigma), 10 μM CDK1 inhibitor RO-3306 (cat. #217699, Millipore-Sigma) or 2 mM thymidine (cat. #T9250, Millipore-Sigma) and harvested for western blotting, flow cytometry or immunostaining. For DNA repair studies, at 3 days post-transfection, U2OS cells were incubated with or without 10 nM LMB for 24 h, exposed to 7.5 Gy ionizing radiation (IR) and then collected at the indicated time points for immunostaining. The cell lines used were tested negative for mycoplasma contamination, using DAPI staining. Cell lines obtained from ATCC were initially amplified in large quantities and then frozen to avoid extended culture. Cell morphology and proliferation rates were always checked.

- **Viral transduction and generation of cell lines stably expressing wild-type or mutant USP16**

U2OS or IMR90 cells stably expressing wild-type or mutant USP16 were generated by lentiviral gene delivery. HEK293T cells were transfected with pLenti-CMV USP16 or mutant plasmids with the packaging vectors psPAX2 (12260, Addgene) and pMD2-G (12259, Addgene). Lentivirus particles were collected and used to transduce cells twice followed by 48 h of puromycin selection (2 μg/ml). The pooled cell populations were used for localization studies within 1 month after selection.

- **siRNA-induced protein depletion and CRISPR/Cas9-mediated gene knockout**

Four siRNA oligonucleotides targeting human USP16 and two siRNA oligonucleotides targeting human Ring1A or Ring1B were purchased from Sigma-Aldrich (Table 3-S2) and pooled as indicated for transfection in U2OS cells using Lipofectamin RNAimax (Life Technologies). USP16 gRNA sequences (21 bp oligonucleotides) were generated using the https://bio.tools/chopchop and https://cm.jefferson.edu/Off-Spotter/ programs to exclude potential off-targets (Table 3-S2). These sequences were synthesized by Biobasic Inc., annealed and cloned into the pLentiCRISPR_V2 plasmid (52961, Addgene). We used the pLentiCRISPR_V2 empty vector as a control. Lentiviruses were generated by transfection in HEK293T cells as described above. Media containing lentivirus particles were used to infect U2OS cells twice. Pooled populations of USP16-knockout cells were selected for 48 h by

treatment with puromycin (2 μg/ml) and the USP16 depletion efficiency assessed by western blotting.

- **Immunofluorescence**

The procedure was carried essentially as previously described (Daou et al., 2011). Briefly, U2OS cells plated on coverslips were treated as indicated, fixed using 3% PFA and permeabilized with PBS solution containing 0.5% NP-40. Non-specific sites were blocked with PBS with 0.1% NP-40 supplemented with 10% FBS. The coverslips were then incubated with mouse monoclonal and/or rabbit polyclonal primary antibodies. Anti-rabbit-IgG conjugated to Alexa Fluor® 594 and anti-mouse-IgG conjugated to Alexa Fluor® 488 (Life Technologies) were used as secondary antibodies. Nuclei were stained with DAPI. Cell membranes were stained on live cells with Alexa Fluor™ 594-conjugated wheat germ agglutinin (WGA) (cat. # W11262, Life Technologies). The cells were observed using imager Zeiss Z2 microscope equipped with Plan-Apochromat 63×1.4 NA and 100×1.4 NA Oil DIC objectives and an AxioCam MRm camera. Cells were also observed with an inverted confocal fluorescence microscope (Olympus FV1000 LSM) with a 60× oil immersion objective lens. Collected images were processed using WCIF-ImageJ program and red-green-blue (RGB) profiles were generated (Schneider et al., 2012). *Z*-stacks were acquired using an inverted confocal fluorescence microscope (Olympus FV1000 LSM) with a 60× oil immersion objective lens. Live cell epifluorescence images were obtained using a LX71 Olympus microscope, with a 60× oil immersion objective, 1.35NA. Automatic time lapse imaging was performed using an in-house LabVIEW program (Binan et al., 2016).

- **Cell counts of USP16 subcellular localization and fluorescence signal determination**

The subcellular localization of USP16 was determined by counting the relevant cell population groups for each experiment. For Figure 3-2B, C2TA is either evenly distributed between the cytoplasm and the nucleus or predominantly nuclear. USP16 is either localized in the cytoplasm or found in both the cytoplasm and nucleus, with no predominant staining in the nucleus. Data is presented for each cell population as the percentage of the total cells expressing C2TA or USP16. For Figures 3-2D,G, 3-3C, 3-6B, 3-7F and 3-8C, Figures 3-S2E, 3-S3D, 3-S4D, 3-S5B, 3-S5F and 3-S6D, USP16 is localized either in the cytoplasm or in both the cytoplasm and nucleus. Thus, we counted all cells with a nuclear staining of USP16 (signal distinctly above background) and reported their percentage relative to all transfected cells

counted. For Figures 3-4B, 3-5C,G, USP16 is cytoplasmic, mostly cytoplasmic but with nuclear staining, evenly distributed between the cytoplasm and the nucleus, mostly nuclear but with cytoplasmic staining or predominantly nuclear. These cell populations were counted, and data is presented as percentage of the total cells expressing USP16. To consolidate cell counts, whenever possible, we also monitored the decrease of H2Aub signal as an indicator of USP16 nuclear accumulation. For Figures 3-1B,C and 3-3A, Figures 3-S1C, 3-S3B and 3-S5D, quantification of USP16 signals in the nucleus and cytoplasm was conducted using ImageJ software. The background signal was taken from cell-free areas and subtracted from cytoplasmic or nuclear signals. The measurement of these signals was conducted on 10 cells and data is presented as mean±s.d.

Overall, the experiments were repeated more than three times to ensure data reproducibility. No particular sample size calculation was done. We did not exclude data unless a major technical problem justified the exclusion. Results in panels represent mean±s.d. for at least three independent experiments.

- **Synchronization and cell cycle analysis**

Transfected or infected U2OS cells were synchronized at G2/M or late G2 following 24 h treatment with 200 ng/ml nocodazole (Hammond-Martel et al., 2010) or 10 μg/ml CDK1 inhibitor (RO-3306) (Daou et al., 2018), respectively. Mitotic cells were enriched using nocodazole treatment, harvested by shake-off, and released from metaphase arrest to enter G1 after replating in nocodazole-free medium. The remaining population of adherent cells was enriched in G2, but also contained a fraction of M cells that resisted shake-off, and this mixed population and was considered as G2/M. G1/S cells were enriched using a thymidine double-block protocol and then released toward S (Daou et al., 2015). Cells were fixed for immunostaining as described above or used for cell cycle analysis. Flow cytometry analysis (FACS) was conducted as described previously (Hammond-Martel et al., 2010). Cells were harvested by trypsinization and fixed using PBS containing 75% (v/v) ethanol. Cells were then treated with 100 μg/ml RNase A and stained with 50 μg/ml propidium iodide. DNA content was analyzed using a FACScan flow cytometer fitted with the CellQuestPro software (BD Biosciences).

- **Immunoblotting**

Total cell extracts were obtained by cell lysis with in a buffer containing 25 mM Tris-HCl pH 7.3 and 1% SDS. Cell extracts were boiled at 95°C for 10 min and then sonicated and used for western blotting. Total proteins were quantified using the bicinchoninic acid (BCA) assay, and then diluted in Laemmli buffer. For western blotting, the band signals were obtained with a LAS-3000 LCD camera coupled to the MultiGauge software (Fuji, Stamford, CT). All immunoblotting data for analysis of protein expression is displayed as Figure 3-S8.

- **Subcellular fractionation**

Nuclear and cytoplasmic fractions were obtained following hypotonic cell lysis. Briefly, semi-confluent dishes were washed twice and incubated for 5 min with hypotonic lysis buffer containing 10 mM Tris-HCl pH 7.3, 10 mM KCl, 1.5 mM MgCl2, 10 mM β-Mercaptoethanol, 1 mM PMSF and protease inhibitors cocktail (Sigma-Aldrich). Cells were then scraped, resuspended and lysed using a dounce homogenizer. Cytoplasmic and nuclear fractions were obtained after centrifugation at 1700 *g* for 15 min. Total cell fractions were harvested directly in the hypotonic buffer and completed to 1% SDS. To minimize cross contaminations, nuclear pellets were resuspended in 3 ml of sucrose buffer S1 (0.1 M sucrose and 10 mM MgCl2) and layered over a 3 ml sucrose cushion S2 (0.35 M sucrose, 0.5 mM MgCl2) by slowly pipetting S1 solution on top of S2. These sucrose cushions were centrifuged at 1500 **g** for 10 min. The sucrose was then removed, and the purified nuclear fractions were resuspended in hypotonic buffer containing 1% SDS.

- **Protein co-immunoprecipitation**

HEK293T cells were transfected with the indicated expression constructs and immunoprecipitation conducted as previously described (Daou et al., 2018).

- **Labeling with DUB activity probes**

U2OS cells expressing various mutants of USP16 were harvested in PBS. Following centrifugation (1700 *g* for 5 min), cell pellets were resuspended in 1:10 (v/v) ratio in 50 mM Tris-HCl pH 7.3, 100 mM NaCl, 5 mM MgCl2, 2.5 mM DTT, 2 mM ATP, 0.1% Igepal, 1 mM PMSF and protease inhibitors cocktail. Following incubation for 20 min on ice, the cell extracts were centrifuged at 25,200 g for 8 min and 20 µl of cell lysates were incubated with 20 µl of buffer with 1 µl of HA-tagged ubiquitin-VME or ubiquitin-Br DUB activity probes

(Borodovsky et al., 2001, 2002). After 2 h incubation at 37°C, cells were added 40 µl of sample buffer and used for immunoblotting detection of USP16.

- **Protein sequences alignment, motifs prediction and structure modeling**

USP16 domains were analyzed using ExPASy from the SIB Bioinformatics Resource Portal (http://www.expasy.org/) (Artimo et al., 2012). NLS and NES predictions was undertaken using the NLStradamus (Nguyen Ba et al., 2009) and NetNES servers (la Cour et al., 2004), respectively. Multiple alignments of USP16 orthologs were performed using Aline (Bond and Schuttelkopf, 2009) or Geneious created by Biomatters (available from http://www.geneious.com) as described in the figure legends. According to a sequence similarity, a homology model of USP16 NES in complex with CRM1 was generated from the crystal structure of PKI NES in complex with CRM1–Ran RanBP1 (PDB 3NBY). The USP16 NES was modeled by manually replacing PKI amino acids (GSLNELALKLGLDI) with USP16 amino acids (GEVDISNGFKNLNL) using Coot (Emsley et al., 2010).

A homology model of the USP16 catalytic domain was generated using SWISS Model (https://swissmodel.expasy.org/). The structural model comprises both parts of the catalytic domain (CD1 and CD2) without the intermediate loop (amino acids from G197 to S394 and A615 to L823). A structural model of the USP16 catalytic domain in complex with ubiquitin was obtained by superimposition of the obtained USP16 catalytic domain homology model with the crystal structure of either USP2 (PDB 2HD5) or USP7 (PDB 1NBF) both in complex with ubiquitin. Structural figures showing USP16 NES, USP16 catalytic domain homology model as well as the polar interactions between USPs and ubiquitin were generated by PyMol (Schrodinger, LLC. 2010. The PyMOL Molecular Graphics System, Version 1.8.0.5).

2.6 Acknowledgements

We thank Diana Adjaoud, Djaileb Abdelhadi, Antoine Simoneau and Emilie Allard for technical assistance and Saad Mengaad for his help with image assembly.

- **Competing interests**

The authors declare no competing or financial interests.

- **Author contributions**

  Conceptualization: N.S.N., E.B.A.; Methodology: N.S.N., S.D., M.U., J.G., N.V.I., H.B., H.Y., L.M., E.F., N.Z.C., N.M., L.B., M.S., F.B., S.C., E.B.A.; Software: N.S.N., S.D., M.U., J.G., N.V.I., H.B., H.Y., L.M., E.F., N.Z.C., N.M., L.B., M.S., F.B., E.B.A.; Validation: N.S.N., S.D., M.U., J.G., N.V.I., H.B., H.Y., L.M., E.F., N.Z.C., N.M., L.B., M.S., F.B., E.B.A.; Formal analysis: N.S.N., S.D., M.U., J.G., N.V.I., H.B., H.Y., L.M., E.F., N.Z.C., N.M., M.S., F.B., E.B.A.; Investigation: N.S.N., S.D., M.U., J.G., N.V.I., H.B., L.M., E.F., N.Z.C., N.M., M.S., F.B., E.B.A.; Resources: N.S.N., E.B.A.; Data curation: N.S.N., S.D., E.B.A.; Writing - original draft: N.S.N., E.B.A.; Writing - review & editing: N.S.N., S.D., M.U., E.D., E.M., H.W., S.C., E.B.A.; Visualization: N.S.N., S.D., E.D., E.M., H.W., S.C., E.B.A.; Supervision: N.S.N., E.B.A.; Project administration: E.B.A.; Funding acquisition: E.B.A.

- **Funding**

  This work was supported by a discovery grant (2015-2021) to E.B.A. from The Natural Sciences and Engineering Research Council of Canada (NSERC), a discovery grant (2013-2019) to H.W. from NSERC, a discovery grant (2018-2023) to E.M. from NSERC and a discovery grant (2016-2021) to S.C. from NSERC. H.W., S.C. and E.B.A. are Scholars of Fonds de la Recherche du Québec en Santé (FRQ-S). J.G. was supported by a Master's scholarship from the FRQ-S. N.S.N. was supported by a PhD scholarship from the FRQ-S. N.M. was supported by a PhD scholarship from Fonds de Recherche du Québec-Nature et Technologies (FRQ-NT). H.Y. was supported by a PhD scholarship from the CIHR.

2.7 References

Adorno, M., Sikandar, S., Mitra, S. S., Kuo, A., Nicolis Di Robilant, B., Haro-Acosta, V., Ouadah, Y., Quarta, M., Rodriguez, J., Qian, D. et al. (2013). Usp16 contributes to somatic stem-cell defects in Down's syndrome. Nature 501, 380-384. doi:10.1038/nature12530

Artimo, P., Jonnalagedda, M., Arnold, K., Baratin, D., Csardi, G., de Castro, E., Duvaud, S., Flegel, V., Fortier, A., Gasteiger, E. et al. (2012). ExPASy: SIB bioinformatics resource portal. Nucleic Acids Res. 40, W597-W603. doi:10.1093/nar/gks400

Binan, L., Mazzaferri, J., Choquet, K., Lorenzo, L.-E., Wang, Y.C.., Affar, E.B., De Koninck, Y., Ragoussis, J., Kleinman, C.L. and Costantinos, S. (2016). Live single-cell laser tag. Nat. Commun. 7, 11636. doi:10.1038/ncomms11636

Bonacci, T., Suzuki, A., Grant, G. D., Stanley, N., Cook, J. G., Brown, N. G. and Emanuele, M. J. (2018). Cezanne/OTUD7B is a cell cycle-regulated deubiquitinase that antagonizes the degradation of APC/C substrates. EMBO J. 37, e98701. doi:10.15252/embj.201798701

Bond, C. S. and Schuttelkopf, A. W. (2009). ALINE: a WYSIWYG protein-sequence alignment editor for publication-quality alignments. Acta Crystallogr. D Biol. Crystallogr. 65, 510-512. doi:10.1107/S0907444909007835

Borodovsky, A., Kessler, B. M., Casagrande, R., Overkleeft, H. S., Wilkinson, K. D. and Ploegh, H. L. (2001). A novel active site-directed probe specific for deubiquitylating enzymes reveals proteasome association of USP14. EMBO J. 20, 5187-5196. doi:10.1093/emboj/20.18.5187

Borodovsky, A., Ovaa, H., Kolli, N., Gan-Erdene, T., Wilkinson, K. D., Ploegh, H. L. and Kessler, B. M. (2002). Chemistry-based functional proteomics reveals novel members of the deubiquitinating enzyme family. Chem. Biol. 9, 1149-1159. doi:10.1016/S1074-5521(02)00248-X

Cai, S.-Y., Babbitt, R. W. and Marchesi, V. T. (1999). A mutant deubiquitinating enzyme (Ubp-M) associates with mitotic chromosomes and blocks cell division. Proc. Natl. Acad. Sci. USA 96, 2828-2833. doi:10.1073/pnas.96.6.2828

Clague, M. J., Heride, C. and Urbé, S. (2015). The demographics of the ubiquitin system. Trends Cell Biol. 25, 417-426. doi:10.1016/j.tcb.2015.03.002

Clague, M. J., Urbé, S. and Komander, D. (2019). Breaking the chains: deubiquitylating enzyme specificity begets function. Nat. Rev. Mol. Cell Biol. 20, 338-352. doi:10.1038/s41580-019-0099-1

Cressman, D. E., O'Connor, W. J., Greer, S. F., Zhu, X.-S. and Ting, J. P. (2001). Mechanisms of nuclear import and export that control the subcellular localization of class II transactivator. J. Immunol. 167, 3626-3634. doi:10.4049/jimmunol.167.7.3626

Daou, S., Mashtalir, N., Hammond-Martel, I., Pak, H., Yu, H., Sui, G., Vogel, J. L., Kristie, T. M. and Affar, E. B. (2011). Crosstalk between O-GlcNAcylation and proteolytic cleavage regulates the host cell factor-1 maturation pathway. Proc. Natl. Acad. Sci. USA 108, 2747-2752. doi:10.1073/pnas.1013822108

Daou, S., Hammond-Martel, I., Mashtalir, N., Barbour, H., Gagnon, J., Iannantuono, N. V. G., Nkwe, N. S., Motorina, A., Pak, H., Yu, H. et al. (2015). The BAP1/ASXL2 histone H2A deubiquitinase complex regulates cell proliferation and is disrupted in cancer. J. Biol. Chem. 290, 28643-28663. doi:10.1074/jbc.M115.661553

Daou, S., Barbour, H., Ahmed, O., Masclef, L., Baril, C., Sen Nkwe, N., Tchelougou, D., Uriarte, M., Bonneil, E., Ceccarelli, D. et al. (2018). Monoubiquitination of ASXLs controls the deubiquitinase activity of the tumor suppressor BAP1. Nat. Commun. 9, 4385. doi:10.1038/s41467-018-06854-2

Eletr, Z. M. and Wilkinson, K. D. (2014). Regulation of proteolysis by human deubiquitinating enzymes. Biochim. Biophys. Acta 1843, 114-128. doi:10.1016/j.bbamcr.2013.06.027

Emsley, P., Lohkamp, B., Scott, W. G. and Cowtan, K. (2010). Features and development of Coot. Acta Crystallogr. D Biol. Crystallogr. 66, 486-501. doi:10.1107/S0907444910007493

Esmaili, A. M., Johnson, E. L., Thaivalappil, S. S., Kuhn, H. M., Kornbluth, S. and Irusta, P. M. (2010). Regulation of the ATM-activator protein Aven by CRM1-dependent nuclear export. Cell Cycle 9, 3913-3920. doi:10.4161/cc.9.19.13138

Fraile, J. M., Quesada, V., Rodríguez, D., Freije, J. M. and Lopez-Otin, C. (2012). Deubiquitinases in cancer: new functions and therapeutic options. Oncogene 31, 2373-2388. doi:10.1038/onc.2011.443

Frangini, A., Sjöberg, M., Roman-Trufero, M., Dharmalingam, G., Haberle, V., Bartke, T., Lenhard, B., Malumbres, M., Vidal, M. and Dillon, N. (2013). The aurora B kinase and the

polycomb protein ring1B combine to regulate active promoters in quiescent lymphocytes. Mol. Cell 51, 647-661. doi:10.1016/j.molcel.2013.08.022

Fu, S. C., Imai, K. and Horton, P. (2011). Prediction of leucine-rich nuclear export signal containing proteins with NESsential. Nucleic Acids Res. 39, e111. doi:10.1093/nar/gkr493

Fung, H. Y., Fu, S. C. and Chook, Y. M. (2017). Nuclear export receptor CRM1 recognizes diverse conformations in nuclear export signals. Elife 6, e23961. doi:10.7554/eLife.23961.046

Garcia-Santisteban, I., Bañuelos, S. and Rodríguez, J. A. (2012). A global survey of CRM1-dependent nuclear export sequences in the human deubiquitinase family. Biochem. J. 441, 209-217. doi:10.1042/BJ20111300

Gelsi-Boyer, V., Trouplin, V., Adelaide, J., Aceto, N., Remy, V., Pinson, S., Houdayer, C., Arnoulet, C., Sainty, D., Bentires-Alj, M. et al. (2008). Genome profiling of chronic myelomonocytic leukemia: frequent alterations of RAS and RUNX1 genes. BMC Cancer 8, 299. doi:10.1186/1471-2407-8-299

Gomez-Diaz, C. and Ikeda, F. (2018). Roles of ubiquitin in autophagy and cell death. Semin. Cell Dev. Biol. 93, 125-135. doi:10.1016/j.semcdb.2018.09.004

Grumati, P. and Dikic, I. (2018). Ubiquitin signaling and autophagy. J. Biol. Chem. 293, 5404-5413. doi:10.1074/jbc.TM117.000117

Gu, Y., Jones, A. E., Yang, W., Liu, S., Dai, Q., Liu, Y., Swindle, C. S., Zhou, D., Zhang, Z., Ryan, T. M. et al. (2016). The histone H2A deubiquitinase Usp16 regulates hematopoiesis and hematopoietic stem cell function. Proc. Natl. Acad. Sci. USA 113, E51-E60. doi:10.1073/pnas.1517041113

Hammond-Martel, I., Pak, H., Yu, H., Rouget, R., Horwitz, A. A., Parvin, J. D., Drobetsky, E. A. and Affar, E. B. (2010). PI 3 kinase related kinases-independent proteolysis of BRCA1 regulates Rad51 recruitment during genotoxic stress in human cells. PLoS ONE 5, e14027. doi:10.1371/journal.pone.0014027

Hammond-Martel, I., Yu, H. and Affar, E. B. (2012). Roles of ubiquitin signaling in transcription regulation. Cell. Signal. 24, 410-421. doi:10.1016/j.cellsig.2011.10.009

Harper, J. W., Ordureau, A. and Heo, J.-M. (2018). Building and decoding ubiquitin chains for mitophagy. Nat. Rev. Mol. Cell Biol. 19, 93-108. doi:10.1038/nrm.2017.129

Heaton, S. M., Borg, N. A. and Dixit, V. M. (2016). Ubiquitin in the activation and attenuation of innate antiviral immunity. J. Exp. Med. 213, 1-13. doi:10.1084/jem.20151531

Hu, H. and Sun, S.-C. (2016). Ubiquitin signaling in immune responses. Cell Res. 26, 457-483. doi:10.1038/cr.2016.40

Jackson, S. P. and Durocher, D. (2013). Regulation of DNA damage responses by ubiquitin and SUMO. Mol. Cell 49, 795-807. doi:10.1016/j.molcel.2013.01.017

Joo, H.-Y., Zhai, L., Yang, C., Nie, S., Erdjument-Bromage, H., Tempst, P., Chang, C. and Wang, H. (2007). Regulation of cell cycle progression and gene expression by H2A deubiquitination. Nature 449, 1068-1072. doi:10.1038/nature06256

Julien, C., Coulombe, P. and Meloche, S. (2003). Nuclear export of ERK3 by a CRM1-dependent mechanism regulates its inhibitory action on cell cycle progression. J. Biol. Chem. 278, 42615-42624. doi:10.1074/jbc.M302724200

Komander, D., Clague, M. J. and Urbé, S. (2009). Breaking the chains: structure and function of the deubiquitinases. Nat. Rev. Mol. Cell Biol. 10, 550-563. doi:10.1038/nrm2731

Kosugi, S., Hasebe, M., Matsumura, N., Takashima, H., Miyamoto-Sato, E., Tomita, M. and Yanagawa, H. (2009). Six classes of nuclear localization signals specific to different binding grooves of importin α. J. Biol. Chem. 284, 478-485. doi:10.1074/jbc.M807017200

La Cour, T., Kiemer, L., Molgaard, A., Gupta, R., Skriver, K. and Brunak, S. (2004). Analysis and prediction of leucine-rich nuclear export signals. Protein Eng. Des. Sel. 17, 527-536. doi:10.1093/protein/gzh062

Lange, A., Mills, R. E., Lange, C. J., Stewart, M., Devine, S. E. and Corbett, A. H. (2007). Classical nuclear localization signals: definition, function, and interaction with importin alpha. J. Biol. Chem. 282, 5101-5105. doi:10.1074/jbc.R600026200

Liu, J. and DeFranco, D. B. (2000). Protracted nuclear export of glucocorticoid receptor limits its turnover and does not require the exportin 1/CRM1-directed nuclear export pathway. Mol. Endocrinol. 14, 40-51. doi:10.1210/mend.14.1.0398

Mashtalir, N., Daou, S., Barbour, H., Sen, N. N., Gagnon, J., Hammond-Martel, I., Dar, H. H., Therrien, M. and Affar, E. B. (2014). Autodeubiquitination protects the tumor suppressor BAP1 from cytoplasmic sequestration mediated by the atypical ubiquitin ligase UBE2O. Mol. Cell 54, 392-406. doi:10.1016/j.molcel.2014.03.002

Mendler, L., Braun, T. and Müller, S. (2016). The ubiquitin-like SUMO system and heart function: from development to disease. Circ. Res. 118, 132-144. doi:10.1161/CIRCRESAHA.115.307730

Mevissen, T. E. T. and Komander, D. (2017). Mechanisms of deubiquitinase specificity and regulation. Annu. Rev. Biochem. 86, 159-192. doi:10.1146/annurev-biochem-061516-044916

Mimnaugh, E. G., Kayastha, G., McGovern, N. B., Hwang, S.-G., Marcu, M. G., Trepel, J., Cai, S.-Y., Marchesi, V. T. and Neckers, L. (2001). Caspase-dependent deubiquitination of monoubiquitinated nucleosomal histone H2A induced by diverse apoptogenic stimuli. Cell Death Differ. 8, 1182-1196. doi:10.1038/sj.cdd.4400924

Murai, N., Murakami, Y. and Matsufuji, S. (2003). Identification of nuclear export signals in antizyme-1. J. Biol. Chem. 278, 44791-44798. doi:10.1074/jbc.M308059200

Nguyen Ba, A. N., Pogoutse, A., Provart, N. and Moses, A. M. (2009). NLStradamus: a simple hidden markov model for nuclear localization signal prediction. BMC Bioinformatics 10, 202. doi:10.1186/1471-2105-10-202

Nijman, S. M. B., Luna-Vargas, M. P., Velds, A., Brummelkamp, T. R., Dirac, A. M., Sixma, T. K. and Bernards, R. (2005). A genomic and functional inventory of deubiquitinating enzymes. Cell 123, 773-786. doi:10.1016/j.cell.2005.11.007

Nishi, R., Wijnhoven, P., le Sage, C., Tjeertes, J., Galanty, Y., Forment, J. V., Clague, M. J., Urbé, S. and Jackson, S. P. (2014). Systematic characterization of deubiquitylating enzymes for roles in maintaining genome integrity. Nat. Cell Biol. 16, 1016-1026. doi:10.1038/ncb3028

Panier, S. and Boulton, S. J. (2014). Double-strand break repair: 53BP1 comes into focus. Nat. Rev. Mol. Cell Biol. 15, 7-18. doi:10.1038/nrm3719

Perrody, E., Abrami, L., Feldman, M., Kunz, B., Urbé, S. and van der Goot, F. G. (2016). Ubiquitin-dependent folding of the Wnt signaling coreceptor LRP6. Elife 5, e19083. doi:10.7554/eLife.19083.018

Popovic, D., Vucic, D. and Dikic, I. (2014). Ubiquitination in disease pathogenesis and treatment. Nat. Med. 20, 1242-1253. doi:10.1038/nm.3739

Reyes-Turcu, F. E., Horton, J. R., Mullally, J. E., Heroux, A., Cheng, X. and Wilkinson, K. D. (2006). The ubiquitin binding domain ZnF UBP recognizes the C-terminal diglycine motif of unanchored ubiquitin. Cell 124, 1197-1208. doi:10.1016/j.cell.2006.02.038

Reyes-Turcu, F. E., Ventii, K. H. and Wilkinson, K. D. (2009). Regulation and cellular roles of ubiquitin-specific deubiquitinating enzymes. Annu. Rev. Biochem. 78, 363-397. doi:10.1146/annurev.biochem.78.082307.091526

Rodier, G., Montagnoli, A., Di Marcotullio, L., Coulombe, P., Draetta, G. F., Pagano, M. and Meloche, S. (2001). p27 cytoplasmic localization is regulated by phosphorylation on Ser10 and is not a prerequisite for its proteolysis. EMBO J. 20, 6672-6682. doi:10.1093/emboj/20.23.6672

Rubinsztein, D. C. (2006). The roles of intracellular protein-degradation pathways in neurodegeneration. Nature 443, 780-786. doi:10.1038/nature05291

Sahtoe, D. D. and Sixma, T. K. (2015). Layers of DUB regulation. Trends Biochem. Sci. 40, 456-467. doi:10.1016/j.tibs.2015.05.002

Schneider, C. A., Rasband, W. S. and Eliceiri, K. W. (2012). NIH Image to ImageJ: 25 years of image analysis. Nat. Methods 9, 671-675. doi:10.1038/nmeth.2089

Schwertman, P., Bekker-Jensen, S. and Mailand, N. (2016). Regulation of DNA double-strand break repair by ubiquitin and ubiquitin-like modifiers. Nat. Rev. Mol. Cell Biol. 17, 379-394. doi:10.1038/nrm.2016.58

Senft, D., Qi, J. and Ronai, Z. A. (2018). Ubiquitin ligases in oncogenic transformation and cancer therapy. Nat. Rev. Cancer 18, 69-88. doi:10.1038/nrc.2017.105

Shanbhag, N. M., Rafalska-Metcalf, I. U., Balane-Bolivar, C., Janicki, S. M. and Greenberg, R. A. (2010). ATM-dependent chromatin changes silence transcription in cis to DNA double-strand breaks. Cell 141, 970-981. doi:10.1016/j.cell.2010.04.038

Soniat, M. and Chook, Y. M. (2015). Nuclear localization signals for four distinct karyopherin-β nuclear import systems. Biochem. J. 468, 353-362. doi:10.1042/BJ20150368

Tanaka, K. and Matsuda, N. (2014). Proteostasis and neurodegeneration: the roles of proteasomal degradation and autophagy. Biochim. Biophys. Acta 1843, 197-204. doi:10.1016/j.bbamcr.2013.03.012

Uckelmann, M. and Sixma, T. K. (2017). Histone ubiquitination in the DNA damage response. DNA Repair 56, 92-101. doi:10.1016/j.dnarep.2017.06.011

Urbé, S., Liu, H., Hayes, S. D., Heride, C., Rigden, D. J. and Clague, M. J. (2012). Systematic survey of deubiquitinase localization identifies USP21 as a regulator of centrosome- and

microtubule-associated functions. Mol. Biol. Cell 23, 1095-1103. doi:10.1091/mbc.e11-08-0668

Vassilev, L. T., Tovar, C., Chen, S., Knezevic, D., Zhao, X., Sun, H., Heimbrook, D. C. and Chen, L. (2006). Selective small-molecule inhibitor reveals critical mitotic functions of human CDK1. Proc. Natl. Acad. Sci. USA 103, 10660-10665. doi:10.1073/pnas.0600447103

Vucic, D., Dixit, V. M. and Wertz, I. E. (2011). Ubiquitylation in apoptosis: a post-translational modification at the edge of life and death. Nat. Rev. Mol. Cell Biol. 12, 439-452. doi:10.1038/nrm3143

Wang, Z., Zhang, H., Liu, J., Cheruiyot, A., Lee, J.-H., Ordog, T., Lou, Z., You, Z. and Zhang, Z. (2016). USP51 deubiquitylates H2AK13,15ub and regulates DNA damage response. Genes Dev. 30, 946-959. doi:10.1101/gad.271841.115

Werner, A., Manford, A. G. and Rape, M. (2017). Ubiquitin-dependent regulation of stem cell biology. Trends Cell Biol. 27, 568-579. doi:10.1016/j.tcb.2017.04.002

Wertz, I. E. and Dixit, V. M. (2010). Regulation of death receptor signaling by the ubiquitin system. Cell Death Differ. 17, 14-24. doi:10.1038/cdd.2009.168

Xu, Y., Yang, H., Joo, H. Y., Yu, J. H., Smith, A. D. T., Schneider, D., Chow, L. T., Renfrow, M. and Wang, H. (2013). Ubp-M serine 552 phosphorylation by cyclin-dependent kinase 1 regulates cell cycle progression. Cell Cycle 12, 3219-3227. doi:10.4161/cc.26278

Yang, W., Lee, Y.-H., Jones, A. E., Woolnough, J. L., Zhou, D., Dai, Q., Wu, Q., Giles, K. E., Townes, T. M. and Wang, H. (2014). The histone H2A deubiquitinase Usp16 regulates embryonic stem cell gene expression and lineage commitment. Nat. Commun. 5, 3818. doi:10.1038/ncomms4818

Yau, R. and Rape, M. (2016). The increasing complexity of the ubiquitin code. Nat. Cell Biol. 18, 579-586. doi:10.1038/ncb3358

Zhang, Z., Yang, H. and Wang, H. (2014). The histone H2A deubiquitinase USP16 interacts with HERC2 and fine-tunes cellular response to DNA damage. J. Biol. Chem. 289, 32883-32894. doi:10.1074/jbc.M114.599605

Zheng, N. and Shabek, N. (2017). Ubiquitin ligases: structure, function, and regulation. Annu. Rev. Biochem. 86, 129-157. doi:10.1146/annurev-biochem-060815-014922

Zhuo, X., Guo, X., Zhang, X., Jing, G., Wang, Y., Chen, Q., Jiang, Q., Liu, J. and Zhang, C. (2015). Usp16 regulates kinetochore localization of Plk1 to promote proper chromosome alignment in mitosis. J. Cell Biol. 210, 727-735. doi:10.1083/jcb.201502044

Zimmermann, M. and de Lange, T. (2014). 53BP1: pro choice in DNA repair. Trends Cell Biol. 24, 108-117. doi:10.1016/j.tcb.2013.09.003

2.8 Supplemental figures and tables

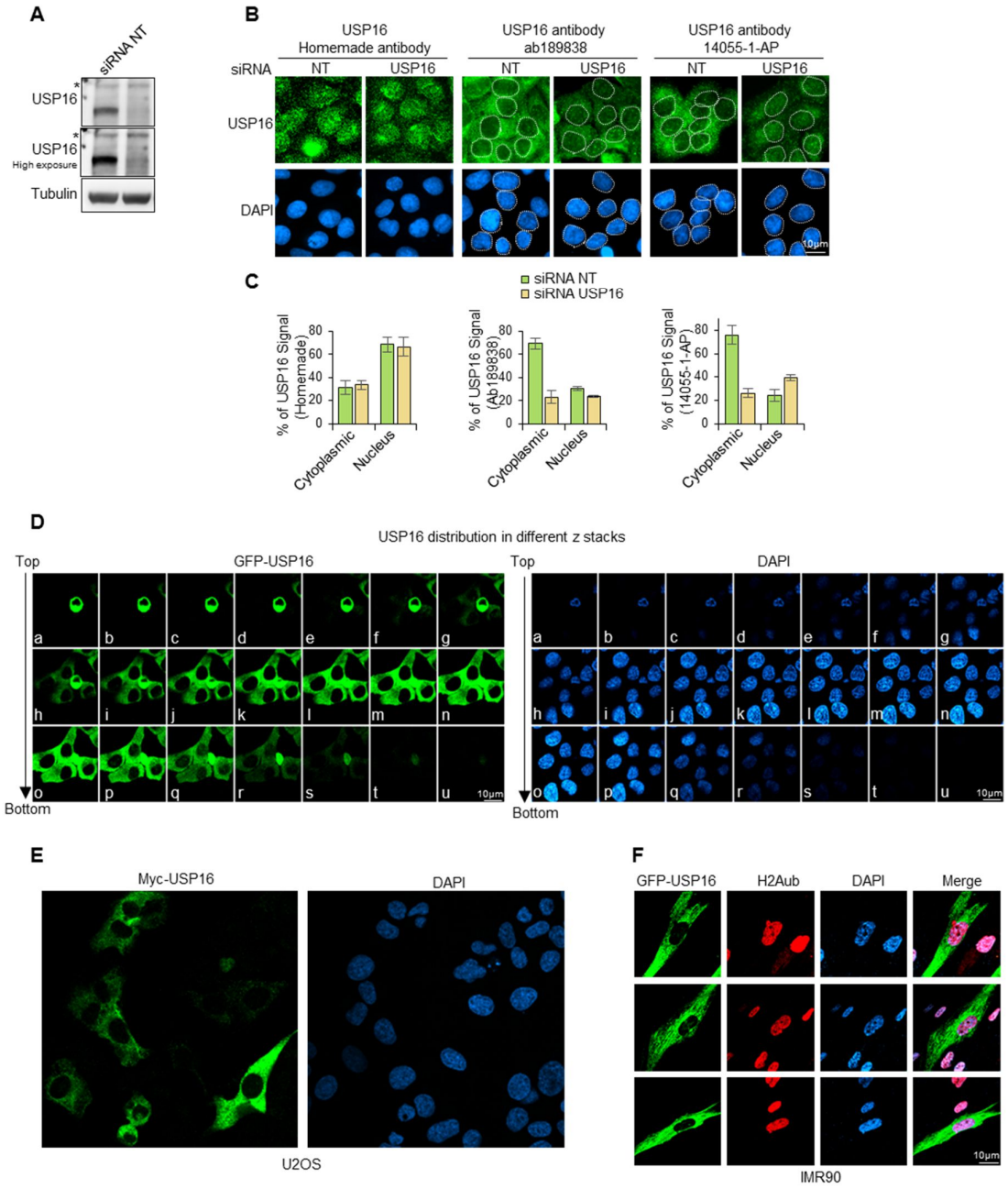

Figure 2-S 1 : USP16 is localized in the cytoplasm in interphase.

(A) Specificity of immunoblotting of USP16 using our homemade antibody. U2OS cells were transfected with non-target control (NT) or USP16 siRNAs for 72 hours. USP16 was detected by immunoblotting on total cell extracts. Tubulin was used as a loading control. The blots of USP16 correspond to two exposure times during chemiluminescence detection. The stars **(B)** U2OS cells were transfected with control (NT) or USP16 siRNAs for 72 hours. USP16

distribution was analyzed by immunofluorescence using homemade or commercial antibodies. **(C)** RGB profiles for the stainings were generated using ImageJ and relative quantification of the fluorescence signal in the nucleus versus cytoplasm was conducted. Data is presented as the percentage of fluorescence signal in each compartment versus total detection. Images were collected at regular intervals to create a stack in the Z axis using a localization of USP16 was determined by fluorescence microscopy. Immunofluorescence indicate non-specific bands or possible modified forms of USP16. n= 5 biological replicates. Signal and corresponds to an average quantification on 10 cells ± SD. n= 2 biological replicates **(D)** U2OS cells stably expressing GFP-USP16 were used for fluorescence confocal microscope. **(E)** U2OS cells stably expressing Myc-USP16 were used for fluorescence detection. Images were collected using a confocal microscope. n= 5 biological replicates **(F)** IMR90 cells stably expressing GFP-USP16 were fixed and the sub-cellular detection of H2Aub was also conducted. n= 3 biological replicates.

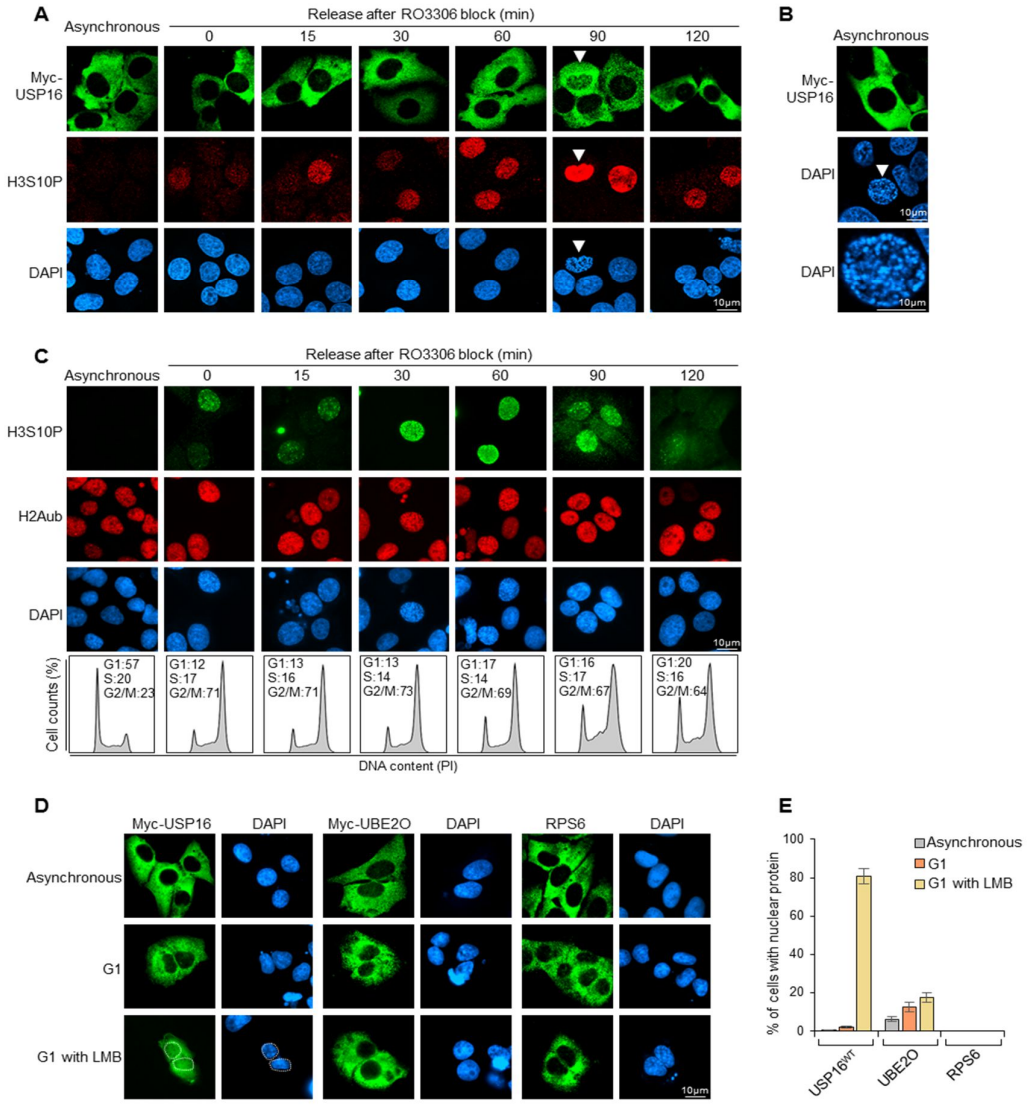

Figure 2-S 2 : USP16 is transiently retained in the nucleus after mitosis.

(A) USP16 is not detected in the nucleus following cell cycle arrest in G2 and during progression towards mitosis. U2OS cells stably expressing Myc-USP16 were enriched in G2 phase with 10 μM of RO3306 treatment and released at selected time points. USP16 subcellular localization and the levels of H3S10P were determined by immunofluorescence as indicated. Note that H3S10P staining could be readily observed, but without a distinct accumulation of USP16 in the nucleus. The arrow indicates a cell starting mitosis. n= 3 biological replicates. **(B)** USP16 is not detected in the nucleus during chromosome condensation. The arrow indicates a nucleus starting chromosome condensation. **(C)** U2OS cells stably expressing Myc-USP16 were enriched in G2 phase with 10 μM of RO3306 treatment and released at selected times. The levels of H2Aub and H3S10P were determined by immunofluorescence as indicated. The

cell cycle profiles were analyzed by propidium iodide staining and FACS (Bottom panels). n= 3 biological replicates. **(D)** U2OS cells were transfected with pDEST Myc-USP16 WT or pDEST Myc-UBE2O for three days. Cells were then synchronized with nocodazole and then released in the absence or presence of 10 nM of LMB for 5 hours. The sub-cellular localization of USP16 or UBE2O as well as endogenous Ribosomal Protein S6 (RPS6) was determined by immunofluorescence as indicated. No cells with nuclear RPS6 were observed. **(E)** Cell counts from experiments performed as indicated in panel D showing the nuclear localization of the indicated proteins. The results are from 3 independent experiments and the values are presented as average ± SD.

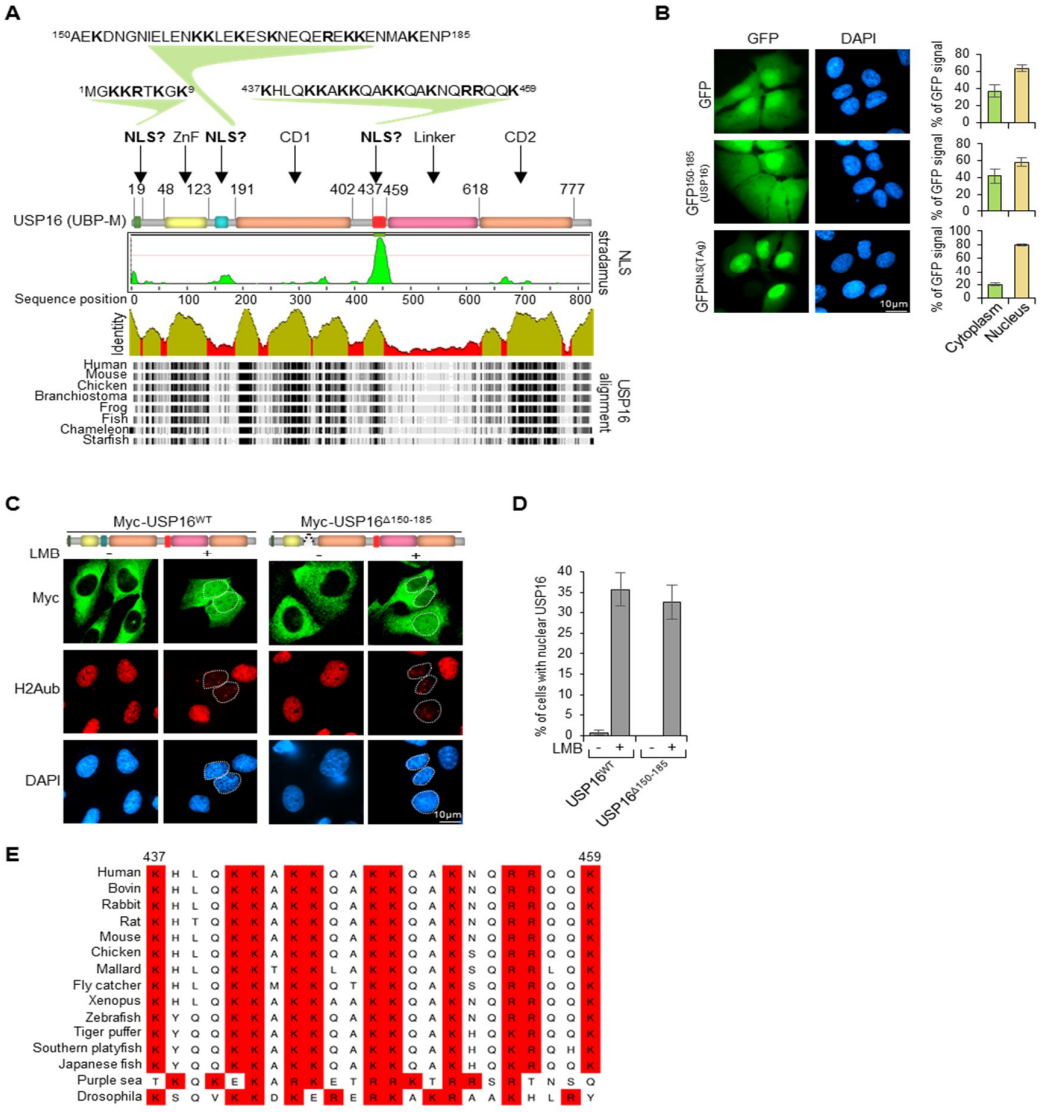

Figure 2-S 3 : Identification of USP16 NLS.

(A) Prediction of NLS sequences in USP16. NLS sequences predictions were done with NLStradamus prediction software. The main functional domains of USP16 as well as the predicted NLS peptides are indicated. Multiple sequences alignment of USP16 across different species is also shown. **(B)** The 150-185 amino acid sequence of USP16 is not sufficient to target GFP to the nucleus. pEGFP N3, GFP N3 150-185(USP16) and pOD35 GFP NLS (TAg) constructs were transfected in U2OS and sub-cellular localization of fusion proteins was detected by fluorescence. T antigen NLS was included as a positive control. Relative quantification of GFP signal in the nucleus versus cytoplasm was conducted on 10 cells and data is presented as average ±SD. n= 3 biological replicates. **(C)** Deletion of the 150-185 amino acid sequence of USP16 does not perturb its localization with or without LMB treatment. U2OS

cells stably expressing Myc-USP16WT or Myc-USP16Δ150-185 were treated with 10 nM of LMB for 24 hours. Sub-localization was determined by immunofluorescence with the indicated antibodies. n= 3 biological replicates. **(D)** Cell counts of USP16 nuclear localization from experiments performed as indicated in panel C. The results are from three independent experiments and the values are presented as average ± SD. n= 3 biological replicates. **(E)** Conservation of USP16 NLS. Sequence alignments of USP16 orthologs. The alignment was performed with Aline using different sequences of USP16 obtained from Uniprot. The lysine and arginine residues forming the NLS are highlighted in red.

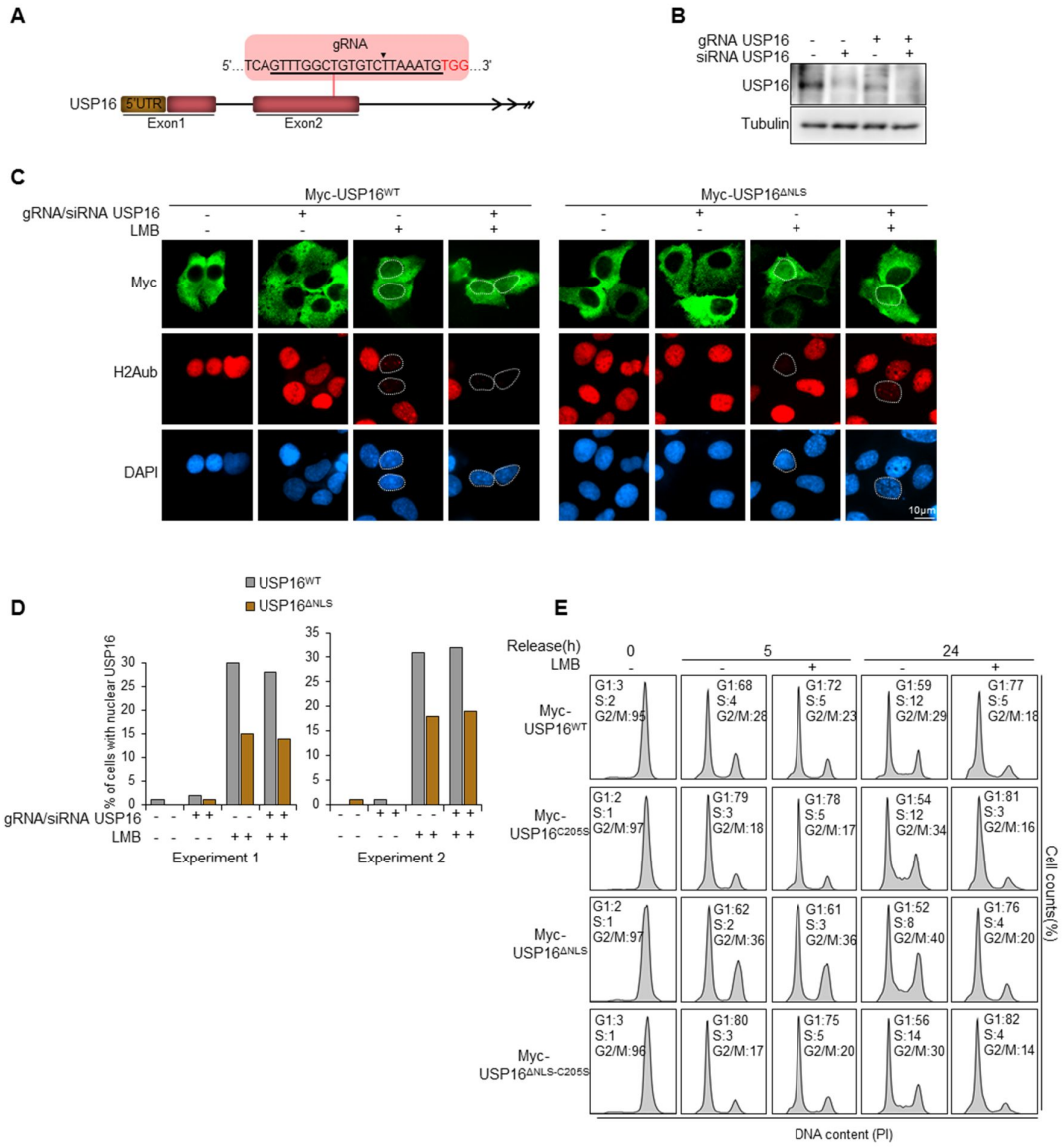

Figure 2-S 4 : Localization of USP16 lacking its NLS in the absence of endogenous USP16.

(A) Graphical representation of USP16 gene and the gRNA sequence used for CRISPR/Cas9 targeting. **(B)** Depletion of USP16 using CRISPR/Cas9 and RNAi approaches. U2OS cells were transfected with USP16 siRNA for 72 hours or infected with CRISPR/Cas9 lentiviruses targeting USP16. U2OS cells were also infected with CRISPR/Cas9 lentiviruses and then subjected to siRNA for 72 hours and then used for USP16 detection by immunoblotting as indicated. Tubulin was used as a loading control. n= 2 biological replicates. **(C)** U2OS cells stably expressing Myc-USP16WT or Myc-USP16ΔNLS were infected with CRISPR/Cas9 lentivirus particles with gRNA targeting USP16. Cells were then also transfected with USP16 siRNA for 72 hours to obtain a strong reduction of USP16 in the majority of the cell population. Cells were then treated with 10 nM LMB for 24 hours and used for immunofluorescence as

indicated. **(D)** Cell counts from two experiments performed as indicated in panel C showing nuclear localization of USP16 and its corresponding mutants. More than 100 cells were counted in each condition. n= 2 biological replicates. **(E)** The cell cycle profile of each population from Figure 4 panel A was analyzed by propidium iodide staining and FACS.

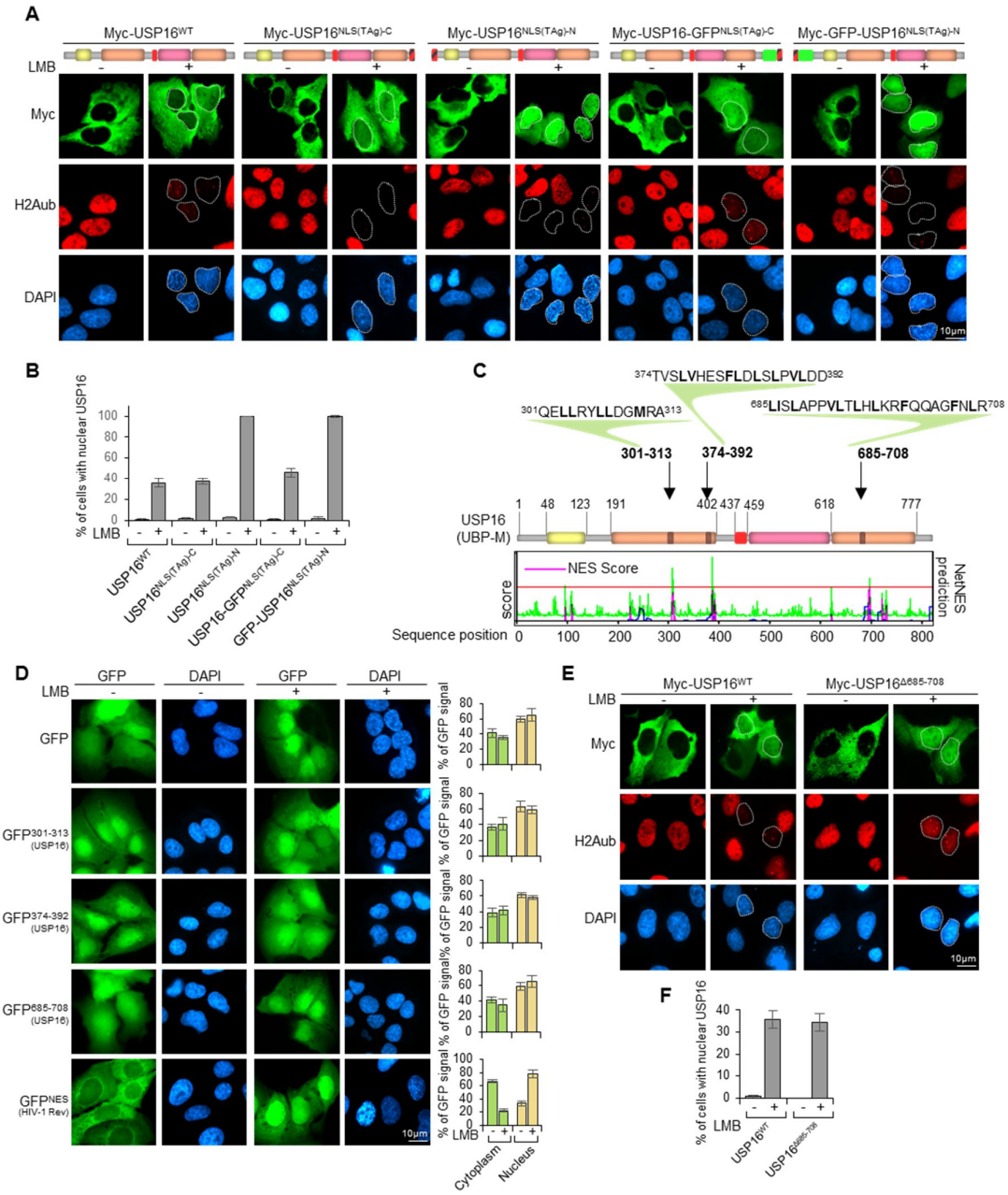

Figure 2-S 5 : Identification of USP16 nuclear export signal.

(A) U2OS cells expressing Myc-USP16WT, Myc-USP16NLS(TAg)-C, Myc-USP16NLS(TAg)-N, USP16-GFPNLS(TAg)-C or USP16-GFPNLS(TAg)-N were treated with

10 nM of LMB for 24 hours. Sub-cellular localization was determined by immunofluorescence using the indicated antibodies. Schematic representation of the different USP16 constructs are shown. n= 3 biological replicates. **(B)** Cell counts from experiments performed as indicated in panel A showing sub-cellular localization of USP16 and its corresponding mutants. More than 100 cells were counted in each condition. The results are from 3 independent experiments and the values are presented as average ± SD. **(C)** NES sequences predictions were done with NetNES 1.1 Server prediction software. The colored lines correspond to different probability score values and the red line represents a probability threshold. The main functional domains of USP16 as well as the predicted NES sequences are shown. **(D)** U2OS cells were transfected with pEGFP N3, GFP-301-313 (USP16), GFP-374-392 (USP16), GFP-685-708 (USP16) or GFP-NES (HIV-1 Rev) expression constructs. Cells were treated with 10 nM of LMB and sub-cellular localization of these GFP-fusion proteins was determined by fluorescence. RGB profiles for GFP staining were generated using ImageJ and relative quantification of fluorescence signals in the nucleus and cytoplasm was conducted. Data is presented as the percentage of fluorescence signal in each compartment versus total signal and corresponds to the average measurements on 10 cells ± SD. n= 3 biological replicates. **(E)** U2OS cells stably expressing USP16WT or USP16Δ685-708 were treated with LMB for 24 hours. The sub-cellular localization of USP16 was determined by immunofluorescence using the indicated antibodies. n= 3 biological replicates. **(F)** Cell counts from experiments performed as indicated in panel E showing the nuclear localization of USP16. The results are from 3 independent experiments and the values are presented as average ± SD.

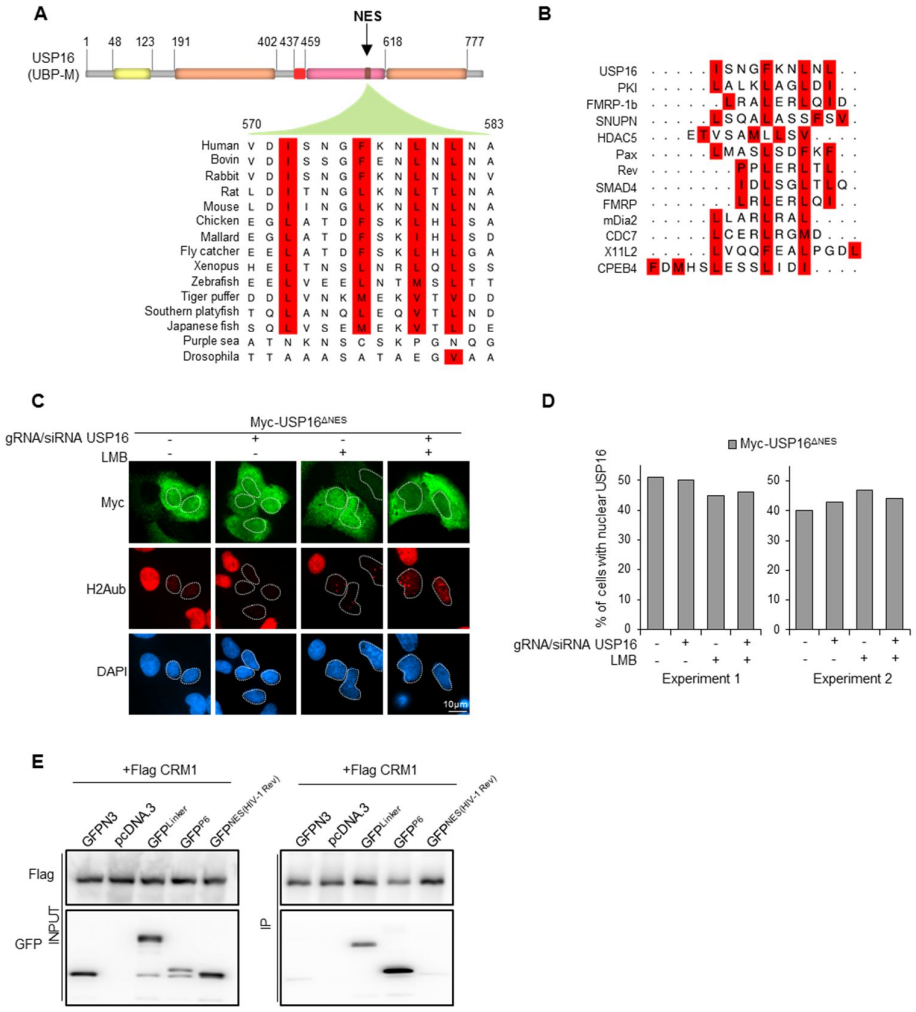

Figure 2-S 6 : Localization of USP16 lacking its NES in the absence of endogenous USP16.

(A) Phylogenetic conservation of USP16 NES. Sequence conservation of the NES region of USP16 between different species. Sequences were obtained from Uniprot database and aligned using Aline software. The hydrophobic amino acids forming the NES are highlighted in red. **(B)** Sequence comparison of the NES region of USP16 with different NES sequences from different proteins. Sequence alignment was done with Aline. The hydrophobic amino acids forming USP16 and the current NES patterns are highlighted in red. **(C)** Localization of Myc-USP16ΔNES following depletion of endogenous USP16. U2OS cells stably expressing Myc-USP16ΔNES were infected with CRISPR/Cas9 lentiviral particles targeting USP16 and then transfected with USP16 siRNA for 72 hours. Cells were then treated with 10 nM of LMB for 24 hours. Sub-cellular localization was determined by immunofluorescence using the indicated antibodies. **(D)** Count from two experiments performed in C showing sub-cellular localization of Myc-USP16ΔNES. At least 100 cells were counted for each condition. n= 2 biological

replicates. **(E)** Interaction between USP16-NES and CRM1/ Exportin1. HEK293T cells were transfected with pEGFP N3, pcDNA, GFP-Linker, GFP-P6, GFP-NES (HIV-1 Rev) or Flag-CRM1 vectors and subjected to immunoprecipitation and immunoblotting. n= 2 biological replicates.

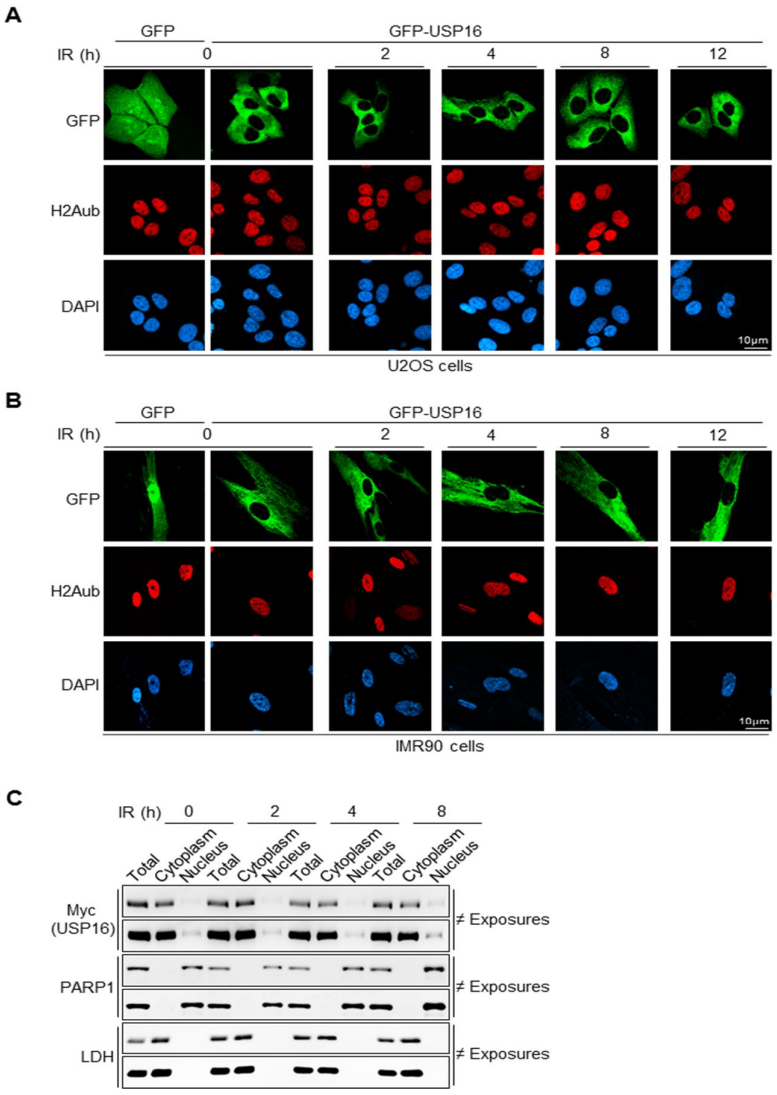

Figure 2-S 7 : Ionizing radiation treatment does not induce USP16 nuclear translocation. USP16 is not translocated into the nucleus during DNA damage by ionizing radiation. (A) U2OS cells stably expressing GFP-USP16 were irradiated with ionizing radiation (7,5 Gy). USP16 sub-cellular localization was determined by fluorescence as indicated. Cells expressing GFP were used as controls for transduction efficiency. (B) IMR90 cells stably expressing GFP-USP16 were treated and analyzed as in panel A. n= 2 biological replicates. (C) U2OS cells stably expressing Myc-USP16 were subjected to ionizing radiation (IR) (7,5 Gy) and harvested at the indicated time points for cell fractionation. Nuclear and cytoplasmic fractions were

prepared at the indicated time points. PARP-1 and LDH were used as fractionation controls for nuclear and cytoplasmic fractions, respectively. n= 3 biological replicates.

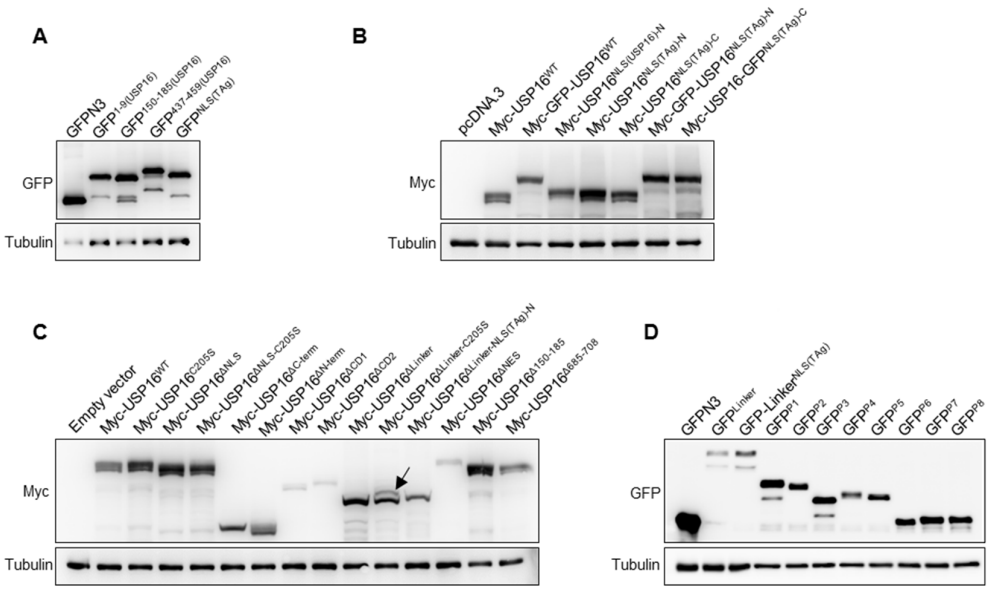

Figure 2-S 8 : Immunoblotting detection of protein expression for the constructs used in this study.

(A) U2OS cells were transfected with expression constructs encoding various GFP-peptide fusions. Three days post-transfection, cells were harvested for immunoblotting using anti-GFP antibody. n= 3 biological replicates. **(B)** U2OS cells were transfected with various expression constructs encoding fusions of USP16 with GFP and/or NLS sequences. Three days later, cells were harvested for immunoblotting using anti-Myc antibody. n= 3 biological replicates. **(C)** U2OS cells were transduced with viruses harboring expression constructs for various deletions or mutations in USP16. Two days later, cells were selected with puromycin for 48 hours and pools of cells stably expressing proteins were harvested for immunoblotting using anti-Myc antibody. n= 3 biological replicates. **(D)** U2OS cells were transfected with expression constructs encoding various GFP-peptide fusions. Three days post-transfection, cells were harvested for immunoblotting using anti-GFP antibody. α-Tubulin was used as a loading control. n= 3 biological replicates.

Table 2-S1 : List of antibodies used.

Antibody	Source	Catalogue number	Dilution	Reference
Mouse monoclonal anti-Flag (M2)	Sigma-Aldrich	F3165	1:2000 (IF)	(Daou et al., 2018)
Mouse monoclonal anti-MYC	Covance	9E10	1:1000 (IF)	(Daou et al., 2018)
Homemade rabbit polyclonal anti-USP16	This study	NA	1:1000 (IF) 1:1000 (WB)	This study
Rabbit polyclonal anti-H2Aub K119 (D27C4)	Cell signaling	8240	1:5000 (IF) 1:10000 (WB)	(Daou et al., 2018)
Mouse monoclonal anti RPS6 (C8)	Santa Cruz	sc-74459	1:1000 (IF)	(Xie et al., 2019)
Mouse monoclonal anti-Tubulin (B-5-1-2)	Santa Cruz	sc-23948	1:2000 (WB)	(Daou et al., 2018)
Mouse monoclonal anti-PARP-1 (F-2)	Santa Cruz	sc-8007	1:2000 (WB)	(Hammond-Martel et al., 2010)
Mouse monoclonal anti-LDH (H-10)	Santa Cruz	sc-133123	1:1000 (WB)	(Daou et al., 2011)
Mouse monoclonal anti-Ring1B (N-32)	Santa Cruz	sc-101109	1:1000 (WB)	(Mashtalir et al., 2014)
Mouse monoclonal anti-Ubiquitin (P4D1)	Santa Cruz	sc-8017	1:500 (WB)	(Hammond-Martel et al., 2010)
Rabbit polyclonal anti-YY1 (H414)	Santa Cruz	sc-1703	1:1000 (WB)	(Daou et al., 2018)
Rabbit polyclonal anti-53BP1 (H300)	Santa Cruz	sc-22760	1:2000 (IF)	(Yu et al., 2014)
Rabbit polyclonal anti-USP16	Proteintech	14055-1-AP	1:500 (IF)	This study
Mouse monoclonal anti-phospho-H3 (Ser10) (3H10)	Millipore-Sigma	05-806	1:2000 (IF)	(Payton et al., 2018)
Rabbit polyclonal anti-phospho-H3 (Ser10)	Millipore-Sigma	06-570	1:1000 (IF)	(Teixeira et al., 2015)
Rabbit polyclonal anti-USP16	Abcam	ab189838	1:1000 (IF)	This study
Mouse anti-HA (home-made)	Homemade	NA	1:1000 (WB)	(Mashtalir et al., 2014)
Anti-mouse Alexa Fluor® 488	Life Technologies	A11029	1:1000 (IF)	(Daou et al., 2018)
Anti-rabbit Alexa Fluor® 594	Life Technologies	A11012	1:1000 (IF)	(Daou et al., 2018)
Alexa FluorTM 594-conjugated wheat germ agglutinin (WGA)	Life Technologies	W11262	1:1000 (IF)	(Yamamoto et al., 2017)

Table 2-S2 : siRNA/gRNA sequences used.

Target	Sequences		Name
hUSP16	siRNA_1	GGAUAAUGAUCUGGAGGUU	SASI_Hs01_00210893
	siRNA_2	GAAUGAUAGUCAUACUCCU	SASI_Hs01_00210894
	siRNA_3	GUGAAAGGAAGCAUGUUUA	SASI_Hs01_00210895
	siRNA_4	CCAAGAACCAACGAAGACA	SASI_Hs01_00210890
	gRNA_Foward	caccgGTTTGGCTGTGTCTTAAATG	N/A
	gRNA_Reverse	AaacCATTTAAGACACAGCCAAACC	N/A
hRing1A	siRNA_1	GAGUGUCCUACCUGCCGAA	SASI_Hs01_00058433
	siRNA_2	GGAAUACGAGGCCCAUCAA	SASI_Hs01_00058434
	siRNA_3	CUAUCUGCCUGGACAUGGU	SASI_Hs01_00058435
	siRNA_4	CACAGAUUCUGCUCUGACU	SASI_Hs02_00334761
hRing1B	siRNA_1	CUAGUGAAAUUGAAUUAGU	SASI_Hs01_00213463
	siRNA_2	GACUACAAAGGAGUGUUUA	SASI_Hs01_00213464
	siRNA_3	GAAUGUCCUACCUGUCGGA	SASI_Hs01_00213465
	siRNA_4	GUUGAUCACUUAUCCAAGU	SASI_Hs02_00343201

CHAPITRE 3

3 ARTICLE : Liquid phase separation of the mammalian nuclear proteasome links amino acid supply to apoptosis

---

Article sous révision à Nature Communication

Maxime Uriarte[1,2], Nadine Sen Nkwe[2,3], Roch Tremblay[2,3], Nazar Mashtalir[4,5], Haithem Barbour[2,6], Salima Daou[2,7], Djaileb Abdelhadi[1,2], Anaïs Darracq[2,3], Nicolas Desjardins-Lecavalier[2], Przemyslaw Sapieha[2,8,9], Jean-Yves Masson[10,11], Mikhail Sergeev[2,12], Eric Milot[2,12], Hugo Wurtele[2,12] and El Bachir Affar[2,12,13]

[1]Department of Biochemistry, University of Montreal, Montreal, Quebec, Canada
[2]Maisonneuve-Rosemont Hospital Research Center, Montréal, QC H1T 2M4, Canada
[3]Molecular Biology Programs, University of Montreal, Montreal, H3A 0G4, Quebec, Canada
[4]Department of Pediatric Oncology, Dana-Farber Cancer Institute and Harvard Medical School, Boston, MA 02215, USA.
[5]Broad Institute of MIT and Harvard, Cambridge, MA 02142, USA.
[6]Biomedical Sciences Programs, University of Montreal, Montreal, H3C 3T5, Quebec, Canada
[7]Lunenfeld-Tanenbaum Research Institute, Sinai Health System, Toronto, ON M5G 1X5, Canada.
[8]Department of Ophthalmology, University of Montréal, Montréal, Québec, Canada.
[9]Department of Neurology-Neurosurgery, McGill University, Montreal, Quebec, Canada
[10]CHU de Québec Research Center, Oncology Division, 9 McMahon, Québec City, QC, G1R 3S3, Canada;
[11] Laval University Cancer Research Center, Québec City, QC, G1V 0A6, Canada
[12]Department of Medicine, University of Montréal, Montréal H3C 3J7, Québec, Canada.
[13]Correspondence: el.bachir.affar@umontreal.ca

Running title: LLPS of the mammalian proteasome in the nucleus

Keywords: Proteasome, Liquid-liquid phase separation, Nutrient starvation, SIPAN, Ubiquitin, RAD23B, Deubiquitinase, Amino acids

Introduction de l'article :

Le chapitre 3 de cette étude est consacré à investiguer l'implication du système ubiquitine protéasome dans la séparation de phase liquide-liquide (LLPS). Les analyses effectuées dans cet article permettront de répondre à la deuxième hypothèse de cette thèse.

Le protéasome 26S est un complexe multi-protéique vital pour les cellules. Cependant, la façon dont le protéasome est régulé pendant les réponses au stress n'est pas bien comprise. Chez la levure *S. Cerevisiae* et chez la plante *Arabidopsis thaliana*, il a été rapporté que le protéasome nucléaire subit une LLPS et migre vers le cytoplasme pour être stocké sous forme de granules en réponse à un stress métabolique. De ce fait, nous nous sommes intéressés au rôle du protéasome lors d'un stress métabolique dans les cellules humaines.

Nos travaux montrent que le protéasome subit une LLPS et s'accumule dans le noyau sous forme de foci après une privation en nutriments. De plus nous avons identifié la protéine Rad23B comme médiateurs nécessaire à la formation de ces foci. De façon intéressante, nous avons pu démontrer que l'absence d'acides aminés non essentiels favoriserait l'apparition de ces foci, ce qui induirait la mort des cellules par apoptose.

Contribution :

En tant que deuxième auteure avec une contribution majeure, ma collaboration est de 30 %. J'ai contribué à la conception et à l'élaboration du rationnel de cet article. J'ai participé à la préparation des protocoles, à la réalisation de plusieurs expériences, à l'analyse de résultats, à l'assemblage de figures et à la correction du manuscrit.

3.1 Abstract

Eukaryotic cells have evolved highly orchestrated protein catabolic machineries responsible for the timely and selective disposal of proteins and organelles, thereby ensuring amino acid recycling. However, how proteasome-mediated protein degradation is coordinated with amino acid supply and protein synthesis has remained largely elusive. Here we show that the mammalian proteasome, including the 20S catalytic, the 19S regulatory and the 11S proteasome activator PSME3 particles, undergo liquid-liquid phase separation (LLPS) in the nucleus upon amino acid deprivation. We termed these proteasome condensates SIPAN (Starvation Induced Proteasome Assemblies in the Nucleus) and show that these are distinct from previously known nuclear foci and bodies. SIPAN are subjected to fusion events and rapidly exchange proteasome components with the surrounding milieu, highlighting their dynamic nature. We also found that SIPAN dissolve quickly following amino acid replenishment, and that their resolution requires deubiquitination. We further show that: (i) SIPAN colocalize with conjugated ubiquitin, (ii) proteasome inhibition accelerate SIPAN formation, and (iii) RAD23B proteasome shuttling factor is required for proteasome LLPS, and this involves its ubiquitin-like and ubiquitin-binding domains. In support of these findings, purified RAD23B drives LLPS *in vitro*. Finally, we found that depletion of RAD23B or PSME3 prevents apoptosis triggered by amino acid depletion. Altogether, our data show that RAD23B orchestrates SIPAN dynamics, and provide evidence that formation of these structures is associated with decreased cell survival during periods of amino acid starvation.

3.2 Introduction

Protein degradation and subsequent recycling of amino acids is fundamental for normal cell physiology. The autophagy system targets large macromolecule complexes, protein aggregates and organelles, all of which are first engulfed within double membrane-delimited structures and subsequently delivered to the lysosome for degradation [288-290]. On the other hand, the proteasome catalyzes the degradation of proteins in surplus, improperly folded or unwanted at a given time or in a specific subcellular location [291-293].

The proteasome is a highly conserved protein degradation machinery that generally recognizes substrates that are polyubiquitinated through the concerted action of E2 ubiquitin conjugating enzymes and E3 ubiquitin ligases. The 26S proteasome is composed of 2 sub-complexes, the 20S cylinder-like catalytic particle (CP) and the 19S regulatory particle (RP) (**Fig. 3-1a**). The CP contains the proteases with caspase-like, trypsin-like and chymotrypsin-

like activities that are responsible for substrate degradation into small peptides, and is the target of the widely used proteasome inhibitors (e.g., MG132 and Bortezomib) [294, 295]. The RP is also a large multi-protein complex that binds the CP to assemble a competent proteasome. The RP is responsible for the recognition and unfolding of polyubiquitinated proteins, as well as their translocation inside the CP. The CP can also associate with other regulatory complexes including the homopentameric ring-shaped 11S complex composed of PSME3 (PA28γ or REG), which targets proteins for ubiquitin-independent degradation (**Fig. 3-1a**) [296].

While a large body of findings have elucidated how the proteasome functions and target its substrates, much less is known about how the proteasome is regulated and how the overall protein degradation is coordinated with protein synthesis and metabolic demands. In the budding yeast, *Saccharomyces cerevisiae*, the 26S proteasome is relocated from the nucleus to the cytoplasm during quiescence [287] . The cytoplasmic proteasome assembles a large condensate termed Proteasome Storage Granule (PSG), and these structures are rapidly dissipated when cells resume proliferation [287]. While nitrogen starvation results in proteasome degradation by autophagy, a process termed proteaphagy; glucose starvation induces the formation of cytoplasmic PSG. It was concluded that PSG protects the proteasome from autophagy, thus promoting yeast cell viability following periods of carbon starvation [297]. Interestingly, carbon deprivation also induces the formation of large cytoplasmic PSG-like structures in Arabidopsis [297] and nitrogen starvation results in proteaphagy [298]. In this organism, proteaphagy requires a multivalent binding of RPN10 subunit of the proteasome with ubiquitin and the ubiquitin-like protein, Autophagy-related protein 8 (Atg8) [298]. These findings further highlight the evolutionary conservation and functional importance of proteasome relocalization and regulation mechanisms.

In animal species, including mammals, the mechanisms that coordinate protein synthesis with degradation are incompletely understood. For instance, conflicting results exist on the link between the mammalian target of rapamycin (mTOR) kinase, which promotes anabolism and protein synthesis; and the signaling pathways that coordinate proteasome function. While mTOR increases proteasome-mediated proteolysis [115], this kinase also negatively regulates the proteasome and autophagy degradation systems [116]. On the other hand, the proteasome was shown to be partly degraded by the autophagy machinery following nutrient starvation [117]. Indeed, amino acid starvation induces proteasome recognition by the ubiquitin-associated domain of p62/SQSTM1 and subsequent engulfment by the autophagy system in the cytoplasm [117]. However, it remained unclear how the nuclear proteasome is

regulated in response to nutrient deprivation. In this study, we show that the mammalian proteasome undergoes liquid-liquid phase separation (LLPS) in the nucleus in response to amino acid starvation. We present a characterization of these heretofore unreported proteasome condensates, which we termed SIPAN (Starvation Induced Proteasome Assemblies in the Nucleus).

3.3 Results

- **Nutrient starvation induces the formation of proteasome foci in the nucleus of mammalian cells.**

In yeast, the 26S proteasome particle translocate to the cytoplasm and form proteasome storage granules (PSG), in response to carbon starvation or quiescence entry [287, 297], but whether the mammalian proteasome is also subjected to a similar regulation has remained unclear. We initially conducted immunostaining following incubation of IMR90 primary human foetal lung fibroblasts in Hank's Balanced Salt Solution (HBSS), which contain 1 g/L of glucose as the only nutrient, and revealed that PSMD4 subunit of the RP localizes in spherical nuclear foci (**Figure 3-1a, b; Figure 3-S1a**). Several components of the CP, e.g., PSMB1, PSMB2, PSMB4, PSMB6 and PSMB7, colocalize with PSMD11 or PSMD4, components of the RP, following incubation of IMR90 in HBSS (**Figure 3-S1b**). C-terminal GFP-tagged versions of PSMB4, PSMB5, PSMD12 or PSMD14, all localize in nuclear foci, following incubation of IMR90 in HBSS starvation (**Figure 3-1c and Figure 3-S1c**). These results suggest that fully assembled 26S proteasome particle is directed to nuclear foci in response to nutrient deprivation. PSME3 proteasome activator complex also localizes in nuclear foci with PSMD14 following incubation of IMR90 in HBSS (**Figure. 3-1d**). Some components of the proteasome are not showed because we did not detect a specific endogenous PSMB or PSMD signal by fluorescence.

We sought to test whether CP and RP are independently assembled in proteasome foci upon nutrient starvation. Following siRNA-mediated depletion of PSMB5, PSMB6 or PSMB7 components of the CP, the global protein levels of the soluble RP components didn't change (**Figure 3-1e**). However, we observed reduced accumulation of the RP components, PSMD4, PSMD7 or the CP component PSMB4, in nuclear foci (**Figure 3-1f and Figure 3-S2a, b**). Conversely, depletion of PSMD4, PSMD7, PSMD11 or PSMD14 components of RP results in reduced assembly of PSMB4 in nuclear foci. Similar results were obtained from treatment of

IMR90 cells stably expressing PSMB4-GFP (**Figure 3-1g and Figure 3-S2b**). We concluded that proteasome integrity is required for PSMD4 or PSMB4 foci formation following nutrient deprivation. In addition to IMR90 cells, nuclear foci of PSMD4 or PSMD7 are found in several other normal or transformed mammalian cell types (**Figure 3-S3a**). Proteasome foci are also observed in mouse embryonic stem cells (mESC) and differentiated 3T3L1 mouse adipocytes upon nutrient starvation (**Figure 3-S3a-c**). We used IMR90 and HCT116 cell lines for further characterization becauce they showed the best nuclear foci formation.

We found that PSMB4 foci are not induced when cells are exposed, in normal culture medium, to osmotic stress (NaCl, mannitol or sucrose), proteotoxic stress (MG132 or Bortezomib), oxidative stress (H_2O_2), heat shock (45 °C), genotoxic stress (ionizing radiation or UVC light) or hypoxia (1% O_2) (**Figure 3-S4a, top panel**). Cell survival was assessed after one week of recovery in normal medium to ensure treatment efficacy (**Figure 3-S4a, bottom panel**). Nuclear proteasome structures, detected with PSMD11 or PSMD4 antibodies, do not correspond to any known nuclear foci, condensates or bodies such as PML bodies (PML staining), nucleoli (Fibrillarin staining), nuclear speckles (SC35 staining) or DNA double strand break foci (53BP1 staining) (**Figure 3-1h and Figure 3-S4b**). Confocal microscopy indicated that PSMB4-GFP foci are preferentially located in low-density chromatin regions (**Figure 3-1i**). This was confirmed by transmission electronic microscopy, which also revealed that nuclear proteasome foci are membrane-less protein condensates (**Figure 3-1j**). We termed the above-described nuclear structures Starvation-Induced Proteasome Assemblies in the Nucleus (SIPAN).

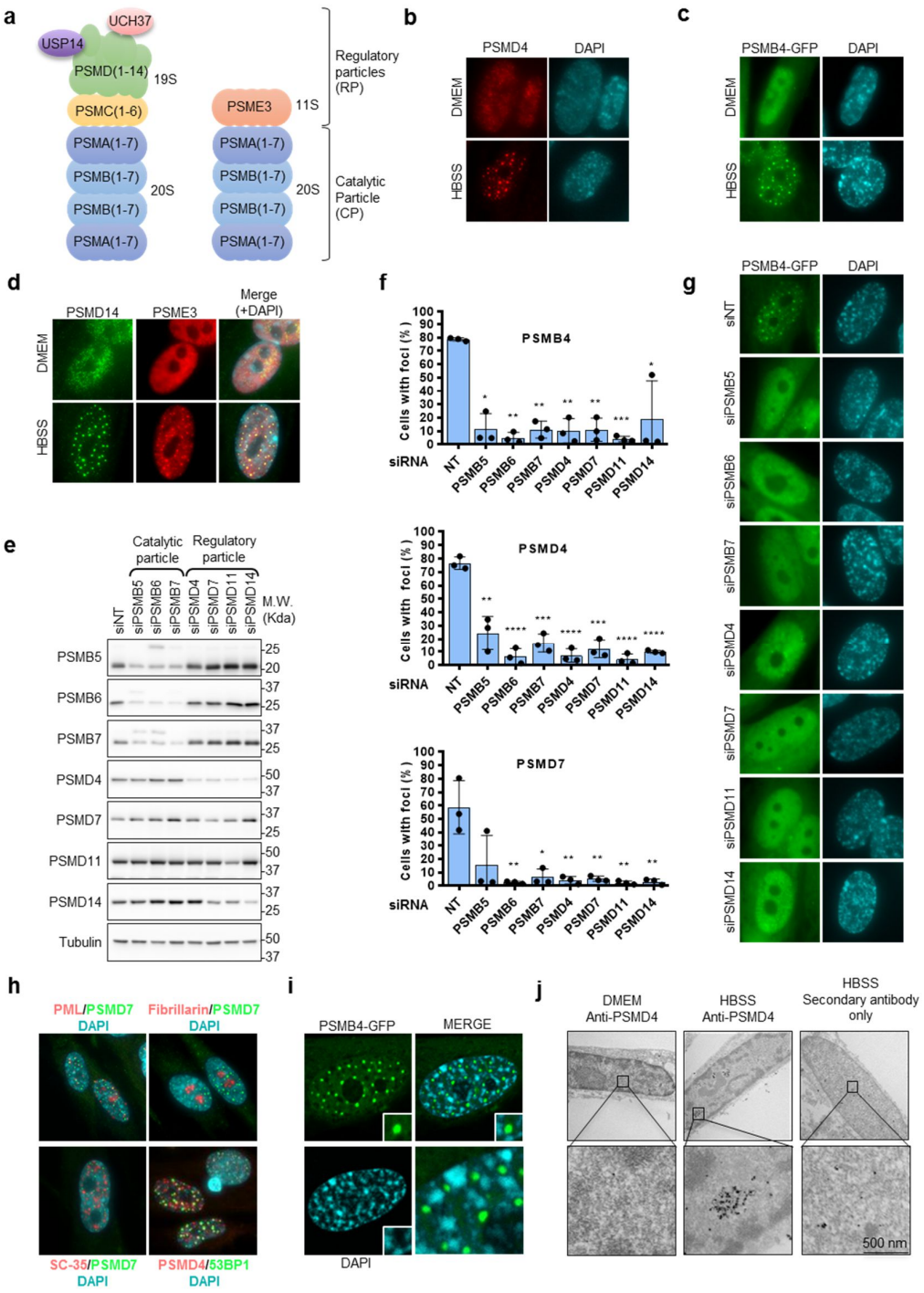

Figure 3-1 : Nutrient starvation induces the formation of proteasome foci in the nucleus of mammalian cells.

a) Schematic representation of the mammalian proteasome, composed by the 20S catalytic particle (CP) and 19S or 11S regulatory particles (RP). **b**) Immunostaining of PSMD4 in IMR90 human fibroblasts showing that this subunit of the 19S RP localizes in distinct nuclear

foci following 6 h incubation in HBSS solution. **c**) PSMB4-GFP localizes in nuclear foci following 6 h incubation of IMR90 in HBSS solution. **d**) Immunostaining of PSME3 in IMR90 human fibroblasts showing that this subunit of the 11S RP localizes with PSMD14 in nuclear foci following 6 h incubation in HBSS. **e-f**) Intact 26S proteasome particle is assembled in nuclear foci following nutrient starvation. **e**) Following siRNA-mediated depletion of components of the RP or CP, IMR90 cells were harvested after three days for immunoblotting. **f**) Three days following transfection by siRNA of components of the RP or CP, IMR90 cells were incubated in HBSS for 6 h and harvested for immunostaining. PSMD4, PSMB4 or PSMD7 do not form foci following depletion of individual components of the proteasome. **g**) PSMB4-GFP does not form foci following depletion of individual components of the proteasome. siRNA depletion was conducted as in panel (**f**)**.** IMR90 cells stably expressing PSMB4-GFP were incubated in HBSS for 6 h and harvested for fluorescence microscopy. **h**) PSMD7 or PSMD4 proteasome foci do not correspond to any known nuclear foci, structure or bodies; including PML bodies (PML staining), nucleoli (Fibrillarin staining), nuclear speckles (SC35 staining) or DNA double strand break foci (53BP1 staining). Staining were conducted following 6 h incubation in HBSS. **i**) Confocal microscopy showing PSMB4-GFP foci in low density chromatin regions. **j**) Transmission electronic microscopy in conjunction with colloidal gold-based immunodetection of PSMD4. Following incubation of IMR90 cells in HBSS for 6 h, cells were fixed and processed for immunodetection and electronic microscopy analysis. PSMD4 condensates are membrane-less and located in regions with reduced chromatin density. Data represent mean ± s.d. (**f**) (n=3 independent experiments). *P<0.05; **P<0.01; ***P<0.001; ****P<0.0001; ns: not significant; 2-tailed unpaired Student's t-test.

- **SIPAN are highly dynamic and undergo fusion events.**

To investigate the dynamics of SIPAN, we first determined the levels of proteasome components (CP and RP) and found that they remain essentially stable during the course of HBSS treatment, except at later time points, where a noticeable decrease could be observed for certain proteasomal factors, e.g., PSMB7 and PSMD14 (**Figure 3-S5a**). The slight decrease in protein levels at later time points possibly reflects autophagy consumption of the cytoplasmic proteasome, as previously reported [117]. Apoptosis was not apparent within the first 12 hours of treatment, as revealed by examination of cell morphology, the absence of proteolytic cleavage of PARP1 or caspase-3, and absence of subG1 cell population (**Figure 3-S5b-d**). Next, we isolated cytoplasmic and nuclear fractions of IMR90 and HCT116 cells, following

incubation in HBSS, and found that, in contrast to yeast [287, 297], no manifest translocation of proteasome components from the nucleus to the cytoplasm was noticed (**Figure 3-S5e-f, see also Figure 3-1b, c**). Thus, in mammalian cells, the nuclear and cytoplasmic proteasomes appear to be subjected to distinct regulatory events.

We then surveyed SIPAN formation as a function of time and found that these structures form as rapidly as 2-3 h with a maximum of cells harboring foci at 6-10 h post-nutrient deprivation (**Figure 3-2a**). The percentage of cells with SIPAN, their signal intensity and number per cell all progressively increased during nutrient starvation (**Figure 3-2a-c**). While signal intensity of SIPAN reach a plateau, their average number per cell decrease at later time points, suggesting SIPAN fusion (**Figure 3-2b-c**). Indeed, live imaging indicated that SIPAN undergo fusion events (**Figure 3-2d**).

To further determine whether SIPAN are reversible, we first induced their formation by depriving cells of nutrients and then replenished the cells with fresh culture medium. We observed that SIPAN, detected by PSMD4 immunostaining, dissipate within 60 min of the addition of culture medium (**Figure 3-2e-g and Figure 3-S6a**). Similar results were obtained for GFP-tagged PSMB4 component of the CP (**Figure 3-S6b**). PSME3 proteasome activator particle also dissipates following addition of culture medium (**Figure 3-S6c**). As disassembly of multi-protein complexes might involve the AAA^+-type ATPase VCP/p97 [299], we blocked this enzyme and determined the impact on SIPAN resolution. Nutrient-deprived IMR90 cells, with preformed SIPAN, were treated with various VCP/p97 inhibitors (DBeQ, ML-240 and NMS-873) in normal culture medium for 1 h. We found that VCP/p97 chaperone is not required for SIPAN resolution (**Figure 3-S6d**). As expected, VCP inhibition results in cell death at later time points, indicating inhibitor efficacy under these experimental conditions (**Figure 3-S6e**).

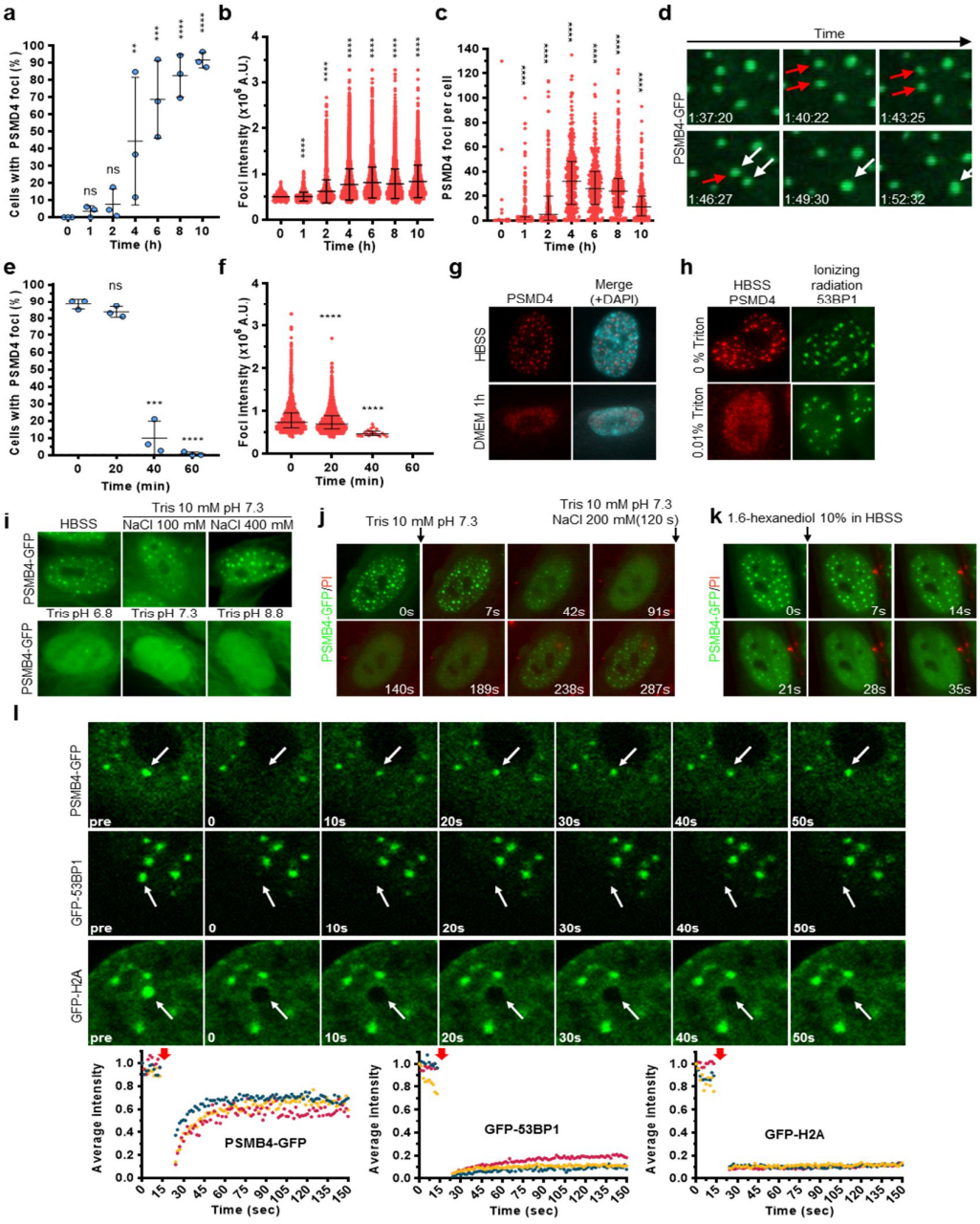

Figure 3-2 : Rapid dynamics of SIPAN assembly and resolution.

a-c) Kinetics of SIPAN formation in IMR90 fibroblasts. **a**) Cells were incubated in HBSS and harvested for immunostaining with PSMD4 antibody. Cells with more than 10 foci were counted. **b**) Signal intensity of SIPAN. Images from control and starved cells were used to estimate SIPAN signals. A.U. (arbitrary units). **c**) Quantification of the number of SIPAN per cell at different time points post-starvation. **d**) Time lapse from live-cell imaging indicating

SIPAN fusion *in vivo*. IMR90 cells expressing PSMB4-GFP were incubated in HBSS and used for live-imaging. Two fusion events are indicated by two arrow colors. **e-g**) SIPAN are reversible. SIPAN formation is induced for 8 h and then normal culture medium or fresh HBSS were added to treated IMR90 for 60 min and harvested for immunostaining. **e**) Cells with more than 10 foci were counted. **f**) Signal intensity of SIPAN. Images from control and starved cells were used to estimate SIPAN signals. **g**) Cell nucleus showing dissipation of PSMD4 signals after medium replenishment. **h**) SIPAN dissipate within two min following incubation of IMR90 cells with very low concentration of Trito. Cells were incubated in HBSS for 8 h and then in the same solution supplemented with Triton before fixation and immunostaining. Alternatively, IMR90 cells were also treated with ionizing radiations for 4 h before treatment with Triton. **i**) SIPAN dissipate following incubation in hypotonic buffers. IMR90 cells expressing PSMB4-GFP were incubated in HBSS for 6 hours and then treated as indicated bore fixation and fluorescence microscopy. **j**) Time lapse from live-cell imaging indicating SIPAN dissipation and recovery following incubation in Tris 10 mM pH 7.3 followed by NaCl 200 mM in Tris 10 mM pH 7.3, respectively. IMR90 cells expressing PSMB4-GFP were incubated in HBSS and used for live-imaging. **k**) Time lapse from live-cell imaging indicating SIPAN dissipation following incubation with 1.6-Hexanediol. **l**) Fluorescence recovery after photobleaching (FRAP) of SIPAN. Bleaching of PSMB4-GFP foci indicate that SIPAN appear rapidly in their original foci following bleaching, while low or no recovery of fluorescence was detected for 53BP1 foci or histone H2A nuclear domains. The arrows indicate the time of laser bleaching. Data represent mean ± s.d. for 3 independent experiments (**a**, **e**) or median with interquartile range for one representative experiment (**b**, **c**, **f**). **P<0.01; ***P<0.001; ****P<0.0001; ns: not significant; one-way ANOVA with Tukey's test (**a**, **e**) or Kruskal-Wallis test with Dunn's test (**b**, **c**, **f**).

- **SIPAN result from liquid-liquid phase separation (LLPS).**

We sought to determine how SIPAN respond to abrupt physico-chemical changes of the cellular environment. SIPAN were assembled by incubation of IMR90 cells in HBSS and were subsequently subjected to other treatments. Interestingly, while SIPAN dissipate within 2 min upon incubation in 0.01 % of Triton X-100, DNA damage-induced 53BP1 foci are resistant to concentrations of this detergent of up to 1% (**Figure 3-2h and Figure 3-S7a,b**). The nuclear staining of PSMD4 does not decrease during the initial time of detergent treatment, suggesting that SIPAN are dissipated in the nucleus as opposed to being expelled from this compartment.

Similar results are obtained with digitonin (**Figure 3-S7c**), a mild detergent that permeabilize cellular membranes with minimal effects on nuclear membrane [300]. Of note, within the same time frame, we observed no noticeable diminution in the signal of the RNA Polymerase II following incubation with low concentration of digitonin (**Figure 3-S7d**). Next, we conducted live imaging of PSMB4-GFP and found that, upon treatment with 0.03 % Triton, SIPAN fluorescence signals become diffuse before reduction of PSMB4-GFP overall intensity and entry of propidium iodide (PI) into the nucleus (**Figure 3-S7e**). These data suggest that SIPAN continuously depend on physico-chemical determinants that quickly dissipate upon plasma membrane permeabilization.

A fundamental characteristic of LLPS is a thermodynamic equilibrium that can shift towards assembly or disassembly depending on the cellular environment [301]. We wanted to determine whether SIPAN assembly/disassembly could be influenced by salt concentration, without plasma membrane permeabilization. We preformed SIPAN in IMR90 cells, which were subsequently incubated in various detergent-free solutions for 2 min. We found that hypotonic treatments induce quick SIPAN dissipation (**Figure 3-2i and Figure 3-S7f**). Changing pH of the hypotonic Tris buffer from 6.8 to 8.8 equally results in SIPAN dissolution, while supplementing this minimal buffer with 100 mM or 400 mM of NaCl maintained SIPAN assembled (**Figure 3-2i**). Live-cell imaging indicated that SIPAN dissipation is followed by quick recovery in the original locations, when hypotonic buffer is supplemented with 200 mM NaCl (**Figure 3-2j, Figure 3-S7g).** Importantly, no staining of DNA with PI was observed, indicating that plasma membrane integrity is not compromised during the course of these treatments. Interestingly, a similar behavior of foci dissipation upon incubation in hypotonic buffer conditions is also observed for PML bodies, which result from LLPS [302] (**Figure 3-S7h**). Finally, we treated IMR90 cells with 1,6-hexanediol, an aliphatic alcohol, which disrupts weak hydrophobic interactions and LLPS [303], and found that this treatment results in a quick SIPAN dissolution (**Figure 3-2k**). Overall, these results indicate that SIPAN are highly sensitive to the physico-chemical environment of the cells and their assembly is governed, at least partly, by hydrophobic interactions.

To further investigate SIPAN dynamics, we conducted fluorescence recovery after photobleaching (FRAP) experiments in HCT116 cells stably expressing PSMB4-GFP. 53BP1-GFP and GFP-H2A, which are tightly associated to DNA [304, 305], were included for comparison with DNA damage foci or high density chromatin domains, respectively. We found that PSMB4-GFP fluorescence recovery is very rapid, while little or no apparent recovery of

fluorescence was detected for 53BP1-GFP or histone GFP-H2A, respectively (**Figure 3-2l**). Taken altogether, these results indicate that SIPAN result from LLPS, and that these structures can be dynamically modulated in response to extracellular cues.

- **RAD23B drives SIPAN formation.**

We sought to determine whether ubiquitin signaling is involved in SIPAN formation. No manifest accumulation of ubiquitin conjugates is observed overtime in IMR90 or HCT116 following incubation in HBSS (**Figure 3-S8a**). Interestingly, SIPAN are enriched with conjugated ubiquitin indicating the presence of ubiquitinated proteins (**Figure 3-3a, b**). In contrast, while SUMO formed foci in untreated cells that likely correspond to PML bodies [306, 307], we did not observe accumulation of this protein in SIPAN (**Figure 3-S8b**). These results suggest that discrete ubiquitination events might play a role in SIPAN dynamics. We reasoned that ubiquitin removal from SIPAN might be required for their resolution upon incubation in normal culture medium. Inhibition of the proteasome-associated deubiquitinases, ubiquitin C-terminal hydrolase 5 (UCHL5) and ubiquitin-specific peptidase 14 (USP14), using the small molecule b-AP15 [308], prevent SIPAN resolution (**Figure 3-3c**). This prompted us to determine whether increasing the pool of ubiquitinated proteins promotes SIPAN formation. Indeed, inhibition of proteasome activity with MG132 results in increased SIPAN formation (**Figure 3-S8c**). Of note, MG132 does not induce SIPAN formation under normal cell culture conditions (**Figure 3-S8d**). Next, we rationalized that ubiquitin binding proteins (UBQLN1, UBQLN2, UBQLN3, UFD1L and SHFM1), and notably proteasome shuttling factors (RAD23A, RAD23B, DDI1 and DDI2), might be involved in SIPAN formation. We found that siRNA depletion of several ubiquitin binding proteins and shuttling factors [309-312], notably RAD23B, inhibit SIPAN formation (**Figure 3-3d**). We validated the effect of RAD23B depletion using additional siRNAs targeting other regions of RAD23B mRNA (**Figure 3-3e**). Of note, depletion of RAD23B does not affect the levels of proteasome components (**Figure 3-S9a**). We expressed RAD23B by lentiviral transduction in IMR90 and found that this factor localizes in SIPAN (**Figure 3-3f**). Interestingly, deletion of the gene encoding the RAD23B orthologue in yeast [313], RAD23, also compromises the assembly of RPN5-GFP (PSMD12) into PSG, suggesting that the role of RAD23B in proteasome phase separation might be conserved throughout evolution (**Figure 3-3g**).

Multivalent interactions ensured by intrinsically disordered regions and/or structured domains are key determinants in LLPS [314, 315]. RAD23B is known to interact with the

proteasome [316], and contains an ubiquitin-like domain (UBL) and two ubiquitin binding motifs, UBA1 and UBA2, which can engage in multivalent interactions (**Figure 3-3h**, left panel) [313, 317]. Bioinformatics analysis of RAD23B and RAD23 showed that intrinsically disordered regions are mainly located between functional domains, while maximal hydrophobicity is found within UBL and UBA domains (**Figure 3-S9b**). As SIPAN appear to depend on hydrophobic interactions, we tested the requirement of the above-mentioned domains for their formations. We expressed several mutants lacking key domains of RAD23B and found that the UBL and UBA domains are required for SIPAN formation (**Figure 3-3h and Figure 3-S9c**). We subsequently purified human RAD23B from bacteria and found that this factor undergoes LLPS in the presence of Ficoll 400 molecular crowding agent, as the protein mixture became turbid and liquid droplets could be readily observed (**Figure 3-3i-j and Figure 3-S9d**). In contrast, BSA did not undergo LLPS in the same conditions. RAD23B LLPS depends on protein concentration and is induced by other molecular crowding agents **(Figure 3-S9e,f)**. Notably, live imaging indicates that RAD23B droplets undergo fusion events *in vitro* (**Figure 3-3k**).

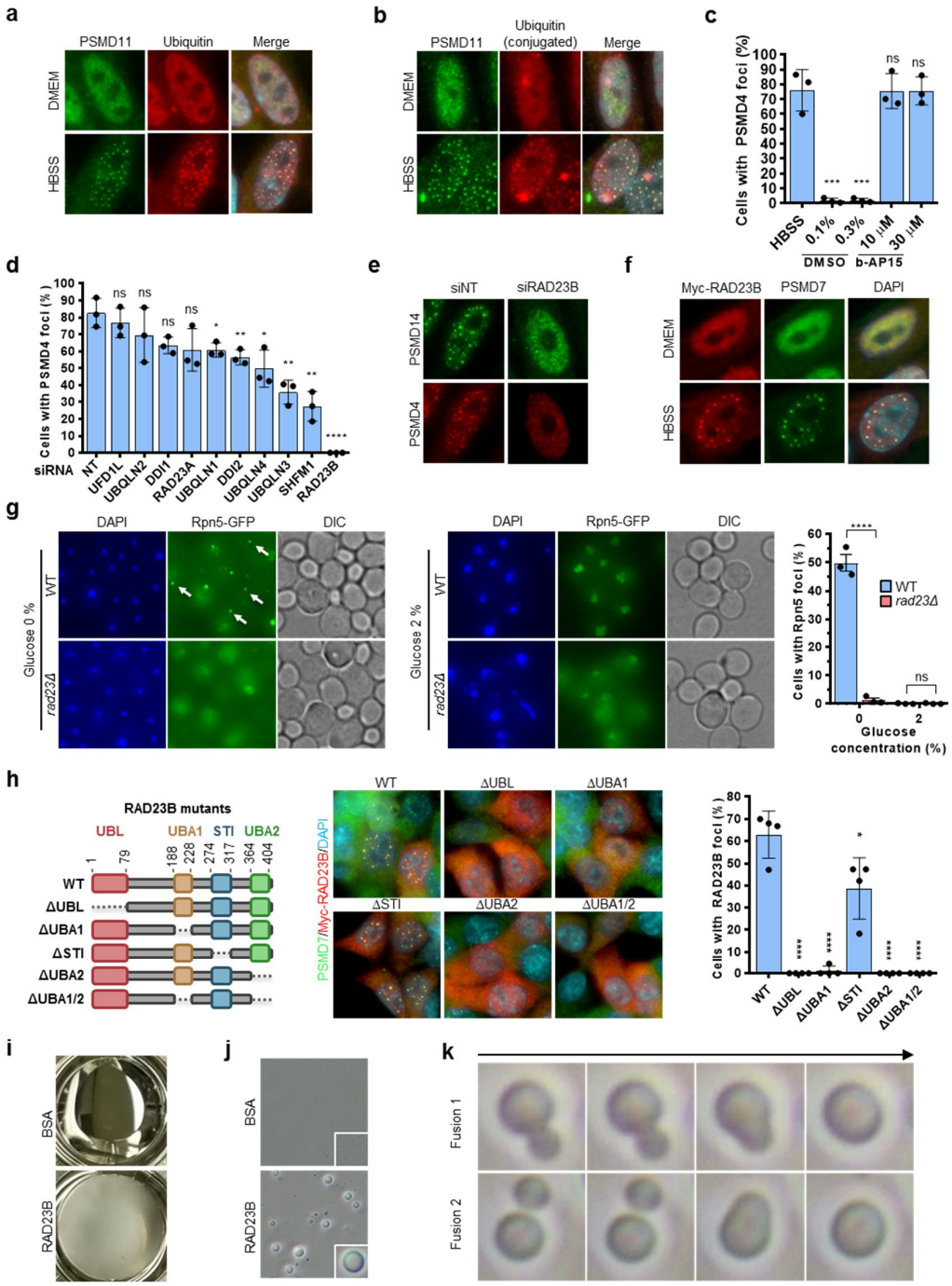

Figure 3-3 : RAD23B is required for proteasome liquid-liquid phase separation.

a-b) Ubiquitin and conjugated ubiquitin colocalize with SIPAN. Immunostaining of PSMD11 and ubiquitin or ubiquitinated proteins (FK2 antibody) following nutrient starvation. IMR90 cells were incubated in HBSS for 6 h and harvested for immunostaining as indicated. **c**) Deubiquitination is required for SIPAN resolution. Cells were incubated in HBSS solution for 6 h and then treated with bAP15 DUB inhibitor in normal culture medium for 1 h. **d**) RAD23B

and other ubiquitin receptors are required for SIPAN formation. Following siRNA depletion of several ubiquitin binding proteins and shuttling factors, IMR90 cells were incubated in HBSS for 6 h and harvested for immunostaining for SIPAN formation. **e**) Validation of RAD23B using additional siRNAs. Following siRNA transfection, IMR90 cells were incubated in HBSS for 6 h and harvested for immunostaining for SIPAN formation. **f**) RAD23B is assembled in SIPAN following nutrient starvation. Following lentiviral infection, IMR90 cells were incubated in HBSS for 6 h and harvested for immunostaining for Myc-RAD23B (anti-Myc) and PSMD7. **g**) RAD23 is required for the formation of proteasome storage granule in yeast. Yeast KO cells were carbon starved and harvested for RPN5 (PSMD12)-GFP fluorescence. Right, Estimation of the number of cells with PSG is indicated. **h**) RAD23B lacking critical domains failed to assemble in SIPAN. Following lentiviral infection, IMR90 cells were incubated in HBSS for 6 h and harvested for immunostaining for Myc-RAD23B (anti-Myc) and PSMD7. Right, Estimation of the number of cells with SIPAN is indicated. **i-k**) RAD23B undergoes LLPS *in vitro*. **i**) Purified RAD23B was mixed with Ficoll 400 and phase separation was visually observed, as RAD23B solution become turbid immediately after solution mixing. **j**) RAD23B droplet were observed by bright-field microscopy. **k**) RAD23B droplet fusion events during phase separation *in vitro*. A portion of RAD23B and Ficoll 400 mixture was added on a microscope slide and a coverslip was applied on the solution near the edge of another coverslip to create space and allow liquid movement. Fusions events were detected by microscopy. Data in graphics represent the mean ± s.d. (n=3 independent experiments). *P<0.05; **P<0.01; ***P<0.001; ****P<0.0001; ns: not significant; 2-tailed unpaired Student's t-test (**c**, **d**, **g**, **h**).

- **Deprivation of non-essential amino acid is responsible for SIPAN formation.**

To further dissect the mechanism that govern SIPAN formation, we supplemented the nutrient-free HBSS solution with specific nutrients and found that addition or removal of glucose or pyruvate does not significantly impact SIPAN formation in IMR90 cells (**Figure 3-4a**). In contrast, addition of fetal bovine serum (FBS) or amino-acid mixture inhibit SIPAN formation (**Figure 3-4a**). Preserving amino acid pools by inhibiting residual protein synthesis with cycloheximide (CHX), during incubation in HBSS, also block SIPAN formation (**Figure 3-4b**). Conversely, preventing amino acid recycling by blocking autophagy with chloroquine or 3-methyladenine accelerates SIPAN formation (**Figure 3-4b**). Of note, blocking mTOR pathway with rapamycin or torin, does not affect SIPAN formation following nutrient deprivation (**Figure 3-4b**). Moreover, no formation of SIPAN was detected following mTOR

inhibition in complete culture medium (**Figure 3-S10a, b).** Next, we deconvolved the amino acid mixture and treated IMR90 with HBSS supplemented with 1 mM of individual amino acids. Interestingly, we found that the majority of non-essential amino acids (NEAA), rather than essential amino acids (EAA), strongly prevent SIPAN formation (**Figure 3-4c**). Similar results were observed on SIPAN resolution, following amino acid replenishment in IMR90 cells (**Figure 3-4d**). More pronounced effects were noticed with high concentrations of amino acids (**Figure 3-S10c, d**). Live-cell imaging on IMR90 expressing PSMB4-GFP further confirmed the rapid resolution of SIPAN following addition of NEAA (**Figure 3-S10e)**. We concluded that deprivation of amino acids, and especially non-essential amino acid, is a major determinant of SIPAN formation and resolution in mammalian cells.

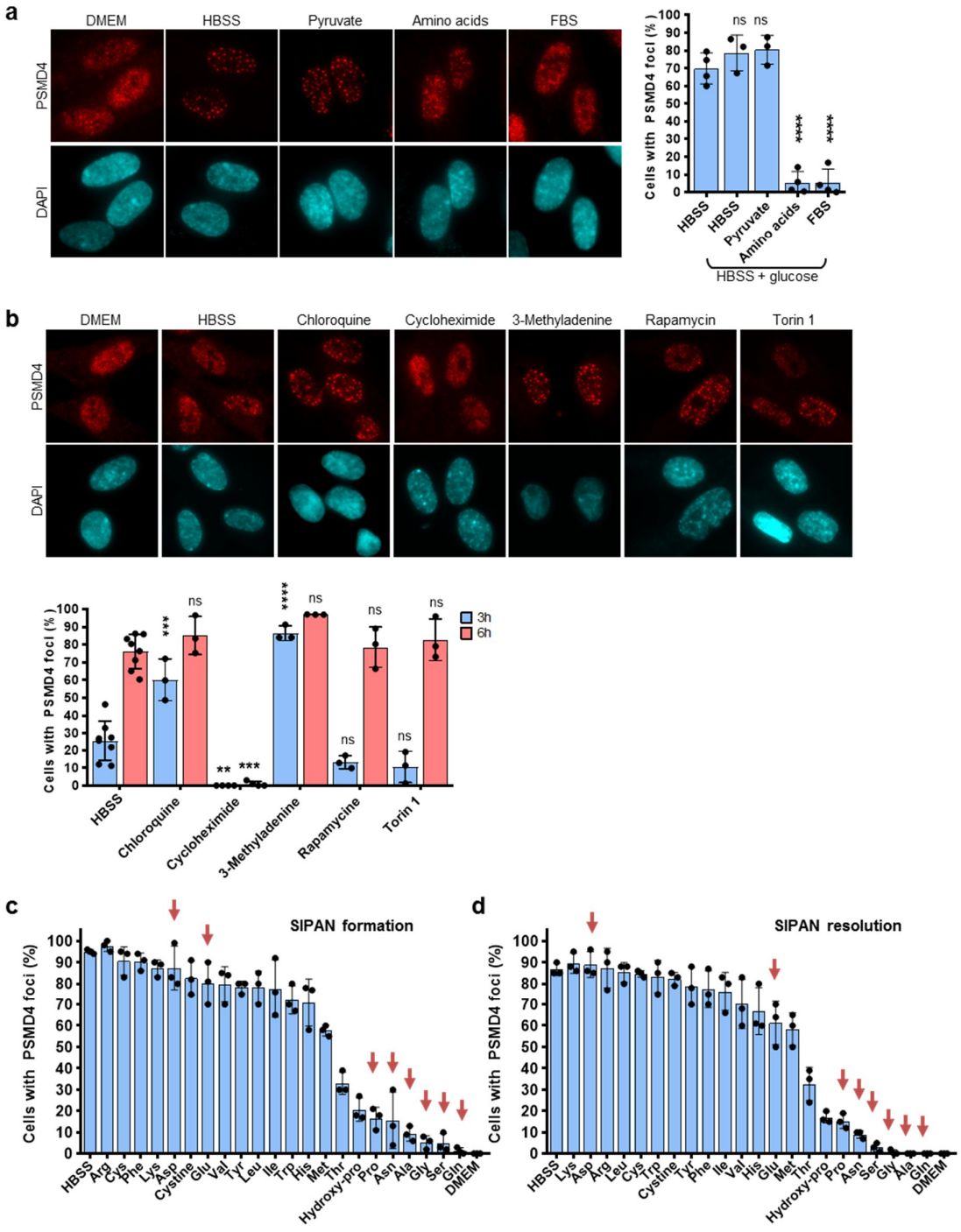

Figure 3-4 : Exhaustion of non-essential amino acid is responsible for SIPAN formation.

a) Addition of amino acids, but not glucose or pyruvate, prevents SIPAN formation in IMR90 cells. Cells were incubated with various nutrients in HBSS solution and harvested after 6 h for immunostaining. **b**) Availability of amino acids regulate SIPAN formation. Cells were incubated with various inhibitors in HBSS solution and harvested after 3 or 6 h for

immunostaining. Inhibition of autophagy by chloroquine accelerates SIPAN formation while inhibition of protein synthesis by cycloheximide inhibits SIPAN formation. Blocking mTOR pathway, with rapamycin or torin, does not affect SIPAN formation following nutrient deprivation. **c**) Non-essential amino acids completely prevented SIPAN formation. IMR90 cells were incubated with individual amino acids in HBSS solution and harvested after 6 h for immunostaining. **d**) Non-essential amino acids promote SIPAN resolution. SIPAN formation is induced and then cells were replenished with fresh medium containing individual amino acids and harvested after 2 h for immunostaining. Red arrows represents NEAA (**c, d**). Data represent mean ± s.d. (n≥3 independent experiments). *P<0.05; **P<0.01; ***P<0.001; ****P<0.0001; ns: not significant; 2-tailed unpaired Student's t-test.

- **RAD23B and PSME3 provide a link between amino acid supply, SIPAN formation and apoptosis.**

In yeast, PSG promote viability and cell fitness following carbon starvation [297]. To provide insights into the significance of SIPAN formation in mammalian cells, we first sought to determine the state of proteasome activity upon amino acid deprivation. We were unable to extract SIPANs to conduct *in vitro* activity studies, as these foci are quickly dissipated in the nucleus upon detergent treatment or hypotonic cell lysis (**Figure 3-2h-j**). We therefore preformed SIPAN in IMR90 cells by incubation in HBSS for 8 h followed by treatment with MG132 in the same solution for 1 hour. Following proteasome inhibition, we observed increased levels of several short-lived nuclear stress-associated transcription factors, including p53, c-fos and c-Jun, suggesting that SIPANs are not associated with proteasome inhibition (**Figure 3-5a**). Immunostaining indicated that SIPAN are not perturbed upon combined HBSS and MG132 treatments (**Figure 3-5b**). Next, we investigated the link between SIPAN formation and cell viability. Treatment of IMR90 cells with chloroquine or 3-MA, which promote SIPAN formation, diminishes cell survival following incubation in HBSS (**Figure 3-5c and Figure 3-S10f**). In contrast, treatment with CHX, which dampens SIPAN formation, protects cells from loss of viability relative to treatment with HBSS alone. As expected, the caspase inhibitor Z-VAD protects IMR90 cells from undergoing apoptosis following nutrient deprivation. NEAA pool, which prevents SIPAN formation, also increases cell viability upon incubation in HBSS; whereas EAA pool decreases cell viability (**Figure 3-5d**). We then used several individual EAA (Lysine, Arginine and Tryptophan), or NEAA (Serine, Glycine, Glutamine, Asparagine and Alanine) whose presence in HBSS has no either clear effect or inhibit SIPAN formation,

respectively. We found that while individual EAA decrease cell viability, individual NEAA have either no effect or significantly increase cell viability (**Figure 3-5d and Figure 3-S10g**). Significantly, we found that depletion of RAD23B or PSME3 results in increased cell viability following amino acid depletion, as determined by MTT transformation assay (**Figure 3-5e**). The protective effect of RAD23B or PSME3 depletion from amino acid depletion-induced cell death was also directly observed by phase contrast microscopy and crystal violet staining (**Figure 3-5f, Figure 3-S10h**). FACS analysis for SubG1 cell population and immunoblotting detection of PARP1 apoptotic cleavage also indicated that depletion of RAD23B or PSME3 protects from cell death induced by amino acid depletion (**Figure 3-5g, h**). Of note, depletion of PSME3 has no impact on protein levels of proteasome components **(Figure 3-S10i**). Based on these results altogether, we concluded that SIPAN formation is associated with amino acid starvation-induced cell death.

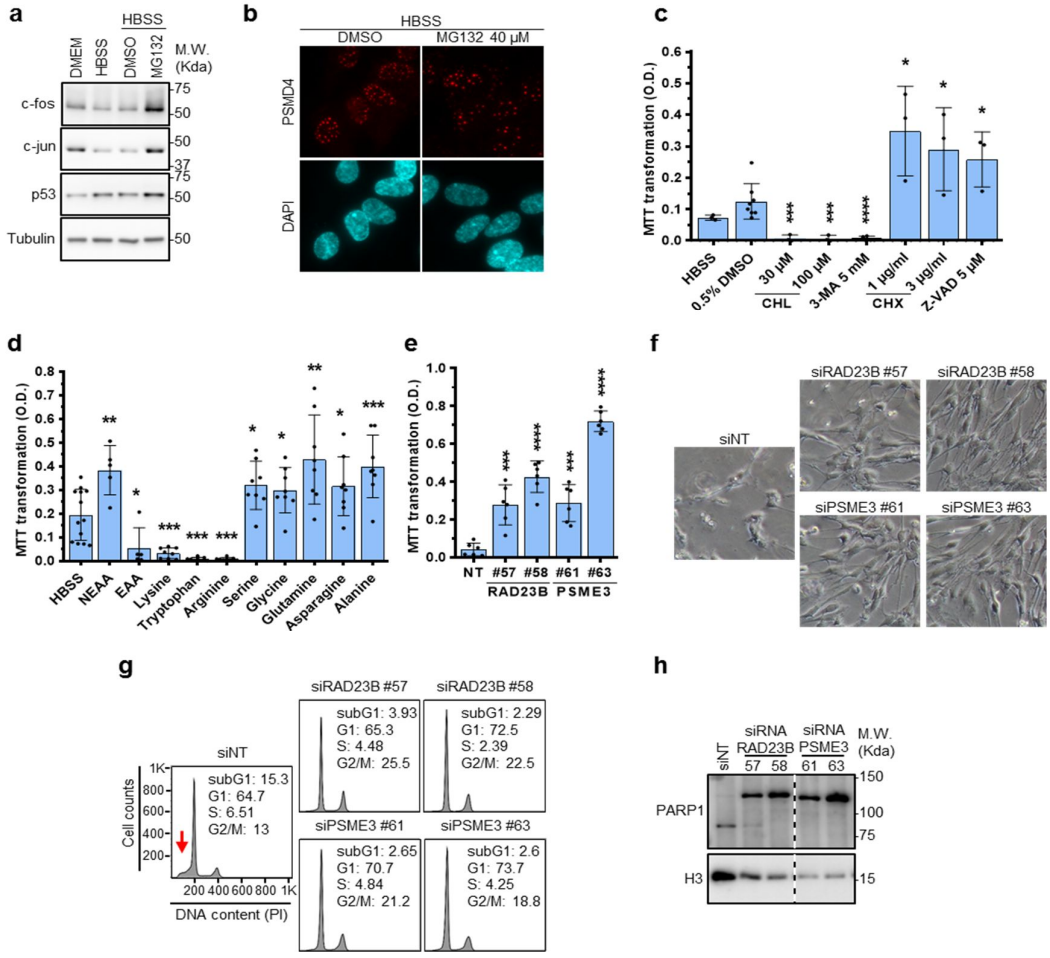

Figure 3-5 : Inhibition of SIPAN formation is associated with apoptosis.

a, b) Proteasome is active under nutrient starvation. IMR90 cells were incubated in HBSS for 8 h and treated with MG132 for 1 hour and harvested for immunoblotting (**a**) or immunostaining (**b**). SIPAN are maintained under conditions of HBSS and MG132 treatments. **c**) Treatments that prevent SIPAN formation result in increased cell survival, whereas those that promote their formation result in increased cell death. IMR90 cells were incubated in HBSS for 48 h in the presence of various inhibitors and harvested for MTT viability assay. **d**) Effects of EAA and NEAA on cell viability. IMR90 cells were incubated in HBSS for 48 h in the presence of individual amino acids and harvested for MTT viability assay. NEAA increase cell survival relative to EAA or HBSS alone. **e-h**) Inhibition of RAD23B or PSME3 result in increased cell survival following nutrient deprivation. Three days following siRNA transfection, IMR90 cells were incubated in HBSS for 48 h and harvested for MTT viability assay (**e**), phase contrast imaging (**f**), FACS analysis (**g**) and Western blotting (**h**). Arrow in in panel **g** represents subG1 apoptotic cell population. Data represent the mean ± s.d. (n≥3 independent experiments) (panels

c, **d**). Data in panel **e** represent the mean ± s.d. (n=6 from 2 independent experiments in triplicate each). *P<0.05; **P<0.01; ***P<0.001; ****P<0.0001; ns: not significant; 2-tailed unpaired Student's t-test.

3.4 Discussion

In this study, we demonstrate that the mammalian proteasome undergoes LLPS upon amino acid deprivation, and this result in SIPAN formation in nuclear regions of low chromatin density. SIPAN undergo fusion events, can be dissipated and reassembled, and rapidly exchange components with the nuclear milieu, reflecting their fast turnover rates. SIPAN therefore constitutes hitherto unknown nuclear substructures common to mammalian cells of various origins.

Our results highlight significant evolutionary divergence in the responses of mammalian and yeast proteasomes to nutrient deprivation. i) SIPAN form in the nucleus, whereas yeast proteasome is exported from the nucleus and form PSG structures in the cytoplasm [287, 297]. ii) SIPAN are formed following amino acid, but not glucose deprivation, while the opposite situation occurs in yeast [297]. iii) Our data suggest that proteasome foci promote cell death in mammalian cells; however, the reverse outcome occurs in yeast, i.e., PSG improve cell fitness and viability [297]. iv) Finally, while SIPAN contain conjugated ubiquitin, PSG contain free ubiquitin [318]. The reasons of these differences between mammalian and yeast proteasome structures are currently unknown, but we emphasize that yeast and high-order metazoan present both common (conserved) and distinct metabolic responses to nutrient deprivation [319]. Wild yeast can face dramatic changes in their environment and have to adapt quickly to maintain survival. In contrast, most of the cells of high-order multicellular organisms are in stable tissular environments, with a generally stable and constant supply of nutriments. In addition, the utilization of nutriments in higher eukaryotes, such as mammalians, depends on growth factor signaling. Moreover, nutrient deprivation is usually a condition of tissue or organ stress [320].

On the other hand, common features unify the responses of the yeast and mammalian proteasomes to nutrient deprivation. The formation of SIPAN or PSG is reversible, as these structures dissipate quickly when nutrients are replenished. SIPAN and PSG contain ubiquitin, and the mammalian ubiquitin binding factor RAD23B and its yeast orthologue RAD23 are important regulators of their formation. RAD23B or RAD23 as well as other factors we identified, e.g., SHFM1 and UBQLN3, provide a link between ubiquitin signaling pathways and the dynamics of SIPAN or PSG. One explanation of our observations is that, under

conditions of nutrient deprivation, increase of E3 ubiquitin ligase activity and/or decreased deubiquitinase activity results in the accumulation of a subset of ubiquitinated substrates. This, in turn, triggers proteasome LLPS, through interaction with RAD23B and other ubiquitin receptors. Consistent with this notion, proteasome inhibition promotes SIPAN formation and proteasome deubiquitinase inhibition prevents SIPAN resolution.

Protein ubiquitination per se is not sufficient to trigger SIPAN formation, as proteasome inhibition alone, under conditions of nutrient availability, does not induce SIPAN. On the other hand, PSME3 which activates proteasome in ubiquitin-independent manner, is also recruited and assembled in SIPAN. Thus, other ubiquitin-independent signals are needed to licence SIPAN formation. Our results indicate that the intracellular levels of amino acids, and notably NEAA, are key determinants in SIPAN assembly and disassembly. Interestingly, NEAA are actively involved in intermediate carbon metabolism, nucleotide metabolism and signaling processes [321, 322], and their presence might favor the formation of metabolic intermediates that might act as hydrotropes, preventing LLPS [323].

What is the biological significance of nuclear proteasome LLPS in mammalian cells? Our data suggest that SIPAN are disadvantageous for the fitness of individual cells. It is possible that, in multicellular organisms, this response has evolved for the benefit of tissues and organs rather than that of individual cells. For instance, SIPAN, by promoting cell death upon nutrient deprivation, might contribute to tissue and organ homeostasis by decreasing competition between cells for nutrients. In addition, release of constituents by dying cells might be beneficial for surrounding cells during periods of nutrient deprivation. In multiple pathological conditions including wound and organ injury, tissue ischemia and tumor development, cells experience drastic nutrient deprivation that could trigger SIPAN formation and cell death. For instance, in pancreatic ductal adenocarcinoma, a poorly vascularized tumor type, it was revealed that certain NEAA, and particularly glutamine and serine, are depleted in tumors, while EAA levels are increased [324]. Glutamine, which has the strongest effect on SIPAN formation, is often depleted in the central region of solid tumours compared to other amino acids [325]. Genetic manipulation of signaling pathways that link proteasome LLPS and amino acid sensing is expected to provide additional insights into the role of SIPAN in human disease.

3.5 Materials and methods

- ***Plasmids***

The cDNAs of human PSMB4, PSMB5, PSMD14 and PSMD12 were generated in a modified pBluescript using gene synthesis (Biobasic Inc). The constructs were then subcloned as fusion with GFP and recombined using gene LR-clonase in lentiviral expression vectors as previously described [326]. SiRNA-resistant constructs for human Rad23B and its corresponding mutants Rad23B ΔUBL, Rad23B ΔUBA1, Rad23B ΔUBA2, Rad23B ΔUBA1/UBA2 and Rad23B ΔSTI were generated using gene synthesis (BioBasic) and then recombined into lentiviral expression constructs. PAX2 (#35002) and pMD2G (#12259) lentiviral packaging plasmids were from Addgene. Human histone H2A was generated by gene synthesis in pENTR gateway plasmid and then recombined into pDEST GFP plasmid. For bacterial expression of RAD23B, His-tagged human RAD23B was generated by recombination of pBluescript into pDEST-His expression vector. pcDNA5-FRT/TO-eGFP-53BP1 (Addgene #60813) is used to express GFP-53BP1.

- **Cell culture**

Human primary lung fibroblasts IMR90 and HDLF cells, MCF7 human breast cancer cell line, human non-small cell lung carcinoma NCI-H1299, AT3 androgen-independent prostate cancer cells, RAW 264.7 murine macrophage cell line, HCT116 human colon cancer cell line, murine C2C12 myoblasts, 3T3-L1 mouse preadipocytes, NIH3T3 mouse fibroblasts were cultured in Dulbecco's modified Eagle's edium (DMEM) supplemented with 10 % foetal bovine serum (FBS), 1% L-glutamine and 1% penicillin/streptomycin. Transformed monkey kidney cells Cos-7, human embryonic kidney HEK293T (HEK293T) cells were cultured in DMEM supplemented with 5% new born calf serum. Mouse embryonic stem cells (mESCs) were cultured on gelatin-coated plates in DMEM medium containing 15 % FBS, 1% L-glutamine, penicillin/streptomycin, 0.1 mM β-mercaptoethanol, 0.1 mM Non-essential amino acids, 1 mM sodium pyruvate and 1,000 U/ml of leukemia inhibitory factor (LIF) (Life technologies). HUVEC cells were cultured in EndoGRO basal medium (Millipore) supplemented with EndoGRO-VEGF Supplement (Millipore, containing 5 ng/mL recombinant human VEGF, 5 ng/mL recombinant human EGF, 5 ng/mL recombinant human FGF basic, 5 ng/mL recombinant human IGF-1, 50 µg/mL Ascorbic Acid, 1 µg/mL Hydrocortisone Hemisuccinate, 0.75 U/mL Heparin Sulfate, 1 % mM L-Glutamine, 2 % FBS, 100 U/mL penicillin, 100 µg/ml streptomycin. Confluent 3T3TL1 were incubated in DMEM

differentiation medium supplemented with 10 % foetal bovine serum, 1 % Glutamine, 1 % penicillin/streptomycin, 1 µM dexamethasone, 1 µg/ml insulin and 500 µM isobutylmethylxanthine (IBMX). 2 days post-induction, culture medium was changed for DMEM medium supplemented with 10 % FBS, 1 % Glutamine, 1 % penicillin/streptomycin and 1 µg/ml insulin. Media were changed every 2 days and cells were harvested at the indicated time points.

- **Nutrient deprivation and chemical treatments**

Following cell culture medium removal, cells were washed three times with PBS (137 mM NaCl, 2.7 mM KCl, 10 mM Na_2HPO_4, 1.76 mM KH_2PO_4, pH 7.4) and then incubated in HBSS (137 mM NaCl, 5.4 mM KCl, 0.34 mM Na_2HPO_4, 1g/L glucose, 0.44 mM KH_2PO_4, 1.3 mM $CaCl_2$, 0.81 mM $MgSO_4$, 4.17 mM $NaHCO_3$,) supplemented with 10 mM HEPES pH 7.3 and 1 % penicillin/streptomycin. HBSS was omitted from glucose or supplemented with other nutrients as indicated in figure legends. For UV treatments, IMR90 cell monolayers grown on coverslips in 6-well plates were washed twice with PBS and incubated in 2 ml of PBS, followed by UVC irradiation with a Philips G25T8 germicidal lamp at fluency of 0.2 J/m^2/s for a total dose of 20 J/m^2. H2O2 was diluted in culture medium at 1 mM and 300 µM. Hypoxia was conducted by incubating IMR90 with 1 % of O_2 for 8 h using a standard hypoxia chamber. Genotoxic stress was induced by treating cells with IR at 7.5 Gy using a Cesium-137 source (Gamma Cell, Atomic energy Canada). Heat shock was conducted by incubating the cell culture plates at 45 ºC for 30 min and then at 37 ºC for the indicated time points. Osmotic stress was induced by supplementing normal culture medium with 100 mM NaCl (243 mM total, 300 mM sucrose or 400 mM mannitol. Chemical inhibitors and others reagents used is listed in supplemental **table 3-S1**.

- **Cell permeabilization**

IMR90 cells were incubated in HBSS or treated with 7.5 Gy ionizing radiations in culture medium and then treated with Triton X-100 (Sigma, X100-1GA) or Digitonin (Sigma, D-5628) at the indicated concentrations and then harvested at the indicated time points for fixation and immunostaining. For live-cell imaging, IMR90 cell permeabilization was conducted in HBSS containing 0.03 % Triton and propidium iodide 50 µg/ml.

- **Cells transfections and lentiviral transductions**

HCT116 cells were transfected with expression plasmids using lipofectamine 2000. Two to three days after the transfection, cells were harvested for immunoblotting or treated

with HBSS and used as indicated. For lentiviral production, expression constructs were transfected in HEK293T, in combination with lentivirus packaging constructs and lentivirus particles were harvested several times post-transfection. IMR90 or HCT116 cells were infected once or multiple times with lentiviral suspension. Two days later, cells were selected with puromycin for 2 days and then used as indicated. siRNA oligonucleotides targeting various factors were purchased from Sigma-Aldrich. IMR90 cells were transfected using Lipofectamine RNAi max with 200 pmol of individual or pooled siRNAs. Three days post-transfection, cells were treated as indicated or directly harvested for immunoblotting or immunostaining. siRNA oligonucleotides used are listed in supplemental **Table 3-S2.**

- **Immunoblotting and antibodies**

Total cell extracts were prepared following cell lysis in 25 mM Tris pH 7.3 and 2 % sodium dodecyl sulfate (SDS). Cell extracts were boiled at 95 °C for 10 min and then sonicated. Total proteins concentration was determined using the bicinchoninic acid (BCA) assay, and samples were diluted in Laemmli buffer. SDS-PAGE and Immunoblotting were done as we previously described [327]. The chemiluminescence band signals were acquired with a LAS-3000 LCD camera and analyzed with a MultiGauge software (Fuji, Stamford, CT, USA) or with Azurec600 chemiluminescence Imaging System. The antibodies used are listed in supplemental **table 3-S3.**

- **Preparation of nuclear and cytoplasmic cell fractions.**

IMR90 cells were incubated in HBSS and fractionated with a hypotonic lysis buffer as previously described [328]. HCT116 cells were incubated in HBSS and nuclear and cytoplasmic fractions were prepared by incubation of cells for 1 min in 10 mM Tris pH 7.3 containing 100 mM KCl, 1 mM mM β-mercaptoethanol, 1 X anti-protease, 1 mM PMSF and 0.1 % NP40. Cells were centrifuged at 6,000 rpm for 1 min and the pellet fraction was washed once in detergent free buffer. All samples were then used for immunoblotting.

- **Colloidal gold-based immunodetection and transmission electronic microscopy.**

This procedure was performed based on previous protocols [329], with the following modifications. Cells were fixed for 30 min in 4 % paraformaldehyde (PFA) in 0.1 M cacodylate buffer pH 7.2 (Tcaco), washed twice in Tcaco buffer and then once in PBS. Cells were permeabilized in PBS containing 0.2 % de NP-40 for 10 min and non-specific sites were saturated with PBS containing 0.04 % NP-40 and 10 % FBS for 30 min (blocking buffer). Cells

were then incubated for 3 h at RT with anti-PSMD4 primary antibody in blocking buffer. Cells were then washed 6 times, 5 min each, with the blocking buffer and incubated with anti-mouse IgG nanogold antibody (Nanoprobes, NY, USA), diluted 1/100 in blocking buffer, followed by several washes in blocking buffer. Coverslips were then incubated in 2 % glutaraldehyde in PBS for 10 min followed by a 10 min incubation in silver enhancement solution (HQ Silver enhancement kit, Nanoprobes, NY, USA) at room temperature. Samples were post-fixed with 1 % OsO_4 in TCaco buffer for 10 min, stained *en bloc* with 1 % uranyl acetate for 5 min. Cells were dehydrated in graded series of ethanol and scrapped off the plates in ethanol and pelleted. The pellets were embedded in Epon [330]. Ultrathin sections of the samples were obtained using a Reichert Ultracut ultramicrotome and mounted on naked nickel grids. Sections were stained with lead citrate and examination was performed with a Philips CM100 transmission electron microscope. Electron micrographs were captured using an AMT XR80 digital camera (Advanced Microscopy Techniques, Corp. MA, USA).

- **Immunofluorescence**

The immunostaining was conducted as previously described [328]. Briefly, culture medium was removed and cells were directly fixed in PBS containing 3 % PFA for 20 min. Cells were permeabilized by incubation in PBS 0.5% Triton. Non-specific sites were blocked for 1 hour using PBS containing 0.1% Triton and 10% FBS. The coverslips were then incubated with primary antibodies for three h at room temperature or overnight at 4°C. After three washes, cells were incubated with secondary Anti-mouse Alexa Fluor® 594, anti-mouse Alexa Fluor® 488, Anti-rabbit Alexa fluor® 488 or anti-rabbit Alexa Fluor® 594 antibodies for 1 hour. Nuclei were stained with 4',6-diamidino-2-phenylindole (DAPI). Cell samples were mounted on a stage of an Olympus BX53 (Olympus Corp., Japan) upright microscope equipped with an Olympus UPlan SApo 60X/1.35 NA oil immersion objective. The corresponding fluorescence cubes (DAPI-1160B, GFP-3035C and Texas-4040C; Semrock Inc, USA) were used to efficiently reflect the excitation wavelengths and pass the emission wavelengths into the CCD camera detection channel. The images were acquired using a monochromatic Peltier cooled 1.4 megapixel CCD Olympus XM10 (Olympus Corp., Japan) CCD camera controlled by the Olympus cellSens software. Gamma, brightness, and contrast were adjusted on displayed

images using the cellSens software. The collected EPI-fluorescence data images was processed using WCIF-ImageJ program [331].

- **EPI-fluorescence and brightfield live-cell microscopy**

Cells stably expressing PSMB4-EGFP were grown on MatTek glass bottom petri dishes (Coverslip thickness No. 1.5, Mattek Corp., Ashland, MA). Cells were rinsed with PBS and then treated with HBSS with or without 100 μM chloroquine. The samples were then mounted on a motorized stage of a Zeiss AxioObserver.Z1/7 inverted microscope equipped with a live-cell incubator and a CO_2 module. Brightfield (DIC) and EPI-fluorescence images were collected using a Zeiss Plan-Apochromat 63x/1.4 NA oil immersion objective lens. GFP was excited with a CoolLED pE-300 lite LED light engine, and the corresponding fluorescence cube (49002 - ET – EGFP/FITC/Cy2, Chroma, Bellows Falls, VT) was used to efficiently reflect the excitation wavelengths and pass the emission wavelengths into the CCD camera detection channel. DIC optics was utilized to enhance specimen detail of brightfield images. The images were acquired every 5 min using a monochromatic Zeiss AxioCam MRm R3 CCD camera (with 1x camera adapter) and Zen Blue v2.6 software. Multiple stage positions were collected using a motorized scanning stage. A combined focus strategy (via Zen's Tiling module assisted with a software autofocus) was utilized to maintain the focal plane over time. The acquisition settings were kept constant for all imaging experiments so that valid comparisons could be made between measurements from different data sets. Acquisition parameters were set within the linear range of the CCD camera detection. Z-series were displayed as maximum Z-projections via the Zen's Extended Depth of Focus image processing module.

- **Automated quantification of SIPAN**

Images were analysed using a custom Python 3.6 program. Briefly, images from cells grown in complete medium were first used to assess background foci intensity. Nuclei were segmented using DAPI staining channel images and images in the other channel (containing SIPAN) were processed using a Python implementation of a band pass filter algorithm (coded by K. Smith and M. Kilfoil) based on bpass.pro (http://www.physics.emory.edu/faculty/weeks/idl/kit/bpass.pro), which was originally developed by J. Crocker and D. Grier [332]. Images were then segmented using a local thresholding algorithm (from the Sci-Kit Python library) to identify regions of elevated signal intensity (foci). Pixel intensity values were then extracted from these foci, and the average "background" signal intensity and standard deviation was calculated. A threshold intensity for

subsequent analyses was set as (average background intensity value + 2*SD). Next, all images (including those originating from cells grown in complete medium) were processed using a similar Python code (band pass filter followed by local thresholding in segmented nuclei regions). Foci that were of intensity < than (background intensity value + 2*SD) or smaller than 3 by 3 pixels were discarded (to remove background noise), and the number of foci per nuclei, as well as their intensity, was calculated.

- **Fluorescence recovery after photobleaching (FRAP) experiments**

PSMB4-GFP expressing HCT116 cells were cultured in 35 mm Mattek chambers and foci formation was induced by incubation in HBSS for 6 h prior to the imaging experiments. HCT116 cells transiently expressing 53BP1-GFP were exposed to gamma irradiation for 4 h to induce the formation of DNA double-strand breaks/repair 53BP1 foci. HCT116 transiently expressing human histone GFP-H2A were directly used. The samples were then mounted on a Prior ProScan III motorized stage of an Olympus IX81 inverted microscope. The FRAP experiments were performed on an Olympus FluoView FV1000 laser scanning confocal (CLSM) system equipped with spectral detectors. Regions of interest [333] from individual cells in the FluoView software were chosen (10x10 pixels with 1.03 μm/pixel) for the FRAP experiments. The 488 nm line of the Argon laser was used for both imaging (attenuated by 95 %) and photobleaching (full 100 % power output) of GFP in combination with a PLAPON 60x/1.4 NA OSC oil immersion lens. The DM405/488 polychroic mirror was used to efficiently reflect the excitation wavelength and pass the emission wavelengths into the corresponding detection channel. Prebleach images (10 frames) were taken prior to FRAP activation for normalization of the data. Photobleaching of EGFP was generated by scanning the selected ROIs for 10 sec (dwell time of 2 μs/pixel). Acquisition parameters (laser intensity, pixel dwell time, photomultiplier tube (PMT) voltage/gain, confocal pinhole aperture) were set within the linear range of the PMT detection. The acquired fluorescence recovery curves were generated using the FluoView software. The values were obtained from the analysis of three independent experiments.

- **MTT assay**

IMR90 cells were plated in 24-well plates and incubated in HBSS with treatments as indicated. For siRNA experiment, the same number of cells (80,000 cells) were plated and treated with HBSS for 48 h. Medium was removed and replaced with complete medium containing 200 μg/ml of MTT (3-(4,5-Dimethylthiazol-2-yl)-2,5-diphenyltetrazolium bromide,

Bioshop, MTT222.1). Cells were then incubated at 37 °C for 2 h. Cells were washed once with PBS and DMSO was added to extract formazan product. The absorbance was measured at 490 nm using a microplate reader (Biotek Instruments).

- **FACS analysis**

Cells were washed with PBS and harvested by trypsinization. Cells were centrifugated, washed once again with PBS and fixed with 75 % cold ethanol. Cells were centrifugated and resuspended in PBS containing 100 µg/ml RNase A and incubated at 37 °C for 30 min. To stain DNA, propidium iodide was added at 50 µg/ml final concentration. DNA content of cells was acquired with BD (Becton Dickinson) FACS Calibur: 2 lasers, 4 detectors and analyzed using a FACScan flow cytometer fitted with CellQuestPro software (BD Biosciences).

- **Colony Forming Assays**

IMR90 cells were plated in 35 mm dishes at the same density. Cells were treated as indicated. For siRNA experiments, transfected IMR90 cells were plated in 6 cm dishes and incubated in HBSS for 48 h. Cells were then changed to normal culture medium and allowed to recover for one week. For all experiments, cells were fixed in PBS contain 3 % PFA for 20 min. Then, cells were washed once with PBS and stained with 0.5 % crystal violet for 30 min and washed several times with water.

- **RAD23B and RAD23 protein sequence Analysis**

Disorder/order analysis of the RAD23 proteins were conducted using PONDR-FIT algorithm [334], PONDR-VLXT and PONDR-VSL2 [335]. 0.5 value in the Y-axis is considered as a threshold. Residues with a score above and below 0.5 are predicted to be disordered and ordered respectively. Hydrophobicity calculation was assessed using Kyte-Doolittle hydropathy algorithm [336]. The highest values indicates the hydrophobic amino acids along the sequence.

- **Purification of RAD23B**

His-RAD23B expression construct was transformed into BL21 RIL bacteria. Cells were grown at 37 °C and then treated with IPTG at 0.4 mM to induce RAD23B production. Then, cells were harvested and centrifuged at 3,000 rpm for 15 min at 4°C. The pellet was washed with cold PBS, centrifuged and frozen on dry ice. Cell pellet was lysed in 50 mM Tris-HCl pH 8.0, 500 mM NaCl, 3 mM β-mercaptoethanol, 1 mM PMSF and 1X protease inhibitors (Sigma-Aldrich). Suspensions were sonicated and centrifuged at 15,000 rpm for 20 min. Supernatants

were incubated with Ni-NTA Agarose resin (Invitrogen, R901–15) overnight at 4 °C. Then, the resin was washed 5 times with 20 volumes of 50 mM Tris-HCl pH 8.0, 500 mM NaCl, 3 mM β-mercaptoethanol, 1 mM PSMF, protease inhibitors, 20 mM imidazole and transferred into a Bio-Spin Disposable Chromatography column (Bio Rad, 731–1550). Proteins were eluted 5 times with 50 mM Tris-HCl pH 8.0, 500 mM NaCl and 200 mM imidazole, 3 mM β-mercaptoethanol and 1 mM EDTA and proteins were used for phase separation or temporarily stored at 4°C.

- **RAD23B *In vitro* phase separation and droplet fusion**

His-RAD23B was concentrated 5 times and the elution buffer was changed with a buffer containing 50 mM HEPES pH 7.2 and 100 mM NaCl using Amicon Ultra-0.5 mL Centrifugal Filters 10KDa (Millipore, UFC501024). For the *in vitro* assay, an equal volume of His-RAD23B and Ficoll 400 (Sigma, F4375, 300 mg/ml prepared in 50 mM HEPES pH 7.2 and 100 mM NaCl buffer) were mixed at room temperature to initiate droplet formation. The droplets were deposited on a glass slide in a chamber formed of 2 overlapping coverslips to allow liquid movements and to observe fusion events. PEG 6000 (Alfa Aesar, A17541) or Dextran 60,000-90,000 (ICN, 101513) prepared in 50 mM HEPES pH 7.2 and 100 mM NaCl buffer was used at 10% or 5% final concentration, respectively. Crystal violet (0.5% w/v) prepared in 25 % methanol is occasionally used to stain droplets (1 µl of crystal violet in 20 µl of droplets).

- **Yeast strains and growth conditions**

Yeast cells were generated and propagated using standard yeast genetics methods. The genotype of the yeast strains used in this study are BY4741 MATa his3Δ1 leu2Δ0 met15Δ0 ura3Δ0 RPN5-GFP::HIS3MX (from Life Technologies Yeast GFP collection, catalog #: 95702) and BY4741 MATa his3Δ1 leu2Δ0 met15Δ0 ura3Δ0 RPN5-GFP::HIS3MX rad23Δ::KanMX (generated for this study). For carbon starvation, cells were grown to saturation in synthetic complete medium containing 2 % glucose. Cells were diluted in the same medium and allowed to grow to the exponential phase overnight. Cells were then washed once in synthetic complete medium without glucose and resuspended in the same medium at a density of 0.1 OD. Cells

were incubated in this medium for 24 h before harvest. Yeast cells were fixed using formaldehyde as described [337], and examined by fluorescence microscopy.

- **Statistical analysis**

When applicable, appropriate statistical tests are used as described in figure legends

3.6 Acknowledgments

We thank Diana Adjaoud for technical assistance, Dr Diane Gingras for help with electronic microscopy and Dr Alain Verreault for yeast strains. This work was supported by grants from the Canadian Institutes of Health Research (CIHR) (MOP159539), the Natural Sciences and Engineering Research Council of Canada (NSERC) (DG 2015-2021) and The Cancer Research Society (2015-2017) to E.B.A, NSERC (DG 2019-2024) to H.W., CIHR MOP126009 to E.M., the CIHR (Foundation grant to J.-Y.M). E.B.A. and H.W are Scholars of the Fonds de la Recherche du Québec-Santé (FRQ-S). J.-Y.M is a FRQS Chair in genome stability. N.K. had a PhD scholarship from the FRQ-S and the Cole Foundation.

Disclosures

The authors declare no competing financial interests.

3.7 Supplemental figures and tables

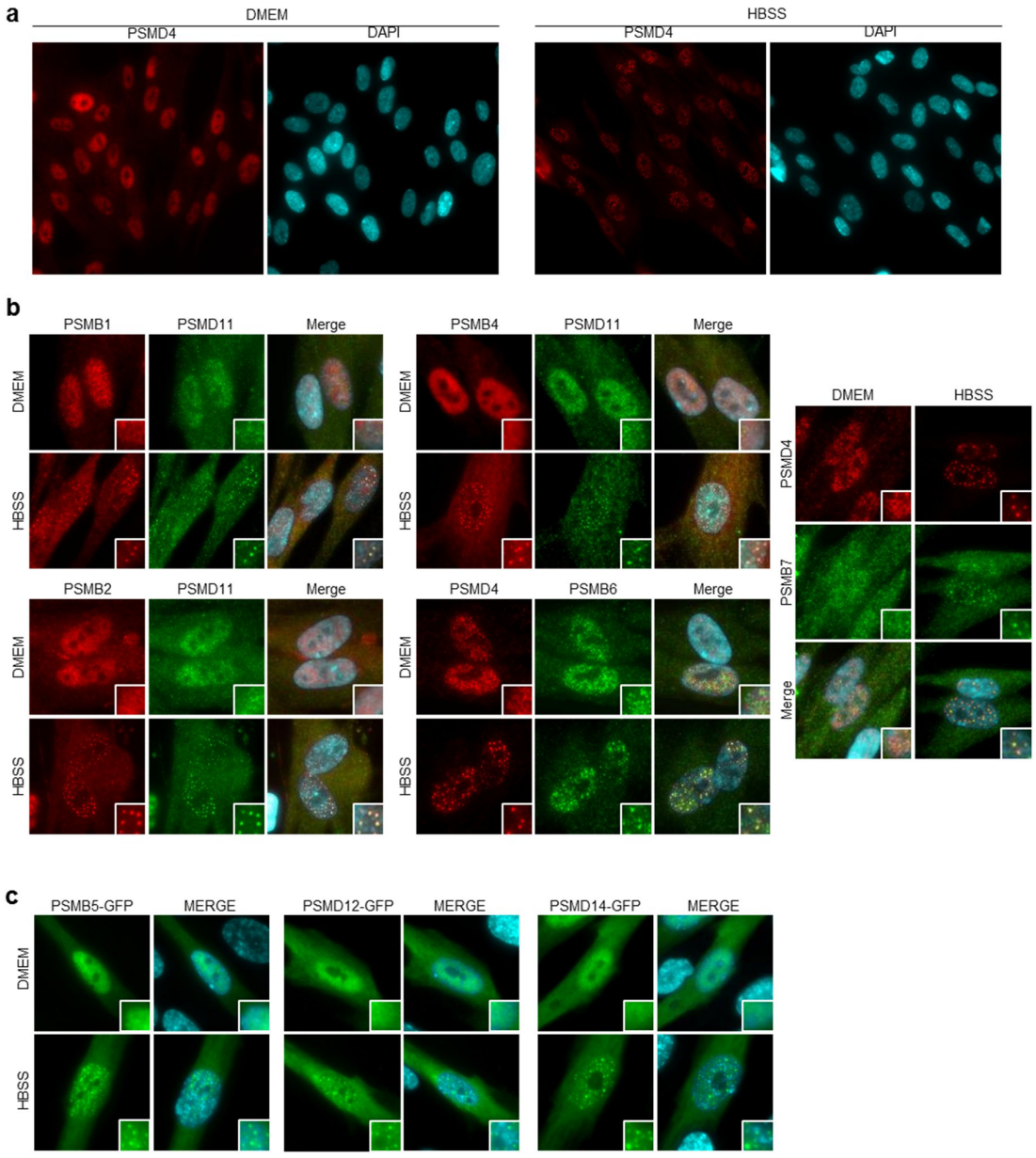

Figure 3-S 1 : Nutrient starvation in human cells induces the formation of nuclear foci containing components of the proteasome.

a) Immunostaining of PSMD4 proteasome component in IMR90 human fibroblasts showing that this component of the RP localizes in distinct nuclear foci following 6 h incubation in HBSS. **b**) Immunostaining of proteasome components in IMR90 human fibroblasts showing that component of the CP and RP co-localize in nuclear foci following 6 h incubation in HBSS. The green (endogenous PSMD11, PSMB6 or PSMB7), red (endogenous PSMB1, PSMB2,

PSMB4 or PSMD4) and blue (DAPI) signals were merged to indicate foci localization within the nucleus. The inset at the bottom right of each picture corresponds to a magnification of small portion of the nucleus as indicated. **c**) PSMB4-GFP localizes in nuclear foci following incubation of IMR90 in HBSS. IMR90 cells were transduced with viral particles generated in HEK293T using a lentiviral PSMB4-GFP constructs along with packaging vectors. Following four days post-infection, cells were incubated in HBSS for 6 h and harvested for fluorescence microscopy. **d**) PSMB5-GFP, PSMD12-GFP, PSMB14-GFP localize in nuclear foci following incubation of IMR90 in HBSS. Cells were transduced and treated as indicated in panel **c**.

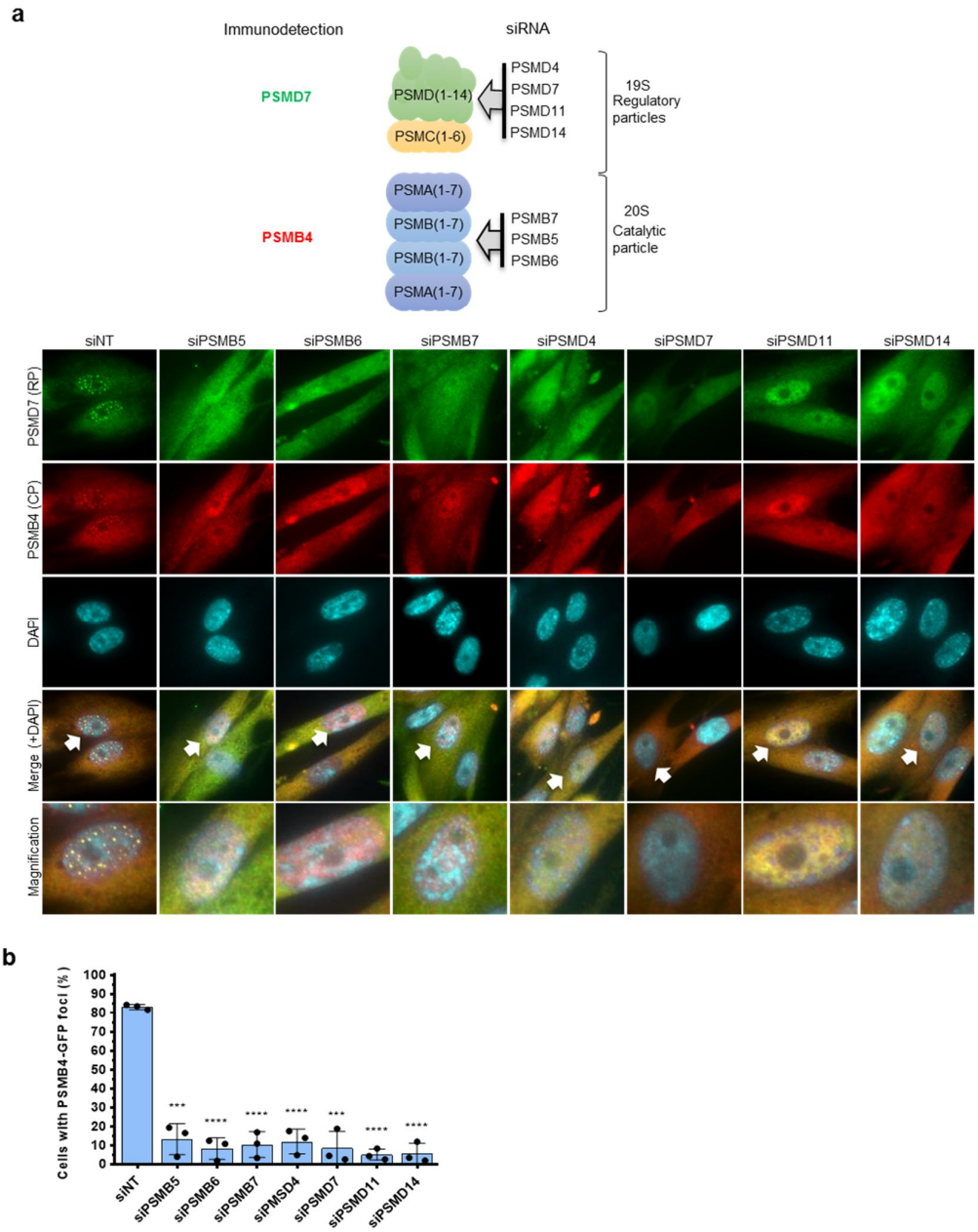

Figure 3-S 2 : Intact proteasome particle is assembled in nuclear foci following nutrient starvation.

a) siRNA-mediated depletion of components of the RP or CP abolish PSMD7 or PSMD4 foci formation. IMR90 cells were transfected twice with the indicated siRNAs. After three days, cells were treated with HBSS for 6 h and harvested for immunostaining of endogenous PSMB4 and PSMD7 proteins. Top panel represents a schematic of the proteasome regulatory and catalytic particles. The images in the bottom represent magnification of the merge as indicated by the arrows. **b**) Reduced PSMB4-GFP foci formation following depletion of individual

components of the proteasome. IMR90 cells expressing PSMB4-GFP were transfected twice with the indicated siRNAs. After three days, cells were treated with HBSS for 6 h and harvested for fluorescence microscopy. Data (panel **b**) represent mean ± s.d. of cells with more than 10 foci counted (n=3 independent experiments). ***P<0.001; ****P<0.0001; ns: not significant; 2-tailed unpaired Student's t-test.

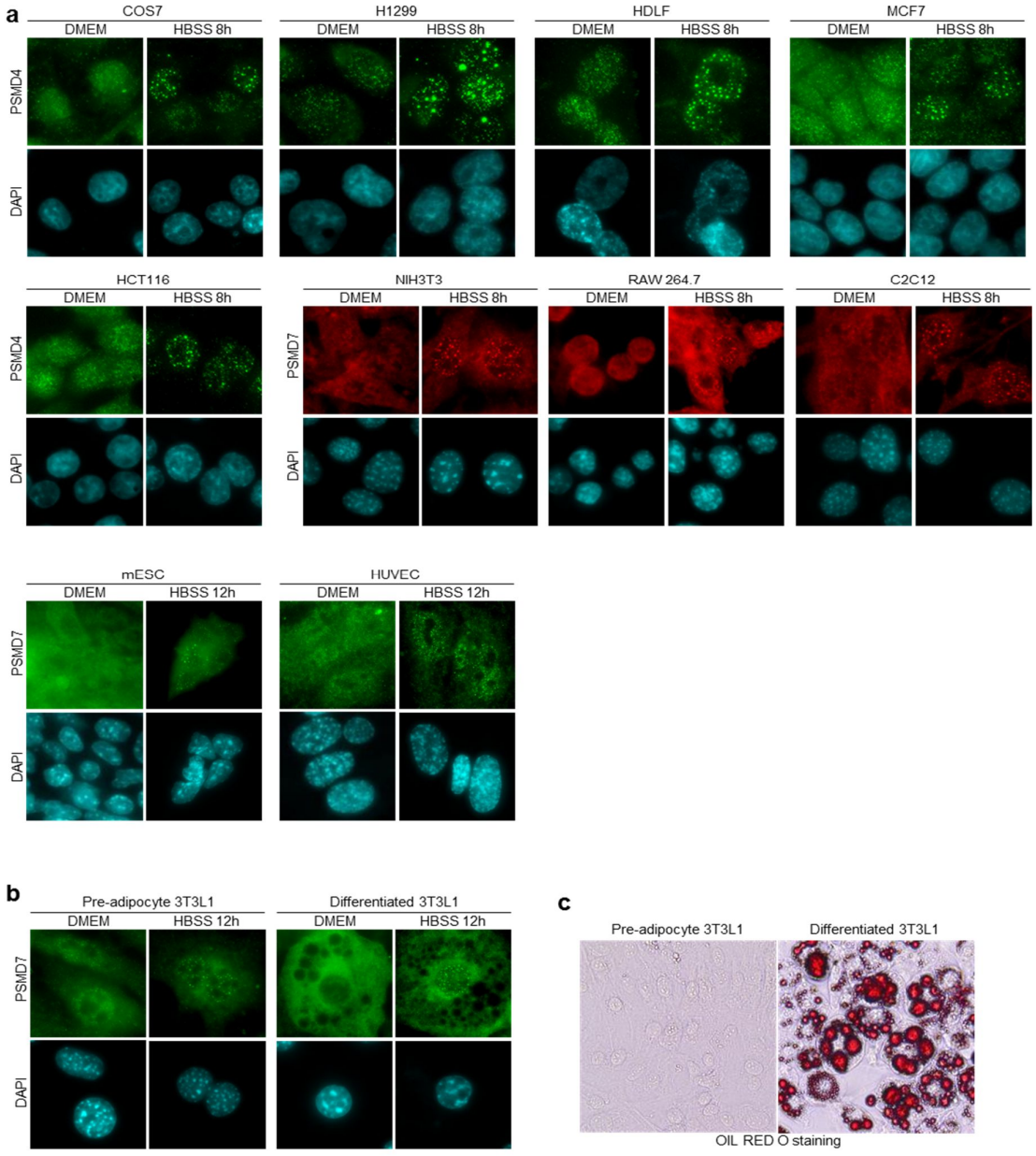

Figure 3-S 3 : SIPAN are a general phenomenon common to many mammalian cell types. **a**) Immunostaining of endogenous PSMD4 or PSMD7 in diverse cell types, showing that these proteins localise in nuclear foci following incubation in HBSS. SIPAN are observed in additional normal primary cells (e.g., HDLF: primary human lung fibroblasts, HUVEC: human

umbilical vein endothelial cells), immortalized cells (e.g., NIH3T3: mouse embryonic fibroblasts, C2C12: mouse myoblast cell line, 3T3L1: mouse preadipocytes), transformed (e.g., Cos7: SV40-transformed simian kidney cells, RAW264.7: Abelson murine leukemia virus transformed macrophage) and tumoral cells (e.g., HCT116: human colorectal carcinoma cell, MCF7: human breast cancer and H1299: human non-small cell lung cancer). **b**) Immunostaining of PSMD7, in mouse preadipocytes 3T3L1 and differentiated adipocytes showing that this protein localises in nuclear foci following incubation in HBSS. **c**) Oil Red O staining was conducted to control for adipocyte differentiation.

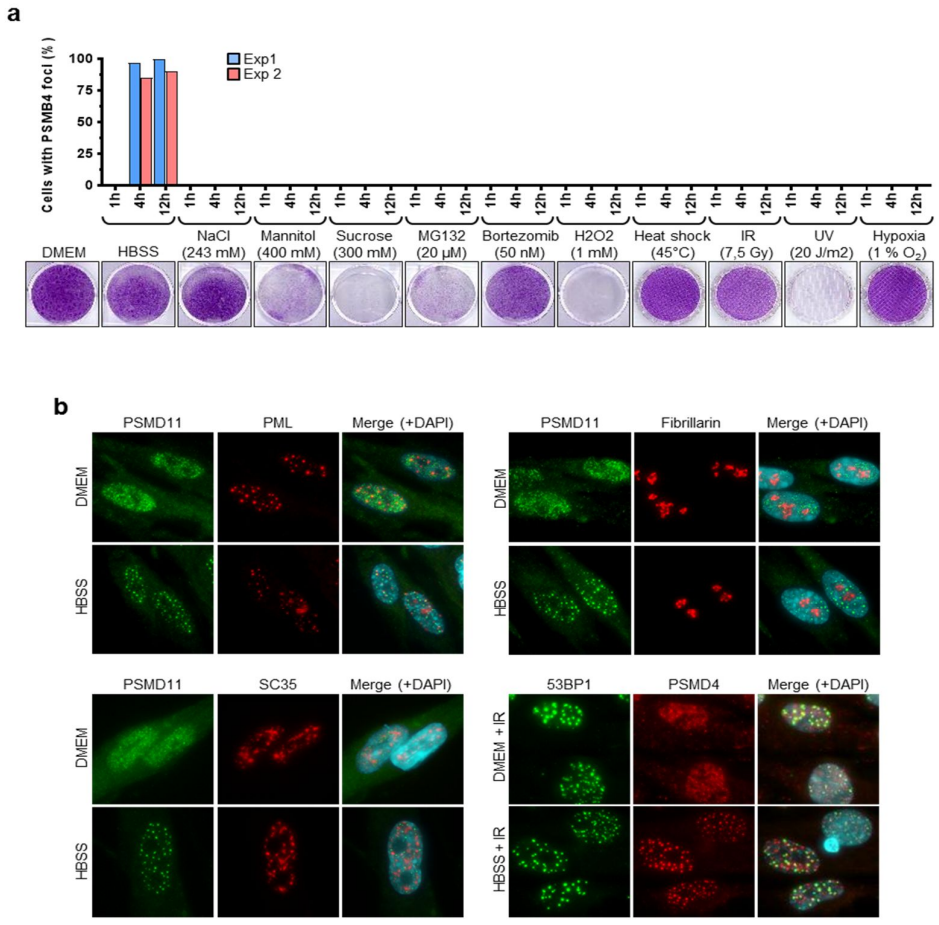

Figure 3-S 4 : SIPAN are selectively induced by metabolic stress and do not correspond to previously known nuclear structures.

a) Proteasome foci are not observed in response to other stress conditions. IMR90 cells were treated with various chemical or physical agents and endogenous PSMB4 was detected by immunostaining at the indicated times. Results of 2 experiments are shown. To ensure treatment efficacy, treated cells were also incubated in normal culture medium for 1 week and then stained with crystal violet. **b**) PSMD11 or PSMD4 proteasome foci do not correspond to any known

nuclear foci, structure or bodies including PML bodies (PML staining), nuclei (Fibrillarin staining), nuclear speckles (SC35 staining) or DNA double strand break foci (53BP1 staining). Staining were conducted following 6 h incubation in HBSS. The merge is shown in Figure 1h.

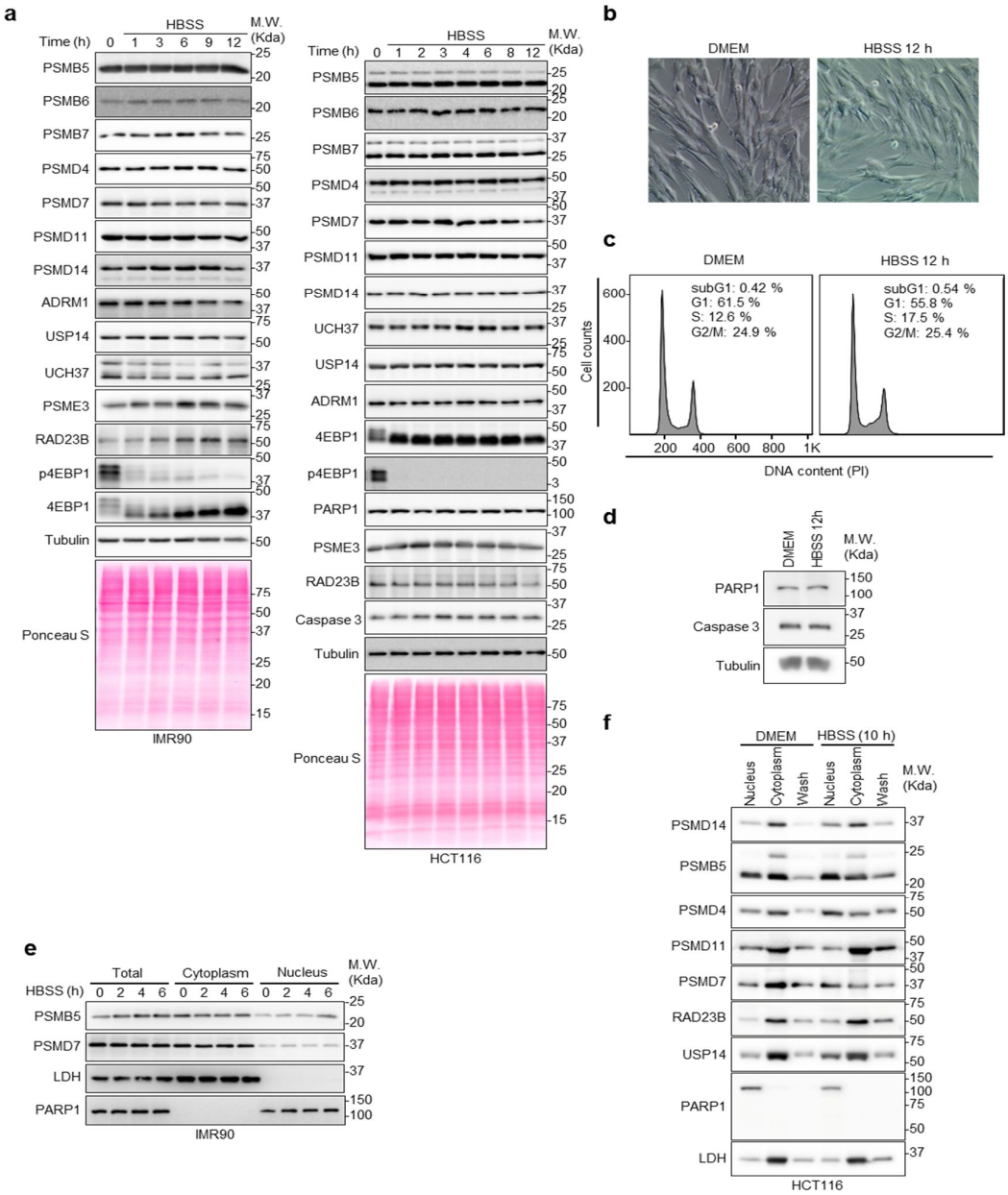

Figure 3-S 5 : Proteasome components are not translocated from the nucleus to the cytoplasm during nutrient starvation.

a) Protein levels of proteasome components and other factors following nutrient deprivation in IMR90 or HCT116 cells. Cells were incubated in HBSS solution and harvested at different times point for immunoblotting. 4EBP1 phosphorylation is included as a control for starvation.

b) Phase contrast pictures of IMR90 cells following incubation in HBSS. **c**) FACS analysis of IMR90 following nutrient deprivation. **d**) Protein levels of PARP1 and Caspase-3 following 12 h nutrient deprivation in IMR90 cells. Cells were incubated in HBSS solution and harvested at different times point for immunoblotting. **e-f**) Fractionation of IMR90 and HCT116 cells and immunoblotting for components of the proteasome. IMR90 cells were fractionated by hypotonic lysis and cytoplasmic and nuclear fractions were used for immunoblotting. HCT116 was fractioned by quick lysis with 0.1 % NP40 detergent and nuclear and cytoplasmic fractions were obtained. The wash fraction corresponds to resuspension of the nuclear pellet in detergent-free buffer followed by an additional centrifugation. LDH and PARP1 were detected as markers of cytoplasmic and nuclear fractions, respectively.

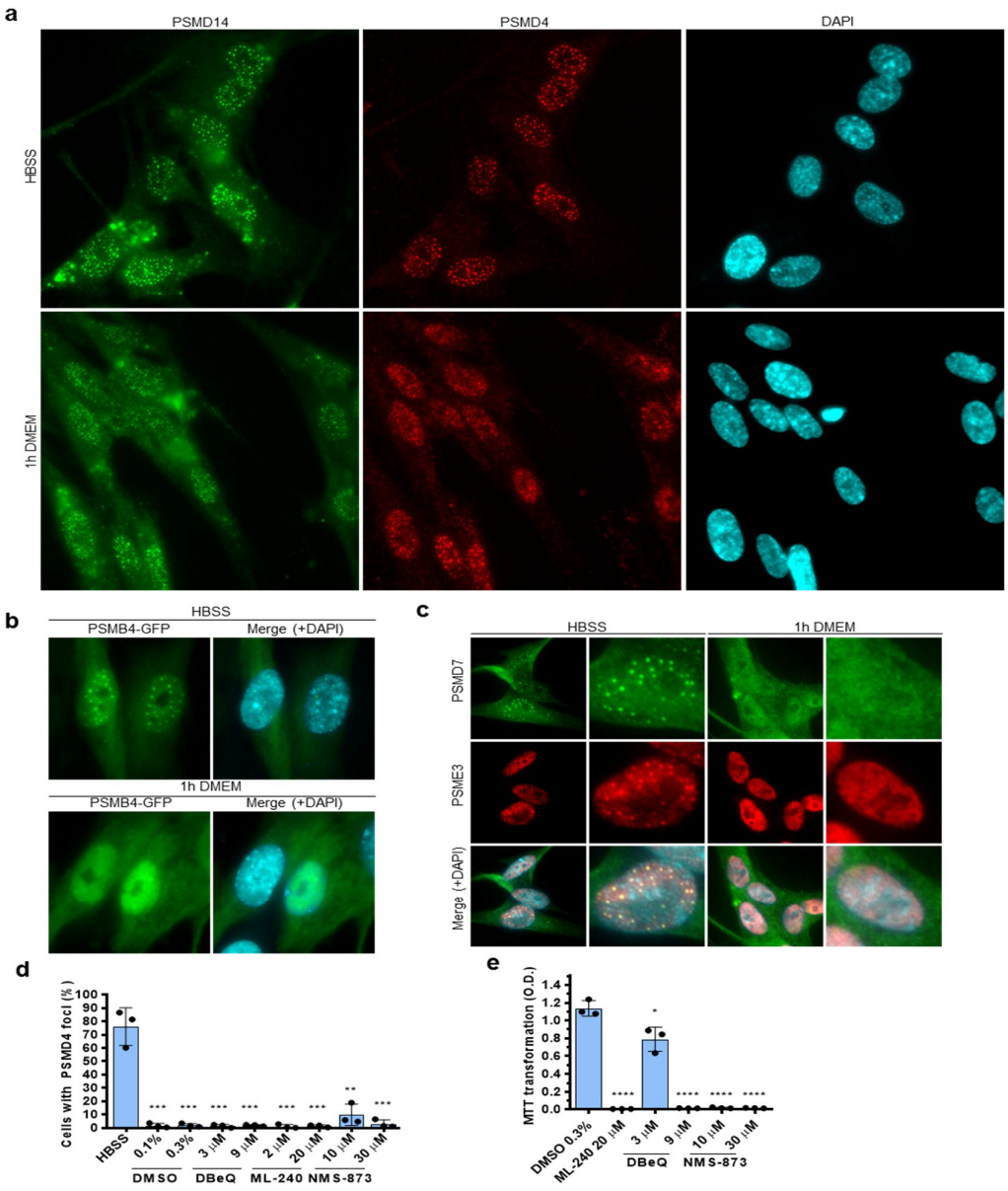

Figure 3-S 6 : Rapid dynamics of SIPAN assembly and resolution.

a-c) SIPAN are reversible. Foci formation is induced following incubation in HBSS and then IMR90 cells were replenished with fresh culture medium (DMEM supplemented with 10% FBS and glutamine) and harvested for immunodetection of PSMD14 and PSMD4 (**a**) or direct detection of PSMB4-GFP fluorescence (**b**), or immunodetection of PSMD7 and PSME3 (**c**). We observed that SIPAN become dissipated as quickly as 1 hour after adding fresh culture medium. **d**) VCP is not required for SIPAN resolution. IMR90 cells were treated with HBSS solution for 6 h and then treated with various VCP/p97 inhibitors (DBeQ, ML-240 and NMS-873) at the indicated concentrations, in complete medium for 1h. Cells with more than 10 foci

are counted. **e**) Inhibition of VCP results in cell death. IMR90 cells were incubated in HBSS for 24 h in the presence of various VCP/p97 inhibitors and harvested for MTT viability assay. Data represent the mean ± s.d. (n=3 independent experiments). Cells with more than 10 foci are counted (**d**). *P<0.05; **P<0.01; ***P<0.001; ****P<0.0001; ns: not significant; 2-tailed unpaired Student's t-test.

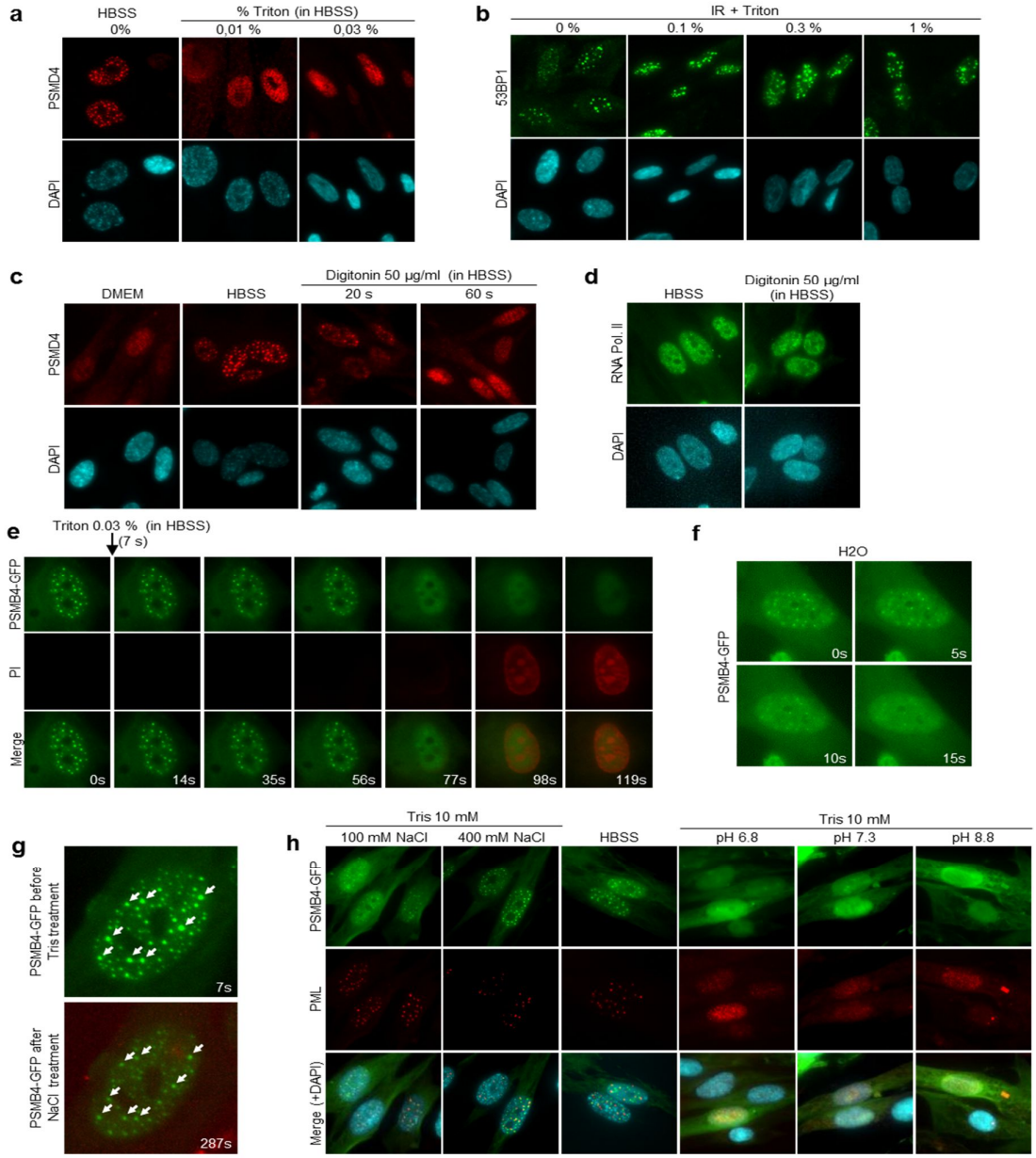

Figure 3-S 7 : SIPAN are highly responsive to physicochemical perturbations of cell environment.

a,b) SIPAN dissipate rapidly following incubation with very low concentration of Triton X-100 detergent. 53BP1 DNA repair foci are not displaced with a concentration of Triton 100 time

more than that used to dissipate SIPAN. IMR90 cells with preformed proteasome foci were treated with Triton in HBSS for 2 min and then harvested for PSMD4 immunostaining. For 53BP1 foci, IMR90 cells were treated with ionizing radiations for 4 h and the used for detergent treatment in HBSS for 2 min before immunostaining. **c**) SIPAN become dissipated rapidly following incubation with digitonin detergent. IMR90 cells were first treated for 8 h to allow SIPAN formation and then treated with digitonin in HBSS for the indicated times. Cells were then harvested for immunostaining. **d**) RNA Polymerase II staining is not affected by digitonin treatment. IMR90 cells with preformed SIPAN were treated with Digitonin in HBSS for 2 min and then harvested for RNA Polymerase II immunostaining. **e**) Live-cell imaging of PSMB4-GFP in IMR90 cells following addition of detergent. IMR90 cells were incubated in HBSS for 8 h to allow SIPAN formation, then treated with 0.03 % Triton X-100 in the presence of 50 µg/ml of propidium iodide (PI). **f)** Live imaging of PSMB4-GFP in IMR90 cells following addition of water. IMR90 cells were incubated in HBSS for 8 h to allow SIPAN formation, then treated as indicated. **g**) Merge of PSMB-GFP before treatment of IMR90 with hypotonic buffer and after addition of 200 mM of NaCl (magnification from **Figure 2j**). **h**) Concomitant detection of SIPAN (PSMB4-GFP) and PML bodies (PML staining) in IMR90 cells following addition of various buffers. Cells were incubated in HBSS for 8 h to allow SIPAN formation and then treated with various Tris buffers for 2 min before fixation and immunostaining.

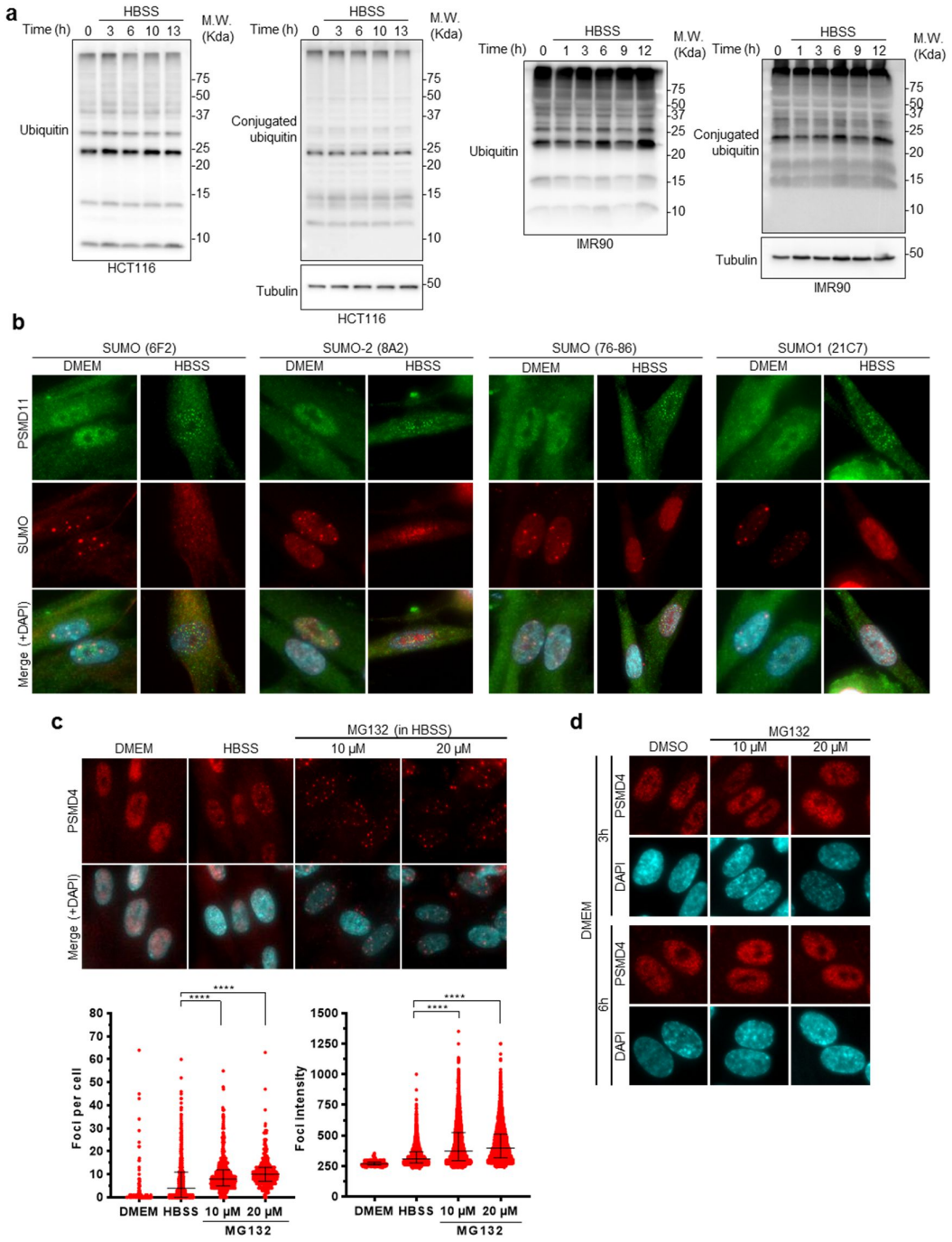

Figure 3-S 8 : SIPAN do not localize with SUMO and are increased with MG132 treatment.

a) Levels of ubiquitin and conjugated ubiquitin following nutrient deprivation in IMR90 or HCT116 cells. Cells were incubated in HBSS solution and harvested at different times point for immunoblotting with anti-ubiquitin or anti-conjugated ubiquitin FK2 antibodies. **b**) SUMO does not colocalize with PSMD11 in SIPAN following nutrient starvation. IMR90 cells were

incubated in HBSS for 6 h and harvested for immunostaining as indicated. Several antibodies against various SUMO epitopes were used. **c**) MG132 treatment increases SIPAN intensity and promote their formation. IMR90 cells were incubated in DMEM, HBSS only or HBSS containing 10 µM or 20 µM of MG132 for 3 h and cells were harvested for immunostaining. **d**) MG132 treatment does not induce SIPAN formation in normal culture conditions. IMR90 cells were incubated in DMEM for 3 or 6 h in the presence or absence of MG132, and cells were harvested for immunostaining. Data (in panel **c**, Bottom) represent the median with interquartile range of a representative experiment; **P<0.01; ***P<0.001; ****P<0.0001; Mann–Whitney U test (**c**).

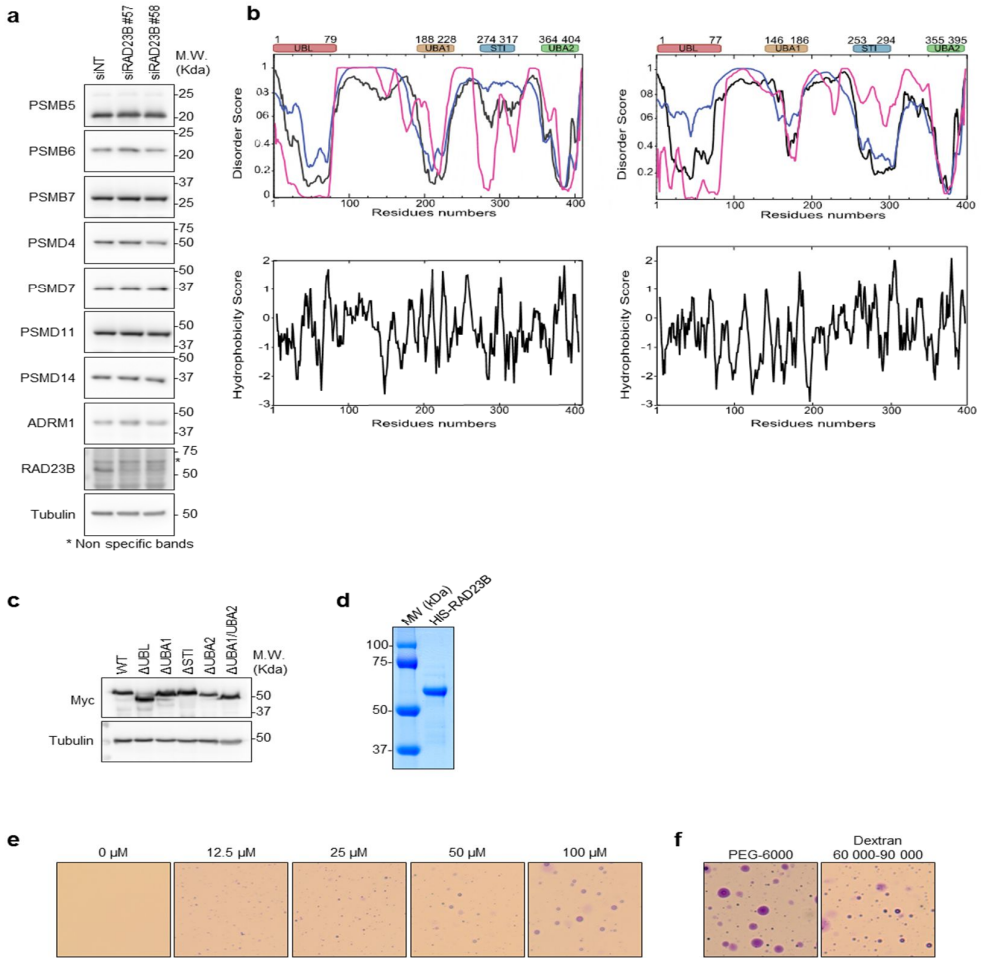

Figure 3-S 9 : RAD23B mediates SIPAN formation.

a) Depletion of RAD23B does not affect components of the proteasome. Following siRNA transfection, IMR90 cells were harvested for immunostaining for SIPAN formation. **b**) Analysis of intrinsically disorder properties of RAD23 proteins. Top panels, prediction of order/disorder

propensity of human RAD23B (left panel, uniprot #P54727) and yeast RAD23 (right panel, uniprot #P32628) based on their protein sequences. Disorder scores were calculated using PONDR-FIT [277], VSL2B (blue) and VLXT (magenta). Diagrams below shows the hydrophobicity distribution derived using Kyte-Doolittle hydropathy algorithm. **c**) Expression levels of RAD23B mutants. RAD23B mutant were expressed in HEK293T to validate expression of mutants. **d**) Purification of human RAD23B following expression in bacteria. **e**) Increasing concentrations of RAD23B and Ficoll 400 mixture was added on a microscope slide and covered with a coverslip for bright-field microscopy. **f**) RAD23B was mixed with Dextran 60,000-90,000 or PEG 6000 and was added on a microscope slide and covered with a coverslip. Crystal violet was used to stain the vesicles (panels **e** and **f**).

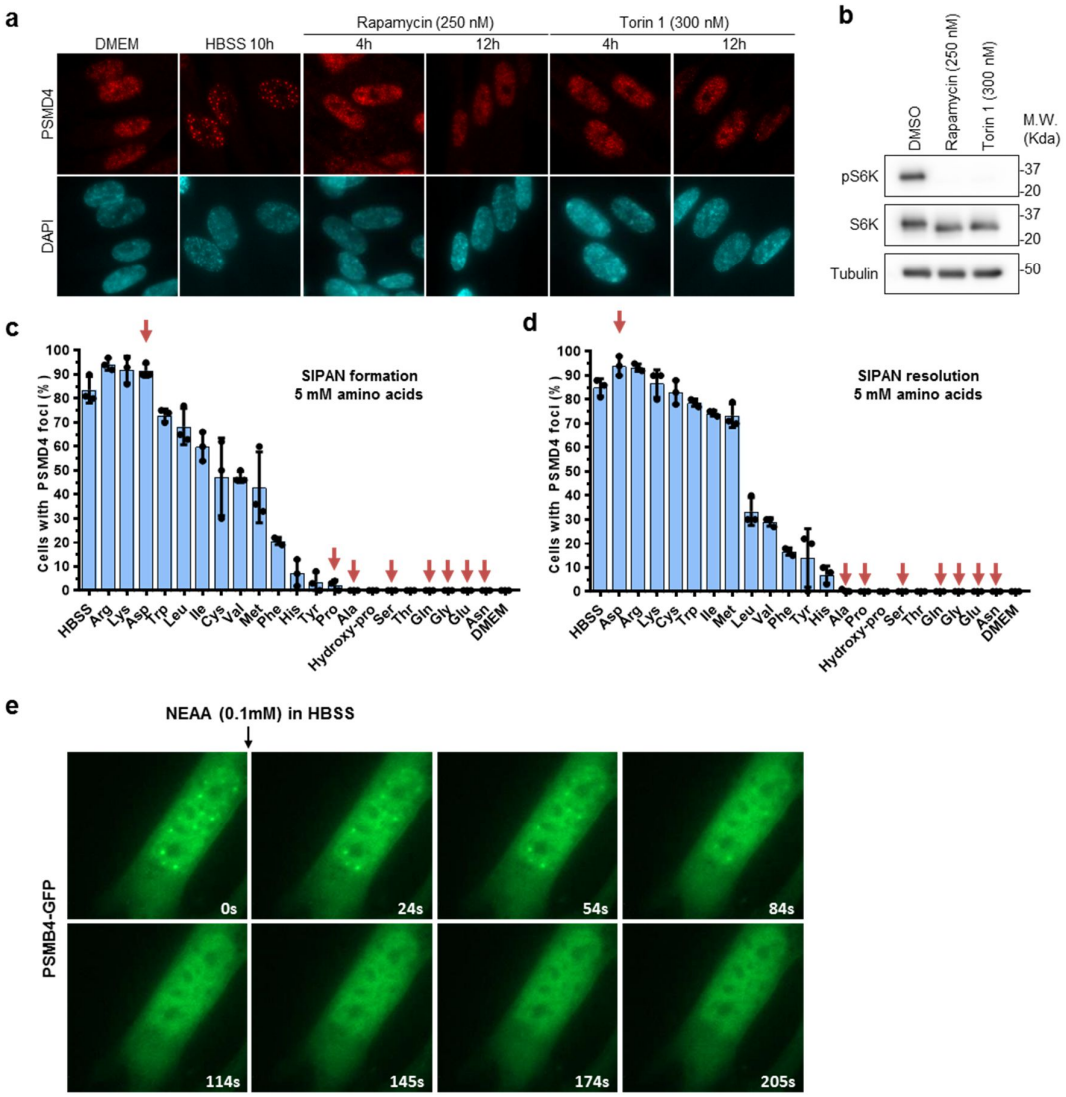

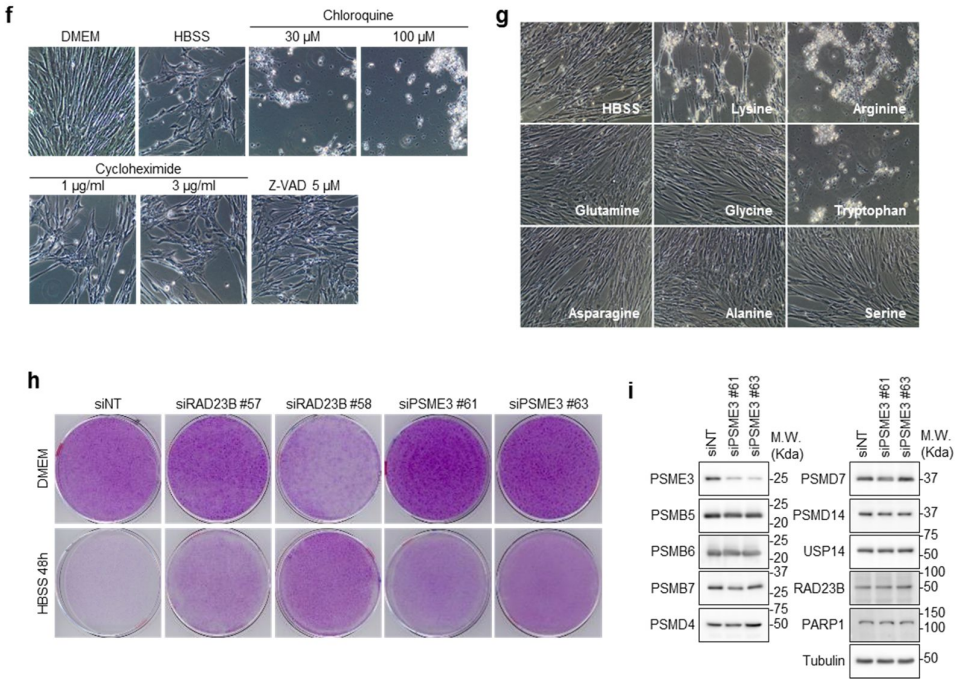

Figure 3-S 10 : Inhibition of RAD23B or PSME3 increases cell survival under conditions of amino acid starvation.

a) Inhibition of mTOR does not result in SIPAN formation. IMR90 cells were incubated with the inhibitors as indicated for immunostaining. **b**) Controls for mTOR inhibition. IMR90 cells were treated with mTOR inhibitors and harvested for immunoblotting with antibodies against the ribosomal protein S6K and its phosphorylated form, as indicated. **c-d**) Non-essential amino acids completely prevented SIPAN formation and promoted their resolution. Left, IMR90 cells were incubated 5 mM concentration of individual amino acids in HBSS solution and harvested after 6 h for immunostaining. Rights, SIPAN formation is induced and then cells were replenished with HBSS containing 5mM concentration of individual amino acids. Cells were harvested after 2 h for immunostaining. Cells with more than 10 foci are counted and the values from three experiments are presented as average ± SD. More pronounced effects on SIPAN were observed compared to 1 mM concentration of amino acids (see **Figure 4c, d**). Red arrows represents NEAA (**c, d**). **e**) Timelapse from live-cell imaging indicating SIPAN dissipation following incubation with 0.1 mM of NEAA. **f-g**) IMR90 cells were treated with various chemicals or amino acids in HBSS and harvested after 48 h for phase contrast imaging. **h**) Following siRNA transfection, IMR90 cells were incubated in HBSS for 48 h and then incubated for one week in normal culture medium and harvested for crystal violet staining. Note that IMR90 cells in the DMEM condition were diluted 10 times before plating to avoid confluency. **i**) Depletion of PSME3 does not result in changes in the levels of proteasome

proteins. Following siRNA depletion of PSME3, IMR90 cells were harvested for western blotting.

Table 3-S1 : Chemicals, Peptides, and Recombinant Proteins.

Chemicals, Peptides, and Recombinant Proteins	Source	Catalog Number
MG132	Sigma	C221
ML-240	Cayman	#17373
NMS-873	Cayman	#17674
Rapamycin	Selleckchem	S1039
Torin 1	Selleckchem	S2827
Sucrose	Sigma	S0389
Mannitol	Sigma	M-4125
Sodium Chloride	Bioshop	SOD002.5
MEM Amino Acids Solution solution, 50X	Wisent	#321-010-EL
NEAA (MEM Nonessential Amino Acids Solution, 100X)	Wisent	#321-011-EL
Chloroquine diphosphate	Bioshop	CHL919.25
Cycloheximide	Bioshop	CYC003.1
Hydrogen peroxide solution	Sigma	#216763
Digitonin	Sigma	DX1390-3
Z-VAD-FMK	Selleckchem	S7023
DBeQ	N/A	N/A
b-AP15	Calbiochem	#662140
3-Methyladenine	Cayman	#13242
Dextran 60000-90000	ICN	#101513
PEG 6000	Alfa Aesar	#A17541
1,6-Hexanediol	Aldrich	#240117
L-Alanine	Bioshop	ALA001.25
L-Arginine hydrochloride	Bioshop	ARG006.25
L-Asparagine anhydrous	Bioshop	ASP001.25
L-Aspartic acid	Bioshop	ASP003.25
L-Cysteine	Bioshop	CYS555.25
L-Cystine	Bioshop	CYS400.25
L-Glutamic acid	Bioshop	GLU202.100
L-Glutamine	Bioshop	GLU102.25
Glycine	Fisher	BP381-5
L-Histidine monohydrochloride monohydrate	Bioshop	HIS200.25
L-4-Hydroxyproline	Bioshop	HYP686.10
L-Isoleucine	Bioshop	ISO910.25
L-Leucine	Bioshop	LEU222.25
L-Lysine monohydrochloride	Bioshop	LYS202.500
L-Methionine	Bioshop	MET222.25
L-Phenylalanine	Bioshop	PHA302.25
L-Proline	Bioshop	PRO222.25
L-Serine	Bioshop	SER333.25
L-Threonine	Bioshop	THR002.25
L-Tryptophan	Bioshop	TRP100.25
L-Tyrosine	Bioshop	TYR333.25
L-Valine	Bioshop	VAL201.25

Table 3-S2 : siRNA sequences used.

Target	siRNA sequences	Names
DDI1	GAGCUUACUGGCAAUGUAA	SASI_Hs01_00215237
	CUUAUGCUCUAGGAUGGUA	SASI_Hs01_00215240
DDI2	GAAUCUACCUCACUGGGAA	SASI_Hs01_00215367
	GUUCCAUCGACCUGAAGAA	SASI_Hs02_00359727
RAD23A	CAGGAGAACCCUCAGCUUU	SASI_Hs01_00145993
	CAGUUCAUCCAGAUGCUGA	SASI_Hs02_00338864
RAD23B	GAAGCUAUAGAAAGGUUAA	SASI_Hs01_00198057
	CUAACUUGUUCACUGGAUU	SASI_Hs01_00198058
	GAAUCAGCCUCAGUUUCAA	SASI_Hs01_00198059
	CUUGGUAUAAGGUAGUAGA	SASI_Hs01_00198061
SHFM1	GGAUGACUUCUCUAAUCA	SASI_Hs01_00017254
	CACAUGUCUGGGAGGAUAA	SASI_Hs01_00017255
UBQLN1	CUGAAAUGAUGGUCCAGAU	SASI_Hs01_00157571
	GACUUACUGUUCACCUUGU	SASI_Hs01_00157573
UBQLN2	CAUGUACACUGACAUUCAA	SASI_Hs01_00115238
	CCUAUUUCCACAAAUAGC	SASI_Hs01_00115239
UBQLN3	GAGAUUGGGCAUAUUCUUA	SASI_Hs01_00189288
	CACAGAUAUUAUGGACCCA	SASI_Hs02_00350087
UBQLN4	CAAACAGCAGGGUGACUUU	SASI_Hs01_00085653
	CUGAUCUGAUGCGUCACAU	SASI_Hs01_00085656
UFD1L	GGAAGAAAGCCCUAAGUGA	SASI_Hs01_00153646
	GACUUUGUAGUUGUAUGCU	SASI_Hs01_00153648
PSMB5	GACAGUGAAGGGAACCGGA	SASI_Hs01_00076892
	CAUGGUGUAUCAGUACAAA	SASI_Hs01_00076894
PSMB6	GUCUGCAAUUCACUGCCAA	SASI_Hs01_00017705
	CUACAUCUAUGGCUAUGUU	SASI_Hs01_00017706
PSMB7	CACUUCAUAUCUCCUAAUA	SASI_Hs02_00334458
	CCAAGAAUCUGGUGAGCGA	SASI_Hs01_00241662
PSMD14	GUGAUUGAUGUGUUUGCUA	SASI_Hs01_00024446
	CAGAAGAUGUUGCUAAAUU	SASI_Hs01_00024447
PSMD11	CCAAGUUGUAUGAUAACUU	SASI_Hs01_00123192
	GCAUUUGAGGGUUAUGACU	SASI_Hs01_00123189
PSMD4	CCAAUUCUACCCUGCUCCU	SASI_Hs01_00179690
	GCACUAUGGUGUGUGUGGA	SASI_Hs01_00179692
PSMD7	CACUUGUUACGAGAUAUCA	SASI_Hs02_00334492
	CGUGUUGUUGGUGUGCUUU	SASI_Hs02_00334491
PSME3	GAAGGAAAGUGCUAGGUGU	SASI_Hs01_00137661
	CUAAUGAAACUCUCAUCUA	SASI_Hs01_00137663

Table 3-S3 : List of antibodies used.

Antibodies	Source	Catalog number
Mouse monoclonal anti-Fibrillarin	Santa Cruz	SC-166001
Mouse monoclonal anti-ADRM1	Santa Cruz	SC-166754
Mouse monoclonal anti-FK2	Millipore	#04-263
Mouse monoclonal anti-LDH	Santa Cruz	SC-133123
Mouse monoclonal anti-PA28γ (PSME3)	Santa Cruz	SC-136025
Mouse monoclonal anti-SC35	Santa Cruz	SC-53518
Mouse monoclonal anti-PSMB1	Santa Cruz	SC-374405
Mouse monoclonal anti-PSMB2	Santa Cruz	SC-365725
Mouse monoclonal anti-PSMB4	Santa Cruz	SC-390878
Rabbit polyclonal anti-PSMB5	Bethyl	#A303-847A
Rabbit Monoclonal anti-PSMB6	Cell Signaling	#13267
Rabbit Monoclonal anti-PSMB7	Cell Signaling	#13207
Rabbit polyclonal anti-PSMD11	Bethyl	#A302-751A
Rabbit Monoclonal anti-PSMD14	Cell Signaling	#4197S
Mouse monoclonal anti-PSMD4	Santa Cruz	SC-393546
Rabbit polyclonal anti-UCH37	Bethyl	A304099A
Rabbit polyclonal anti-PSMD7	Bethyl	A303-828A
Mouse monoclonal anti-RAD23B	Santa Cruz	SC-166507
Mouse monoclonal anti-Tubulin	Santa Cruz	SC-23948
Mouse monoclonal anti-Ub	Santa Cruz	SC-8017
Rabbit polyclonal anti-c-fos	Santa Cruz	SC-7202
Mouse monoclonal anti-PARP1	Santa Cruz	SC-8007
Mouse monoclonal anti-p53	Santa Cruz	SC-126
Mouse monoclonal anti-c-jun	Santa Cruz	SC-74543
Rabbit polyclonal anti-53BP1	Santa Cruz	SC-22760
Mouse monoclonal anti-PML	Santa Cruz	SC-966
Mouse monoclonal anti-H3	Cell Signaling	#14269S
Mouse monoclonal anti-RNA polymerase II	Millipore	#05-952
Mouse monoclonal anti-SUMO1 21C7	DSHB	SUMO1 21C7
Mouse monoclonal anti-SUMO1 76-86	DSHB	SUMO1 76-86
Mouse monoclonal anti-SMUO-2 8A2	DSHB	SMUO-2 8A2
Mouse monoclonal anti-SUMO 6F2	DSHB	SUMO 6F2
Mouse monoclonal anti-caspase 3	Santa Cruz	SC-56053
Mouse monoclonal anti-USP14	Santa Cruz	SC-100630
Rabbit monoclonal anti-S6 ribosomal protein	Cell Signaling	#2217S
Rabbit monoclonal anti-P-S6 ribosomal protein	Cell Signaling	#4858S
Rabbit polyclonal anti-P-4EBP1	Cell Signaling	#9459S
Rabbit monoclonal anti-4EBP1	Cell Signaling	#9644S
Mouse monoclonal anti-MYC	This paper	homemade

CHAPITRE 4

4 DISCUSSION

L'objectif général de cette thèse est l'étude des mécanismes régulant l'assemblage et le désassemblage des foci nucléaires formés suite à une LLPS. Les deux articles discutés dans ce manuscrit ont pour cible la régulation de la LLPS suite à des stress nocifs pour la cellule, causés soit par des radiations ionisantes, soit par une privation de nutriments.

Le deuxième chapitre de cette étude s'est intéressé essentiellement au rôle de la déubiquitinase cytoplasmique USP16 dans la régulation de H2AK119ub. Cette modification est impliquée dans la répression de l'expression génique, la progression du cycle cellulaire et la régulation de la réponse aux dommages à l'ADN. Bien que plusieurs études reconnaissent l'implication de USP16 dans diverses signalisations nucléaires, son mécanisme d'action reste mal connu. Ainsi, la caractérisation moléculaire et fonctionnelle de USP16 nous a permis de comprendre le mécanisme complexe qui gouverne la localisation subcellulaire de cette déubiquitinase et son implication dans la régulation de H2AK119ub.

Le troisième chapitre de cette étude s'est intéressé plus en profondeur aux mécanismes de régulation des foci du protéasome dans le noyau de la cellule. Étant donné que l'UPS régule la majeure partie des processus cellulaires, comprendre davantage comment les protéines du protéasome, ainsi que ses partenaires participent à la formation de ces foci est primordial pour mieux appréhender le rôle de l'UPS dans le développent et la progression du cancer.

4.1 Transport et localisation de la protéine USP16

Dans le but d'investiguer les mécanismes qui coordonnent la localisation de USP16, nous avons effectué des expériences d'immunofluorescence et de fractionnement subcellulaire. Nos travaux montrent la présence de USP16 exclusivement dans le cytoplasme des cellules durant l'interphase du cycle cellulaire et suite aux dommages à l'ADN [338]. Nous avons donc conclu que USP16 pourrait indirectement réguler la formation des foci de dommages à l'ADN. Ce résultat est très inattendu, compte tenu du rôle prédit de USP16 dans la déubiquitination de l'histone H2AK119ub. Par ailleurs, aucune des études antérieures de USP16 n'a pu démontrer, de façon convaincante, sa présence dans le noyau dans des conditions normales. Toutefois, les techniques d'immunofluorescence et de fractionnement subcellulaire sont potentiellement critiquables, car elles ne permettent pas de visualiser de très faibles niveaux de USP16 dans le noyau qui sont en dessous de la limite de détection.

En revanche, une accumulation nucléaire de USP16 n'est observée que lorsqu'on traite les cellules à la leptomycine B, un inhibiteur de l'export nucléaire. Aussi, des analyses plus approfondies de la distribution de USP16 ont indiqué que bien qu'elle possède un motif NLS fonctionnelle, USP16 diffuse passivement à l'intérieur du noyau après rupture de la membrane nucléaire lors de la mitose. Ensuite, elle est très transitoirement retenue dans le noyau en début de phase G1, et exportée par la suite dans le cytoplasme. Il est possible que la disparition du pool de USP16 dans le noyau soit concomitante avec la réorganisation de ce dernier. Au vu de tous ces résultats, nous avons donc conclu que USP16 est principalement localisée dans le cytoplasme. Ces résultats ont soulevé un grand nombre de questions :

(a) A quoi sert le NLS fonctionnelle de USP16 ?
(b) USP16 est-elle impliquée dans le remodelage de la chromatine ?
(c) Comment s'effectue la régulation de USP16 ?
(d) Avec quels partenaires USP16 interagit ?
(e) Y a-t-il un rôle de USP16 dans le cytoplasme ?

Nous avons tenté d'apporter des éléments de réponses par différentes approches discutées dans les paragraphes suivants.

4.1.1 À quoi sert le NLS fonctionnel de USP16 ?

Malgré le fait que USP16 soit principalement cytoplasmique, nous avons pu identifier un signal de localisation nucléaire (NLS) dans sa séquence suggérant son implication dans des événements nucléaires. Cependant, si USP16 diffuse passivement à l'intérieur du noyau après rupture de la membrane nucléaire lors de la mitose, à quoi sert son NLS ?

Des études ont rapporté que la présence d'un NLS dans une protéine ne garantit pas nécessairement son importation vers le noyau [339]. La présence d'un NLS fonctionnel dans la séquence protéique de USP16 et son absence du noyau pourrait suggérer une forte régulation de ce motif. Dans le cytoplasme, ce motif pourrait être caché selon la conformation de USP16. Par exemple :

- Étant donné que ce NLS est situé entre les 2 régions du domaine catalytique, il est possible que la conformation ou le repliement de USP16 masque l'accessibilité du signal [338].
- L'interaction de USP16 avec lui-même (homo-tetramerization) ou avec d'autres protéines pourrait inhiber sa capacité à être importée vers le noyau [171].

- Des modifications post-traductionnelles de USP16 pourraient rendre impossible son accès vers le noyau.

Afin de déterminer si certains évènements masquent l'accessibilité du NLS de USP16, une comparaison de la capacité d'interaction de la protéine USP16 avec le complexe importine α/β, en absence et en présence d'un extrait cellulaire, pourrait être envisagée. Toutefois, nous devons aussi envisager la possibilité qu'il n'y ait pas de mécanisme actif transportant USP16 du cytoplasme vers le noyau ou que ce NLS est très peu efficace dans le contexte de la protéine USP16. Par conséquent, USP16 serait tout simplement exclu du noyau via son signal d'export nucléaire.

4.1.2 USP16 est-elle impliquée dans le remodelage de la chromatine ?

Les analyses effectuées dans le chapitre 2 nous ont permis de constater que lorsque USP16 est catalytiquement inactive, elle reste accrochée à l'ubiquitine ce qui empêche son exportation vers le cytoplasme. Dans le même ordre d'idée, Cai et son équipe ont révélé que lorsque USP16 est dépourvue de sa cystéine active, elle s'associe aux chromosomes mitotiques lors de la division cellulaire et reste à l'intérieur du noyau pendant la période postmitotique [149].

L'entrée des cellules en mitose est généralement initiée par une condensation des chromosomes, qui atteint son maximum en métaphase, ceci pour permettre la ségrégation des chromatides [340]. De plus, le complexe PRC1, responsable de H2AK119ub a déjà été impliqué dans le mécanisme de compaction et de remodelage de la chromatine [341, 342]. Malgré le haut niveau de compaction des chromosomes lors de la mitose, des études ont montré qu'il existe différents facteurs épigénétiques permettant l'accès à la chromatine durant la métaphase [343]. En effet, des différences d'accessibilité entre les loci alléliques sur la chromatine en métaphase ont été observées [343, 344]. Ce qui signifie qu'il pourrait exister des régions décondensées au niveau des chromosomes mitotiques de la métaphase. Au vu de ces différents résultats, il est donc possible que USP16 se lie de manière transitoire à H2AK119ub pour enlever cette marque répressive et permettre un relâchement local de la chromatine. Ceci augmenterait l'accessibilité des protéines responsables de la progression de la phase mitotique du cycle cellulaire.

Parallèlement, d'autres travaux ont suggéré que lors de la métaphase, la PLK1, une protéine importante pour la division cellulaire, est monoubiquitinée par l'ubiquitine ligase CUL3-KLHL22 [181, 182]. Cette modification promeut sa dissociation des kinetochores et permet à la cellule mitotique d'entrer en anaphase [181]. Afin d'assurer le bon déroulement

de la division cellulaire, Zhuo et al. ont proposé que durant la prométaphase, USP16 se lie à PLK1 pour assurer sa déubiquination et le maintien de PLK1 au niveau des kinetochores [184]. Cette déubiquitination va permettre à PLK1 de promouvoir l'alignement des chromosomes de la prométaphase jusqu'en métaphase [184]. Ainsi, la déplétion de USP16 induirait un mauvais alignement chromosomique au niveau de la plaque métaphasique.

En considérant ces différents résultats, nous proposons un scénario selon lequel suite à la rupture de la membrane nucléaire en mitose, USP16 diffuse passivement dans le noyau pour déubiquitiner H2A afin d'assurer le relâchement de la chromatine, l'accessibilité des gènes et permettre l'avancement de la mitose. En parallèle, USP16 déubiquitine PLK1 pour promouvoir un alignement optimal des chromosomes et permettre une division cellulaire harmonieuse. Une fois la mitose terminée, nous proposons que USP16 doive impérativement sortir du noyau pour éviter une éventuelle activité protéase non spécifique. Ainsi, la membrane nucléaire jouerait le rôle de barrière pour empêcher USP16 de se localiser dans le noyau et induire une déubiquitination excessive des protéines pouvant conduire à des maladies telles que le syndrome de Down [151].

Toutefois, la possibilité que USP16 déubiquitine d'autres substrats à l'intérieur du noyau après la rupture de l'enveloppe nucléaire pour permettre la progression de la mitose et la division cellulaire n'est pas exclue. De manière intrigante, des études ont montré que USP16 est enrichie au niveau des promoteurs et dans des sites d'initiation de la transcription de 2461 gènes [198]. Étant donné le rôle de USP16 dans le développement postérieur chez le Xénope et dans l'expression des gènes des cellules souches embryonnaires et hématopoïétiques [171, 198, 199], il est toujours possible que la fonction remplie par USP16 dans le noyau soit de réguler l'expression des gènes responsables de la progression du cycle cellulaire et du développement. De toute évidence, d'autres expériences seront nécessaires pour tester ces différentes hypothèses.

4.1.3 Régulation de USP16 par d'autres PTMs

Nos résultats indiquent que bien que USP16 possède un NLS fonctionnel, elle se trouve principalement dans le cytoplasme. Une explication à cela est qu'elle possède aussi un NES très fort, responsable de sa rétention cytoplasmique. Cependant, au cours de ces dernières années, plusieurs études suggérant que les PTMs seraient capables de réguler l'activation et la localisation de USP16 ont fait l'objet de plusieurs contradictions.

Tout d'abord en 1999, Cai et son équipe ont montré que USP16 est phosphorylée durant la pro-métaphase par le complexe CDC2/cycline B, puis déphosphorylée en anaphase. De plus, ces auteurs précisent que la phosphorylation et la déphosphorylation de USP16 seraient respectivement corrélées à la déubiquitination et re-ubiquitination de l'histone H2A [149]. Par la suite, en 2013, il a été suggéré que USP16 est phosphorylée sur la sérine 552 par le complexe CDK1/cycline B à la barrière G2/M. Cette phosphorylation semblerait faciliter sa localisation nucléaire et serait importante pour la progression du cycle cellulaire [158]. La même année, Frangini et son équipe ont proposé que la kinase AuroraB serait capable de phosphoryler USP16, ce qui promeut son activité déubiquitinase [345]. En 2015, la protéine PLK1 a été identifiée comme étant la kinase capable de phosphoryler et d'activer USP16 durant la mitose [183]. Récemment, en 2017, Stratford et al, a indiqué que la kinase TTK (aussi connu sous le nom de Mps1 : Monopolar spindle 1) induirait la phosphorylation de USP16 sur les résidus S415, S552 et T554 et cette modification conduirait à une dégradation protéasomale de USP16 [346]. Face à de toutes ses différentes affirmations qui semblent contradictoires, nous avons essayé d'apporter quelques explications.

Pour déterminer si les PTMs de USP16 affectent son activité déubiquitinase, nous avons synchronisé la lignée cellulaire HeLa S3 exprimant de manière stable Flag-HA-USP16 en phase G2/M après 24 heures de traitement au nocodazole. Ensuite, les complexes USP16 ont été purifiés à partir de cellules non synchronisées et mitotiques (**Figure 4-1A et B**). Fait intéressant, nous avons observé un changement de la mobilité de USP16 pendant la mitose suggérant qu'elle est fortement phosphorylée pendant cette phase du cycle cellulaire (**Figure 4-1C**). Nous avons identifié par spectrométrie de masse plusieurs sites de phosphorylation (**Figure 4-1D**). Ensuite, nous avons mis en place un test de déubiquitination *in vitro* sur un substrat nucléosomal contenant H2AK119ub, et avons observé que USP16, purifiée à partir de cellules mitotiques ou non synchronisées, est capable de déubiquitiner l'histone H2A (**Figure 4-1C**). La phosphorylation de USP16 ne semble donc pas avoir un impact direct ni sur son activité DUB, ni sur sa stabilité.

Par la suite, nous avons voulu savoir si cette phosphorylation a un impact sur la localisation subcellulaire de USP16. Nous avons ainsi généré des constructions d'expression myc-USP16 de type sauvage (myc-USP16 WT) et myc-USP16 mutées dans ses sites de phosphorylation (myc-USP16 PM, tous les sites de phosphorylation convertis en alanines) (**Figure 4-1E**). Nous avons analysé par immunofluorescence, l'effet de ces mutations sur la localisation de USP16 et avons montré que dans des conditions normales, USP16 WT et USP16

PM étaient principalement cytoplasmiques (**Figure 4-1F**). Aussi, l'enrichissement de USP16 dans le noyau suite au traitement à la LMB semble être indépendant de sa phosphorylation (**Figure 4-1F**).

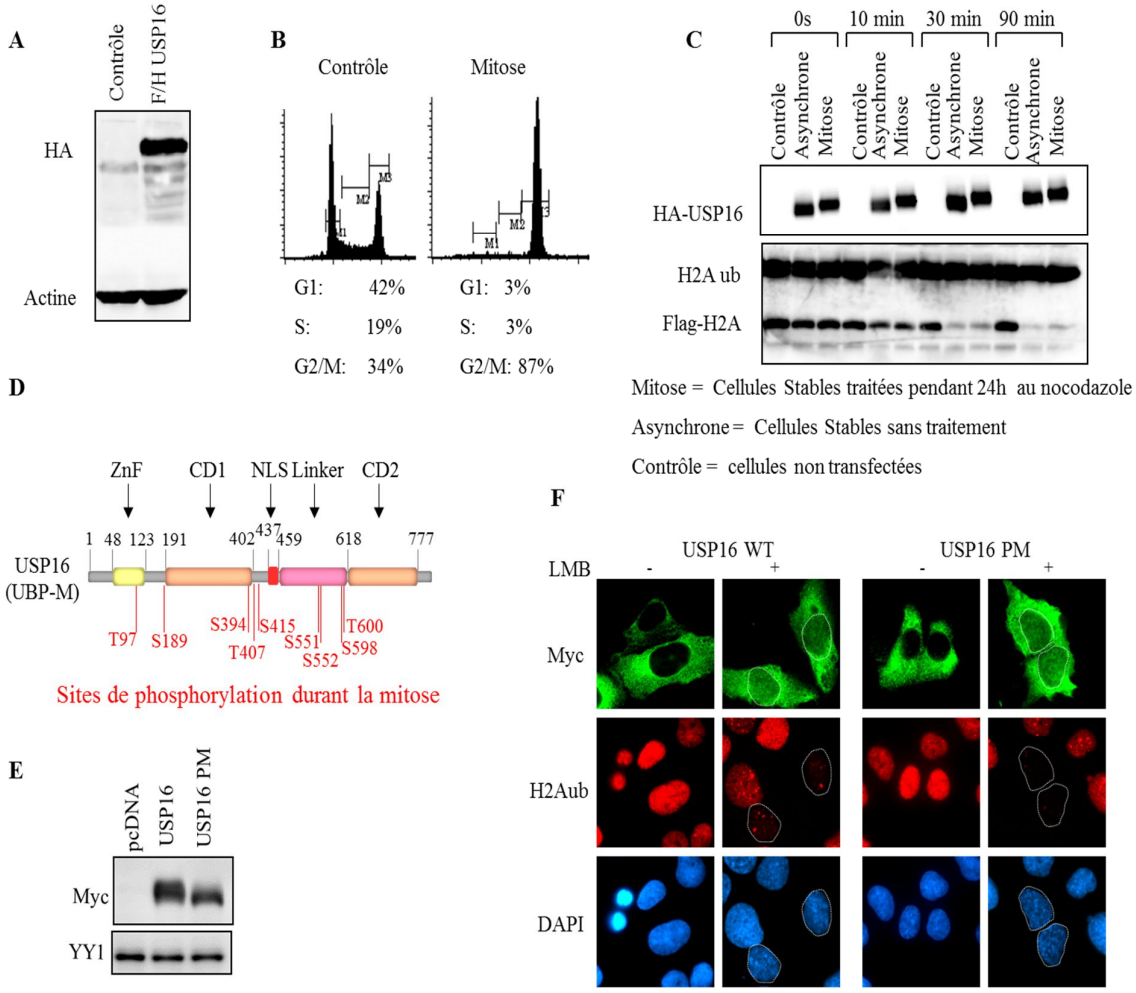

Figure 4-1 : Rôle de la phosphorylation de USP16 dans sa localisation et son activité.

(A, B) La protéine Flag-HA-USP16 a été purifiée à partir des cellules HeLa S3 synchronisées en phase M en utilisant un traitement au nocodazole à 200 ng/ml. Le profil du cycle cellulaire a été analysé par cytométrie en flux à l'aide d'iodure de propidium pour garantir la synchronisation des cellules. **(C)** L'activité de la déubiquitinase USP16 a été détectée par un essai DUB *in vitro* suivi d'un western blot. Les protéines purifiées Flag-HA-USP16 provenant de cellules interphasiques et mitotiques ont été incubées avec un substrat H2AK119ub nucléosomique à différents moments. **(D)** Flag-HA-USP16 purifié à partir de cellules non synchronisées ou mitotiques a été analysée par spectrométrie de masse et de nombreux sites de phosphorylation USP16 ont été identifiés. **(E)** Myc-USP16 de type sauvage (USP16 WT) et

myc-USP16 mutée en alanine dans ses sites de phosphorylation (USP16 PM) ont été générés pour déterminer la localisation subcellulaire de USP16. **(F)** L'analyse par immunofluorescence a été effectuée pour déterminer l'effet de ces mutations sur la localisation subcellulaire de USP16 en présence ou en absence de 10 ng/mL de leptomycine B.

L'importance de la phosphorylation lors du cycle cellulaire et, en particulier, dans les cellules qui traversent la mitose est reconnue depuis longtemps [347, 348]. Plusieurs scénarios peuvent donc expliquer la phosphorylation de USP16. En effet, l'entrée des cellules en mitose est caractérisée par une activation massive de plusieurs kinases dont : CDK1/cycline B, PLK, Aurora A et B, Greatwall (GWL), Wee, Haspin, TTK, etc. Ensemble, ces kinases ont la capacité de phosphoryler plus de 1000 protéines nécessaires pour la rupture de l'enveloppe nucléaire, la condensation adéquate des chromosomes et la formation des fuseaux mitotiques [349]. Le processus inverse a été observé en fin de mitose où on assiste à une désactivation et à une dégradation des kinases, permettant ainsi une déphosphorylation massive des substrats [350].

Une des hypothèses possibles de la phosphorylation de USP16 serait qu'elle soit une conséquence de sa présence dans le noyau suite à la rupture de la membrane nucléaire. Étant donné que chez les eucaryotes, l'enveloppe nucléaire est entièrement rompue en prophase et prométaphase, il est possible que USP16 se disperse dans le noyau durant cette période et devienne la cible de nombreuses kinases. Ce qui pourrait expliquer nos observations selon lesquelles la phosphorylation n'affecterait pas la localisation de USP16. Par ailleurs, la déphosphorylation de USP16 à la fin de la mitose comme l'a indiqué Cai et a. [149], serait la résultante de la dégradation des kinases mitotiques. Ainsi, lors du réassemblage de l'enveloppe nucléaire, USP16 serait activement exclu du noyau en raison de la présence de son NES.

Comme autre alternative au rôle de la phosphorylation de USP16, il se pourrait que cette modification soit nécessaire pour coordonner l'interaction de USP16 avec ses partenaires et/ou pour son implication dans d'autres processus cellulaires. Par exemple, des auteurs ont révélé la protéine HERC2, une ubiquitine ligase connue pour interagir avec USP16 [279], se localise au niveau des centrosomes pour maintenir leur intégrité [351]. Aussi, HERC2 a été impliquée dans le contrôle de la duplication des centrioles via son interaction et sa stabilisation avec la protéine NudCL2 [352]. Étant donné le rôle de USP16 dans la régulation de la localisation des kinétochores au niveau de la région centromérique, il serait possible que USP16 et HERC2 interagissent pour réguler la métaphase. Basés sur ce scénario, nous ne pouvons exclure la possibilité que la phosphorylation de USP16 au cours de la mitose serait nécessaire pour la régulation de cette interaction. Toutefois, des études supplémentaires sont clairement

nécessaires pour déterminer si la phosphorylation de USP16 et son interaction avec HERC2 auraient un impact sur la division cellulaire.

Comme autre modèle, il serait possible que hormis la phosphorylation, d'autres PTMs pourraient réguler l'action de USP16. Par exemple, la base de données protéomiques « phosphositeplus » indique que USP16 pourrait être phosphorylée, ubiquitinée ou acétylée (**Figure 4-2**). Lors de notre étude, nous avons observé que USP16 nucléaire catalytiquement inactif (USP16 ΔLinker-C205S) pouvait était être ubiquitinée (**Figure 2-6C et Figure 2-S8C**). Ce qui suggère que USP16 de type sauvage aurait la capacité de s'autodéubiquitiner. Ce mécanisme d'ubiquitination/déubiquitination de USP16 pourrait constituer un processus de régulation largement utilisé par la cellule.

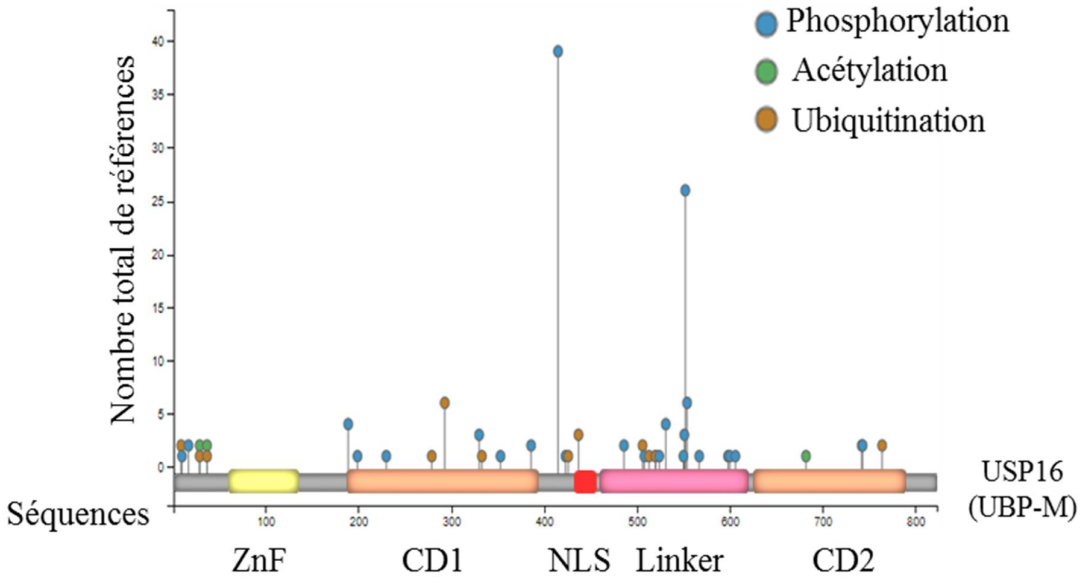

Figure 4-2 : Les différentes PTMs de USP16.

La base de données phosphositeplus (http://www.phosphosite.org) rapporte quarante sites de PTMs de la protéine USP16 chez l'humain.

4.1.4 Rôle de USP16 dans la LLPS lors des dommages à l'ADN

À la suite de l'induction des DSB, plusieurs protéines subissent une LLPS et sont rapidement recrutées sur des sites de dommages à l'ADN pour former des foci de réparation. C'est le cas des protéines γH2AX, 53BP1 et BRCA1 [230, 266].

Contrairement à ce qui a été rapporté par Zhang et son équipe qui stipule que la surexpression ou la déplétion de USP16 perturbe la réparation du DSB [279], une étude récente

a montré que la surexpression de USP16 n'a pas d'impact sur les foyers de réparation du DSB [353]. Ainsi, il n'était pas clair si USP16 pouvait avoir un impact sur la réparation des dommages. Nos données indiquent que le traitement des cellules par IR n'induit pas de changements perceptibles dans la localisation de USP16. Par contre, une accumulation forcée de USP16 dans le noyau via la délétion de son NES inhibe la réparation des DSB. Nous avons donc conclu que USP16 est activement exclu du noyau et qu'elle pourrait indirectement réguler la réparation du DSB.

Plusieurs scénarios peuvent être envisagés pour expliquer le rôle indirect de USP16 dans la régulation des foci de dommages. La E3 ligase HERC2 se localise à la fois dans le cytoplasme et le noyau. Des études ont rapporté que cette ligase renferme un motif NLS actif dans sa séquence qui le déplace vers le noyau, suggérant que HERC2 est une protéine navette nucléaire-cytoplasmique [354]. Étant donné qu'il a été trouvé que USP16 interagit avec la protéine HERC2 [279], il est possible que cette interaction dans le cytoplasme ait un impact sur la réponse aux dommages à l'ADN dans le noyau.

Étant donné que HERC2 interagit aussi avec RNF8 et RNF168 pour permettre le recrutement de BRCA1 et 53BP1 sur le site du dommage [278, 280], nous avons fait quelques expériences préliminaires démontrant les conséquences de la déplétion de USP16 sur la réparation des DSB. Premièrement, nous avons déplété USP16 dans les cellules U2OS en utilisant l'ARN interférant (siRNA USP16) et nous avons observé des niveaux accrus de γH2AX en réponse aux IR ainsi qu'un retour retardé au niveau de base pendant la phase de réparation des DSB (**Figure 4-3A**). Pour valider davantage nos résultats, nous avons inactivé le gène USP16 dans les cellules U2OS par knock-out (KO) en utilisant le système CRISPR/Cas9 et avons observé des résultats comparables (**Figure 4-3B**). Il convient de noter que les cellules USP16 KO sont une population polyclonale et une petite fraction de cellules sans inactivation génique persiste souvent après la sélection à la puromycine, comme le révèle le western blot (**Figure 4-2B**). Parallèlement aux changements dans les niveaux de protéines γH2AX, nous avons observé que la formation et la résolution des foci 53BP1 et BRCA1 étaient également retardées dans les cellules déplétées en USP16, ce qui indique à son tour un retard dans la réparation de l'ADN (**Figure 4-3C**). Tandis que le nombre de foci 53BP1 et BRCA1 est significativement réduit dans les cellules contrôles, le nombre de ces foci atteint son maximum dans les cellules USP16 KO (**Figure 4-3C**).

En résumé, nos différents résultats suggèrent que USP16 est retenue dans le cytoplasme pendant la DDR. Cependant, sa déplétion lors d'un dommage ralentit la réparation. Pris

ensemble, ces résultats renforcent l'idée selon laquelle USP16 pourrait agir de façon indirecte sur la réponse aux dommages à l'ADN.

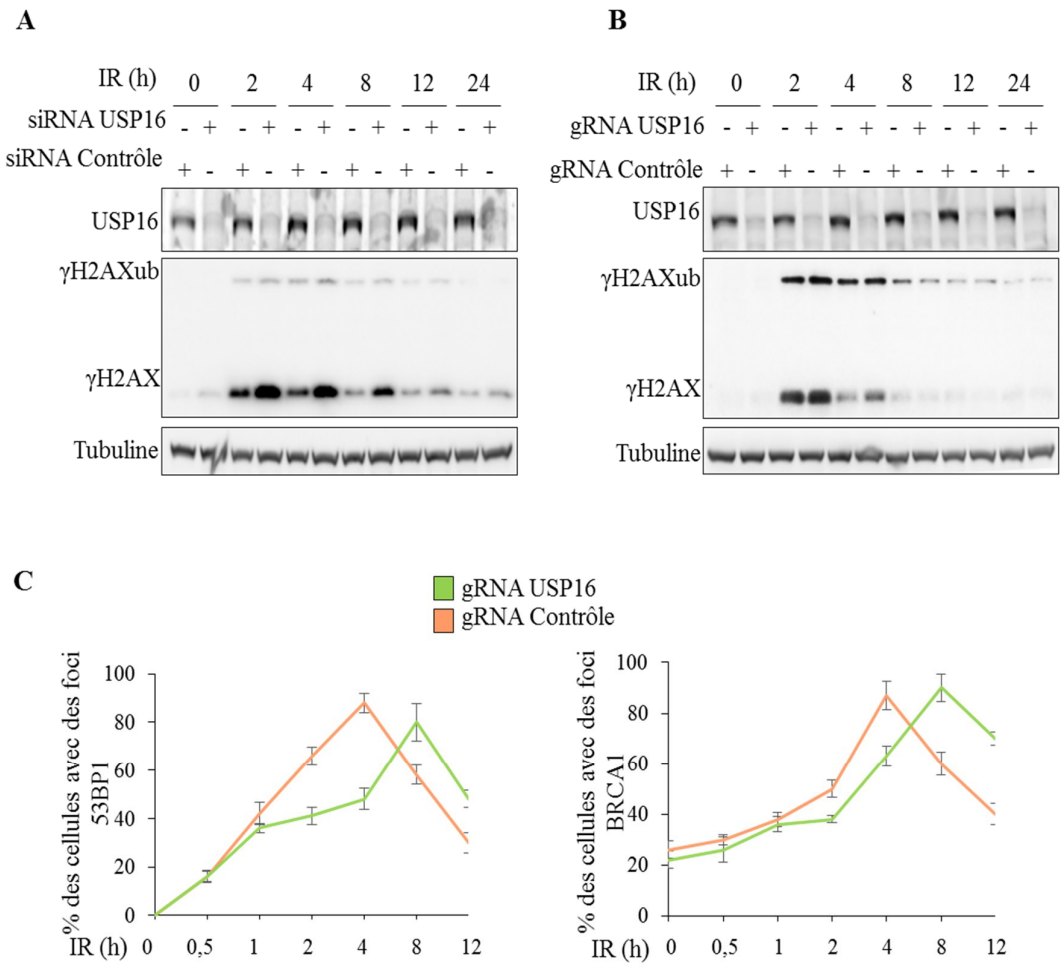

Figure 4-3 : La déplétion de USP16 retarde la réparation de la cassure de l'ADN double brin.

(A) La déplétion de USP16 entraîne des niveaux élevés de γH2AX. Les cellules U2OS ont été transfectées avec des siRNA contrôle ou USP16 pendant 72 heures. Les cellules ont été soumises à des radiations ionisantes (7,5 Gy) et les niveaux de protéines de USP16 et de γH2AX ont été détectés par western blot. **(B)** Les cellules U2OS ont été infectées par des particules lentivirales CRISPR/Cas9 ciblant USP16 et sélectionnées pour leur résistance à la puromycine. Les cellules ont été traitées avec des radiations ionisantes et les niveaux protéiques de USP16 et de γH2AX ont été détectés par western blot. **(C)** Des cellules U2OS déficientes en USP16 ont été traitées par IR. Le pourcentage de cellules hébergeant des foci 53BP1 ou BRCA1 a été

quantifié et comparé au vecteur vide (contrôle). Les résultats sont issus de 3 expériences indépendantes et les valeurs sont présentées en moyenne ± SD.

4.1.5 Rôle éventuel de USP16 dans le cytoplasme

L'activité et la fonction de USP16 restent à ce jour une énigme dans le sens où c'est une protéine principalement cytoplasmique capable de lier l'ubiquitine et dont le principal substrat connu se trouve dans le noyau. Comme nous n'avons pas observé d'accumulation de USP16 endogène dans le noyau en condition normale, il serait peut-être possible que celle-ci ait un rôle dans le cytoplasme. De nombreuses études antérieures ont apporté des éléments de réponses à cette théorie.

Récemment, des chercheurs ont rapporté que USP16 régule la biogenèse des ribosomes au niveau du cytoplasme [203]. En effet, ces auteurs ont montré que USP16 s'associe à la sous-unité pré-40S du ribosome et cette liaison va permettre la déubiquitination de la protéine ribosomale RPS27a sur sa lysine K113. Cela va ainsi favoriser la maturation de la sous-unité ribosomique 40S [203].

D'autre part, il est connu que l'ubiquitine est synthétisée sous forme de précurseurs. Ces précurseurs sont soit de l'ubiquitine en fusion avec les protéines ribosomales. C'est le cas du précurseur UBA80 qui est composé de l'ubiquitine associée à la protéine ribosomale RPS27A et du précurseur UBA52 composé de l'ubiquitine associée à la protéine ribosomale RPL40 (**Figure 4-4A**). Soit les précurseurs sont des multimères d'ubiquitine liés tête-à-queue et contenant une extrémité C-terminale. C'est le cas des précurseurs UBB et UBC [124, 355] (**Figure 4-4A**). Il apparaît que la fusion entre les protéines ribosomales et l'ubiquitine facilite la biogenèse du ribosome [355]. Ces données soulèvent la question sur le rôle éventuel de USP16 dans le clivage de l'ubiquitine au niveau des précurseurs dans le cytoplasme en général et au niveau de la protéine RPS27A du précurseur UBA80 en particulier.

Dans le même ordre d'idée, des recherches d'interaction protéines-protéines de la base de données STRING (Search Tool for the Retrieval of Interacting Genes / Proteins) ont prédit que USP16 pourrait s'associer aux protéines ribosomales ainsi qu'aux précurseurs d'ubiquitine (**Figure 4-4B**). De plus, différents travaux ont montré que USP16 possède un domaine de reconnaissance à l'ubiquitine et est capable de lier l'ubiquitine libre sur son côté C-terminal [154, 155]. Ces analyses renforcent davantage l'idée d'un rôle potentiel de USP16 dans le

clivage des précurseurs d'ubiquitine et le maintien constant du niveau d'ubiquitine libre dans la cellule (**Figure 4-4C**).

De manière intéressante, des expériences ont montré que les niveaux protéiques de USP16 semblent affecter la formation de foci d'ubiquitine après un dommage à l'ADN [279]. Il serait possible que la perturbation des niveaux de USP16, causée par sa déplétion ou sa surexpression dans le cytoplasme, altère le processus de biogenèse des ribosomes, ainsi que les pools d'ubiquitine libre. Ce qui aurait un impact majeur sur la transcription, la réparation des dommages à l'ADN ou le cycle cellulaire (**Figure 4-4C**).

L'histone H2A est l'une des protéines les plus ubiquitinées et est considérée comme un réservoir d'ubiquitine, car elle renferme près de 10 % de H2A totale dans la cellule [58]. Un modèle envisageable serait que lors de la mitose, USP16 assure la déubiquitination massive de H2A afin d'enrichir le pool d'ubiquitine libre dans la cellule.

Des analyses supplémentaires devront être menées pour prouver cette hypothèse notamment en : (a) étudiant l'interaction entre USP16 et les précurseurs d'ubiquitine, (b) analysant la déubiquitination des précurseurs d'ubiquitine *in vitro* par USP16, (c) investiguant l'effet de la déplétion de USP16 sur la biogenèse des ribosomes et la génération de l'ubiquitine libre dans la cellule.

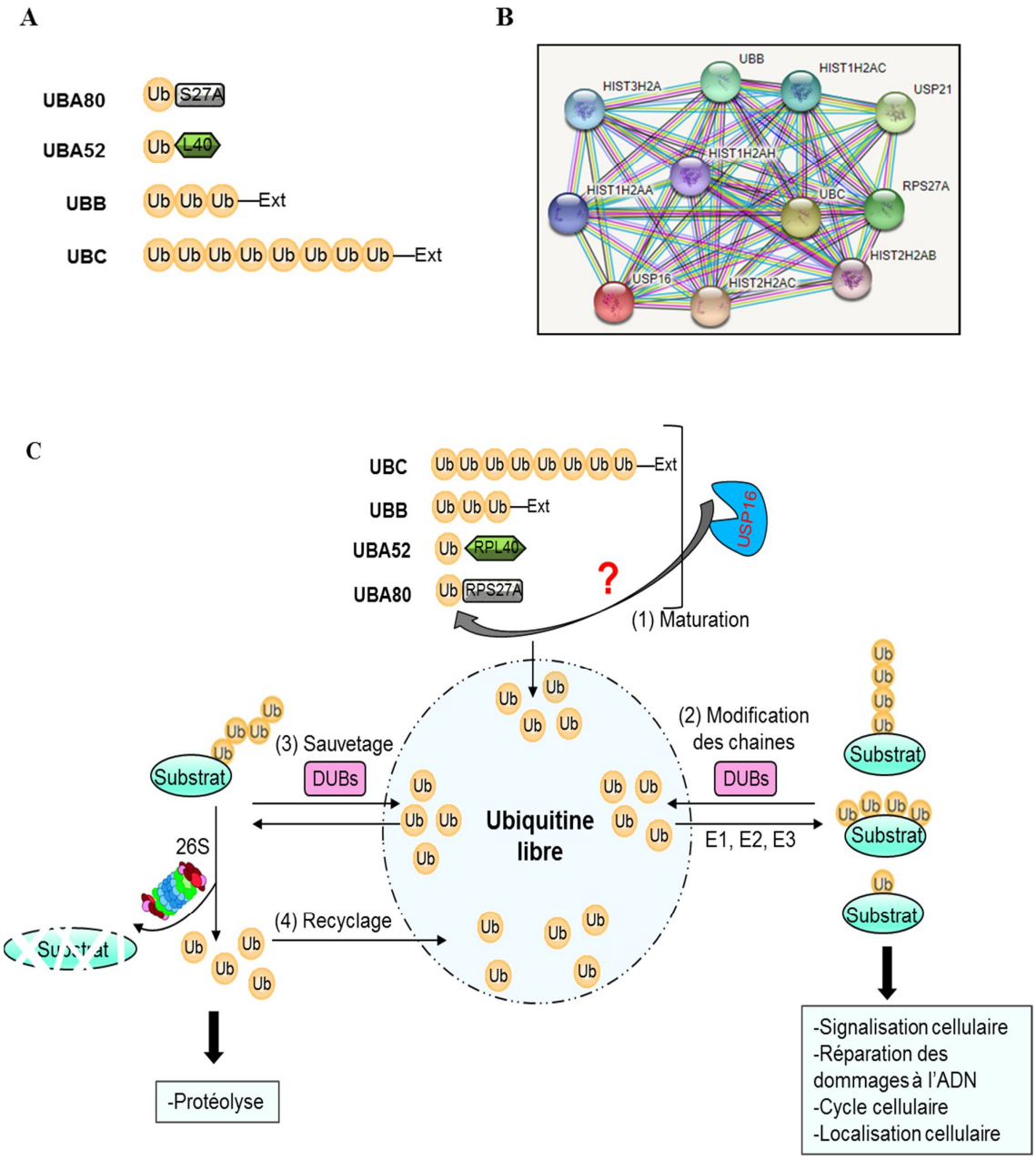

Figure 4-4 : Prédiction des partenaires et des autres rôles potententiels USP16

(A) Représentation schématique des précurseurs d'ubiquitine chez l'humain. **(B)** prédiction des interactions entre USP16 et ses partenaires selon la base de données STRING. On y retrouve plusieurs types d'histone H2A, la déubiquitinase USP21, la protéine ribosomale RPS27A ainsi que les précurseurs d'ubiquitine UBB et UBC. **(C)** Processus de génération du pool d'ubiquitine libre. (1) Les précurseurs d'ubiquitine peuvent être clivés par des DUBs pour former des monomères d'ubiquitine libres matures. (2) L'ubiquitine conjuguée peut être clivée par des DUBs dans le but de modifier le signal. (3) Les DUBs peuvent participer au sauvetage des

protéines de la dégradation en éliminant les marqueurs de polyubiquitine. (4) Les DUBs peuvent assurer le recyclage des chaînes de polyubiquitine après dégradation des protéines cibles par le protéasome. Modifiée de [356]

4.2 Les multiples facettes de l'UPS

Le protéasome a toujours été considéré comme une puissante machinerie nécessaire à la dégradation des protéines et au maintien de l'homéostasie dans la cellule. Toutefois, le devenir du protéasome en situation de stress a fait l'objet de plusieurs études ces dernières années. Des travaux ont montré que suite à un stress induit par un épuisement en acides aminés, les récepteurs d'ubiquitine associés au protéasome sont polyubiquitinés, cette polyubiquitination va être reconnue par la protéine adaptatrice P62 qui va permettre la dégradation du protéasome par autophagie [117, 357].

Chez la levure, lors d'un stress induit par un manque de glucose, le protéasome sort du noyau et s'accumule dans le cytoplasme sous forme de granules. Ces granules formés via une LLPS vont protéger le protéasome de la dégradation par autophagie, favorisant ainsi la viabilité des cellules [114]. Quant à la plante *Arabidopsis taliana,* la formation de granules de protéasome survient après une privation en carbone [114]. Cependant, peu de choses sont connues sur les changements possibles du protéasome chez l'espèce humaine.

Le troisième chapitre de cette thèse montre que suite à une privation de nutriments, le protéasome subit une LLPS permettant la formation de foci (nommé SIPAN « Starvation Induced Proteasome Assemblies in the Nucleus ») dynamiques dans le noyau cellulaire. Aussi, nos résultats indiquent que la présence des SIPAN, due principalement à l'absence d'acides aminés non essentiels, est corrélée à une augmentation de l'apoptose dans les cellules. Bien que cette étude nous ait fourni de bons indices quant au devenir du protéasome en situation de stress, plusieurs questions restent sans réponse. (a) On ignore encore comment le métabolisme des acides aminés régule la formation des SIPAN. (b) Est-ce que les SIPAN sont toxiques pour la cellule et peuvent entraîner des maladies ? (c) Les protéines contenues dans les SIPAN peuvent-elles encore remplir leur fonction biologique ? Dans les sections suivantes, nous discuter de plusieurs possibilités de réponses.

4.2.1 Structure et mécanisme de formation des SIPAN

Dans notre étude, nous avons identifié des structures nucléaires appelées SIPAN, induites par un stress métabolique et contenant les protéines du complexe protéasomal. Des expériences *in vivo* de FRAP (Fluorescence recovery after photobleaching) ont montré que ces structures sont dynamiques et peuvent être modulées en réponse à des signaux extracellulaires. Ce qui suggère un échange continuel de ses composants, d'où la difficulté de la purification des SIPAN. Étant donné qu'il existe plusieurs structures nucléaires à l'intérieur du noyau (les corps de cajal, les corps PML, les foci de dommages à l'ADN et bien d'autres), il serait important de mieux définir les SIPAN afin de démontrer leurs spécificités par rapport aux autres structures connues.

Il existe une technique appelée FFS « fluorescence fluctuation spectroscopy » permettant de quantifier la mobilité moléculaire dans les compartiments intracellulaires [358]. La FFS enregistre les variations d'intensité créées par les particules fluorescentes traversant une petite surface et caractérise les propriétés des particules par analyse statistique du signal mesuré. Cette approche pourra être efficace pour suivre les mouvements coordonnés de Rad23B ou des protéines du protéasome en présence ou en absence de stress métabolique afin d'apporter de nouvelles connaissances sur les propriétés moléculaires de la structure formée par les SIPAN.

Une autre possibilité intéressante serait de comprendre les évènements permettant la formation des SIPAN par des tests *in vitro*. La LLPS *in vitro* pourrait se faire en présence de protéasome, de polyubiquitine et de Rad23B, tous marqués à des fluorophores différents. Après le mélange, nous observerons par microscopie la formation et la distribution des SIPAN avec des signaux de fluorescence différents. Les analyses de FRAP pourraient être nécessaires pour comprendre les échanges rapides entre les composants de ces foci lors de la séparation de phase *in vitro*.

Il a été suggéré dans notre étude que les SIPAN ne correspondent pas aux structures nucléaires connues antérieurement. Étant donné que nous n'avons pas pu tester la colocalisation des SIPAN avec toutes les structures nucléaires, il serait peut-être intéressant de purifier les protéines Flag-Rad23B ou Flag-PSMD4 en présence ou en absence de stress métabolique et d'identifier par spectrométrie de masse l'abondance des peptides associés à ces protéines. Ceci

pourra nous donner des indices sur la composition des SIPAN et de vérifier s'ils seraient associés à d'autres structures connues dans la littérature.

4.2.2 Rôle du métabolisme des acides aminés dans la régulation des SIPAN

Les résultats de notre étude ont montré que suite à une privation en acides aminés, le protéasome des mammifères subit une LLPS pour former des corps nucléaires appelés SIPAN. Étant donné que le métabolisme des acides aminés et d'autres sources de carbone sont primordiaux pour de nombreux processus cellulaires, il serait important d'investiguer le mécanisme de signalisation des acides aminés lors de la formation des SIPAN.

La protéine mTOR est une kinase conservée de la levure à l'homme. Des études antérieures ont rapporté que mTOR joue un rôle clé dans le contrôle de la croissance cellulaire via les synthèses protéiques, lipidiques et nucléotidiques [359] et la régulation de l'autophagie [360]. Aussi, mTOR a été impliquée dans le contrôle du métabolisme cellulaire via l'import et l'utilisation des nutriments [361]. De manière intéressante des travaux ont mentionné que le retrait des acides aminés, particulièrement la leucine du milieu culture cellulaire inhibe la signalisation de mTOR [362]. Considérant ces résultats, il serait donc possible que la formation des SIPAN causée par l'absence des acides aminés passe par la régulation de la voie mTOR. Cette hypothèse soulève la question sur le lien entre mTOR et le protéasome.

Des résultats contradictoires existent sur le lien entre la signalisation de mTOR et celle du protéasome. En effet, tandis que les travaux de Zhang et al. ont indiqué que mTOR augmente la protéolyse médiée par le protéasome [115]. Zhao et son équipe ont suggéré que l'inhibition de mTOR augmente la protéolyse induite par l'UPS et l'autophagie [116]. Par ailleurs, d'autres travaux ont signalé qu'en situation de stress induit par une absence en acides aminés, la voie mTOR facilite le processus de dégradation du protéasome par autophagie [117].

Cependant, nos travaux montrent que le blocage de la voie mTOR avec la rapamycine ou la torine n'affecte pas la formation de SIPAN après une privation de nutriments. De plus, aucune formation de SIPAN n'a été détectée suite à l'inhibition de mTOR dans un milieu de culture complet. Pour expliquer cela, nous pensons qu'étant donné que la voie mTOR est déjà

inhibée en absence d'acide aminé [362], l'ajout de la rapamycine ou de la torine n'aura donc aucun effet sur les SIPAN.

D'autre part, comme l'ont suggéré Zhao et son équipe, l'inhibition de mTOR pourrait augmenter la protéolyse induite par l'autophagie [116]. Cette activation de l'autophagie suite à l'épuisement en acides aminés pourrait provoquer la dégradation du protéasome dans le cytoplasme [117, 357]. Pris ensemble, nous proposons le modèle de signalisation suivant : pour se protéger d'une éventuelle destruction par autophagie dans le cytoplasme après une privation en nutriments, le protéasome va subir une LLPS et va s'accumuler sous forme SIPAN à l'intérieur du noyau. Plusieurs expériences devront être réalisées pour tester cette hypothèse.

Par la suite, nos résultats ont montré que le blocage de l'autophagie via le traitement de la chloroquine ou du 3-methyladenine accélère la formation des SIPAN. Ceci peut être dû au fait qu'en absence de nutriment, l'autophagie génère un approvisionnement en acides aminés dans la cellule via la dégradation des protéines dans les lysosomes. Son inhibition pourrait diminuer la présence des acides aminés de façon drastique, ce qui conduit à une accélération de la formation de SIPAN. Toutes ces observations suggèrent qu'une relation complexe existe entre les acides aminés, mTOR, l'autophagie et le protéasome et cette relation est nécessaire pour maintenir l'homéostasie protéique dans la cellule.

Plus loin dans notre étude, nous avons constaté que plusieurs composants sont capables de bloquer la formation des SIPAN.

(a) La majorité des acides aminés non essentiels, contrairement aux acides aminés essentiels, empêchent fortement la formation de SIPAN.
(b) La déplétion du récepteur d'ubiquitine Rad23B abolit l'apparition de ces SIPAN.

La plupart des acides aminés non essentiels sont des glucoformateurs et entrent dans le métabolisme de la néoglucogenèse, du cycle de Krebs et de la voie des pentoses phosphates en libérant le α -k, oxaloacétate, le fumarate, le succinyl-CoA et le pyruvate [363, 364]. Cela assure la production d'énergie et la synthèse de nucléotide dans la cellule. Ainsi, il est probable que l'absence des acides aminés non essentiels entraîne des altérations au niveau de ces voies métaboliques, ce qui favorise la formation de SIPAN. Cette situation est bien illustrée dans le cas de la glycine, la sérine, l'asparagine et la glutamine qui sont des composantes majeures dans

de nombreuses voies métaboliques et jouent un rôle clé dans la synthèse des nucléotides [365-367]. Dans des conditions de privation en nutriments, il est possible que l'ajout de ces acides aminés fournisse une voie métabolique alternative permettant la synthèse des nucléotides *de novo*. Ce qui va altérer la formation des SIPAN.

De façon intéressante, nous avons montré dans notre étude que la déplétion du récepteur d'ubiquitine Rad23B abolit l'apparition de ces SIPAN. De plus, nos analyses indiquent que ces SIPAN colocalisent avec de l'ubiquitine conjuguée. Il est donc possible que la signalisation de l'ubiquitine médiée par Rad23B soit impliquée dans le processus de LLPS induisant les SIPAN. Par ailleurs, des études récentes ont rapporté que chez la levure, Rad23B est capable de se lier à la protéine Rad4, impliquée dans la réponse aux dommages à l'ADN. Ainsi le complexe formé Rad4-Rad23 favorise la survie en régulant les pools de la désoxyribonucléoside triphosphate (dNTP) qui ont un rôle central dans le métabolisme cellulaire [368]. Il est possible que plusieurs voies métaboliques soient dérégulées en absence de Rad23B, ce qui aurait un impact sur l'apparition des SIPAN.

Pris ensemble, ces données suggèrent que la privation de nutriments provoque une perturbation du métabolisme des acides aminés et de la signalisation de l'ubiquitine. Ceci favorise l'apparition des SIPAN. Une investigation minutieuse de l'impact du métabolisme des acides aminés non essentiel sur les SIPAN devra être accomplie.

4.2.3 Implication des SIPAN dans la mort cellulaire

Notre étude a suggéré que les SIPAN facilitent l'apoptose induite par la déplétion des acides aminés. Cependant, le mécanisme moléculaire démontrant le rôle direct des SIPAN dans la mort des cellules n'a pas été clairement établi. Nous pouvons donc nous demander si les SIPAN sont la cause directe de la mort des cellules ou si l'induction de l'apoptose est une conséquence de la séquestration du protéasome sous forme de foci. Plusieurs travaux ont montré que le suppresseur de tumeur p53 joue un rôle critique dans l'arrêt du cycle cellulaire et le déclenchement de l'apoptose via l'activation des protéines pro-apoptotiques telles que BAX, NOXA, PUMA [369, 370]. De même, Kaur et son équipe ont indiqué que lors d'un stress induit par des agents génotoxiques, la protéine Rad23B interagit avec p53 et est essentielle à son activation et à l'induction de l'apoptose [371]. Il semble donc y avoir un lien entre Rad23B et le déclenchement de l'apoptose. De manière intéressante, l'étude du dynamisme des protéines associées au SIPAN a révélé une augmentation des niveaux de Rad23B au cours du traitement

HBSS (**Figure 3-S5a**). Il est donc possible que lors d'un stress induit par une privation en nutriment, la cellule stressée puisse, via les SIPAN, réguler sélectivement l'expression des protéines permettant l'arrêt du cycle cellulaire. Puisque la formation de SIPAN semble stabiliser Rad23B, un inducteur d'apoptose, il serait important d'investiguer si les cellules stressées sont en mesure d'accumuler des protéines impliquées dans les voies de signalisation apoptotiques à l'intérieur des foci, telles NOXA, BAX, PUMA.

Pour vérifier cette hypothèse, nous allons tout d'abord vérifier par microscopie si les protéines pro-apoptotiques peuvent effectuer une séparation de phase et colocaliser avec les SIPAN. Par la suite, nous allons effectuer une co-immunoprécipitation de Rad23B et de PSME3 pour tester si ces protéines interagissent avec les protéines pro-apopotique en présence ou en absence de stress métabolique. Aussi, les analyses de spectrométrie de masse de la protéine Rad23B purifiée dans les conditions de stress métabolique nous donneront des indices sur le rôle potentiel des SIPAN comme lieu de stockage, de stabilisation et d'activation des protéines induisant la mort cellulaire.

4.2.4 Implication des SIPAN dans l'apparition des tumeurs

Il est bien connu que les mutations qui surviennent dans les protéines oncogènes ou les suppresseurs de tumeurs peuvent causer une prolifération accrue et incontrôlée des cellules induisant la formation des tumeurs. Cependant, la question sur le rôle potentiel des SIPAN dans l'apparition des cancers nous intrigue.

Contrairement aux études chez la levure qui proposent que suite à une absence en carbone, les granules du protéasome augmentent la viabilité cellulaire [297], nos travaux suggèrent que dans les cellules de mammifères, les foci du protéasome favorisent la mort cellulaire après privation de nutriments. Même s'il est possible que les voies de signalisations qui relient la LLPS du protéasome diffèrent entre la levure et les mammifères, les raisons de cette divergence entre ces deux espèces sont actuellement inconnues.

Les études ont montré qu'entraver la fonction du protéasome pourrait favoriser la mort des cellules cancéreuses. C'est le cas par exemple du bortézomib, un inhibiteur du protéasome qui est utilisé dans de nombreux traitements contre le cancer. Les études ont montré que le bortezomib augmente la toxicité et permet l'entrée en apoptose des cellules [372]. Étant donné que nos résultats indiquent que l'inhibition du protéasome dans les cellules privées de nutriments accélère la formation de SIPAN, il est donc possible que les SIPAN jouent un rôle

dans la suppression des tumeurs. Néanmoins, dans ce cas, nous devons nous assurer de la fonctionnalité du protéasome et déterminer si la LLPS induite par un manque d'apport en nutriments pourrait altérer la fonction du protéasome.

Un des principaux résultats du troisième chapitre de cette thèse est que les acides aminés sont des déterminants majeurs dans la formation de SIPAN. Étant donné que la division anarchique des cellules cancéreuses entraîne un développement important de la tumeur, ce qui aura pour conséquence un manque d'apport en nutriments. Nous pensons que ces SIPAN pourraient être présents dans les cellules cancéreuses ayant subi des variations métaboliques majeures. De manière intéressante, nos données montrent que la privation en acides aminés non essentiels tels que la glutamine, la sérine, la glycine, l'alanine, l'asparagine ou la proline est impliquée dans la formation des SIPAN.

Tandis que les études ont montré qu'en comparaison à des tissus sains, la glutamine est l'acide aminé non essentiel le plus consommé et le plus appauvri dans la plupart des cancers [373, 374]. L'élimination de la sérine et de la glycine réduit la prolifération des cellules cancéreuses du sein [375]. Il est important de noter que les cellules cancéreuses du myélome et du glioblastome dépendent de la glutamine pour leur croissance et leur survie [376, 377]. Par ailleurs, la présence d'asparagine et de proline pourrait devenir une condition essentielle dans certaines tumeurs [375]. Pris ensemble, ces observations suggèrent que les acides aminés non essentiels ont une place particulière dans le développement des tumeurs. Il serait donc raisonnable de supposer que la privation de ces acides aminés induisant la formation des SIPAN pourrait induire la mort des cellules cancéreuses.

4.2.5 Influence des mutants de Rad23B et de USP16 dans l'apparition de maladies

Tous nos résultats, pris ensemble, mettent en avant les mécanismes cellulaires qui influencent la séparation de phase liquide-liquide dans la réponse aux dommages à l'ADN, la survie et la mort des cellules. De plus, les protéines Rad23B et USP16, toutes deux impliquées dans la LLPS, jouent aussi un rôle dans l'apparition des cancers [211, 378]. Ceci soulève la question à savoir si les mutations de Rad23B pourraient influencer la formation des SIPAN ou encore si des altérations de USP16 pourraient avoir un impact sur sa localisation subcellulaire.

Plusieurs études ont indiqué que Rad23B fait partie d'un mécanisme complexe permettant la réparation des dommages à l'ADN suite à une excision de nucléotides (NER)

[108]. En effet, Rad23B peut se lier à XPC pour former le complexe Rad23B-XPC qui joue un rôle important dans la reconnaissance de l'ADN endommagé. Hormis son rôle dans la réparation des dommages à l'ADN, des groupes de chercheurs ont impliqué Rad23B dans la progression des cancers [378-380]. Leurs études ont indiqué qu'il existe des polymorphismes mononucléotidiques (SNP) dans la région du gène Rad23B qui pourraient être associés à un risque de cancer [378, 380]. Par exemple, le variant de Rad23B (rs1805329) entraîne un changement d'acide aminé (Ala249Val) qui pourrait avoir un impact sur sa fonction protéique [378]. De plus, des études de populations ont montré que ce variant était significativement associé au risque de cancer du sein dans tous les modèles testés [378]. Cependant, la fonction précise de ce mutant cancer de Rad23B reste méconnue.

D'autres travaux récents ont suggéré que la régulation négative de Rad23B induirait l'invasion et l'adhésion des lignées cellulaires de cancer du sein *in vitro* [379]. De plus, il s'avère que Rad23B est moins exprimée dans les lignées de cellules mammaires hautement invasives par rapport à des lignées de cellules mammaires peu invasives [379]. Il est donc possible que le variant rs1805329 de Rad23B agisse comme un dominant négatif et inhibe l'action menée par Rad23 sauvage. Ce qui pourrait avoir pour conséquence une diminution de la capacité de réparation des dommages à l'ADN, une incapacité à former des SIPAN après un stress et une prolifération anarchique des cellules.

Quant à la déubiquitinase USP16, il a été montré que sa surexpression diminue la prolifération des fibroblastes, tandis que sa régulation négative favorise la prolifération des cellules [209]. USP16 agit également comme un suppresseur de tumeur dans certains cancers, tel que le carcinome hépatocellulaire [211]. D'autre part, des données cliniques ont dévoilé une aberration chromosomique impliquant USP16 comme une cause de leucémie myélomonocytaire chronique (CMML) [150]. En effet, ces auteurs rapportent que chez plusieurs patients atteints de la CMML, le transcrit de USP16 se trouve en fusion avec le facteur de transcription RUNX1. Ce transcrit chimérique contient plusieurs codons d'arrêt dans sa partie N-terminale. Il est donc possible que la perte de fonction de USP16 causée soit par des mutations, soit par des translocations chromosomiques empêche la déubiquitination de H2A durant la mitose ou suite aux dommages à l'ADN. De façon intéressante, BMI1, qui stimule fortement l'activité de l'ubiquitine ligase E3 de RING1B, responsable de l'ubiquitination de H2A, est surexprimée dans le cancer du pancréas, le glioblastome, le cancer colorectal et la

leucémie myéloïde aiguë [60, 381, 382]. Pris ensemble, ces différentes études suggèrent un rôle eventuel de USP16 comme suppresseur de tumeur via la déubiquitination de H2A.

Il existe un catalogue qui repertorie les différentes mutations somatiques potentielles des protéines dans les cancers « https://cancer.sanger.ac.uk/ ». Leurs données rapporte plus de quatre cents mutations somatiques de la protéine USP16 chez l'humain. Cependant, qu'adviendrait-il s'il existe des mutations qui bloquent le signal d'export nucléaire de USP16, l'empêchant d'être retenu dans le cytoplasme ? Dans ce dernier cas, USP16 induirait une déubiquitination abondante de l'histone H2A, altérant la formation des foci de réparation des dommages à l'ADN. Ce qui conduirait probablement à une mort cellulaire excessive et à une perte de l'homéostasie tissulaire [151, 209, 383].

CONCLUSION GÉNÉRALE

Les travaux présentés dans le cadre de cette thèse ont eu pour but l'étude des mécanismes de signalisation et de régulation de la LLPS suite à différents stress.

Dans la première partie de cette étude, nous avons montré que la déubiquitinase USP16 est essentiellement cytoplasmique et serait capable de déubiquitiner l'histone H2A suite à une entrée forcée de cette déubiquitinase dans le noyau. Malgré son signal de localisation nucléaire fonctionnel, USP16 semble posséder un signal d'export nucléaire très fort qui maintient cette déubiquitinase dans le cytoplasme au cours de l'interphase ou suite à des radiations ionisantes. Par conséquent, nous avons pu conclure que USP16 pourrait réguler de façon indirecte les foci de dommages à l'ADN. Nos résultats ont donné un aperçu de la nature complexe de la localisation subcellulaire USP16 et de son rôle indirect dans la régulation des foci de dommage à l'ADN formés suite à une LLPS.

Dans la deuxième partie de cette thèse, nous avons caractérisé les mécanismes qui coordonnent la LLPS du protéasome suite à une privation en nutriments. Nos résultats suggèrent que le protéasome subit une LLPS pour former des foci nucléaires appelés SIPAN suite à une privation de nutriments. Ces SIPAN semblent être dirigés par le récepteur d'ubiquitine Rad23B et par l'absence des acides aminés non essentiels. Aussi, nos données soutiennent le modèle selon lequel la formation des SIPAN conduit à la mort cellulaire par apoptose. Dans l'ensemble, cette étude nous donne un aperçu des voies de signalisation qui régulent la LLPS du protéasome. De plus, elle apporte des réponses sur le lien complexe qui existe entre le système ubiquitine protéasome et le métabolisme des acides aminés.

.

RÉFÉRENCES

1. Progida, C. and O. Bakke, *Bidirectional traffic between the Golgi and the endosomes – machineries and regulation.* Journal of Cell Science, 2016. **129**(21): p. 3971.
2. Ballabio, A., *The awesome lysosome.* EMBO molecular medicine, 2016. **8**(2): p. 73-76.
3. Meyer-Schwesinger, C., *The ubiquitin–proteasome system in kidney physiology and disease.* Nature Reviews Nephrology, 2019. **15**(7): p. 393-411.
4. Hershko, A., et al., *Proposed role of ATP in protein breakdown: conjugation of protein with multiple chains of the polypeptide of ATP-dependent proteolysis.* Proceedings of the National Academy of Sciences, 1980. **77**(4): p. 1783.
5. Wilkinson, K.D., M.K. Urban, and A.L. Haas, *Ubiquitin is the ATP-dependent proteolysis factor I of rabbit reticulocytes.* J Biol Chem, 1980. **255**(16): p. 7529-32.
6. Ciechanover, A. and R. Ben-Saadon, *N-terminal ubiquitination: more protein substrates join in.* Trends Cell Biol, 2004. **14**(3): p. 103-6.
7. Pelzer, C., et al., *UBE1L2, a novel E1 enzyme specific for ubiquitin.* J Biol Chem, 2007. **282**(32): p. 23010-4.
8. Ye, Y. and M. Rape, *Building ubiquitin chains: E2 enzymes at work.* Nature reviews. Molecular cell biology, 2009. **10**(11): p. 755-764.
9. Stewart, M.D., et al., *E2 enzymes: more than just middle men.* Cell research, 2016. **26**(4): p. 423-440.
10. Deshaies, R.J. and C.A. Joazeiro, *RING domain E3 ubiquitin ligases.* Annu Rev Biochem, 2009. **78**: p. 399-434.
11. Rotin, D. and S. Kumar, *Physiological functions of the HECT family of ubiquitin ligases.* Nat Rev Mol Cell Biol, 2009. **10**(6): p. 398-409.
12. Ohi, M.D., et al., *Structural insights into the U-box, a domain associated with multi-ubiquitination.* Nat Struct Biol, 2003. **10**(4): p. 250-5.
13. Hatakeyama, S., et al., *U box proteins as a new family of ubiquitin-protein ligases.* J Biol Chem, 2001. **276**(35): p. 33111-20.
14. Martino, L., et al., *Determinants of E2-ubiquitin conjugate recognition by RBR E3 ligases.* Sci Rep, 2018. **8**(1): p. 68.
15. Dove, K.K. and R.E. Klevit, *RING-Between-RING E3 Ligases: Emerging Themes amid the Variations.* J Mol Biol, 2017. **429**(22): p. 3363-3375.
16. Xu, P., et al., *Quantitative proteomics reveals the function of unconventional ubiquitin chains in proteasomal degradation.* Cell, 2009. **137**(1): p. 133-145.
17. Komander, D. and M. Rape, *The ubiquitin code.* Annu Rev Biochem, 2012. **81**: p. 203-29.
18. Jia, R. and J.S. Bonifacino, *Regulation of LC3B levels by ubiquitination and proteasomal degradation.* Autophagy, 2020. **16**(2): p. 382-384.
19. Livneh, I., et al., *Monoubiquitination joins polyubiquitination as an esteemed proteasomal targeting signal.* Bioessays, 2017. **39**(6).

20. Ronai, Z.A., *Monoubiquitination in proteasomal degradation.* Proc Natl Acad Sci U S A, 2016. **113**(32): p. 8894-6.

21. Braten, O., et al., *Numerous proteins with unique characteristics are degraded by the 26S proteasome following monoubiquitination.* Proc Natl Acad Sci U S A, 2016. **113**(32): p. E4639-47.

22. Koegl, M., et al., *A novel ubiquitination factor, E4, is involved in multiubiquitin chain assembly.* Cell, 1999. **96**(5): p. 635-44.

23. Stolz, A. and I. Dikic, *Heterotypic Ubiquitin Chains: Seeing is Believing.* Trends in cell biology, 2018. **28**(1): p. 1-3.

24. Huang, Y., et al., *An E4 ligase facilitates polyubiquitination of plant immune receptor resistance proteins in Arabidopsis.* Plant Cell, 2014. **26**(1): p. 485-96.

25. Hoppe, T., *Multiubiquitylation by E4 enzymes: 'one size' doesn't fit all.* Trends Biochem Sci, 2005. **30**(4): p. 183-7.

26. Akutsu, M., I. Dikic, and A. Bremm, *Ubiquitin chain diversity at a glance.* Journal of Cell Science, 2016. **129**(5): p. 875.

27. Hock, A.K. and K.H. Vousden, *The role of ubiquitin modification in the regulation of p53.* Biochimica et Biophysica Acta (BBA) - Molecular Cell Research, 2014. **1843**(1): p. 137-149.

28. Brooks, C.L. and W. Gu, *p53 ubiquitination: Mdm2 and beyond.* Molecular cell, 2006. **21**(3): p. 307-315.

29. Petroski, M.D. and R.J. Deshaies, *Mechanism of Lysine 48-Linked Ubiquitin-Chain Synthesis by the Cullin-RING Ubiquitin-Ligase Complex SCF-Cdc34.* Cell, 2005. **123**(6): p. 1107-1120.

30. Nakayama, K.I. and K. Nakayama, *Ubiquitin ligases: cell-cycle control and cancer.* Nat Rev Cancer, 2006. **6**(5): p. 369-81.

31. Glotzer, M., A.W. Murray, and M.W. Kirschner, *Cyclin is degraded by the ubiquitin pathway.* Nature, 1991. **349**(6305): p. 132-8.

32. Hannah, J. and P. Zhou, *Regulation of DNA damage response pathways by the cullin-RING ubiquitin ligases.* DNA repair, 2009. **8**(4): p. 536-543.

33. Dwane, L., et al., *The Emerging Role of Non-traditional Ubiquitination in Oncogenic Pathways.* J Biol Chem, 2017. **292**(9): p. 3543-3551.

34. Zlotorynski, E., *H1 — a linker of ubiquitylation and repair.* Nature Reviews Molecular Cell Biology, 2015. **16**(12): p. 700-701.

35. Ciccia, A. and S.J. Elledge, *The DNA damage response: making it safe to play with knives.* Molecular cell, 2010. **40**(2): p. 179-204.

36. Ohtake, F., et al., *The K48-K63 Branched Ubiquitin Chain Regulates NF-κB Signaling.* Molecular cell, 2016. **64**(2): p. 251-266.

37. Zhang, L., et al., *Both K63 and K48 ubiquitin linkages signal lysosomal degradation of the LDL receptor.* Journal of lipid research, 2013. **54**(5): p. 1410-1420.

38. Kulathu, Y. and D. Komander, *Atypical ubiquitylation - the unexplored world of polyubiquitin beyond Lys48 and Lys63 linkages.* Nature reviews. Molecular cell biology, 2012. **13**(8): p. 508-523.

39. Chastagner, P., A. Israël, and C. Brou, *Itch/AIP4 mediates Deltex degradation through the formation of K29-linked polyubiquitin chains.* EMBO reports, 2006. **7**(11): p. 1147-1153.

40. Yuan, W.-C., et al., *K33-Linked Polyubiquitination of Coronin 7 by Cul3-KLHL20 Ubiquitin E3 Ligase Regulates Protein Trafficking.* Molecular Cell, 2014. **54**(4): p. 586-600.

41. Fulda, S., K. Rajalingam, and I. Dikic, *Ubiquitylation in immune disorders and cancer: from molecular mechanisms to therapeutic implications.* EMBO molecular medicine, 2012. **4**(7): p. 545-556.

42. Pien, S. and U. Grossniklaus, *Polycomb group and trithorax group proteins in Arabidopsis.* Biochim Biophys Acta, 2007. **1769**(5-6): p. 375-82.

43. Martinez, A.M., et al., *Polycomb group-dependent Cyclin A repression in Drosophila.* Genes Dev, 2006. **20**(4): p. 501-13.

44. Schuettengruber, B., et al., *Genome regulation by polycomb and trithorax proteins.* Cell, 2007. **128**(4): p. 735-45.

45. Wang, L., et al., *Hierarchical recruitment of polycomb group silencing complexes.* Mol Cell, 2004. **14**(5): p. 637-46.

46. Kennison, J.A., *The Polycomb and trithorax group proteins of Drosophila: trans-regulators of homeotic gene function.* Annu Rev Genet, 1995. **29**: p. 289-303.

47. Cao, R. and Y. Zhang, *SUZ12 is required for both the histone methyltransferase activity and the silencing function of the EED-EZH2 complex.* Mol Cell, 2004. **15**(1): p. 57-67.

48. Yu, J.-R., et al., *PRC2 is high maintenance.* Genes & development, 2019. **33**(15-16): p. 903-935.

49. Shao, Z., et al., *Stabilization of chromatin structure by PRC1, a Polycomb complex.* Cell, 1999. **98**(1): p. 37-46.

50. Chittock, E.C., et al., *Molecular architecture of polycomb repressive complexes.* Biochemical Society transactions, 2017. **45**(1): p. 193-205.

51. Lanzuolo, C. and V. Orlando, *Memories from the polycomb group proteins.* Annu Rev Genet, 2012. **46**: p. 561-89.

52. Turner, S.A. and A.P. Bracken, *A "complex" issue: deciphering the role of variant PRC1 in ESCs.* Cell Stem Cell, 2013. **12**(2): p. 145-6.

53. Cao, R., et al., *Role of Histone H3 Lysine 27 Methylation in Polycomb-Group Silencing.* Science, 2002. **298**(5595): p. 1039.

54. Sparmann, A. and M. van Lohuizen, *Polycomb silencers control cell fate, development and cancer.* Nature Reviews Cancer, 2006. **6**(11): p. 846-856.

55. Blackledge, N.P., et al., *Variant PRC1 complex-dependent H2A ubiquitylation drives PRC2 recruitment and polycomb domain formation.* Cell, 2014. **157**(6): p. 1445-59.

56. Cooper, S., et al., *Targeting polycomb to pericentric heterochromatin in embryonic stem cells reveals a role for H2AK119u1 in PRC2 recruitment.* Cell Rep, 2014. **7**(5): p. 1456-1470.

57. Nickel, B.E. and J.R. Davie, *Structure of polyubiquitinated histone H2A.* Biochemistry, 1989. **28**(3): p. 964-8.

58. Zhang, Z., et al., *Role of remodeling and spacing factor 1 in histone H2A ubiquitination-mediated gene silencing.* Proceedings of the National Academy of Sciences, 2017. **114**(38): p. E7949.

59. Fang, J., et al., *Ring1b-mediated H2A Ubiquitination Associates with Inactive X Chromosomes and Is Involved in Initiation of X Inactivation.* Journal of Biological Chemistry, 2004. **279**(51): p. 52812-52815.

60. Cao, R., Y. Tsukada, and Y. Zhang, *Role of Bmi-1 and Ring1A in H2A ubiquitylation and Hox gene silencing.* Mol Cell, 2005. **20**(6): p. 845-54.

61. Endoh, M., et al., *Histone H2A mono-ubiquitination is a crucial step to mediate PRC1-dependent repression of developmental genes to maintain ES cell identity.* PLoS genetics, 2012. **8**(7): p. e1002774-e1002774.

62. Wunsch, A.M., A.L. Haas, and J. Lough, *Synthesis and ubiquitination of histones during myogenesis.* Dev Biol, 1987. **119**(1): p. 85-93.

63. Mueller, R.D., et al., *Identification of ubiquitinated histones 2A and 2B in Physarum polycephalum. Disappearance of these proteins at metaphase and reappearance at anaphase.* J Biol Chem, 1985. **260**(8): p. 5147-53.

64. Walters, K.J., *Ubiquitin in disguise unveils a cryptic binding site in 1.2-MDa anaphase-promoting complex/cyclosome.* Proceedings of the National Academy of Sciences, 2019. **116**(35): p. 17142.

65. Wang, H., et al., *Role of histone H2A ubiquitination in Polycomb silencing.* Nature, 2004. **431**(7010): p. 873-878.

66. Budenholzer, L., et al., *Proteasome Structure and Assembly.* Journal of molecular biology, 2017. **429**(22): p. 3500-3524.

67. Adams, J., *The proteasome: structure, function, and role in the cell.* Cancer treatment reviews, 2003. **29 Suppl 1**: p. 3-9.

68. Hauer, M.H., et al., *Histone degradation in response to DNA damage enhances chromatin dynamics and recombination rates.* Nature structural & molecular biology, 2017. **24**(2): p. 99-107.

69. Sledź, P., F. Förster, and W. Baumeister, *Allosteric effects in the regulation of 26S proteasome activities.* Journal of molecular biology, 2013. **425**(9): p. 1415-1423.

70. Tanaka, K., *The proteasome: overview of structure and functions.* Proceedings of the Japan Academy. Series B, Physical and biological sciences, 2009. **85**(1): p. 12-36.

71. Humbard, M.A. and J.A. Maupin-Furlow, *Prokaryotic proteasomes: nanocompartments of degradation.* Journal of molecular microbiology and biotechnology, 2013. **23**(4-5): p. 321-334.

72. Arendt, C.S. and M. Hochstrasser, *Identification of the yeast 20S proteasome catalytic centers and subunit interactions required for active-site formation.* Proceedings of the National Academy of Sciences of the United States of America, 1997. **94**(14): p. 7156-7161.

73. Vangala, J.R., et al., *Regulation of PSMB5 protein and β subunits of mammalian proteasome by constitutively activated signal transducer and activator of transcription 3 (STAT3): potential role in bortezomib-mediated anticancer therapy.* The Journal of biological chemistry, 2014. **289**(18): p. 12612-12622.

74. Davies, K.J.A., *Degradation of oxidized proteins by the 20S proteasome.* Biochimie, 2001. **83**(3): p. 301-310.

75. Dikic, I., *Proteasomal and Autophagic Degradation Systems.* Annu Rev Biochem, 2017. **86**: p. 193-224.

76. Gomes, A.V., *Genetics of proteasome diseases.* Scientifica, 2013. **2013**: p. 637629-637629.

77. Cascio, P., *PA28αβ: the enigmatic magic ring of the proteasome?* Biomolecules, 2014. **4**(2): p. 566-584.

78. Ustrell, V., et al., *PA200, a nuclear proteasome activator involved in DNA repair.* The EMBO journal, 2002. **21**(13): p. 3516-3525.

79. Blickwedehl, J., et al., *Role for proteasome activator PA200 and postglutamyl proteasome activity in genomic stability.* Proceedings of the National Academy of Sciences, 2008. **105**(42): p. 16165.

80. Khor, B., et al., *Proteasome activator PA200 is required for normal spermatogenesis.* Mol Cell Biol, 2006. **26**(8): p. 2999-3007.

81. Rosenzweig, R., et al., *Rpn1 and Rpn2 coordinate ubiquitin processing factors at proteasome.* The Journal of biological chemistry, 2012. **287**(18): p. 14659-14671.

82. Husnjak, K., et al., *Proteasome subunit Rpn13 is a novel ubiquitin receptor.* Nature, 2008. **453**(7194): p. 481-488.

83. Sakata, E., et al., *Localization of the proteasomal ubiquitin receptors Rpn10 and Rpn13 by electron cryomicroscopy.* Proceedings of the National Academy of Sciences of the United States of America, 2012. **109**(5): p. 1479-1484.

84. Schreiner, P., et al., *Ubiquitin docking at the proteasome through a novel pleckstrin-homology domain interaction.* Nature, 2008. **453**(7194): p. 548-552.

85. Shi, Y., et al., *Rpn1 provides adjacent receptor sites for substrate binding and deubiquitination by the proteasome.* Science, 2016. **351**(6275).

86. Sutovsky, P., *Sperm proteasome and fertilization.* Reproduction (Cambridge, England), 2011. **142**(1): p. 1-14.

87. Paraskevopoulos, K., et al., *Dss1 is a 26S proteasome ubiquitin receptor.* Molecular cell, 2014. **56**(3): p. 453-461.

88. Saeki, Y., *Ubiquitin recognition by the proteasome.* The Journal of Biochemistry, 2017. **161**(2): p. 113-124.

89. Luan, B., et al., *Structure of an endogenous yeast 26S proteasome reveals two major conformational states.* Proceedings of the National Academy of Sciences, 2016. **113**(10): p. 2642.

90. Bohn, S., et al., *Localization of the regulatory particle subunit Sem1 in the 26S proteasome.* Biochemical and Biophysical Research Communications, 2013. **435**(2): p. 250-254.

91. Pathare, G.R., et al., *Crystal structure of the proteasomal deubiquitylation module Rpn8-Rpn11.* Proceedings of the National Academy of Sciences, 2014. **111**(8): p. 2984.

92. Lasker, K., et al., *Molecular architecture of the 26S proteasome holocomplex determined by an integrative approach.* Proceedings of the National Academy of Sciences of the United States of America, 2012. **109**(5): p. 1380-1387.

93. Boehringer, J., et al., *Structural and functional characterization of Rpn12 identifies residues required for Rpn10 proteasome incorporation.* The Biochemical journal, 2012. **448**(1): p. 55-65.

94. Liu, C.-W. and A.D. Jacobson, *Functions of the 19S complex in proteasomal degradation.* Trends in biochemical sciences, 2013. **38**(2): p. 103-110.

95. Peth, A., et al., *Ubiquitinated proteins activate the proteasomal ATPases by binding to Usp14 or Uch37 homologs.* The Journal of biological chemistry, 2013. **288**(11): p. 7781-7790.

96. Aviram, S. and D. Kornitzer, *The Ubiquitin Ligase Hul5 Promotes Proteasomal Processivity.* Molecular and Cellular Biology, 2010. **30**(4): p. 985.

97. Hicke, L., H.L. Schubert, and C.P. Hill, *Ubiquitin-binding domains.* Nat Rev Mol Cell Biol, 2005. **6**(8): p. 610-21.

98. Grice, G.L. and J.A. Nathan, *The recognition of ubiquitinated proteins by the proteasome.* Cellular and molecular life sciences : CMLS, 2016. **73**(18): p. 3497-3506.

99. Saeki, Y., *Ubiquitin recognition by the proteasome.* J Biochem, 2017. **161**(2): p. 113-124.

100. Sahtoe, D.D., et al., *Mechanism of UCH-L5 activation and inhibition by DEUBAD domains in RPN13 and INO80G.* Molecular cell, 2015. **57**(5): p. 887-900.

101. Cohen-Kaplan, V., A. Ciechanover, and I. Livneh, *Stress-induced polyubiquitination of proteasomal ubiquitin receptors targets the proteolytic complex for autophagic degradation.* Autophagy, 2017. **13**(4): p. 759-760.

102. Cohen-Kaplan, V., I. Livneh, and A. Ciechanover, *Proteasome phase separation: a novel layer of quality control.* Cell Research, 2020. **30**(5): p. 374-375.

103. Kim, I., K. Mi, and H. Rao, *Multiple interactions of rad23 suggest a mechanism for ubiquitylated substrate delivery important in proteolysis.* Molecular biology of the cell, 2004. **15**(7): p. 3357-3365.

104. Elsasser, S., et al., *Rad23 and Rpn10 serve as alternative ubiquitin receptors for the proteasome.* The Journal of biological chemistry, 2004. **279**(26): p. 26817-26822.

105. Kim, I., K. Mi, and H. Rao, *Multiple interactions of rad23 suggest a mechanism for ubiquitylated substrate delivery important in proteolysis.* Mol Biol Cell, 2004. **15**(7): p. 3357-65.

106. Xie, Z., et al., *Roles of Rad23 protein in yeast nucleotide excision repair.* Nucleic acids research, 2004. **32**(20): p. 5981-5990.

107. Yokoi, M. and F. Hanaoka, *Two mammalian homologs of yeast Rad23, HR23A and HR23B, as multifunctional proteins.* Gene, 2017. **597**: p. 1-9.

108. Dantuma, N.P., C. Heinen, and D. Hoogstraten, *The ubiquitin receptor Rad23: at the crossroads of nucleotide excision repair and proteasomal degradation.* DNA repair, 2009. **8**(4): p. 449-460.

109. Gödderz, D., et al., *The deubiquitylating enzyme Ubp12 regulates Rad23-dependent proteasomal degradation.* Journal of Cell Science, 2017. **130**(19): p. 3336.

110. Lee, J.-H., et al., *Structure of a peptide:N-glycanase-Rad23 complex: Insight into the deglycosylation for denatured glycoproteins.* Proceedings of the National Academy of Sciences of the United States of America, 2005. **102**(26): p. 9144.

111. Sümegi, M., et al., *26S proteasome subunits are O-linked N-acetylglucosamine-modified in Drosophila melanogaster.* Biochemical and Biophysical Research Communications, 2003. **312**(4): p. 1284-1289.

112. Zhang, F., et al., *O-GlcNAc Modification Is an Endogenous Inhibitor of the Proteasome.* Cell, 2003. **115**(6): p. 715-725.

113. Zhang, F., et al., *Proteasome Function Is Regulated by Cyclic AMP-dependent Protein Kinase through Phosphorylation of Rpt6.* Journal of Biological Chemistry, 2007. **282**(31): p. 22460-22471.

114. Marshall, R.S. and R.D. Vierstra, *Proteasome storage granules protect proteasomes from autophagic degradation upon carbon starvation.* eLife, 2018. **7**: p. e34532.

115. Zhang, Y., et al., *Coordinated regulation of protein synthesis and degradation by mTORC1.* Nature, 2014. **513**(7518): p. 440-3.

116. Zhao, J., et al., *mTOR inhibition activates overall protein degradation by the ubiquitin proteasome system as well as by autophagy.* Proceedings of the National Academy of Sciences of the United States of America, 2015. **112**(52): p. 15790-15797.

117. Cohen-Kaplan, V., et al., *p62- and ubiquitin-dependent stress-induced autophagy of the mammalian 26S proteasome.* Proc Natl Acad Sci U S A, 2016. **113**(47): p. E7490-e7499.

118. Swatek, K.N. and D. Komander, *Ubiquitin modifications.* Cell research, 2016. **26**(4): p. 399-422.

119. He, M., et al., *The emerging role of deubiquitinating enzymes in genomic integrity, diseases, and therapeutics.* Cell & Bioscience, 2016. **6**(1): p. 62.

120. Mevissen, T.E.T. and D. Komander, *Mechanisms of Deubiquitinase Specificity and Regulation.* Annual Review of Biochemistry, 2017. **86**(1): p. 159-192.

121. Clague, M.J., et al., *Deubiquitylases from genes to organism.* Physiological reviews, 2013. **93**(3): p. 1289-1315.

122. Liang, J., et al., *MCP-induced protein 1 deubiquitinates TRAF proteins and negatively regulates JNK and NF-kappaB signaling.* The Journal of experimental medicine, 2010. **207**(13): p. 2959-2973.

123. Abdul Rehman, S.A., et al., *MINDY-1 Is a Member of an Evolutionarily Conserved and Structurally Distinct New Family of Deubiquitinating Enzymes.* Molecular cell, 2016. **63**(1): p. 146-155.

124. Grou, C.P., et al., *The de novo synthesis of ubiquitin: identification of deubiquitinases acting on ubiquitin precursors.* Scientific reports, 2015. **5**: p. 12836-12836.

125. Lund, P.K., et al., *Nucleotide sequence analysis of a cDNA encoding human ubiquitin reveals that ubiquitin is synthesized as a precursor.* The Journal of biological chemistry, 1985. **260**(12): p. 7609-7613.

126. Seo, D., et al., *The deubiquitinating enzyme PSMD14 facilitates tumor growth and chemoresistance through stabilizing the ALK2 receptor in the initiation of BMP6 signaling pathway.* EBioMedicine, 2019. **49**: p. 55-71.

127. Lee, B.H., et al., *USP14 deubiquitinates proteasome-bound substrates that are ubiquitinated at multiple sites.* Nature, 2016. **532**(7599): p. 398-401.

128. de Poot, S.A.H., G. Tian, and D. Finley, *Meddling with Fate: The Proteasomal Deubiquitinating Enzymes.* Journal of molecular biology, 2017. **429**(22): p. 3525-3545.

129. de la Peña, A.H., et al., *Substrate-engaged 26S proteasome structures reveal mechanisms for ATP-hydrolysis-driven translocation.* Science (New York, N.Y.), 2018. **362**(6418): p. eaav0725.

130. Wertz, I.E., et al., *De-ubiquitination and ubiquitin ligase domains of A20 downregulate NF-kappaB signalling.* Nature, 2004. **430**(7000): p. 694-699.

131. Komander, D., M.J. Clague, and S. Urbé, *Breaking the chains: structure and function of the deubiquitinases.* Nature Reviews Molecular Cell Biology, 2009. **10**(8): p. 550-563.

132. Yuan, J., et al., *USP10 regulates p53 localization and stability by deubiquitinating p53.* Cell, 2010. **140**(3): p. 384-396.

133. Zhuang, M., et al., *Substrates of IAP ubiquitin ligases identified with a designed orthogonal E3 ligase, the NEDDylator.* Molecular cell, 2013. **49**(2): p. 273-282.

134. Hicke, L., H.L. Schubert, and C.P. Hill, *Ubiquitin-binding domains.* Nature Reviews Molecular Cell Biology, 2005. **6**(8): p. 610-621.

135. Dikic, I., S. Wakatsuki, and K.J. Walters, *Ubiquitin-binding domains — from structures to functions.* Nature Reviews Molecular Cell Biology, 2009. **10**(10): p. 659-671.

136. Lim, M., et al., *A Ubiquitin-Binding Domain that Binds a Structural Fold Distinct from that of Ubiquitin.* Structure, 2019. **27**(8): p. 1316-1325.e6.

137. Drag, M., et al., *Positional-scanning fluorigenic substrate libraries reveal unexpected specificity determinants of DUBs (deubiquitinating enzymes).* The Biochemical journal, 2008. **415**(3): p. 367-375.

138. Yu, H., et al., *Tumor suppressor and deubiquitinase BAP1 promotes DNA double-strand break repair.* Proc Natl Acad Sci U S A, 2014. **111**(1): p. 285-90.

139. Daou, S., et al., *The BAP1/ASXL2 Histone H2A Deubiquitinase Complex Regulates Cell Proliferation and Is Disrupted in Cancer.* The Journal of biological chemistry, 2015. **290**(48): p. 28643-28663.

140. Machida, Y.J., et al., *The deubiquitinating enzyme BAP1 regulates cell growth via interaction with HCF-1.* The Journal of biological chemistry, 2009. **284**(49): p. 34179-34188.

141. Misaghi, S., et al., *Association of C-Terminal Ubiquitin Hydrolase BRCA1-Associated Protein 1 with Cell Cycle Regulator Host Cell Factor 1.* Molecular and Cellular Biology, 2009. **29**(8): p. 2181.

142. Ruan, H.-B., et al., *O-GlcNAc transferase/host cell factor C1 complex regulates gluconeogenesis by modulating PGC-1α stability.* Cell metabolism, 2012. **16**(2): p. 226-237.

143. Mashtalir, N., et al., *Autodeubiquitination protects the tumor suppressor BAP1 from cytoplasmic sequestration mediated by the atypical ubiquitin ligase UBE2O.* Molecular cell, 2014. **54**(3): p. 392-406.

144. Cooper, E.M., et al., *K63-specific deubiquitination by two JAMM/MPN+ complexes: BRISC-associated Brcc36 and proteasomal Poh1.* The EMBO journal, 2009. **28**(6): p. 621-631.

145. Brooks, C.L., et al., *The p53--Mdm2--HAUSP complex is involved in p53 stabilization by HAUSP.* Oncogene, 2007. **26**(51): p. 7262-7266.

146. Li, M., et al., *Deubiquitination of p53 by HAUSP is an important pathway for p53 stabilization.* Nature, 2002. **416**(6881): p. 648-653.

147. Sun, X.-X. and M.-S. Dai, *Deubiquitinating enzyme regulation of the p53 pathway: A lesson from Otub1.* World journal of biological chemistry, 2014. **5**(2): p. 75-84.

148. Hanpude, P., et al., *Deubiquitinating enzymes in cellular signaling and disease regulation.* IUBMB life, 2015. **67**(7): p. 544-555.

149. Cai, S.Y., R.W. Babbitt, and V.T. Marchesi, *A mutant deubiquitinating enzyme (Ubp-M) associates with mitotic chromosomes and blocks cell division.* Proceedings of the National Academy of Sciences of the United States of America, 1999. **96**(6): p. 2828-2833.

150. Gelsi-Boyer, V., et al., *Genome profiling of chronic myelomonocytic leukemia: frequent alterations of RAS and RUNX1 genes.* BMC Cancer, 2008. **8**: p. 299.

151. Xu, J.-c., V.L. Dawson, and T.M. Dawson, *Usp16: key controller of stem cells in Down syndrome.* The EMBO journal, 2013. **32**(21): p. 2788-2789.

152. Reyes-Turcu, F.E., et al., *The ubiquitin binding domain ZnF UBP recognizes the C-terminal diglycine motif of unanchored ubiquitin.* Cell, 2006. **124**(6): p. 1197-208.

153. Yang, Y., et al., *Structural and functional studies of USP20 ZnF-UBP domain by NMR.* Protein Science, 2019. **28**(9): p. 1606-1619.

154. Hard, R.L., et al., *HDAC6 and Ubp-M BUZ domains recognize specific C-terminal sequences of proteins.* Biochemistry, 2010. **49**(50): p. 10737-46.

155. Pai, M.T., et al., *Solution structure of the Ubp-M BUZ domain, a highly specific protein module that recognizes the C-terminal tail of free ubiquitin.* J Mol Biol, 2007. **370**(2): p. 290-302.

156. Faesen, Alex C., et al., *The Differential Modulation of USP Activity by Internal Regulatory Domains, Interactors and Eight Ubiquitin Chain Types.* Chemistry & Biology, 2011. **18**(12): p. 1550-1561.

157. Nijman, S.M.B., et al., *A Genomic and Functional Inventory of Deubiquitinating Enzymes.* Cell, 2005. **123**(5): p. 773-786.

158. Xu, Y., et al., *Ubp-M serine 552 phosphorylation by cyclin-dependent kinase 1 regulates cell cycle progression.* Cell Cycle, 2013. **12**(19): p. 3219-27.

159. Lange, A., et al., *Classical nuclear localization signals: definition, function, and interaction with importin alpha.* The Journal of biological chemistry, 2007. **282**(8): p. 5101-5105.

160. Lange, A., et al., *Expanding the definition of the classical bipartite nuclear localization signal.* Traffic (Copenhagen, Denmark), 2010. **11**(3): p. 311-323.

161. Fontes, M.R.M., T. Teh, and B. Kobe, *Structural basis of recognition of monopartite and bipartite nuclear localization sequences by mammalian importin-α11Edited by K. Nagai.* Journal of Molecular Biology, 2000. **297**(5): p. 1183-1194.

162. Goldfarb, D.S., et al., *Importin α: a multipurpose nuclear-transport receptor.* Trends in Cell Biology, 2004. **14**(9): p. 505-514.

163. Stewart, M., *Molecular mechanism of the nuclear protein import cycle.* Nature Reviews Molecular Cell Biology, 2007. **8**(3): p. 195-208.

164. Xu, D., et al., *Sequence and structural analyses of nuclear export signals in the NESdb database.* Molecular biology of the cell, 2012. **23**(18): p. 3677-3693.

165. Fung, H.Y.J., S.-C. Fu, and Y.M. Chook, *Nuclear export receptor CRM1 recognizes diverse conformations in nuclear export signals.* eLife, 2017. **6**: p. e23961.

166. Kutay, U. and S. Güttinger, *Leucine-rich nuclear-export signals: born to be weak.* Trends in Cell Biology, 2005. **15**(3): p. 121-124.

167. Nijman, S.M., et al., *A genomic and functional inventory of deubiquitinating enzymes.* Cell, 2005. **123**(5): p. 773-86.

168. Prigent, C. and S. Dimitrov, *Phosphorylation of serine 10 in histone H3, what for?* Journal of Cell Science, 2003. **116**(18): p. 3677.

169. Sauvé, D.M., et al., *Phosphorylation-induced rearrangement of the histone H3 NH2-terminal domain during mitotic chromosome condensation.* The Journal of cell biology, 1999. **145**(2): p. 225-235.

170. Crosio, C., et al., *Mitotic phosphorylation of histone H3: spatio-temporal regulation by mammalian Aurora kinases.* Mol Cell Biol, 2002. **22**(3): p. 874-85.

171. Joo, H.Y., et al., *Regulation of cell cycle progression and gene expression by H2A deubiquitination.* Nature, 2007. **449**(7165): p. 1068-72.

172. Frangini, A., et al., *The aurora B kinase and the polycomb protein ring1B combine to regulate active promoters in quiescent lymphocytes.* Mol Cell, 2013. **51**(5): p. 647-61.

173. Goto, H., et al., *Aurora-B phosphorylates Histone H3 at serine28 with regard to the mitotic chromosome condensation.* Genes Cells, 2002. **7**(1): p. 11-7.

174. Akopyan, K., et al., *Assessing kinetics from fixed cells reveals activation of the mitotic entry network at the S/G2 transition.* Mol Cell, 2014. **53**(5): p. 843-53.

175. van de Weerdt, B.C. and R.H. Medema, *Polo-like kinases: a team in control of the division.* Cell Cycle, 2006. **5**(8): p. 853-64.

176. Lee, K.S., et al., *Self-regulated mechanism of Plk1 localization to kinetochores: lessons from the Plk1-PBIP1 interaction.* Cell Div, 2008. **3**: p. 4.

177. Kang, Y.H., et al., *Self-regulated Plk1 recruitment to kinetochores by the Plk1-PBIP1 interaction is critical for proper chromosome segregation.* Mol Cell, 2006. **24**(3): p. 409-22.

178. Kishi, K., et al., *Functional dynamics of Polo-like kinase 1 at the centrosome.* Mol Cell Biol, 2009. **29**(11): p. 3134-50.

179. Lera, R.F., et al., *Plk1 protects kinetochore-centromere architecture against microtubule pulling forces.* EMBO Rep, 2019. **20**(10): p. e48711.

180. Sumara, I., et al., *Roles of polo-like kinase 1 in the assembly of functional mitotic spindles.* Curr Biol, 2004. **14**(19): p. 1712-22.

181. Beck, J., et al., *Ubiquitylation-dependent localization of PLK1 in mitosis.* Nat Cell Biol, 2013. **15**(4): p. 430-9.

182. Beck, J. and M. Peter, *Regulating PLK1 dynamics by Cullin3/KLHL22-mediated ubiquitylation.* Cell cycle (Georgetown, Tex.), 2013. **12**(16): p. 2528-2529.

183. Zhuo, X., et al., *Usp16 regulates kinetochore localization of Plk1 to promote proper chromosome alignment in mitosis.* The Journal of cell biology, 2015. **210**(5): p. 727-735.

184. Liu, J. and C. Zhang, *The equilibrium of ubiquitination and deubiquitination at PLK1 regulates sister chromatid separation.* Cellular and molecular life sciences : CMLS, 2017. **74**(12): p. 2127-2134.

185. Higashi, M., S. Inoue, and T. Ito, *Core histone H2A ubiquitylation and transcriptional regulation.* Exp Cell Res, 2010. **316**(17): p. 2707-12.

186. Wang, H., et al., *Role of histone H2A ubiquitination in Polycomb silencing.* Nature, 2004. **431**(7010): p. 873-8.

187. Zhou, W., X. Wang, and M.G. Rosenfeld, *Histone H2A ubiquitination in transcriptional regulation and DNA damage repair.* Int J Biochem Cell Biol, 2009. **41**(1): p. 12-5.

188. Uckelmann, M. and T.K. Sixma, *Histone ubiquitination in the DNA damage response.* DNA Repair, 2017. **56**: p. 92-101.

189. Plys, A.J., et al., *Phase separation of Polycomb-repressive complex 1 is governed by a charged disordered region of CBX2.* Genes & development, 2019. **33**(13-14): p. 799-813.

190. Tatavosian, R., et al., *Nuclear condensates of the Polycomb protein chromobox 2 (CBX2) assemble through phase separation.* J Biol Chem, 2019. **294**(5): p. 1451-1463.

191. Morgan, B.A., *Hox genes and embryonic development.* Poult Sci, 1997. **76**(1): p. 96-104.

192. Noordermeer, D., et al., *The dynamic architecture of Hox gene clusters.* Science, 2011. **334**(6053): p. 222-5.

193. Mallo, M. and C.R. Alonso, *The regulation of Hox gene expression during animal development.* Development, 2013. **140**(19): p. 3951.

194. Zhang, Z., et al., *Role of remodeling and spacing factor 1 in histone H2A ubiquitination-mediated gene silencing.* Proceedings of the National Academy of Sciences, 2017: p. 201711158.

195. Baarends, W.M., et al., *Silencing of Unpaired Chromatin and Histone H2A Ubiquitination in Mammalian Meiosis.* Molecular and Cellular Biology, 2005. **25**(3): p. 1041.

196. Simon, J.A., *Chromatin compaction at Hox loci: a polycomb tale beyond histone tails.* Mol Cell, 2010. **38**(3): p. 321-2.

197. Francis, N.J., R.E. Kingston, and C.L. Woodcock, *Chromatin Compaction by a Polycomb Group Protein Complex.* Science, 2004. **306**(5701): p. 1574.

198. Gu, Y., et al., *The histone H2A deubiquitinase Usp16 regulates hematopoiesis and hematopoietic stem cell function.* Proc Natl Acad Sci U S A, 2016. **113**(1): p. E51-60.

199. Yang, W., et al., *The histone H2A deubiquitinase Usp16 regulates embryonic stem cell gene expression and lineage commitment.* Nat Commun, 2014. **5**: p. 3818.

200. Zhang, Y., et al., *USP16-mediated deubiquitination of calcineurin A controls peripheral T cell maintenance.* J Clin Invest, 2019. **129**(7): p. 2856-2871.

201. Rusnak, F. and P. Mertz, *Calcineurin: form and function.* Physiol Rev, 2000. **80**(4): p. 1483-521.

202. Park, Y.-J., et al., *The Role of Calcium–Calcineurin–NFAT Signaling Pathway in Health and Autoimmune Diseases.* Frontiers in Immunology, 2020. **11**(195).

203. Montellese, C., et al., *USP16 counteracts mono-ubiquitination of RPS27a and promotes maturation of the 40S ribosomal subunit.* Elife, 2020. **9**.

204. Nerurkar, P., et al., *Eukaryotic Ribosome Assembly and Nuclear Export.* Int Rev Cell Mol Biol, 2015. **319**: p. 107-40.

205. Zemp, I. and U. Kutay, *Nuclear export and cytoplasmic maturation of ribosomal subunits.* FEBS Lett, 2007. **581**(15): p. 2783-93.

206. Otálora-Otálora, B.A., et al., *RUNX family: Oncogenes or tumor suppressors (Review).* Oncology reports, 2019. **42**(1): p. 3-19.

207. Choi, A., et al., *RUNX1 is required for oncogenic Myb and Myc enhancer activity in T-cell acute lymphoblastic leukemia.* Blood, 2017. **130**(15): p. 1722-1733.

208. Sood, R., Y. Kamikubo, and P. Liu, *Role of RUNX1 in hematological malignancies.* Blood, 2017. **129**(15): p. 2070-2082.

209. Adorno, M., et al., *Usp16 contributes to somatic stem-cell defects in Down's syndrome.* Nature, 2013. **501**(7467): p. 380-4.

210. Pawlikowski, B., et al., *Muscle stem cell dysfunction impairs muscle regeneration in a mouse model of Down syndrome.* Scientific reports, 2018. **8**(1): p. 4309-4309.

211. Qian, Y., et al., *USP16 Downregulation by Carboxyl-terminal Truncated HBx Promotes the Growth of Hepatocellular Carcinoma Cells.* Scientific reports, 2016. **6**: p. 33039-33039.

212. Hyman, A.A., C.A. Weber, and F. Jülicher, *Liquid-Liquid Phase Separation in Biology.* Annual Review of Cell and Developmental Biology, 2014. **30**(1): p. 39-58.

213. Nott, T.J., et al., *Phase transition of a disordered nuage protein generates environmentally responsive membraneless organelles.* Mol Cell, 2015. **57**(5): p. 936-947.

214. A, P. and S.C. Weber, *Evidence for and against Liquid-Liquid Phase Separation in the Nucleus.* Noncoding RNA, 2019. **5**(4).

215. Dumetz, A.C., et al., *Protein phase behavior in aqueous solutions: crystallization, liquid-liquid phase separation, gels, and aggregates.* Biophysical journal, 2008. **94**(2): p. 570-583.

216. Brangwynne, C.P., et al., *Germline P granules are liquid droplets that localize by controlled dissolution/condensation.* Science, 2009. **324**(5935): p. 1729-32.

217. Conicella, A.E., et al., *TDP-43 α-helical structure tunes liquid-liquid phase separation and function.* Proc Natl Acad Sci U S A, 2020. **117**(11): p. 5883-5894.

218. Murthy, A.C., et al., *Molecular interactions underlying liquid-liquid phase separation of the FUS low-complexity domain.* Nature structural & molecular biology, 2019. **26**(7): p. 637-648.

219. Gabryelczyk, B., et al., *Hydrogen bond guidance and aromatic stacking drive liquid-liquid phase separation of intrinsically disordered histidine-rich peptides.* Nature Communications, 2019. **10**(1): p. 5465.

220. Amaya, J., V.H. Ryan, and N.L. Fawzi, *The SH3 domain of Fyn kinase interacts with and induces liquid-liquid phase separation of the low-complexity domain of hnRNPA2.* The Journal of biological chemistry, 2018. **293**(51): p. 19522-19531.

221. Wegmann, S., et al., *Tau protein liquid-liquid phase separation can initiate tau aggregation.* The EMBO journal, 2018. **37**(7): p. e98049.

222. Rhoads, S.N., et al., *The Role of Post-Translational Modifications on Prion-Like Aggregation and Liquid-Phase Separation of FUS.* International journal of molecular sciences, 2018. **19**(3): p. 886.

223. Shin, Y. and C.P. Brangwynne, *Liquid phase condensation in cell physiology and disease.* Science, 2017. **357**(6357): p. eaaf4382.

224. Bernardi, R. and P.P. Pandolfi, *Structure, dynamics and functions of promyelocytic leukaemia nuclear bodies.* Nature Reviews Molecular Cell Biology, 2007. **8**(12): p. 1006-1016.

225. Molliex, A., et al., *Phase separation by low complexity domains promotes stress granule assembly and drives pathological fibrillization.* Cell, 2015. **163**(1): p. 123-33.

226. Lee, C.-Y.S., et al., *Recruitment of mRNAs to P granules by condensation with intrinsically-disordered proteins.* eLife, 2020. **9**: p. e52896.

227. Brangwynne, C.P., T.J. Mitchison, and A.A. Hyman, *Active liquid-like behavior of nucleoli determines their size and shape in Xenopus laevis oocytes.* Proc Natl Acad Sci U S A, 2011. **108**(11): p. 4334-9.

228. Luo, Y., Z. Na, and S.A. Slavoff, *P-Bodies: Composition, Properties, and Functions.* Biochemistry, 2018. **57**(17): p. 2424-2431.

229. Courchaine, E.M., A. Lu, and K.M. Neugebauer, *Droplet organelles?* The EMBO Journal, 2016. **35**(15): p. 1603-1612.

230. Kilic, S., et al., *Phase separation of 53BP1 determines liquid-like behavior of DNA repair compartments.* The EMBO Journal, 2019. **38**(16): p. e101379.

231. A, P. and S.C. Weber, *Evidence for and against Liquid-Liquid Phase Separation in the Nucleus.* Non-coding RNA, 2019. **5**(4): p. 50.

232. Patel, A., et al., *A Liquid-to-Solid Phase Transition of the ALS Protein FUS Accelerated by Disease Mutation.* Cell, 2015. **162**(5): p. 1066-77.

233. Efimova, A.D., et al., *The FUS protein: Physiological functions and a role in amyotrophic lateral sclerosis.* Molecular Biology, 2017. **51**(3): p. 341-351.

234. Bosco, D.A., et al., *Mutant FUS proteins that cause amyotrophic lateral sclerosis incorporate into stress granules.* Hum Mol Genet, 2010. **19**(21): p. 4160-75.

235. Liu-Yesucevitz, L., et al., *Tar DNA binding protein-43 (TDP-43) associates with stress granules: analysis of cultured cells and pathological brain tissue.* PLoS One, 2010. **5**(10): p. e13250.

236. Sharma, V., et al., *Oxidative stress at low levels can induce clustered DNA lesions leading to NHEJ mediated mutations.* Oncotarget, 2016. **7**(18): p. 25377-25390.

237. Srinivas, U.S., et al., *ROS and the DNA damage response in cancer.* Redox Biology, 2019. **25**: p. 101084.

238. Manhart, C.M. and E. Alani, *DNA replication and mismatch repair safeguard against metabolic imbalances.* Proceedings of the National Academy of Sciences, 2017. **114**(22): p. 5561.

239. Rastogi, R.P., et al., *Molecular mechanisms of ultraviolet radiation-induced DNA damage and repair.* Journal of nucleic acids, 2010. **2010**: p. 592980-592980.

240. Lomax, M.E., L.K. Folkes, and P. O'Neill, *Biological Consequences of Radiation-induced DNA Damage: Relevance to Radiotherapy.* Clinical Oncology, 2013. **25**(10): p. 578-585.

241. Arthur, A., et al., *Binding of nuclear proteins associated with mammalian DNA repair to the mitomycin C-DNA interstrand crosslink.* Environmental and molecular mutagenesis, 1998. **31**: p. 70-81.

242. Lundin, C., et al., *Methyl methanesulfonate (MMS) produces heat-labile DNA damage but no detectable in vivo DNA double-strand breaks.* Nucleic acids research, 2005. **33**(12): p. 3799-3811.

243. Chatterjee, N. and G.C. Walker, *Mechanisms of DNA damage, repair, and mutagenesis.* Environmental and molecular mutagenesis, 2017. **58**(5): p. 235-263.

244. Cannavo, E., et al., *Characterization of the Interactome of the Human MutL Homologues MLH1, PMS1, and PMS2.* Journal of Biological Chemistry, 2007. **282**(5): p. 2976-2986.

245. Candelli, A., et al., *Visualization and quantification of nascent RAD51 filament formation at single-monomer resolution.* Proceedings of the National Academy of Sciences of the United States of America, 2014. **111**(42): p. 15090-15095.

246. Jensen, R.B., A. Carreira, and S.C. Kowalczykowski, *Purified human BRCA2 stimulates RAD51-mediated recombination.* Nature, 2010. **467**(7316): p. 678-83.

247. Pannunzio, N.R., G. Watanabe, and M.R. Lieber, *Nonhomologous DNA end-joining for repair of DNA double-strand breaks.* The Journal of biological chemistry, 2018. **293**(27): p. 10512-10523.

248. McVey, M., et al., *Eukaryotic DNA Polymerases in Homologous Recombination.* Annual review of genetics, 2016. **50**: p. 393-421.

249. Stinson, B.M., et al., *A Mechanism to Minimize Errors during Non-homologous End Joining.* Mol Cell, 2020. **77**(5): p. 1080-1091.e8.

250. Heidenreich, E., et al., *Non-homologous end joining as an important mutagenic process in cell cycle-arrested cells.* Embo j, 2003. **22**(9): p. 2274-83.

251. Decottignies, A., *Alternative end-joining mechanisms: a historical perspective.* Frontiers in genetics, 2013. **4**: p. 48-48.

252. Iliakis, G., T. Murmann, and A. Soni, *Alternative end-joining repair pathways are the ultimate backup for abrogated classical non-homologous end-joining and homologous recombination repair: Implications for the formation of chromosome translocations.* Mutat Res Genet Toxicol Environ Mutagen, 2015. **793**: p. 166-75.

253. Sallmyr, A. and A.E. Tomkinson, *Repair of DNA double-strand breaks by mammalian alternative end-joining pathways.* J Biol Chem, 2018. **293**(27): p. 10536-10546.

254. Reuven, N., et al., *Recruitment of DNA Repair MRN Complex by Intrinsically Disordered Protein Domain Fused to Cas9 Improves Efficiency of CRISPR-Mediated Genome Editing.* Biomolecules, 2019. **9**(10).

255. Lou, D.I., et al., *An Intrinsically Disordered Region of the DNA Repair Protein Nbs1 Is a Species-Specific Barrier to Herpes Simplex Virus 1 in Primates.* Cell Host Microbe, 2016. **20**(2): p. 178-88.

256. Murthy, A.C. and N.L. Fawzi, *The (un)structural biology of biomolecular liquid-liquid phase separation using NMR spectroscopy.* The Journal of biological chemistry, 2020. **295**(8): p. 2375-2384.

257. Sołtys, K. and A. Ożyhar, *Ordered structure-forming properties of the intrinsically disordered AB region of hRXRγ and its ability to promote liquid-liquid phase separation.* The Journal of Steroid Biochemistry and Molecular Biology, 2020. **198**: p. 105571.

258. Kijas, A.W., et al., *ATM-dependent phosphorylation of MRE11 controls extent of resection during homology directed repair by signalling through Exonuclease 1.* Nucleic acids research, 2015. **43**(17): p. 8352-8367.

259. Georgoulis, A., et al., *Genome Instability and γH2AX.* International journal of molecular sciences, 2017. **18**(9): p. 1979.

260. Gardiner, M., et al., *Identification and characterization of FUS/TLS as a new target of ATM.* Biochem J, 2008. **415**(2): p. 297-307.

261. Deng, Q., et al., *FUS is Phosphorylated by DNA-PK and Accumulates in the Cytoplasm after DNA Damage.* The Journal of Neuroscience, 2014. **34**(23): p. 7802.

262. Lenzken, S.C., et al., *FUS-dependent phase separation initiates double-strand break repair.* bioRxiv, 2019: p. 798884.

263. Murthy, A.C., et al., *Molecular interactions underlying liquid-liquid phase separation of the FUS low-complexity domain.* Nat Struct Mol Biol, 2019. **26**(7): p. 637-648.

264. Mastrocola, A.S., et al., *The RNA-binding protein fused in sarcoma (FUS) functions downstream of poly(ADP-ribose) polymerase (PARP) in response to DNA damage.* J Biol Chem, 2013. **288**(34): p. 24731-41.

265. Valnegri, P., et al., *RNF8/UBC13 ubiquitin signaling suppresses synapse formation in the mammalian brain.* Nat Commun, 2017. **8**(1): p. 1271.

266. Panier, S. and S.J. Boulton, *Double-strand break repair: 53BP1 comes into focus.* Nature reviews. Molecular cell biology, 2014. **15**(1): p. 7-18.

267. Bader, A.S., et al., *The roles of RNA in DNA double-strand break repair.* British Journal of Cancer, 2020. **122**(5): p. 613-623.

268. Citterio, E., *Fine-tuning the ubiquitin code at DNA double-strand breaks: deubiquitinating enzymes at work.* Frontiers in genetics, 2015. **6**: p. 282-282.

269. Nakada, S., et al., *Non-canonical inhibition of DNA damage-dependent ubiquitination by OTUB1.* Nature, 2010. **466**(7309): p. 941-6.

270. Kato, K., et al., *Fine-tuning of DNA damage-dependent ubiquitination by OTUB2 supports the DNA repair pathway choice.* Mol Cell, 2014. **53**(4): p. 617-30.

271. Sharma, N., et al., *USP3 counteracts RNF168 via deubiquitinating H2A and gammaH2AX at lysine 13 and 15.* Cell Cycle, 2014. **13**(1): p. 106-14.

272. Mosbech, A., et al., *The deubiquitylating enzyme USP44 counteracts the DNA double-strand break response mediated by the RNF8 and RNF168 ubiquitin ligases.* The Journal of biological chemistry, 2013. **288**(23): p. 16579-16587.

273. Sy, S.M., et al., *The ubiquitin specific protease USP34 promotes ubiquitin signaling at DNA double-strand breaks.* Nucleic Acids Res, 2013. **41**(18): p. 8572-80.

274. Plys, A.J., et al., *Phase separation of Polycomb-repressive complex 1 is governed by a charged disordered region of CBX2.* Genes Dev, 2019. **33**(13-14): p. 799-813.

275. Strom, A.R., et al., *Phase separation drives heterochromatin domain formation.* Nature, 2017. **547**(7662): p. 241-245.

276. Shakya, A., et al., *Liquid-Liquid Phase Separation of Histone Proteins in Cells: Role in Chromatin Organization.* Biophysical Journal, 2020. **118**(3): p. 753-764.

277. Shanbhag, N.M., et al., *ATM-dependent chromatin changes silence transcription in cis to DNA double-strand breaks.* Cell, 2010. **141**(6): p. 970-81.

278. Bekker-Jensen, S., et al., *HERC2 coordinates ubiquitin-dependent assembly of DNA repair factors on damaged chromosomes.* Nat Cell Biol, 2010. **12**(1): p. 80-6; sup pp 1-12.

279. Zhang, Z., H. Yang, and H. Wang, *The histone H2A deubiquitinase USP16 interacts with HERC2 and fine-tunes cellular response to DNA damage.* J Biol Chem, 2014. **289**(47): p. 32883-94.

280. Danielsen, J.R., et al., *DNA damage-inducible SUMOylation of HERC2 promotes RNF8 binding via a novel SUMO-binding Zinc finger.* The Journal of cell biology, 2012. **197**(2): p. 179-187.

281. Narcis, J.O., et al., *Accumulation of poly(A) RNA in nuclear granules enriched in Sam68 in motor neurons from the SMNDelta7 mouse model of SMA.* Sci Rep, 2018. **8**(1): p. 9646.

282. Charlier, C., et al., *Ultrastructural detection of nucleic acids within heat shock-induced perichromatin granules of HeLa cells by cytochemical and immunocytological methods.* J Struct Biol, 2009. **166**(3): p. 329-36.

283. Schoborg, T., et al., *Chromatin insulator bodies are nuclear structures that form in response to osmotic stress and cell death.* J Cell Biol, 2013. **202**(2): p. 261-76.

284. Hoischen, C., et al., *Multimodal Light Microscopy Approaches to Reveal Structural and Functional Properties of Promyelocytic Leukemia Nuclear Bodies.* Frontiers in oncology, 2018. **8**: p. 125-125.

285. Bernardi, R. and P.P. Pandolfi, *Structure, dynamics and functions of promyelocytic leukaemia nuclear bodies.* Nat Rev Mol Cell Biol, 2007. **8**(12): p. 1006-16.

286. Sampuda, K.M., M. Riley, and L. Boyd, *Stress induced nuclear granules form in response to accumulation of misfolded proteins in Caenorhabditis elegans.* BMC Cell Biol, 2017. **18**(1): p. 18.

287. Laporte, D., et al., *Reversible cytoplasmic localization of the proteasome in quiescent yeast cells.* J Cell Biol, 2008. **181**(5): p. 737-45.

288. Harper, J.W., A. Ordureau, and J.M. Heo, *Building and decoding ubiquitin chains for mitophagy.* Nat Rev Mol Cell Biol, 2018. **19**(2): p. 93-108.

289. Grumati, P. and I. Dikic, *Ubiquitin signaling and autophagy.* J Biol Chem, 2018. **293**(15): p. 5404-5413.

290. Dikic, I. and Z. Elazar, *Mechanism and medical implications of mammalian autophagy.* Nat Rev Mol Cell Biol, 2018. **19**(6): p. 349-364.

291. Stadtmueller, B.M. and C.P. Hill, *Proteasome activators.* Mol Cell, 2011. **41**(1): p. 8-19.

292. Finley, D., X. Chen, and K.J. Walters, *Gates, Channels, and Switches: Elements of the Proteasome Machine.* Trends Biochem Sci, 2016. **41**(1): p. 77-93.

293. Rousseau, A. and A. Bertolotti, *Regulation of proteasome assembly and activity in health and disease.* Nat Rev Mol Cell Biol, 2018. **19**(11): p. 697-712.

294. Bhattacharyya, S., et al., *Regulated protein turnover: snapshots of the proteasome in action.* Nat Rev Mol Cell Biol, 2014. **15**(2): p. 122-33.

295. Livneh, I., et al., *The life cycle of the 26S proteasome: from birth, through regulation and function, and onto its death.* Cell Res, 2016. **26**(8): p. 869-85.

296. Demartino, G.N. and T.G. Gillette, *Proteasomes: machines for all reasons.* Cell, 2007. **129**(4): p. 659-62.

297. Marshall, R.S. and R.D. Vierstra, *Proteasome storage granules protect proteasomes from autophagic degradation upon carbon starvation.* Elife, 2018. **7**.

298. Marshall, R.S., et al., *Autophagic Degradation of the 26S Proteasome Is Mediated by the Dual ATG8/Ubiquitin Receptor RPN10 in Arabidopsis.* Mol Cell, 2015. **58**(6): p. 1053-66.

299. van den Boom, J. and H. Meyer, *VCP/p97-Mediated Unfolding as a Principle in Protein Homeostasis and Signaling.* Mol Cell, 2018. **69**(2): p. 182-194.

300. Adam, S.A., R. Sterne-Marr, and L. Gerace, *Nuclear protein import using digitonin-permeabilized cells.* Methods Enzymol, 1992. **219**: p. 97-110.

301. Zhou, H.X., et al., *Why Do Disordered and Structured Proteins Behave Differently in Phase Separation?* Trends Biochem Sci, 2018. **43**(7): p. 499-516.

302. Uversky, V.N., *Intrinsically disordered proteins in overcrowded milieu: Membrane-less organelles, phase separation, and intrinsic disorder.* Curr Opin Struct Biol, 2017. **44**: p. 18-30.

303. Kroschwald, S., et al., *Promiscuous interactions and protein disaggregases determine the material state of stress-inducible RNP granules.* Elife, 2015. **4**: p. e06807.

304. Anderson, L., C. Henderson, and Y. Adachi, *Phosphorylation and rapid relocalization of 53BP1 to nuclear foci upon DNA damage.* Mol Cell Biol, 2001. **21**(5): p. 1719-29.

305. Yadav, T., J.P. Quivy, and G. Almouzni, *Chromatin plasticity: A versatile landscape that underlies cell fate and identity.* Science, 2018. **361**(6409): p. 1332-1336.

306. Sternsdorf, T., K. Jensen, and H. Will, *Evidence for covalent modification of the nuclear dot-associated proteins PML and Sp100 by PIC1/SUMO-1.* J Cell Biol, 1997. **139**(7): p. 1621-34.

307. Muller, S., M.J. Matunis, and A. Dejean, *Conjugation with the ubiquitin-related modifier SUMO-1 regulates the partitioning of PML within the nucleus.* EMBO J, 1998. **17**(1): p. 61-70.

308. D'Arcy, P., et al., *Inhibition of proteasome deubiquitinating activity as a new cancer therapy.* Nat Med, 2011. **17**(12): p. 1636-40.

309. Finley, D., *Recognition and processing of ubiquitin-protein conjugates by the proteasome.* Annu Rev Biochem, 2009. **78**: p. 477-513.

310. Paraskevopoulos, K., et al., *Dss1 is a 26S proteasome ubiquitin receptor.* Mol Cell, 2014. **56**(3): p. 453-61.

311. Suzuki, R. and H. Kawahara, *UBQLN4 recognizes mislocalized transmembrane domain proteins and targets these to proteasomal degradation.* EMBO Rep, 2016. **17**(6): p. 842-57.

312. Hjerpe, R., et al., *UBQLN2 Mediates Autophagy-Independent Protein Aggregate Clearance by the Proteasome.* Cell, 2016. **166**(4): p. 935-949.

313. Watkins, J.F., et al., *The Saccharomyces cerevisiae DNA repair gene RAD23 encodes a nuclear protein containing a ubiquitin-like domain required for biological function.* Mol Cell Biol, 1993. **13**(12): p. 7757-65.

314. Wang, Z. and H. Zhang, *Phase Separation, Transition, and Autophagic Degradation of Proteins in Development and Pathogenesis.* Trends Cell Biol, 2019. **29**(5): p. 417-427.

315. Alberti, S., A. Gladfelter, and T. Mittag, *Considerations and Challenges in Studying Liquid-Liquid Phase Separation and Biomolecular Condensates.* Cell, 2019. **176**(3): p. 419-434.

316. Schauber, C., et al., *Rad23 links DNA repair to the ubiquitin/proteasome pathway.* Nature, 1998. **391**(6668): p. 715-8.

317. Chen, L., et al., *Ubiquitin-associated (UBA) domains in Rad23 bind ubiquitin and promote inhibition of multi-ubiquitin chain assembly.* EMBO Rep, 2001. **2**(10): p. 933-8.

318. Gu, Z.C., et al., *Ubiquitin orchestrates proteasome dynamics between proliferation and quiescence in yeast.* Mol Biol Cell, 2017. **28**(19): p. 2479-2491.

319. Broach, J.R., *Nutritional control of growth and development in yeast.* Genetics, 2012. **192**(1): p. 73-105.

320. Palm, W. and C.B. Thompson, *Nutrient acquisition strategies of mammalian cells.* Nature, 2017. **546**(7657): p. 234-242.

321. Wu, G., et al., *Amino acid nutrition in animals: protein synthesis and beyond.* Annu Rev Anim Biosci, 2014. **2**: p. 387-417.

322. Broer, S. and A. Broer, *Amino acid homeostasis and signalling in mammalian cells and organisms.* Biochem J, 2017. **474**(12): p. 1935-1963.

323. Patel, A., et al., *ATP as a biological hydrotrope.* Science, 2017. **356**(6339): p. 753-756.

324. Kamphorst, J.J., et al., *Human pancreatic cancer tumors are nutrient poor and tumor cells actively scavenge extracellular protein.* Cancer Res, 2015. **75**(3): p. 544-53.

325. Pan, M., et al., *Regional glutamine deficiency in tumours promotes dedifferentiation through inhibition of histone demethylation.* Nat Cell Biol, 2016. **18**(10): p. 1090-101.

326. Daou, S., et al., *The BAP1/ASXL2 Histone H2A Deubiquitinase Complex Regulates Cell Proliferation and Is Disrupted in Cancer.* J Biol Chem, 2015. **290**(48): p. 28643-63.

327. Mashtalir, N., et al., *Autodeubiquitination protects the tumor suppressor BAP1 from cytoplasmic sequestration mediated by the atypical ubiquitin ligase UBE2O.* Mol Cell, 2014. **54**(3): p. 392-406.

328. Daou, S., et al., *Crosstalk between O-GlcNAcylation and proteolytic cleavage regulates the host cell factor-1 maturation pathway.* Proc Natl Acad Sci U S A, 2011. **108**(7): p. 2747-52.

329. Melo, R.C., et al., *Pre-embedding immunogold labeling to optimize protein localization at subcellular compartments and membrane microdomains of leukocytes.* Nat Protoc, 2014. **9**(10): p. 2382-94.

330. Luft, J.H., *Improvements in epoxy resin embedding methods.* J Biophys Biochem Cytol, 1961. **9**: p. 409-14.

331. Gupta, A., et al., *PARK2 Depletion Connects Energy and Oxidative Stress to PI3K/Akt Activation via PTEN S-Nitrosylation.* Mol Cell, 2017. **65**(6): p. 999-1013 e7.

332. Crocker, J.C. and D.G. Grier, *Methods of Digital Video Microscopy for Colloidal Studies.* Journal of Colloid and Interface Science, 1196. **179**(1): p. 298-310.

333. Oberoi, J., et al., *Structural basis of poly(ADP-ribose) recognition by the multizinc binding domain of checkpoint with forkhead-associated and RING Domains (CHFR).* J Biol Chem, 2010. **285**(50): p. 39348-58.

334. Xue, B., et al., *PONDR-FIT: a meta-predictor of intrinsically disordered amino acids.* Biochim Biophys Acta, 2010. **1804**(4): p. 996-1010.

335. Romero P, O.Z., Li X, Garner EC, Brown CJ, Dunker AK., *Sequence complexity of disordered protein.* Proteins. **42**(1): p. 38-48.

336. Kyte J, D.R., *A simple method for displaying the hydropathic character of a protein.* J Mol Biol, 1982. **157**(1): p. 105-132.

337. Wurtele, H., et al., *Histone H3 lysine 56 acetylation and the response to DNA replication fork damage.* Mol Cell Biol, 2012. **32**(1): p. 154-72.

338. Sen Nkwe, N., et al., *A potent nuclear export mechanism imposes USP16 cytoplasmic localization during interphase.* Journal of cell science, 2020: p. jcs.239236.

339. Garcia-Lozano, J.R., et al., *Cytoplasmic detection of a novel protein containing a nuclear localization sequence by human autoantibodies.* Clinical and experimental immunology, 1997. **107**(3): p. 501-506.

340. Antonin, W. and H. Neumann, *Chromosome condensation and decondensation during mitosis.* Curr Opin Cell Biol, 2016. **40**: p. 15-22.

341. Francis, N.J., R.E. Kingston, and C.L. Woodcock, *Chromatin compaction by a polycomb group protein complex.* Science, 2004. **306**(5701): p. 1574-7.

342. Grau, D.J., et al., *Compaction of chromatin by diverse Polycomb group proteins requires localized regions of high charge.* Genes Dev, 2011. **25**(20): p. 2210-21.

343. Khan, W.A., P.K. Rogan, and J.H. Knoll, *Localized, non-random differences in chromatin accessibility between homologous metaphase chromosomes.* Mol Cytogenet, 2014. **7**(1): p. 70.

344. Khan, W.A., P.K. Rogan, and J.H.M. Knoll, *Reversing chromatin accessibility differences that distinguish homologous mitotic metaphase chromosomes.* Molecular cytogenetics, 2015. **8**: p. 65-65.

345. Frangini, A., et al., *The aurora B kinase and the polycomb protein ring1B combine to regulate active promoters in quiescent lymphocytes.* Molecular cell, 2013. **51**(5): p. 647-661.

346. Stratford, J.K., et al., *Genetic and pharmacological inhibition of TTK impairs pancreatic cancer cell line growth by inducing lethal chromosomal instability.* PloS one, 2017. **12**(4): p. e0174863-e0174863.

347. Fisher, D., et al., *Phosphorylation network dynamics in the control of cell cycle transitions.* Journal of Cell Science, 2012. **125**(20): p. 4703.

348. Ohta, S., et al., *Identification of Mitosis-Specific Phosphorylation in Mitotic Chromosome-Associated Proteins.* Journal of Proteome Research, 2016. **15**(9): p. 3331-3341.

349. Dephoure, N., et al., *A quantitative atlas of mitotic phosphorylation.* Proceedings of the National Academy of Sciences, 2008. **105**(31): p. 10762.

350. Irniger, S., *Cyclin destruction in mitosis: a crucial task of Cdc20.* FEBS Letters, 2002. **532**(1): p. 7-11.

351. Al-Hakim, A.K., et al., *Interaction proteomics identify NEURL4 and the HECT E3 ligase HERC2 as novel modulators of centrosome architecture.* Mol Cell Proteomics, 2012. **11**(6): p. M111.014233.

352. Li, M., et al., *NudC-like protein 2 restrains centriole amplification by stabilizing HERC2.* Cell death & disease, 2019. **10**(9): p. 628-628.

353. Wang, Z., et al., *USP51 deubiquitylates H2AK13,15ub and regulates DNA damage response.* Genes & development, 2016. **30**(8): p. 946-959.

354. Wu, W., et al., *HERC2 is an E3 ligase that targets BRCA1 for degradation.* Cancer Res, 2010. **70**(15): p. 6384-92.

355. Finley, D., B. Bartel, and A. Varshavsky, *The tails of ubiquitin precursors are ribosomal proteins whose fusion to ubiquitin facilitates ribosome biogenesis.* Nature, 1989. **338**(6214): p. 394-401.

356. Radici, L., et al., *Ubiquitin C gene: Structure, function, and transcriptional regulation.* Advances in Bioscience and Biotechnology, 2013. **Vol.04No.12**: p. 6.

357. Hoeller, D. and I. Dikic, *How the proteasome is degraded.* Proceedings of the National Academy of Sciences, 2016. **113**(47): p. 13266.

358. Jameson, D.M., J.A. Ross, and J.P. Albanesi, *Fluorescence fluctuation spectroscopy: ushering in a new age of enlightenment for cellular dynamics.* Biophysical reviews, 2009. **1**(3): p. 105-118.

359. Saxton, R.A. and D.M. Sabatini, *mTOR Signaling in Growth, Metabolism, and Disease.* Cell, 2017. **168**(6): p. 960-976.

360. Schmeisser, K. and J.A. Parker, *Pleiotropic Effects of mTOR and Autophagy During Development and Aging.* Frontiers in Cell and Developmental Biology, 2019. **7**(192).

361. Marçais, A., et al., *The metabolic checkpoint kinase mTOR is essential for IL-15 signaling during the development and activation of NK cells.* Nature immunology, 2014. **15**(8): p. 749-757.

362. Kimball, S.R. and L.S. Jefferson, *Signaling pathways and molecular mechanisms through which branched-chain amino acids mediate translational control of protein synthesis.* The Journal of nutrition, 2006. **136**(1 Suppl): p. 227S-31S.

363. DeBerardinis, R.J. and T. Cheng, *Q's next: the diverse functions of glutamine in metabolism, cell biology and cancer.* Oncogene, 2010. **29**(3): p. 313-324.

364. Hu, Q., U. Agarwal, and B.J. Bequette, *Gluconeogenesis, non-essential amino acid synthesis and substrate partitioning in chicken embryos during later development.* Poultry Science, 2017. **96**(2): p. 414-424.

365. Lane, A.N. and T.W.M. Fan, *Regulation of mammalian nucleotide metabolism and biosynthesis.* Nucleic Acids Research, 2015. **43**(4): p. 2466-2485.

366. Amelio, I., et al., *Serine and glycine metabolism in cancer.* Trends in biochemical sciences, 2014. **39**(4): p. 191-198.

367. Locasale, J.W., *Serine, glycine and one-carbon units: cancer metabolism in full circle.* Nature reviews. Cancer, 2013. **13**(8): p. 572-583.

368. Zhou, Z., et al., *UV induced ubiquitination of the yeast Rad4-Rad23 complex promotes survival by regulating cellular dNTP pools.* Nucleic acids research, 2015. **43**(15): p. 7360-7370.

369. Chipuk, J.E., et al., *Direct activation of Bax by p53 mediates mitochondrial membrane permeabilization and apoptosis.* Science, 2004. **303**(5660): p. 1010-4.

370. Haupt, S., et al., *Apoptosis - the p53 network.* Journal of Cell Science, 2003. **116**(20): p. 4077.

371. Kaur, M., et al., *hHR23B is required for genotoxic-specific activation of p53 and apoptosis.* Oncogene, 2007. **26**(8): p. 1231-7.

372. Poulaki, V., et al., *The proteasome inhibitor bortezomib induces apoptosis in human retinoblastoma cell lines in vitro.* Invest Ophthalmol Vis Sci, 2007. **48**(10): p. 4706-19.

373. Mashimo, T., et al., *Acetate is a bioenergetic substrate for human glioblastoma and brain metastases.* Cell, 2014. **159**(7): p. 1603-1614.

374. Yuneva, M., et al., *Deficiency in glutamine but not glucose induces MYC-dependent apoptosis in human cells.* The Journal of cell biology, 2007. **178**(1): p. 93-105.

375. Geck, R.C. and A. Toker, *Nonessential amino acid metabolism in breast cancer.* Advances in biological regulation, 2016. **62**: p. 11-17.

376. Bolzoni, M., et al., *Dependence on glutamine uptake and glutamine addiction characterize myeloma cells: a new attractive target.* Blood, 2016. **128**(5): p. 667-679.

377. van den Heuvel, A.P.J., et al., *Analysis of glutamine dependency in non-small cell lung cancer: GLS1 splice variant GAC is essential for cancer cell growth.* Cancer biology & therapy, 2012. **13**(12): p. 1185-1194.

378. Pérez-Mayoral, J., et al., *Genetic polymorphisms in RAD23B and XPC modulate DNA repair capacity and breast cancer risk in Puerto Rican women.* Mol Carcinog, 2013. **52 Suppl 1**(0 1): p. E127-38.

379. Linge, A., et al., *Identification and functional validation of RAD23B as a potential protein in human breast cancer progression.* J Proteome Res, 2014. **13**(7): p. 3212-22.

380. Shen, M., et al., *Polymorphisms in the DNA nucleotide excision repair genes and lung cancer risk in Xuan Wei, China.* Int J Cancer, 2005. **116**(5): p. 768-73.

381. Jeusset, L.M. and K.J. McManus, *Developing Targeted Therapies That Exploit Aberrant Histone Ubiquitination in Cancer.* Cells, 2019. **8**(2).

382. Wang, W., et al., *Polycomb Group (PcG) Proteins and Human Cancers: Multifaceted Functions and Therapeutic Implications.* Med Res Rev, 2015. **35**(6): p. 1220-67.

383. Cao, G., et al., *Bmi-1 absence causes premature brain degeneration.* PLoS One, 2012. **7**(2): p. e32015.

ANNEXE

ARTICLE DE REVUE - Ubiquitination interplay with other post-translational modifications in orchestrating cellular processes

---

Article en cours de finalisation pour publication

Haithem Barbour*, **Nadine Sen Nkwe***, Salima Daou[♯], Frederick A Mallette[♯] and El Bachir Affar[♯]

Maisonneuve-Rosemont Hospital Research Center and Department of Medicine, University of Montréal, Montréal H3C 3J7, Québec, Canada

* These authors contributed equally to this work

[♯] To whom correspondence should be addressed:
Salima Daou: sdaou@lunenfeld.ca
Frederick A Mallette: fa.mallette@umontreal.ca
El Bachir Affar: el.bachir.affar@umontreal.ca

Running title: Crosstalk between ubiquitination and other post-translational modifications

Keywords: Ubiquitin E3 ligase; deubiquitinase; Ubiquitination; Sumoylation; Neddylation; Phosphorylation; Acetylation; Methylation; O-GlcNAcylation; PARylation; Hydroxylation; S-Nitrosylation

Introduction de l'article :

L'ubiquitination est une modification post-traductionnelle importante pour la régulation et l'activité des protéines. Ce mécanisme émerge comme un processus majeur qui coordonne le dynamisme de tout le réseau de signalisation cellulaire. Comme beaucoup d'autres modifications, l'ubiquitination est réversible et peut être régulée par des enzymes appelées déubiquitinases. Outre que les déubiquitinases, il existe d'autres mécanismes pouvant moduler le processus d'ubiquitination. En effet, des travaux montrent qu'il existe des échanges entre les différentes modifications post-traductionnelles capables d'induire ou d'inhiber le signal d'ubiquitination.

Dans cette revue, nous nous sommes intéressés à la manière dont les autres modifications post-traductionnelles régulent l'ubiquitination. Nous avons caractérisé de façon détaillée les interactions entre les différentes modifications et nous avons discuté de l'impact de la dérégulation de celle-ci sur l'apparition des maladies.

Contribution :

En tant que co-première auteure de cet article, ma contribution est de 40 %. J'ai activement participé à la conception du projet, à la préparation des figures et à la rédaction du manuscrit en collaboration avec Dr Barbour.

1. Abstract

Ubiquitination is an important post-translational modification found in virtually all kingdoms of life. The covalent attachment of the ubiquitin moiety to protein substrates involves the sequential action of E1 ubiquitin-activating, E2 ubiquitin-conjugating and E3 ubiquitin-ligase enzymes. The E2 and E3 enzymes are responsible for writing the ubiquitin signal which is interpreted by a wide spectrum of ubiquitin-binding proteins, resulting in protein change of function or degradation by the proteasome. Ubiquitination is reversed by deubiquitinases (DUBs) which act as erasers of this post-translational modification, ensuring the fine-tuning or termination of ubiquitin signaling. All the above-mentioned factors constitute the Ubiquitin Proteasome System (UPS), which regulates a large spectrum of cellular processes including gene expression, DNA replication and repair, cell cycle, cell death, differentiation, endocytic trafficking, protein quality control, as well as immune and stress responses. Not surprisingly, abnormalities in the UPS play causal roles in an ever-increasing number of human pathologies. For instance, several E3 ligases and DUBs act as either oncogenes or tumor suppressors and deregulations of their cognate signaling pathways drive neoplastic transformation and tumor progression. Much progress has been made during the last two decades in understanding how ubiquitin ligases recognize their substrates and how this post-translational modification is coordinated. Several mechanisms of regulation have evolved to prevent promiscuity including the assembly of ubiquitin ligases in complexes with dedicated subunits and specific post-translational modifications of these enzymes and their cofactors. Here we discuss another layer of complexity involving the coordinated access of E3 ligases to substrates. Several models have emerged in which ubiquitination of substrates is regulated by an ever-increasing number of post-translational modifications of the same targets dictating ON and OFF switches, and thus increasing both the specificity of ubiquitination as well as its crosstalk with other cellular pathways ensuring cell homeostasis.

2. Introduction

Ubiquitination is a post-translational modification (PTM) playing important roles in regulating protein stability, activity and localization, and constitutes a major biochemical process coordinating a vast majority of cell signaling networks [1-6]. This modification is catalyzed by the concerted action of three distinct enzymes, E1 ubiquitin-activating, E2 ubiquitin-conjugating and E3 ubiquitin ligase culminating in the covalent attachment of the 76 amino acids ubiquitin protein to an internal lysine or the N-terminal residue of substrates [1, 3, 7]. The E1 enzyme binds and activates ubiquitin through a thioester bond between the C-terminal glycine of ubiquitin and the catalytic cysteine site of the E1 in ATP-dependent manner. The E2 recognizes the activated ubiquitin which is then transferred to a cysteine residue of the E2 active site [1, 8]. The E3 ligase interacts with the charged E2 and then promote the ubiquitin attachment through the formation of an isopeptide bond between the carboxyl group of the ubiquitin and the epsilon-amino group of the substrate lysine [1, 7]. E3 ligases can also target the alpha amine group of the N-terminal residue resulting in the formation of an amide bond between ubiquitin and the substrate [9]. Humans have two E1s, ~40 E2s and more than 600 E3s [10-13]. There are two major groups of E3 ligases, the RING domain-containing enzymes which catalyze the transfer of ubiquitin from E2 enzyme directly to their substrate and the HECT domain containing E3 enzymes, which form a thioester bond with ubiquitin prior to its transfer to the substrate [7, 10, 14]. Ubiquitin can be attached to substrates in different configurations. Monoubiquitination corresponds to the attachment of one ubiquitin molecule to the substrate, while attachment of individual ubiquitin molecules to several lysines of the substrate corresponds to multi-monoubiquitination. In contrast, polyubiquitination corresponds to the formation of an ubiquitin chain as ubiquitin itself contains, in addition to the N-terminus, seven lysines (K6, K11, K27, K29, K33, K48 and K63) that can be used for ubiquitin attachment [4-6, 15, 16]. It has long been known that ubiquitination through K48 is associated with protein degradation by the proteasome, while K63 ubiquitin chain formation is often involved in complex assembly and protein activation [4-6]. Similar to many other PTMs, ubiquitination is reversible, and ubiquitin removal from substrates is catalyzed by deubiquitinases (DUBs). The DUBs compose a relatively large superfamily of proteases classified into at least seven families according to similarities of their catalytic domains and mechanisms of catalysis [17-20]. DUBs play important roles in ubiquitin maturation, recycling and the maintenance of adequate pools of free and conjugated ubiquitin in the cell. For instance, PSMD14, a zinc metalloprotease DUB and a component of the 19S proteasome regulatory

particle, is required for deubiquitination of substrates prior to their degradation by the 20S catalytic portion of the proteasome [21]. DUBs have also emerged as highly selective regulators of ubiquitination events and as such can control diverse cellular processes [18, 22]. Deubiquitination of proteins modified by K48 or K11 ubiquitin chains can rescue them from proteasomal degradation, while deubiquitination of substrates that are either monoubiquitinated or polyubiquitinated through other chains could result in change of activity or localization, thus impacting protein function in proteolysis-independent manner, reminiscent of other PTMs [18, 22].

Due to its bulky nature, protein ubiquitination can have a major impact on protein function. Moreover, ubiquitination mediates events often with rapid spatiotemporal dynamics [23, 24]. Thus, this reaction has to be extremely controlled to avoid unwanted proteolysis or promiscuous change in activity. A significant progress has been made during the last decades to determine how ubiquitination is regulated at different levels, notably by other PTMs. For example, ubiquitination of the tumor suppressor and transcription factor p53 can be regulated by phosphorylation, acetylation, methylation, and SUMOylation, allowing fine control of its stability and functional states [25]. However, how these and other PTMs of substrates can promote or antagonize ubiquitination events, remain an area of active investigations. Here, we summarize and discuss the current state of knowledge on the crosstalk between ubiquitination and a diverse spectrum of PTMs in the regulation of protein stability and function. The mechanisms of regulation of E3 ligases or DUBs have been previously documented [7, 26-29], and will not be covered in this review. Central to this review is the impact of the multiple PTMs on the substrate itself. We provide examples on the intricate mechanisms of recognition and ubiquitination of substrates proteins. Finally, we also stress some of the unaddressed questions and highlight new directions for future studies.

3. Cooperation and antagonism between SUMO, NEDD8, ISG15 and Ubiquitin

Despite low sequence conservation, the 3D structures of ubiquitin and the ubiquitin-like proteins (UBL, including SUMO (Small Ubiquitin-like MOdifier), NEDD8 (Neural Precursor Cell Expressed, Developmentally Down-Regulated 8) and ISG15 (Interferon-stimulated gene 15), are remarkably similar and all share a core β-grasp (β-Golgi Reassembly Stacking Protein) fold containing secondary structure elements arranged in a ββαβββ order [30-32] (**Figure 1A**). Although, there are substantial mechanistic similarities between ubiquitination and UBLs-

mediated reactions, specific properties of each system selectively contribute in determining the fate of the modified protein [3, 30]. Because Ubiquitin and UBLs target lysine residues, it is expected that a certain degree of crosstalk would occur between these modifications. Thus, how these PTMs act in unison or opposition to orchestrate protein function?

While ubiquitination generally does not target a canonical peptide sequence, the core SUMOylation consensus motif, ΨKXE/D (where Ψ represents a large hydrophobic residue and X is any amino acid) in which the lysine serves as the acceptor site, constitutes the target for isopeptidic link with SUMO. SUMO modification is minimally catalyzed by a single E2 enzyme, UBC9 (ubiquitin conjugating enzyme 9) [33-35], and this reaction involves about a dozen SUMO E3 ligases which ensure the specificity of substrate modification *in vivo* [36]. Similar to ubiquitination, SUMOylation can have different effects on protein function, including stimulation or inhibition of activity, change in subcellular localization, and modulation of protein stability [36-38]. In some cases, these two modifications exert opposite effects and SUMOylation can antagonize ubiquitination by competing for the same lysine in substrates. This is the case for IkappaBalpha (IκBα), an inhibitor of the transcription factor NF-κB, which is targeted for proteasomal degradation upon TNF receptor stimulation by phosphorylation-mediated ubiquitination of K21 and K22 residues [39-41]. Instead, SUMOylated IκBα on K21 is resistant to signal-induced degradation and this sequesters inactive NF-κB in the cytoplasm, limiting its transcriptional functions in the nucleus [42]. (**Figure 1B**). In addition, while phosphorylation of IκBα on S32 and S36 is required for ubiquitination, these PTMs appear to inhibit SUMOylation indicating a hierarchy in signaling events that orchestrate IκBα stability and NF-κB activation [42]. However, the role of SUMOylation in regulating IκBα appears to be more complex than anticipated, since SUMOylated IκBα on K21 and K22 can be directly recruited to chromatin to exert nuclear functions in keratinocytes, independently of NF-κB [43]. SUMOylated IκBα mediates Polycomb group-dependent transcriptional repression through interaction with components of the PRC2 complex. In this context, IκBα regulates the expression of developmental genes, including Hox and IRX gene families, a function that becomes disrupted during oncogenic transformation [43]. Of note, in some conditions, phosphorylated and SUMOylated IκBα can be found in the nucleus, although it remains unclear whether the same molecules can simultaneously harbor these two PTMs [43]. It was also found that IκBα can be targeted by SUMO-ubiquitin hybrid chains, promoting its degradation [44]. Thus, how ubiquitination-SUMOylation switches orchestrate IκBα function still remains incompletely understood. In

addition, how deSUMOylation could potentially orchestrates IκBα stability and function remains to be determined, particularly when taking into account that NF-κB promote feedback mechanisms that involve transcription regulation of SENP proteases [45].

SUMOylation and ubiquitination can act in synergy to propagate signaling pathways through orchestrated and timely intervention of these PTMs. Perhaps the best example illustrating the concerted action of SUMOylation and ubiquitination relates to promyelocytic leukemia (PML) protein. The polySUMOylation on K160 of PML triggers the recruitment of STUbL (SUMO-targeted Ubiquitin ligase) such as RNF4 (RING finger protein 4, also known as Snurf or Small nuclear ring finger protein), which recognizes SUMOylated PML, through SUMO interacting motifs (SIM) and catalyzes SUMO chains polyubiquitination. This initial step is followed by the generation of SUMO-ubiquitin hybrids and subsequent degradation of PML through the proteasome [46, 47]. Mechanistically, RNF4 activity appears to be regulated by dimerization through binding to SUMO chains [48]. RNF4 is monomeric in the absence of SUMO chains, and during stress conditions, a local increase of SUMO modification results in the recruitment of RNF4, through SIMs, inducing Ring finger dimerization and ubiquitin ligase activation. Structural studies indicated that the ring dimer of RNF4 binds the E2-ubiquitin complex and facilitates catalysis [49]. Interestingly, PML was also shown to ensure a protein quality control mechanism by catalyzing SUMOylation and subsequent recruitment of RNF4 to promote the degradation of nuclear misfolded proteins [50]. Of note, substrate SUMOylation-induced ubiquitination and proteasomal degradation appears to be more complex than initially anticipated. For instance, the ubiquitin ligase Arkadia/RNF111 is another STUbL that uses its SIM and SUMO one binding (SOB) motif to interact with SUMO1-capped SUMO2-SUMO3 chains, and this results in substrate proteasomal degradation [51].

Another interesting case of a concerted signaling cascade involves the SUMOylation of MDC1 (Mediator of DNA damage Checkpoint 1) protein which recruits RNF4 to trigger its ubiquitination and removal from the DSB site, thereby inducing the disassembly of 53BP1 and promoting homologous recombination repair of DNA double strand breaks (DSB) [52]. This pathway is subjected to another layer of complexity involving the regulation of MDC1 by both deubiquitination and deSUMOylation. It was found that the DUB Ataxin-3, which is also recruited, in a SUMOylation-dependent manner, counteracts MDC1 ubiquitination and promote its residency time at the site of DNA damage [53]. Here, SUMOylation of MDC1 appears to play opposite roles in promoting or preventing MDC1 removal from chromatin. In addition, deSUMOylation of MDC1 by SENP2 also prevents RNF4 activation and MDC1 clearance from

the site of DNA damage, and this event appears to promote DSB repair by nonhomologous end joining (NHEJ) [54]. It will be interesting to further investigate how SUMOylation/deSUMoylation are coordinated with ubiquitination/deubiquitination events, thus determining when signaling through MDC1 recruitment and its downstream factors need to be consolidated or terminated.

Analogous to ubiquitination and SUMOylation, NEDDylation also needs E1 and E2 enzymes for NEDD8 conjugation to the substrate [55]. This system uses multiple ubiquitin E3 ligases to promote the conjugation of the UbL protein on lysine residues of its target [55]. It is well recognized that the Cullin-RING ubiquitin E3 Ligases (CRLs) are major targets of NEDD8. Cullins are scaffold proteins required for the assembly of multicomponent RING E3 ligase complexes (CRLs) whose E3 ubiquitin ligase activity is stimulated by NEDDylation [56-58]. NEDDylation of non-cullin targets has also been described and this modification protects some proteins from ubiquitin-mediated degradation. For instance, the proto-oncogene and ubiquitin E3 ligase Casitas B-lineage lymphoma (C-CBL), a downstream effector of the Transforming Growth Factor beta (TGFβ) antiproliferative signaling, NEDDylates TGFβ type II receptor (TbetaRII) ensuring its stabilization [59]. On the other hand, it was also established that TGFβ receptors is internalized through two endocytic pathways, clathrin-mediated or caveolin-mediated, leading to two opposite outcomes. While clathrin-mediated TbetaRII internalization results in the maintenance of signal transduction, caveolin-mediated TbetaRII compartmentalization triggers receptor degradation and signal termination [60]. In further elucidating the mechanism of action involved, it was found that C-CBL-mediated NEDDylation promotes TbetaRII internalization through clathrin-dependent endocytosis, thus sustaining TGFβ signaling [59]. Of note, Smad2 and its anchoring protein Smad Anchor for Receptor Activation (SARA) are highly enriched in the early endosome, comparatively to the caveolin-positive compartment [60]. This raises the question of whether distinct factors associated with each endocytic compartment play a role in sorting the NEDDylated versus unmodified TbetaRII. While the example above illustrates how NEDDylation and ubiquitination can exert opposite functions on the substrate, it was also shown that these modifications sometimes act in a concerted manner to promote a signaling pathway. The degradation of the proto-oncogene c-Src involves both NEDDylation and polyubiquitination, resulting in the inhibition of the PI3K-AKT signaling pathway and reduction of cell migration and metastasis [61]. Here, the E3 ligase C-CBL NEDDylates c-Src and this appears to be a prerequisite for polyubiquitination

and proteasomal degradation. Whether a conformational change or the recruitment of additional proteins mediate the NEDDylation-ubiquitination crosstalk remain to be determined.

The crosstalk between ubiquitin and multiple Ubls within the same substrate is best illustrated by Proliferating Cell Nuclear Antigen (PCNA) which is subjected to several PTMs that ensure coordination between DNA replication and repair machineries. Although, established primarily in yeast, the regulation of PCNA by UBLs is highly conserved in eukaryotes. PCNA is a homotrimeric ring-shaped DNA clamp complex acting as a processivity factor for DNA polymerase δ/ε and required for DNA synthesis during replication [62]. PCNA could be modified by ubiquitin or other UBLs on the same K residue, but with different functional consequences [63, 64] (**Figure 1C**). It is interesting to note that the competition between SUMO and ubiquitin for the same site regulate DNA-dependent processes in a degradation-independent manner. In normally growing yeast, SUMOylation of PCNA on K164 induces the recruitment of Srs2 protein to the replication fork, blocking unwanted homologous recombination. Srs2 interacts with PCNA through a PCNA-interacting protein (PIP) box-like motif within the carboxy-terminal domain and a SUMO-Interacting Motif (SIM) that binds SUMOylated PCNA, and Srs2-PCNA interaction prevents Rad51 filament formation and subsequent homologous recombination [65-68]. Similar observed were made in human cells, whereby SUMOylation of PCNA appear to prevent DSB formation and blocks homologous recombination at the stalled replication fork [69]. More recently, SUMOylation of PCNA was also found to promote replication block release by stimulating error-free template switch [70]. In contrast, during DNA damage, the E2-E3 complex Rad6-Rad18 mediates the monoubiquitination of PCNA at K164 triggering the recruitment of Y-family damage-tolerant DNA polymerases (Pol η, Pol ι, Pol κ, REV1 and Pol ζ) in order to bypass the lesion in a process called translesion DNA synthesis (TLS) [64, 71]. The binding of monoubiquitinated PCNA by the TLS DNA polymerase involve the PCNA-interacting protein (PIP) domain as well as UBM or UBZ ubiquitin-binding motifs [72, 73]. PCNA can also be polyubiquitinated on K164, through K63-chains, by Ubc13–Mms2 (E2) and Rad5 (E3), and this event has been involved in template switching (TS) in yeast, resulting in error free repair, although the detailed mechanism remains incompletely understood [74, 75]. In mammalian cells, K63-chain polyubiquitination of PCNA promotes the recruitment of ZRANB3 translocase, which stimulates replication fork

reversal and inhibits recombination events that could take place during template switching, thus maintaining genomic integrity [76-79].

PCNA is also regulated by deubiquitination. In mammalian cells, under normal conditions, USP1 deubiquitinates PCNA, thus protecting against unsolicited TLS. During DNA damage such as pyrimidine dimers induced by UV exposure, USP1 is inactivated by autocleavage, involving a mechanism reminiscent of ubiquitin maturation, as the cleavage site contains an ubiquitin-like diglycine motif [80]. In yeast, UBP8 and UBP10 deubiquitinate PCNA at lysine 164, thus opposing Rad18 E3 ligase function. PCNA deubiquitination prevents TLS and template switch events and might play central roles in damage tolerance during replication [81, 82].

Finally, PCNA was recently shown to be targeted by other UBLs including NEDD8 and ISG15. PCNA K164 NEDDylation appears to inhibits its ubiquitination and the recruitment of polymerase η, and this PTM is reversed by the deNEDDylase NEDP1 [83]. PCNA ISGylation on K164 and/or K168 residues is catalyzed by EFP ISG15 E3 ligase after the recruitment of TLS polymerase, promoting TLS termination. Mechanistically, PCNA K164 mono-ubiquitination promotes the recruitment of EFP and this event leads to PCNA ISGylation. In turn, PCNA ISGylation promotes the recruitment of USP10 for PCNA deubiquitination, leading to pol η release from DNA. Finally, DeISGylatation of PCNA is mediated by UBP43 ensuring TLS termination and reestablishment of normal DNA replication [84].

Overall, while it is increasingly appreciated that PCNA is a major platform for molecular switches between ubiquitin and UBLs, it is still unclear how these switches operate and how other PTMs act in concert with ubiquitin and UBLs to mediate distinct functional outcomes. In particular, PCNA is also known to be phosphorylated, methylated and acetylated on multiple residues [85-89], and its remains to be determined how all these PTMs orchestrate PCNA function in DNA replication and repair.

Taken altogether, although much progress has been made during the last decade, the exact mechanisms of action coordinating the crosstalk between Ubiquitin and UBLs remain incompletely understood. Further investigations are needed to decipher how crosstalks are impacted by the interaction interfaces of the substrate. Dynamic protein-protein interactions including the recruitment of UBLs readers as well as conformation changes resulting from additional PTMs are expected to be at play. Capturing these interactions through structural

studies should help understanding the interplay between signaling events and positioning these PTMs in the context of cellular processes and physiopathology.

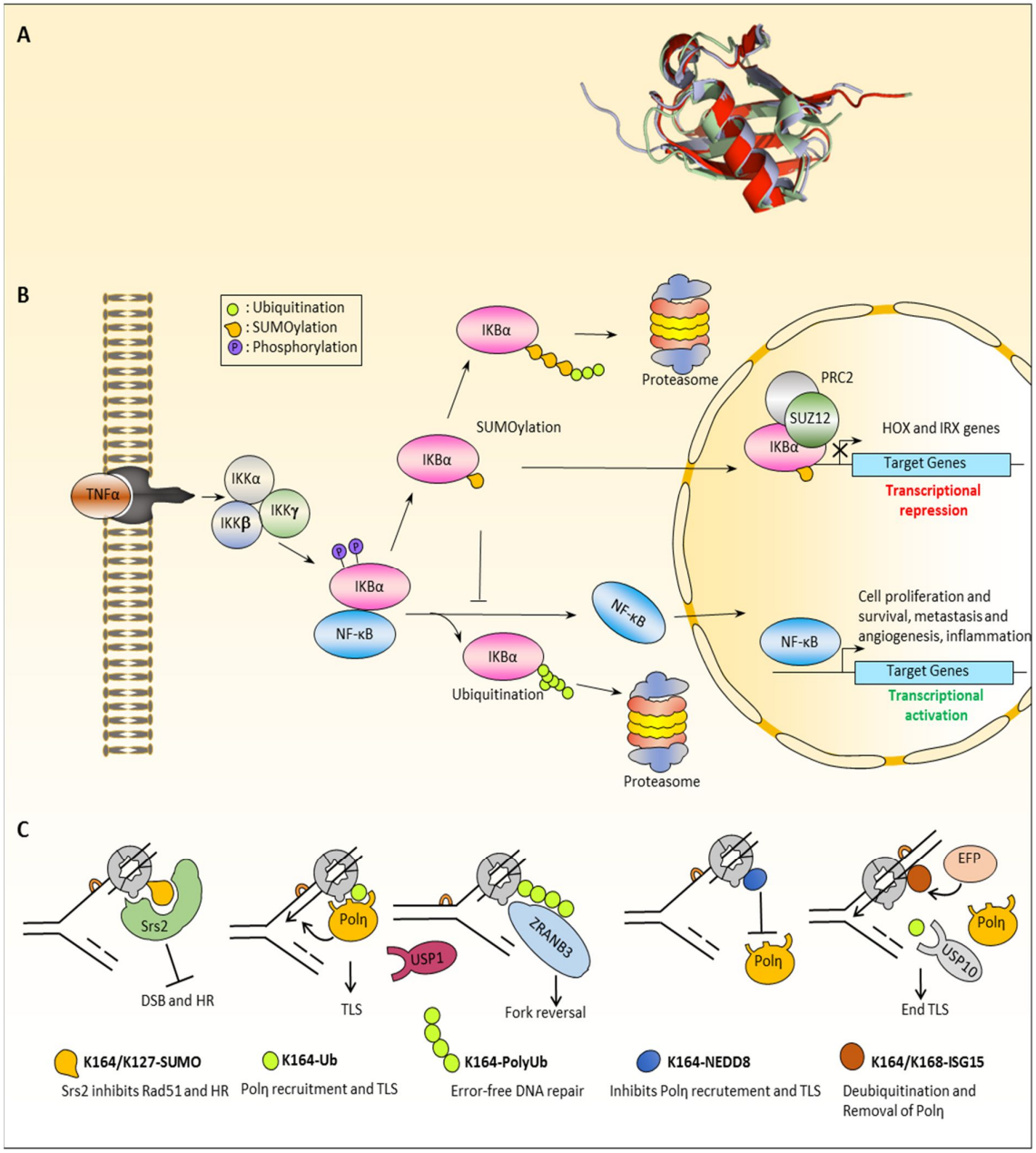

Figure 1 : Crosstalk between ubiquitin-like posttranslational modifications and ubiquitination.

A) Ubiquitin-like proteins, SUMO2, NEDD8 and ISG15 share significant structural similarity with ubiquitin (PDB: 1ubq). **B-C)** Ubiquitin-like modifications compete with ubiquitination on target proteins with variable outcomes on protein stability and functions. **B)** Polyubiquitination of the NF-κB inhibitor, IKBα, leads to its proteasomal degradation and release of NF-κB to

execute its transcriptional activity. However, SUMOylation on the same residue of IKBα blocks its degradation, while hybrid SUMO-Ubiquitin chain extension can re-engage the proteasomal proteolysis pathway. SUMOylated IKBα can also enter the nucleus and repress transcription in concert with the PRC2 complex. **C)** Attachment of SUMO, ubiquitin, NEDD and ISG15 moieties on PCNA is associated with different outcomes on DNA replication and repair.

4. Extensive crosstalk between protein phosphorylation and ubiquitination

Similar to ubiquitination, phosphorylation is a widespread signaling biochemical reaction catalysed by more than 500 kinases in mammals, and reversed by over than 150 phosphatases [90-92]. This modification consists in the attachment of a phosphoryl group (PO_3^{2-}) on serine, threonine and tyrosine residues of target proteins. Much work has been done to determine how phosphorylation regulates cellular processes, and systematic approaches have now revealed the immense repertoire of the phosphoproteome [93]. It is therefore not surprising that ubiquitination and phosphorylation are extensively interconnected involving a complex interplay of cooperative and antagonistic interactions. For instance, a recent global proteomics survey indicated that, in Saccharomyces cerevisiae, about 2,100 phosphorylation sites coexist with 2,189 ubiquitylation sites in hundreds of cellular proteins [94]. The link between phosphorylation and ubiquitination has been studied at different levels such as cell membrane receptor signalling and trafficking, immune responses, DNA replication, cell cycle progression, apoptosis, transcription and DNA damage repair. Generally, the interplay between phosphorylation and ubiquitination is associated with protein degradation. Protein phosphorylation on a conserved short motif of amino acids, called phosphodegron, is recognized by an E3 ubiquitin ligase complex leading to polyubiquitination and proteasomal degradation of the targeted substrate. In particular, the multi-protein E3 ligase Skip1-Culin-F-box (SCF) complex family has been shown to be one of the main players in mediating phosphorylation-inducing degradation (**Figure 2A**). The F-box protein family are responsible for the recognition and binding of the phosphorylated degron motif with one of the first F-box protein identified being the *S. cerevisiae* Cdc4 [95]. Of note substrate ubiquitination is usually preceded by priming phosphorylation events that occur on adjacent sites, involving other kinases than those phosphorylating the degron, indicating the tight control of the phospho-ubiquitin signaling cascades. SCF-mediated ubiquitination covers a wide range of phosphorylated target proteins including many cell cycle effectors. One example is the Cyclin-

dependent kinase inhibitor 1B ($p27^{Kip1}$), which binds and prevents the activation of cyclin E-CDK2 or cyclin A-CDK2 complexes [96, 97]. Previous studies established that phosphorylation of $p27^{Kip1}$ on T187 was essential for its proteasomal degradation by the E3 ligase SKP2 [98, 99], and that this concerted reaction requires the CDK subunit 1 (Cks1) [100]. The crystal structure of the quaternary complex: Skp1-Skp2-Cks1-Phospho $p27^{Kip1}$ reveals that Cks1 binds to both the leucine-rich repeat domain and the C-terminal tail of SKP2 (**Figure 2B**). $p27^{Kip1}$ establishes contacts with both Cks1 and Skp2, a configuration that position Cks1 phospho-binding motif for interaction with the phosphorylated T187 side chain of $p27^{Kip1}$ [101]. Interestingly, $p27^{Kip1}$ binding to Skp1-Skp2-Cks1 is in majority coordinated by intramolecular interactions between the $p27^{Kip1}$ phospho T187 and Cks1 and $p27^{Kip1}$ E185 with both Cks1 and Skp2. This conformation allows $p27^{Kip1}$ phospho T187 recognition and its ubiquitination. Additionally, $p27^{Kip1}$ is also phosphorylated by the oncogenic tyrosine kinase Src on Y88, promoting a conformational change that results in disruption of $p27^{Kip1}$ interaction with the CDK2 catalytic cleft. The released cyclin A-CDK2 become in an active state promoting p27 phosphorylation on T187, which stimulates its ubiquitination and proteasomal degradation [102, 103].

On the other hand, phosphorylation is also known to prevent substrate ubiquitination and degradation. This is exemplified by dual leucine zipper-bearing kinase (DLK/MAP3K12), an evolutionarily conserved member of the mixed lineage kinase (MLK) family that plays an important role in c-Jun N-terminal kinases (JNK) signaling and apoptosis. DLK protein stability is regulated through the action of the E3 ubiquitin ligase PHR1 and the DUB USP9X [104]. During retrograde signaling, neurons respond to axonal damage by inducing a site-specific phosphorylation of DLK by JNK that prevents its ubiquitination (**Figure 2C**). Stabilized DLK acts in turn to promote downstream JNK signaling and apoptosis [104]. This signaling cascade illustrates how ubiquitination and phosphorylation crosstalk can be exploited to amplify a stress response, thereby quickly reacting to extracellular cues.

There are many examples where phosphorylation promotes ubiquitination in signaling events, independently of proteolysis. The DNA double strand break repair (DSB) pathway is subjected to an intricate level of regulation coordinating multiple points of the DNA damage response signaling cascade including, initiation, pathway choice and termination. The extent of DNA end resection highly influences the pathway choice between non-homologous end-joining (NHEJ) and homologous recombination (HR) [105-107]. While NHEJ can function in all phases of the cell cycle, HR is highly active in S and G2 phases, as sister chromatids can be

used for recombination [108, 109]. The increase of Cyclin-dependent kinases (CDKs) activity at G1/S transition results in the coordinated phosphorylation of key chromatin-associated and DNA repair factors, thus promoting DNA resection and HR pathway. For instance, RECQL4, a RecQ-type helicase required for genomic integrity, regulates both NHEJ and HR depending on cell cycle phases [109]. Mechanistically RECQL4 forms a complex with Ku70 and facilitates NHEJ. Increased CDK1 and CDK2 activity in S and G2 results in the phosphorylation of RECQL4 on S89 and S251, which promotes its interaction with MRE11. Phosphorylated RECQL4 becomes a substrate of DDB1-CUL4A E3 ubiquitin ligase, which catalyses its ubiquitination and recruitment to DSB sites to mediate DNA end resection and HR (**Figure 2D**) [109].

Reciprocal phosphorylation-ubiquitination switches are provided by the Fanconi anemia (FA) pathway, a complex DNA repair mechanism that protect against DNA interstrand crosslinks (ICL) [110, 111]. The phosphorylation status of FANCI/FANCD2 complex determines its activation state through site-specific monoubiquitination of FANCI and FANCD2 at the DNA damage site [112]. This monoubiquitination event has been found to depend on phosphorylation of FANCI by ATR following DNA damage [113, 114]. Mechanistically, phosphorylation of FANCI results in its dissociation from FANCD2 and subsequent monoubiquitination of these DNA repair factors by the FA complex [115]. Interestingly, while phosphorylation of FANCI on S556 leads to monoubiquitination of FANCI/FANCD2, maintaining the monoubiquitination state is achieved by phosphorylation of FANCI on neighbouring S559/S565 residues (**Figure 2E**) [116]. The latter phosphorylation events block USP1, a DUB for FANCI/FANCD2, and promotes DNA ICL repair. Intriguingly, depletion of USP1 leads to excessive FANCI/FANCD2 monoubiquitination, absence of S559/S565 phosphorylation and defective DNA ICL repair [116]. Clearly an intricate interplay between phosphorylation and ubiquitination/deubiquitination can take place and might provide a platform for the establishment of additional regulatory loops, thus fine-tuning the signaling events that coordinate the FA pathway, ensuring timely and effective removal of replication and transcription blocking DNA lesions.

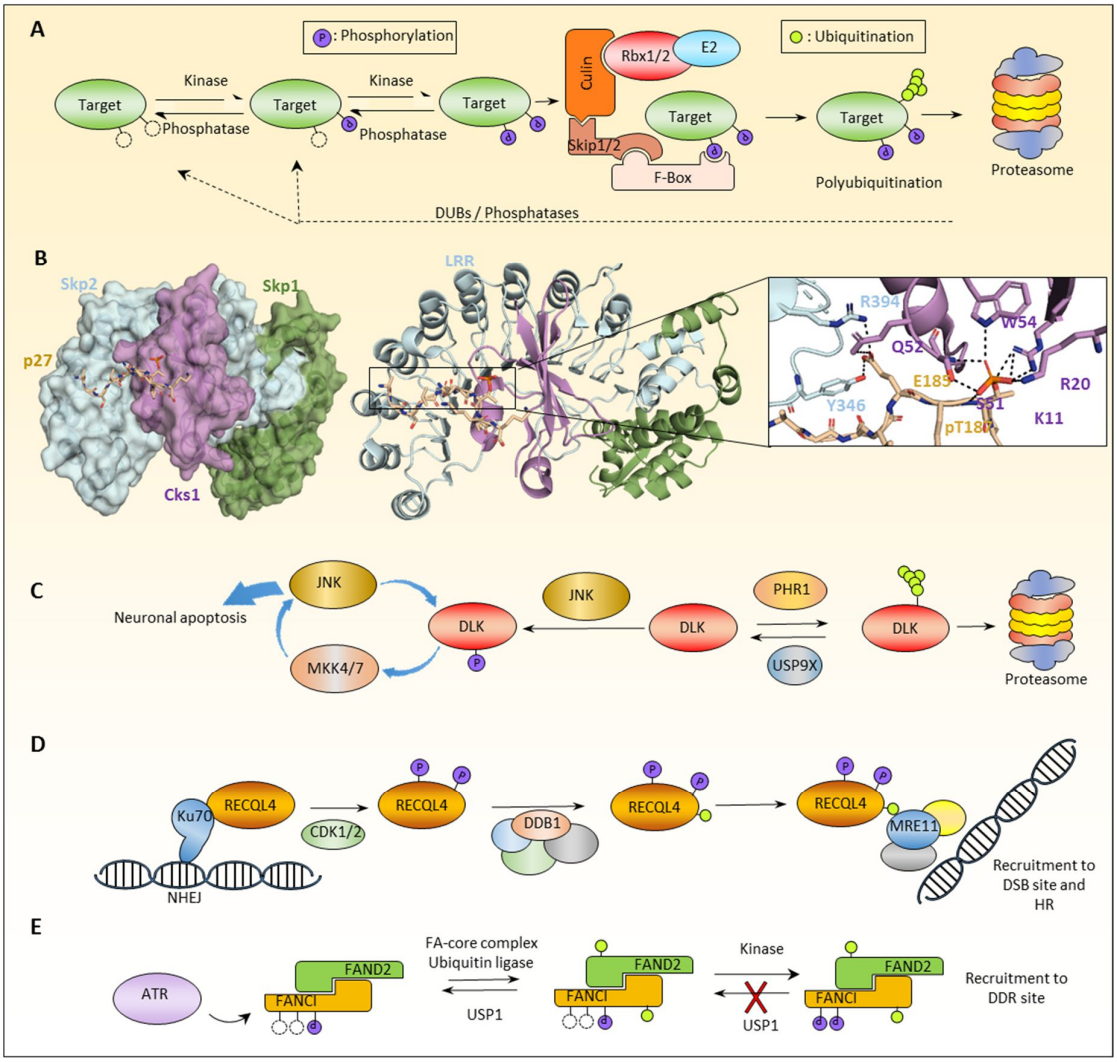

Figure 2 : Model of interplay between protein phosphorylation and ubiquitination.

A) Phosphorylation of a target protein creates a signal recognized by E3 ubiquitin ligase complexes (in this case the SCF or Skip-Culin-F-box complex family). Generally the F-box factor positions the targeted protein in the vicinity of the Culin ligase and its co-factors/E2 enzymes leading to its ubiquitination and proteasomal degradation. **B)** Crystal structure of the quaternary complex: Skp1-Skp2-Cks1-Phospho $p27^{Kip1}$ (PDB: 2AST). Left panel, overall representation of the complex showing the specific positioning of the p27 peptide within Cks1 and Skp2 binding pockets. Right panel, close up view of the phosphorylated $p27^{Kip1}$ interaction with Cks1 and Skp2. Phosphorylated $p27^{Kip1}$ intercalates into a Cks1/Skp2 pocket formed by Skp2 leucine-rich repeat (LRR) and Cks1 phospho binding site. pT187 is recognized by Cks1 phospho binding site residues whereas E185 binds to both Cks1 and Sp2. The hydrogen bounds

between amino acids are shown in the bottom by the dash lines. **C)** Phosphorylation of DLK blocks its ubiquitination and degradation while promoting the downstream JNK signaling pathway. **D**) Phosphorylation triggers monoubiquitination of RECQL4 leading to its accumulation at DNA damage sites. **E)** FANC1/FAND2 heterodimer is phosphorylated by ATR following DNA interstrand crosslinks which triggers the FA-core complex to monoubiquitinate both proteins. These modifications are removed by USP1 to ensure proper DNA repair, while subsequent FANC1 phosphorylation was shown to block its deubiquitination.

5. Opposing functions of protein acetylation and ubiquitination: a rule with exceptions

Mostly known for its function on histone and chromatin structure, protein lysine acetylation is a widespread PTM catalyzed by lysine acetyltransferases (KATs/HATs) and reversed by lysine deacetylases (KDACs/HDACs) [117-119]. Acetylation plays critical roles in the regulation of various cellular functions including chromatin-dependent processes [117, 119, 120]. Crosstalk between acetylation and ubiquitination is a critical regulatory mechanism controlling vital cellular processes. Protein acetylation can promote protein stability by blocking ubiquitination-mediated proteasomal degradation. One of the first observations validating this notion is the regulation of p53 degradation, as its ubiquitination by the E3 ubiquitin ligase MDM2 can be is inhibited through acetylation of p53 C-terminal domain by p300 [121]. However, acetylation of p53 can also inhibit its ubiquitination not only at ubiquitinated lysines, but also at non-ubiquitinated residues [121]. This observation suggests that, in addition to acetylation directly blocking ubiquitination at specific residues, it may also attenuate ubiquitination by inducing potential conformational change or possibly by preventing substrate recognition by E3 ligases [121]. To counteract this mechanism, the ubiquitin ligase MDM2 functions in part by recruiting the histone deacetylase 1 (KDAC1/HDAC1) to deacetylate p53, thus allowing ubiquitination and subsequent degradation [122]. The model of negative regulation of protein ubiquitination by acetylation has been expanded to many other substrates.

A cooperative relationship between acetylation and ubiquitination can also take place in other contexts. For example, the TIP60 KAT interacts with the ubiquitin-conjugating enzyme UBC13 to catalyze a concerted acetylation-ubiquitination cascade during DNA damage. TIP60 is recruited at the DSB site to induce acetylation of H2AX which is prerequisite for the

ubiquitination of this histone variant and its release from chromatin [123]. This timely removal of ubiquitinated H2AX, promote chromatin remodeling and facilitates DNA repair. In the same context of chromatin-associated acetylation, the regulation of DNA methyltransferase DNMT1 has been shown to be linked to a dynamic acetylation/ubiquitination interplay. Following DNA methylation, DNMT1 is acetylated by TIP60, leading to its polyubiquitination by the E3 ligase UHRF1 and triggering its proteasomal degradation [124]. In contrast, DNMT1 could be rescued from degradation by simultaneous deacetylation by HDAC1 and deubiquitination by herpes virus-associated ubiquitin-specific protease USP7 (HAUSP). This rescue mechanism appears to be deregulated in colon cancer, as a positive correlation between DNMT1 and USP7 expression levels is observed in tumors [124]. However, it remains unclear how the acetylation-dependent ubiquitination switch of DNMT1 is executed, and how this could be reconciled with the prevalent model of UHFR1-mediated DNMT1 recruitment to hemimethylated DNA. Nonetheless, it has been proposed that UHRF1 could have dual roles of recruiting DNMT1 to chromatin, followed by its ubiquitination once DNMT1-driven DNA methylation is completed [124]. A recent structural study showed that DNMT1 interacts with USP7 through an acidic interface in its Lysine-Glycine rich motif (KG linker). Acetylation of the KG linker by TIP60 disrupts USP7 and DNMT1 interaction, an event that favors UHRF1-driven ubiquitination of DNMT1 [125]. Another example for a cooperative and dynamic relationship between acetylation and ubiquitination is exemplified by the regulation of phosphoenolpyruvate carboxykinase (PEPCK1), a cataplerotic enzyme playing a key role in the regulation of gluconeogenesis and cell metabolism [126]. PEPCK1 is degraded in response to high glucose through acetylation-induced ubiquitination by the HECT domain containing E3 ubiquitin ligase UBR5 [126]. The p300-mediated acetylation of PEPCK1 is counteracted by the NAD-dependent deacetylase Sirtuin-2 (SIRT2), contributing to the stabilization of PEPCK1 [126]. Mechanistic insights are needed to fully understand how glucose sensing impacts PEPCK1 stability and how PEPCK1 acetylation is recognized by UBR5 for subsequent ubiquitination. Moreover, it will be interesting to determine whether deregulation of this signaling cascade underlie human metabolic disorders.

6. The link between protein methylation and ubiquitination

Protein methylation consists in adding one to three methyl groups on lysines or one to two methyl groups on arginines by enzymes termed methyltransferases [127-130]. Histones can undergo numerous methylation events, which allow the coordination of chromatin structure, thus impacting gene expression, DNA replication and the DNA damage response. An

interesting mechanism of histone methylation-induced histone ubiquitination is provided by the multidomain protein UHRF1 (Ubiquitin-Like PHD and RING Finger Domain-Containing Protein 1). UHRF1 contains a ubiquitin-like domain (UBL), a tandem Tudor Domain (TTD), a plant homeodomain (PHD), a SET- and RING-associated (SRA) domain, and a RING finger domain. The TTD and PHD are readers of di- or tri-methylated histone H3K9 and unmodified H3R2, respectively, while SRA binds methylated DNA. Through its RING finger, UHFR1 catalyzes ubiquitination of histone H3K23, an event stimulated by UBL. The proper positioning of UHFR on nucleosomal marks and subsequent ubiquitination are prerequisite for DNA methylation (**Figure 3A**) [131-136]. The crystal structure of UHRF1 provided a molecular explanation for the bivalent recognition of histone H3 (**Figure 3B**) [132]. Notably, the PHD and the TTD are linked with 17 residues linker that plays an important role in maintaining a proper structural conformation of the PHD-Tudor module for the bivalent recognition of the H3 tail and the positioning of the RING finger in close proximity of H3K23. This conformation is inhibited by phosphorylation of the S298 residue within the linker of UHRF1[132]. Overall, recognition of histone methylation and DNA methylation are cooperatively involved in ensuring H3 ubiquitination, which in turn promote DNA methylation and transcriptional repression.

Protein methylation has a broader substrate target range than histones [137]. Non-histone methylation/ubiquitination interplay is often linked to protein stability as shown for the orphan nuclear receptor RORα whose methylation is driven by the Polycomb group protein and methyl-transferase EZH2 [138] (**Figure 3C**). EZH2 specifically monomethylates RORα on K38, a methyl-degron motif resembling the H3K27 LxxxxxRKS methyl acceptor motif. Once methylated, RORα(me1) is recognized and bound by the DDB1/CUL4B associated factor DCAF1 which is known to act as an adaptor for CUL4A/B E3 ubiquitin ligases [139]. RORα is then polyubiquitinated and degraded by the proteasome, thus inducing transcriptional repression of RORα target genes and inhibition of its tumor suppressor properties. Interestingly, DCAF1 recognizes specifically the mono-methylated RORα through its C-terminal chromodomain, but not other methylated proteins such as H3K27, which restricts the spectrum of target proteins to be ubiquitinated by DDB1/CUL4B [138]. Moreover, EZH2 targets other proteins for methylation such as GATA4 and STAT3, and it will be interesting to determine whether these methylation events could induce proteasomal degradation [140, 141].

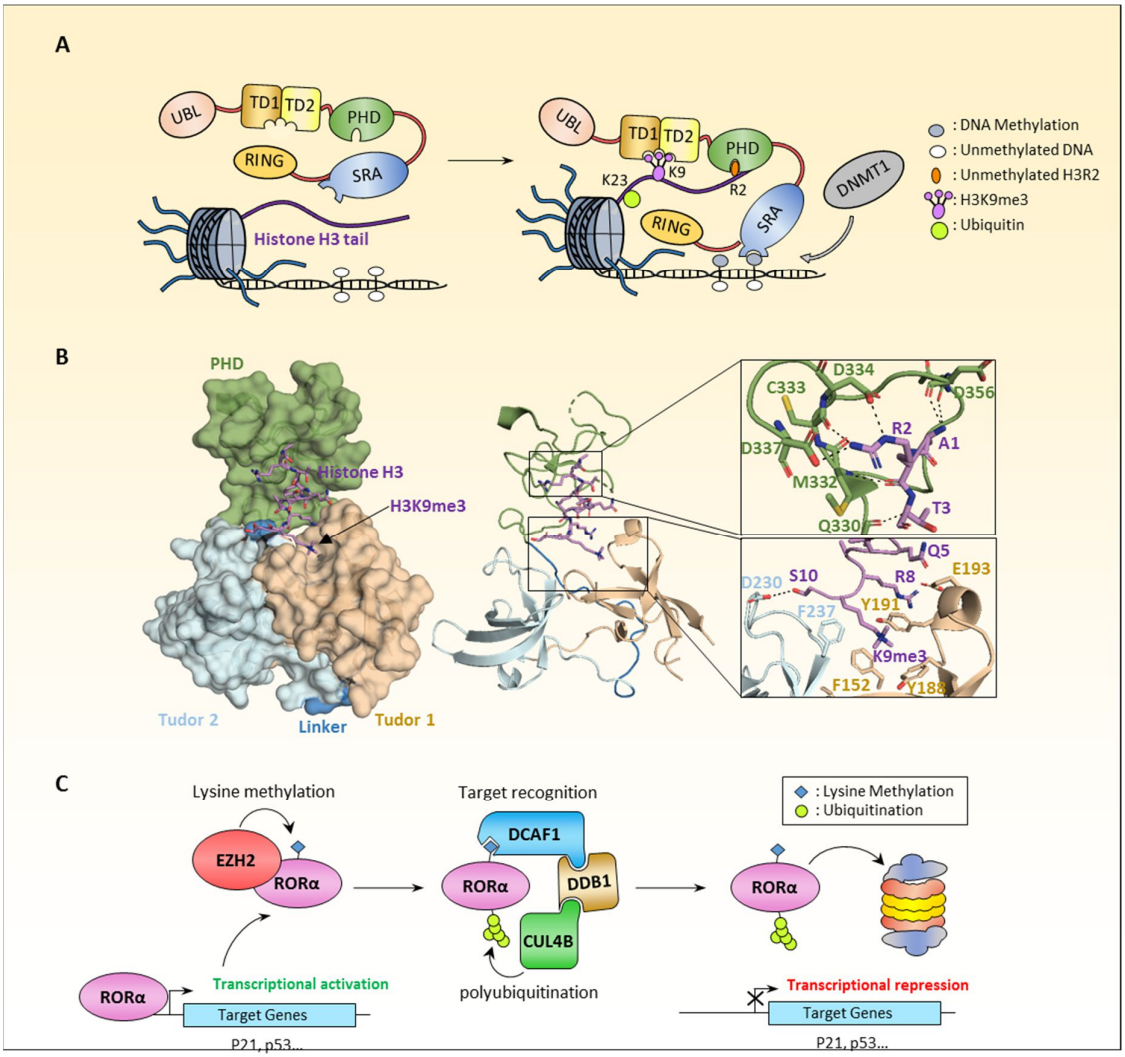

Figure 3 : Crosstalk between methylation and ubiquitination.

A) Bivalent recognition of unmethylated H3R2 and methylated H3K9 by the multidomain E3 ligase, UHRF1, leading to ubiquitination of H3K23. **B)** Surface representation of the crystal structure of the E3 ubiquitin ligase UHRF1 in complex with Histone H3 peptide (PDB: 3ASK). The Tudor domains and the PHD domain (TTD-PHD) used for the crystallization are shown in the left panel. Right panel, zoom in view of the interaction between Histone H3 peptide with the PHD domain (**top picture**) and the Tudor1/2 domains (bottom picture). The H3 peptide is composed by two cassettes. Cassette 1 encompassing H3R2, is positioned within the PHD acidic pocket. Cassette 2 containing H3 K9me3 is recognized by an "aromatic cage" surface within Tudor 1. The hydrogen bounds between amino acids are shown by the dash lines. The structure shows that the unmodified H3 R2 intercalates into an acidic pocket within the PHD finger domain where hydrogen bounds can be formed with the PHD C333, D334 and D337 side

chains residues. The Tudor domain 1 accommodated the H3 peptide C-terminus residues forming H3 K9me3 and S10. The H3 K9me3 fits into an "aromatic cage" surface formed by Tudor 1 F152, Y188 and Y191 while the H3 S10 form hydrogen bound with Tudor D230. **C)** Regulation of the RORα nuclear receptor by a methylation/ubiquitination crosstalk. RORα is subjected to monomethylation by the PRC2 methyl-transferase EZH2. This monomethylated RORα is bound by the chromo-domain of DCAF1 recruiting it to the DCAF1/DDB1/CUL4B ubiquitin ligase complex, resulting in proteasomal degradation of RORα and repression of its target genes.

The extensively studied tumor suppressor p53 is also subjected to regulation by methylation. The C-terminal domain of p53 is methylated by at least three different methyltransferases: SET8 (KMT5A), SMYD2 (KMT3C) and SET9 (KMT5) [142-144]. Depending on which residue of the C-terminal domain, p53 methylation could have different outcomes, including change in protein localization, stability and transcriptional activation (**Figure 4**). SET9 methylates K372 and promotes p53 stability and transcriptional activity [142]. p53 methylation on K370 by SMYD2 represses its activity, an event inhibited by K372 methylation [143]. Moreover, SET8 monomethylates p53 at K382, which also suppresses its transcriptional activity [144]. However, p53 methylation was found to be more complex, as several sites undergo dimethylation [145, 146]. Dimethylated p53 at K370 or K382 could be bound by the TUDOR domain of PHF20 which stabilizes and activates p53 through inhibition of MDM2-induced ubiquitination and degradation [147]. The tandem Tudor domains of 53BP1 also act as readers of K370me2 and K382me2 linking p53 methylation to its stabilization and transcriptional activation [145].

p53 is also subjected to active demethylation involving the lysine-specific demethylase LSD1 (KDM1A) which inhibits the transcriptional activity of p53 and its apoptosis promoting functions [145] (**Figure 4**). Mechanistically, LSD1 demethylates K370me2, and this inhibits p53 interaction with 53BP1. Additionally, lysine demethylation of p53 could take place in order to prevent a permanent stabilization of p53 by PHF20 [145]. This has not been proven until recently when p53 was shown to be actively demethylated then directed to ubiquitination and proteasomal degradation, unexpectedly by the SCF^{FBXO22}/KDM4A ubiquitin ligase/demethylase complex [148]. Mechanistically, p53 interacts with the FIST-N domain of FBXO22 protein, which also binds through its FIST-C domain to the lysine demethylase KDM4A, while binding the SCF complex via its F-box domain. This scaffold-like structure would position p53 between the catalytic domain of KDM4A and the RING domain of the SCF

complex. Interestingly, this configuration seems to target exclusively methylated p53, but not its acetylated form, while the demethylase activity of KDM4A seems to also be required for subsequent ubiquitination and degradation of p53 [148]. In addition, p53 interaction with PHF20 was enhanced after depletion of FBXO22 or with co-expression of an inactive form of KDM4A. According to these data, the SCF^{FBXO22}/KDM4A could simultaneously demethylate and ubiquitinate dimethylated p53 leading to its proteasomal degradation [148]. Moreover, acetylation of p53 C-terminal domain inhibits p53 interaction with FBXO22 suggesting an interplay between acetylation and methylation in coordinating p53 stability. This model of switch from methylation to ubiquitination on the C-terminal domain of p53 by the same protein complex could allow rapid regulation of p53 stability in response to stress. Nonetheless, validation of this model with structure studies is needed to reveal the spatial organization of such complex, especially when taking into account a previous study showing that the interaction between KDM4A and FBXO22 is mediated by the JmjN and JmjC catalytic domain of KDM4A which targets it for ubiquitination and degradation by SCF^{FBXO22} [149]. These studies raised interesting questions on how KDM4A demethylates p53 and interacts with FBXO22 through its catalytic domain and what determines whether the complex SCF^{FBXO22} targets either p53 or KDM4A for ubiquitination and degradation?

It is becoming increasingly appreciated that the crosstalk between methylation and ubiquitination can involve additional signaling pathways, adding other layers of complexity to this regulation. An interesting example of methylation-phosphorylation switch in regulating protein ubiquitination and stability is provided by the transcription factor SOX2, which plays an important role in maintaining embryonic stem cell (ESS) pluripotency [150]. SET7 methylates SOX2 on K119 and this results in the recruitment of the HECT domain containing E3 ligase, WWP2. This event triggers SOX2 polyubiquitination and proteasomal degradation. On the other hand, AKT1 phosphorylates SOX2 on a nearby residue of K119, T118, and this event blocks methylation and ubiquitination of this transcription factor. Interestingly, the HECT domain of WWP2 recognizes methylated K119 of SOX2, suggesting a mechanism by which SOX2 ubiquitination could be disrupted by phosphorylation. While structural studies should provide insights into how phosphorylation-inhibits methylation, this example illustrates the importance of crosstalk between multiples PTMs of SOX2 in directing stem cells toward stemness or differentiation.

Protein methylation could also promote non-degradative polyubiquitination, resulting in protein activation. A recent example of methylation promoting substrate ubiquitination and

activation was shown for AKT kinase which constitutes a major regulator of cell proliferation and its overactivation promotes cancer development [151]. The methyltransferase SETDB1 interacts with AKT and induces its di- or tri-methylation on K64 residue in response to IGF-1 or EGF signaling. This results in AKT T308 phosphorylation and recruitment at plasma membrane. Interestingly, methylation of AKT K64 creates a docking site for the lysine demethylase JMJD2A, which in turn promotes the recruitment of TRAF6 or SKP2 E3 ubiquitin ligases, catalyzing K63-linked ubiquitination of AKT and its activation. Here, an adapter function, rather than the catalytic activity of JMJD2A, appears to be required for AKT activation. While this study raises several questions on the exact mechanism of AKT activation, it also provided a new paradigm for potential therapeutic manipulation of this important oncogenic pathway.

Finally, while several studies focused on lysine methylation, increasing evidence indicates that arginine methylation could also interfere with ubiquitination events [152]. For instance, PRMT5-driven arginine methylation of the transcription factor KLF4 inhibits it ubiquitination and proteasomal degradation by the VHL/VBC ubiquitin ligase complex. This stabilizing effect contributes to the oncogenic function of KLF4 in breast cancer initiation and invasion [153]. It will be interesting to further investigate the molecular basis of this interplay and determine whether a similar mechanism regulate the function of other cellular factors.

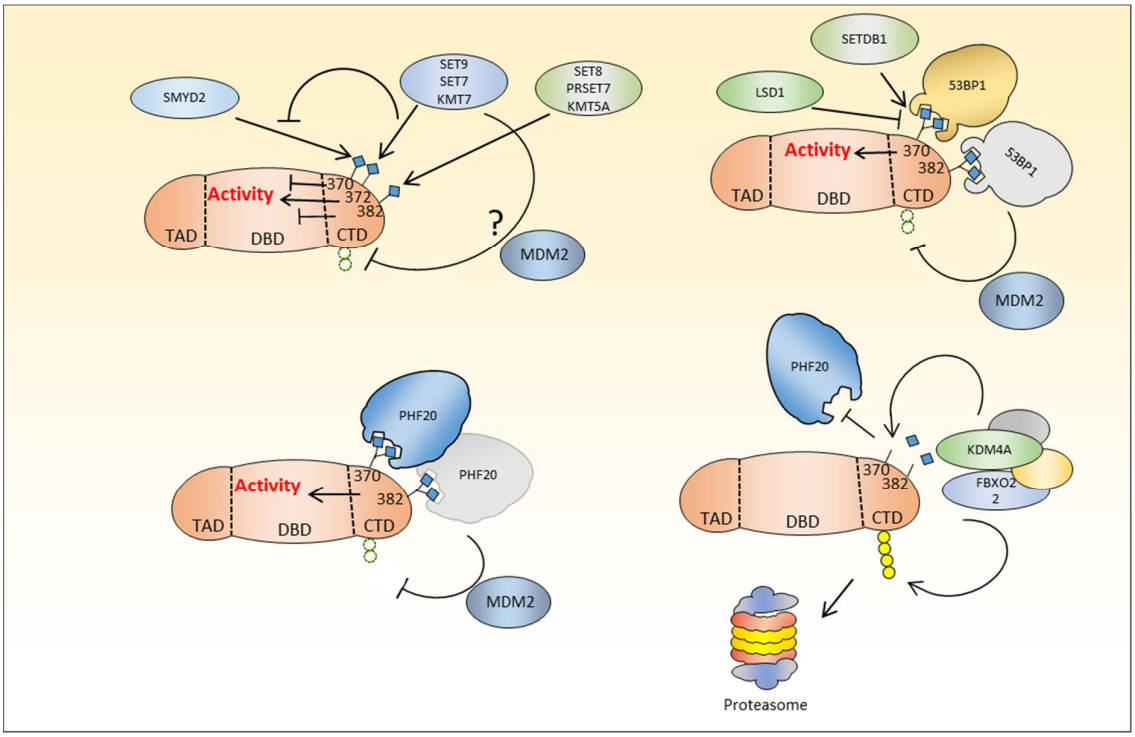

Figure 4 : Crosstalk between methylation and ubiquitination in regulating p53 stability and function.

The tumor suppressor p53 undergo mono or dimethylation on several sites at its C-terminal domain. Depending on the site and the extent of site methylation, p53 transcriptional activity or stability can be inhibited or promoted. These events are dynamically regulated by demethylation. Methyl-binding proteins such as PHF20 or 53BP1 associate with p53, inhibit its degradation and promote its transcriptional activity.

7. Impact of O-GlcNAcylation on protein ubiquitination

O-GlcNAcylation has recently emerged as an important player in the coordination of other PTMs including phosphorylation and ubiquitination [154]. This modification consists in the O-linked attachment of β-N-acetylglucosamine (O-GlcNAc) group on S or T residues of target proteins, and is catalyzed by the O-GlcNAc transferase (OGT) [154, 155]. The synthesis of UDP-GlcNAc, the donor of the O-GlcNAc group, involves the hexosamine biosynthesis pathway, a proposed metabolic sensor incorporating intermediates derived from glucose, glutamine, fatty acid and nucleotide metabolism [156, 157]. O-GlcNAcylation regulates the ubiquitination of numerous target proteins either directly or through the involvement of other PTMs such as phosphorylation. The O-GlcNAcylation of proteins generally results in a negative regulatory action on ubiquitination, thus leading to increased protein stability. For

example, p53 O-GlcNAcylation interferes with the p53/MDM2 interaction resulting in increased p53 protein stability [158]. In addition, p53 is phosphorylated on multiple residues, including S15, S20 and T18, and these events prevent p53 ubiquitination and its proteasomal degradation upon DNA damage [159-161]. However, inhibiting the O-GlcNAcylation of p53 does not affect its phosphorylation status on those sites suggesting the existence of other mechanisms by which p53 is stabilized [158]. Indeed, O-GlcNAcylation of p53 on S149 prevents the COP9 signalosome-specific phosphorylation of p53 on T155, an event known to label p53 for degradation [162] **(Figure 5A)**. Another interesting example of interplay between the O-GlcNAcylation and ubiquitination pertains to the two circadian clock proteins BMAL1 and CLOCK. The circadian clock system is a machinery that living cells use to synchronize their biological processes with the external environment, exhibiting 24 hours-long cycles [163]. Notably, the molecular circadian clock involves transcriptional and post-transcriptional control mechanisms as well as feedback loops that ensure proper synchrony of the rhythm [164]. Through dimerization, BMAL1 and CLOCK form a transcription activator complex inducing the expression of the Period genes (Per1, Per2) along with two Cryptochrome genes (Cry1 and Cry2) [164]. Both BMAL1 and CLOCK proteins are stabilized by O-GlcNAcylation which prevents proteasomal degradation [165] (**Figure 5B**). The crystal structure of the BMAL1/CLOCK complex suggests that the O-GlcNAcylation site on BMAL1 (S418) is less likely to be involved in the interaction with CLOCK since it is located far from the interaction interface between both proteins [166]. It is possible that O-GlcNAcylation site could be in close proximity to BMAL1 ubiquitination site(s). Indeed, BMAL1 K404 and K415 are ubiquitination sites and this might explain how O-GlcNAcylation prevents substrate ubiquitination [167]. Alternatively, O-GlcNAcylation sites might be located within an E3 ligase interacting motif and this can also dictate the outcome of subsequent ubiquitination. Interestingly, OGT acts along with the DUB BAP1 to stabilize the BMAL1/CLOCK complex in response to nutrient abundance [165]. This suggests that deubiquitination might be required for the O-GlcNAcylation of an adjacent site on BMAL1 or that O-GlcNAcylation occurs first and deubiquitination of adjacent lysine residue(s) is the consequence. While further studies are required to determine the exact molecular mechanism, these findings indicate that O-GlcNAcylation and ubiquitination could orchestrate an intricate signaling cascade that fine tune the functions of target proteins. At the physiological level, the impact of O-GlcNAcylation on the function of BMAL1/CLOCK complex provides a framework that can be further expanded to identify how this signaling axis regulates organ function in response to hormones and

environmental cues. It will also be interesting to determine how deregulation of cell metabolism impacts the circadian clock.

O-GlcNAcylation may also impact ubiquitination by competing over the same site of phosphorylation as shown for the zinc-finger protein Snail1. Snail1 is an epithelial to mesenchymal transition-promoting transcription factor repressing the cell adhesion junction factor E-cadherin [168, 169]. Snail1 is phosphorylated by glycogen synthase kinase-3β (GSK-3β) on two consensus motifs, creating a docking site for $SCF^{\beta\text{-}TRCP}$ E3 ubiquitin ligase and leading to the degradation of Snail1 [170]. Snail1 O-GlcNAcylation can also occur on S112 within the GSK-3β consensus motif [171]. This prevents Snail1 polyubiquitination and degradation under hyperglycemic conditions, inducing down-regulation of E-cadherin and promoting epithelial to mesenchymal transition [171]. These finding reveal a molecular switch from phosphorylation to O-GlcNAcylation, which inhibit the recruitment of an E3 ligase responsible for targeting Snail1 for polyubiquitination and subsequent downregulation.

O-GlcNAcylation could also promote protein polyubiquitination and degradation, in opposition to the established dogma of antagonism between these two PTMs [172]. Following DNA damage, the DNA-lesion-bypassing DNA polymerase η (Polη) is O-GlcNAcylated on T457 which induces its polyubiquitination by $CRL4^{CDT2}$ and subsequent extraction from chromatin by the p97 segregase [172]. This contributes to Polη dissociation from replication forks after the completion of TLS. Interestingly, cells expressing T457A mutant were more sensitive to DNA damage inducing agents such as cisplatin, suggesting that O-GlcNAcylation of Polη could be linked to drug resistance. However, it remains unclear whether OGT specifically triggers the O-GlcNAcylation of Polη at DNA lesions. It will also be interesting to determine how O-GlcNAcylated Polη is recognized by the $CRL4^{CDT2}$ and whether this event involves a potential O-GlcNAc receptor within $CRL4^{CDT2}$. Lastly, this also brings about the question of how cell metabolism-associated O-GlcNAcylation is linked to TLS-mediated DNA repair.

Finally, O-GlcNAcylation can also modulate ubiquitination in a degradation-independent manner. O-GlcNAcylation of S112 histone H2B promotes its monoubiquitination on K120, an event associated with transcriptional activation [173]. However, the molecular mechanism involved remains unknown and the occurrence of histone O-GlcNAcylation as has been recently disputed [174].

Overall, both O-GlcNAcylation and ubiquitination are important PTMs intimately involved in cellular processes. As these PTMs dynamically target a wide spectrum of substrates, it is anticipated that a significant interplay between the signaling pathways that deposit these PTMs take place in response to nutrient availability and microenvironment sates of the cells. A better understanding of these crosstalk will shed new light on normal and disease-associated mechanisms of action.

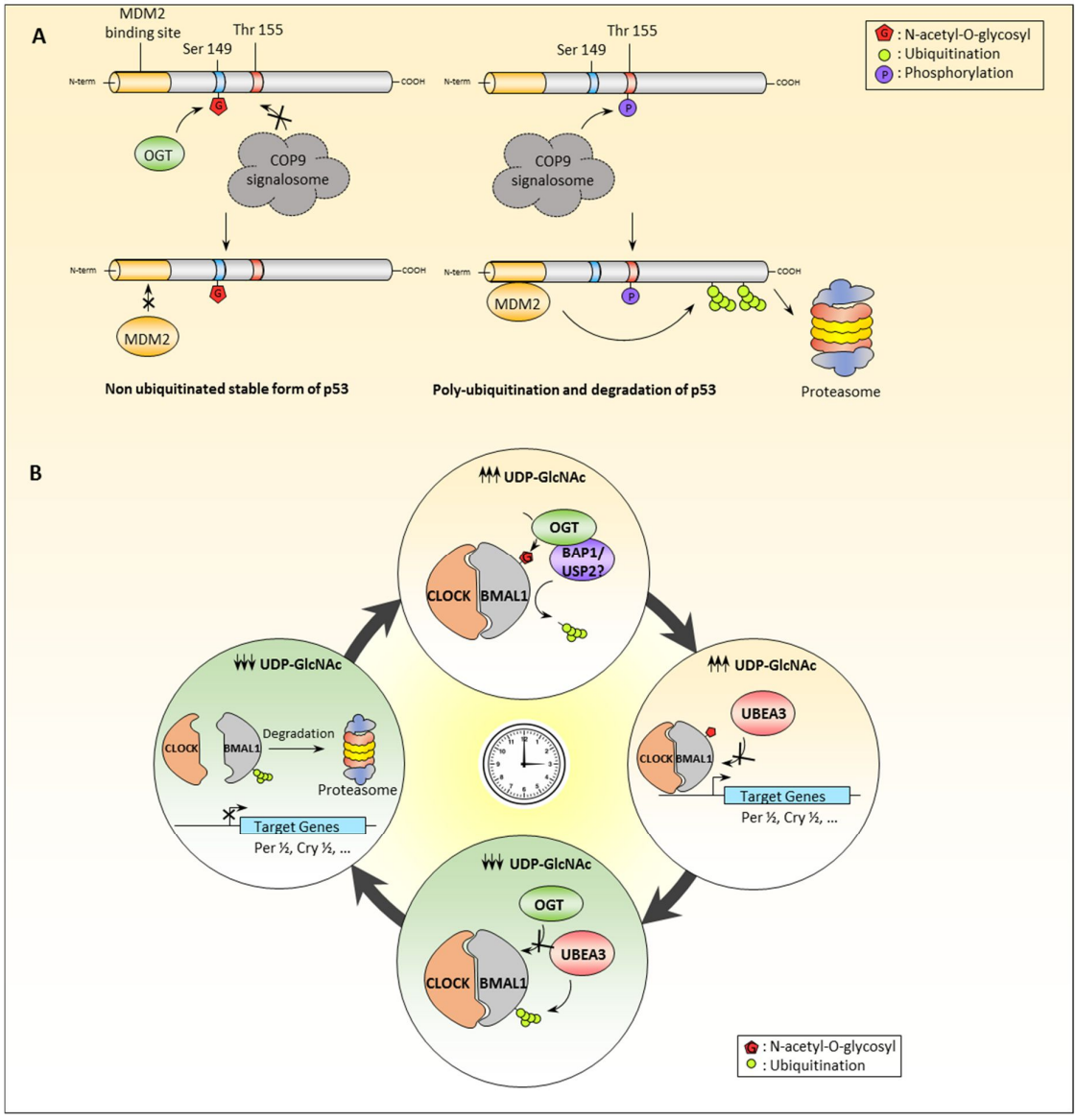

Figure 5 : Crosstalk between O-GlcNAcylation and ubiquitination.

A) Example of crosstalk between O-GlcNAcylation and ubiquitination regulating p53 stability. Phosphorylation of te Thr155 residue of p53 by the signalosome complex leads to MDM2 E3 ubiquitin ligase binding and polyubiquitination-inducing proteasomal degradation of p53. This

cascade is blocked by the O-GlcNAcylation of an adjacent Ser149 residue by OGT, inducing stabilization of p53. **B)** Example of crosstalk between O-GlcNAcylation and ubiquitination regulating the circadian cycle. The CLOCK/BMAL1 complex ensures the transcription of critical genes in the circadian rhythm in a cyclic manner. Depending on the availability of the metabolism-associated O-GlcNAc group donor, UDP-GlcNAc, BMAL1 could be O-GlcNAcylated which is suggested to prevent its polyubiquitination by UBEA3 ligase and enhancing the activity/recruitment of deubiquitinases such as BAP1/USP2, thus stabilizing the CLOCK/BMAL1 complex. Low presence of UDP-GlcNAc during slow metabolism phase of the circadian cycle induces a reduced BMAL1 O-GlcNAcylation leading to its polyubiquitination and proteasomal degradation and thus repression of the CLOCK/BMAL1 complex target genes.

8. N-linked glycan signals for ubiquitination-mediated degradation

Several protein quality control mechanisms have evolved to ensure that proteins are correctly folded before reaching their final destination or otherwise degraded by the proteasome, thus avoiding undesirable protein interactions that can lead to protein aggregation and human disease. For instance, in the endoplasmic reticulum, inadequately folded proteins are recognized and eliminated by the ERAD (Endoplasmic Reticulum-Associated Degradation) system [175-178]. It was initially revealed that the ubiquitin-proteasome system is indeed a critical component of the ERAD process [179-183]. Processing misfolded proteins involve three essential steps: (i) the recognition of target protein through a specific signal which is usually a PTM, (ii) the recruitment of the protein to the ER-membrane embedded E3 ligase complex, and (iii) the ubiquitination and export of the protein through the ER membrane to the proteasome by a process called retrotranslocation. Depending on the location of the misfolded protein (inside the ER lumen, inside the ER membrane or at the cytoplasmic side of the ER membrane), the target protein are differently processed by either ERAD-L (luminal), ERAD-M (membranellar) or ERAD-C (cytoplasmic) pathways respectively [184, 185]. The ERAD-C pathway requires the E3 ubiquitin ligase DoA10 to polyubiquitinate its substrates. On the other hand, the E3 ubiquitin ligase Hrd1p is required for both ERAD-L and ERAD-M pathways [184, 186]. However, Doa10 has been recently shown to be required for the degradation of transmembrane proteins, suggesting that it could be required for both ERAD-C and ERAD-M [187]. A key step for all ERAD pathways is the recognition of the defective target protein among all the protein species in the ER. While the exact mechanisms are still not fully

established, N-linked glycosylation plays an important role in targeting proteins to ERAD [176].

When entering the ER, proteins are enzymatically modified *en bloc* on an asparagine residue by a branched oligosaccharide composed by three glucose, nine mannose and two N-acetylglucosamine residues ($GlcNAc_2Man_9Glc_3$) [188]. These glycan groups are trimmed during the protein journey inside the ER until its export as a fully folded protein. However, if the protein is delayed inside the ER due to a folding issue, a late glycan processing enzyme such as the mannosidase Htm1 (EDEM in mammals) will generate an oligosaccharide that directs the improperly folded substrate for ubiquitination and proteasomal degradation [189]. Since the Htm1 enzymatic activity is relatively slower than other glycan processing enzymes and that its output product ($Man_7GlcNAc_2$ with an exposed α1,6-linked mannosyl residue) is essential for ERAD pathway, it has been proposed that the ERAD machinery should have a "reader" for this modification [189, 190]. For instance, Yos9 (OS-9 in mammals) has been identified as a lectin capable of binding glycan products generated by Htm1 [191, 192]. However, the binding of Yos9 to the α1,6-linked mannose is not sufficient to induce the degradation of the target protein. In order to do so, Yos9 must bind a glycan attached to the unstructured region of the target protein which should be bound also by Hrd3 (component of the Hrd1 complex) [193, 194] (**Figure 6A**). Other mechanisms have also been proposed for the Htm1 glycan-processing enzyme since its activity represents the trigger for downstream degradation of the target protein. The association of the yeast protein Htm1p into a Htm1p-Pdi1p complex selectively guides Htm1p activity towards misfolded N-glycoprotein targets due to the Pdip1 adapter function [195, 196]. This dual action of Htm1p-Pdi1p on one hand and Yos9 on the other hand adds another layer of control to the ERAD pathway to carefully select the misfolded targets. After the recognition and binding steps by Yos9, the target protein is polyubiquitinated by Hrd1 and dragged through the ER membrane to be retrotranslocated to the cytoplasm where it is recognized by the Cdc48/p97 ATPase complex [197]. The Cdc48/p97 complex binds the polyubiquitin chains, added by Hrd1 on the target protein in the cytoplasmic side of the ER, and pulls it off, so it could be processed by the proteasome [198, 199] (**Figure 6A)**. This example of target protein selection for polyubiquitination and proteasomal degradation shows how tight is the control for protein fate decision by adapting a multi-step mechanism, which is highly conserved through evolution.

Signaling protein degradation by N-linked glycan ligation can also occur in the cytoplasm in ERAD-dependent or -independent manner [200]. An F-box E3 ubiquitin ligase

subfamily has been identified for its ability to recognize N-glycan [201-203]. For instance, SCF^{Fbs1} ubiquitin ligase complex that contains Fbs1/Fbx2/NFB42 was identified as an E3 ligase that recognizes N-linked glycoproteins through a sugar-binding domain (SBD) [200, 203]. To reveal the mechanism of ubiquitination of N-glycoproteins by the SCF^{Fbs1} complex, the crystal structures of Skp1 in complex with Fbs1 as well as SBD with Ribonuclease B (RNase B) have been solved [204, 205] RNase B was used as glycoprotein for the co-structure as it has a single oligosaccharide ($Man_{6-8}GlcNAc_2$) linked to its N34 residue. The SBD-sugar binding surface is composed by nine residues that makes hydrogen and/or van der Waals bounds with $Man_3GlcNAc_2$. GlcNAc 1 is positioned within a hydrophobic pocket formed by SBD F117, Y279 and K281. GlcNAc 2 also make hydrogen bound with K281 and W280. Man 1 and Man 2 contacts Fbs1 through hydrogen bounds with D216 and N159 side chains, respectively. The overall SCF^{Fbs1}-RNase B-E2 complex model (**Figure 6B),** indicates that RNase B is positioned in a distance that is accessible for ubiquitination by E2 (UBCH7). In addition, a linker loop between the F box and SBD domains of Fbs1 would endow SCF^{Fbs1} with a certain rotational flexibility to accommodate diverse substrates.

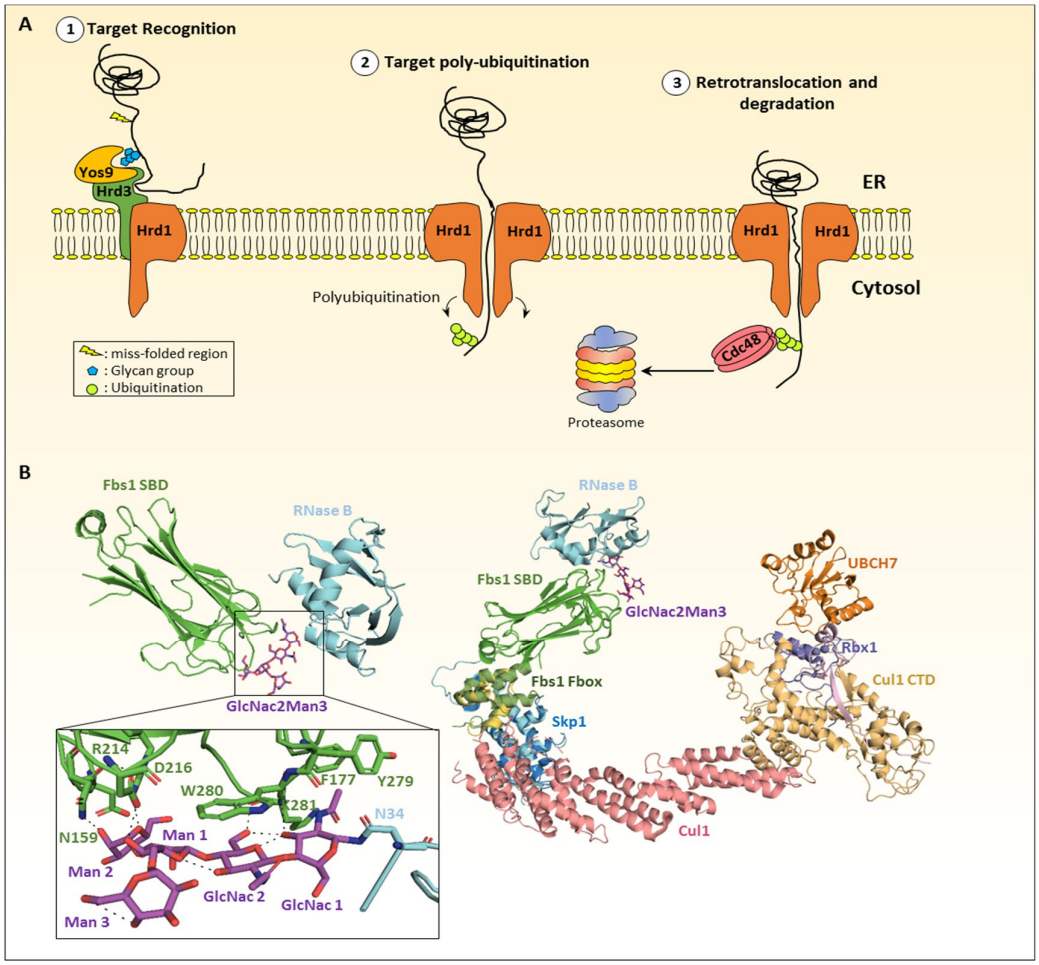

Figure 6 : N-linked glycan signals for ubiquitination-mediated degradation.

A) The ERAD-L pathway regulation by oligosaccharide/ubiquitination interplay in S. cerevisiae. The unprocessed glycan groups on misfolded proteins in the lumen of the Endoplasmic Reticulum (ER) are recognized by the Yos9 protein which triggers the misfolded protein recruitment to the Hrd3/Hrd1 complex within ER membrane. The Hrd1 ubiquitin ligase is then triggered for dimerization forming a transmembrane channel to facilitate the pass-through of misfolded polypeptide and its ubiquitination by Hrd1 cytoplasmic RING domain. The last step is the engagement of the cytoplasmic Cdc48/p97 ATPase complex which drags the polyubiquitinated polypeptide to the proteasome for degradation. **B)** N-linked glycoproteins recognition by the F-box E3ligase complex. Structural overview of the Fbs1 SBD in complex with modified RNase B (top left panel) (PDB: 2E33). Close up view of the RNase B Man3GlcNAc2 moiety binding with the SBD domain (bottom left panel). Structural model of the SCF^{Fbs1} ubiquitin ligase complex bound to modified RNase and the E2, UBCH7 (right panel). The model was generated by superimposing the current crystal structure of the

SBD/RNase B with Skp1/Cul1/Rbx1 (PDB: 1LDK) and c-Cbl-UBCH7 (PDB: 1FBV) structures. The hydrogen bounds between amino acids are shown by the dash lines.

9. Protein PARylation and crosstalk with ubiquitination

Since its discovery during the early 1960s, ADP-ribosylation has emerged as an interesting PTM adding another dimension of complexity to the regulation of multiple cellular processes including transcription, DNA repair and apoptosis [206-209]. ADP-ribosylation is a reaction conducted by any enzyme of the 18 family members called PARPs (Poly-ADP-Ribose Polymerases). Having a Nicotinamide Adenine Dinucleotide (NAD^+)-dependent catalytic activity, PARPs add one or multiple negatively-charged ADP-ribose molecules (PAR) on target proteins, allowing the regulation of their functions [209-212]. One of the most studied members of the PARP family is PARP1, which coordinates transcription and DNA repair through chromatin regulation [209, 212-214].

The majority of studies investigating the biological function(s) of poly-ADP-ribosylation (PARylation) were conducted in the context of DNA damage response (DDR) since PARylation by PARP1 is known to be among the first signals of DDR [215]. As most PTMs, PARylation has multiple specific binding motifs called readers of PAR [216]. At least three major groups of PAR-binding domains were described including the PAR-binding macrodomain, PAR-binding zinc finger (PBZ) and most recently the WWE domain linking PARylation to ubiquitin signaling [216-220]. The basis of the interplay between PARylation and other PTMs is based on the recognition of PAR by "reader" proteins, which, in turn, catalyze the attachment of other PTMs on the targeted substrate. Many of these reader proteins (or associated complexes) have been reported to include an E3 ubiquitin ligase domain such as RNF146, BAL1/BBAP complex, BARD1/BRCA1 complex and Checkpoint with forkhead-associated and RING domains, CHFR [218, 220-223], suggesting an extensive interplay between PARylation and ubiquitination.

One notable example of PARylation/ubiquitination crosstalk which relies on the WWE domain used for recognition and binding of the E3 ubiquitin ligase RNF146 (*Iduna*) to PAR. RNF146 has been shown to promote PAR-dependent ubiquitination of many DDR and chromatin-associated proteins, such as KU70, XRCC1, DNA-ligase III and interestingly PARP1 and PARP2 themselves [221]. A hint on the mechanism by which PARylation promotes ubiquitination has been revealed by recent studies reporting interaction of RNF146 with PARylated target proteins of the Wnt signaling pathway [224, 225]. In the absence of the Wnt-

ligand, β-catenin is driven to degradation through its assembly in a specific proteolysis-inducing complex [226]. In the presence of Wnt-ligand, β-catenin is released from its degradation complex and translocated into the nucleus to transduce the Wnt signaling. The β-catenin destruction complex is formed by multiple subunits including axin which is a concentration limiting factor essential for complex assembly [226, 227]. To avoid sustained activation of β-catenin, stabilization of axin protein is ensured through inhibition of the Tankyrases PARPs (TNKS1 and TNKS2 a.k.a. PARP5A and PARP5B, respectively) responsible of axin PARylation and degradation [224]. RNF146 is the E3 ubiquitin ligase responsible of axin polyubiquitination and degradation upon PARylation by TNKS1/TNKS2 [228]. Interestingly, RNF146 interacts with both the Tankyrase and the PARylated target protein through its WWE domain. The crystal structures of RNF146/UbcH5a (E2 conjugating enzyme) and RNF146/TNKS in the presence of PAR suggest an interesting multi-step activation mechanism by which RNF146 ubiquitinates PARylated substrates in the presence of TNKS and UbcH5a [225] (**Figure 7**). The first step is the PARylation of the target substrate followed by RNF146 binding the TNKS's five *Ankyrin Repeat Clusters* (ARCs) domain by its C-terminal domain exposing the PAR chain to the RING/WWE domains of the E3 ligase. Next, the PAR chain is immobilized by the WWE domain and the proximal RING domain, and this new conformation induces an allosteric change in the structure of the E3 catalytic domain resulting in enhanced ubiquitin ligase activity [225]. This mode of regulation increases specificity and would avoid any promiscuous degradation of PARylated proteins. On the other hand, the cell cycle checkpoint protein CHFR, has been reported to use PBZ motif to bind PARylated proteins [218, 229]. The mechanism of PBZ recognition of PAR is different from RNF168, as two ADP-ribose molecules can be accommodated within the binding site used by CHFR. Interestingly, CHFR also targets auto-PARylated PARP1 for ubiquitination, which is thought to be a mechanism for that limits its continuous activation during the mitotic checkpoint [230, 231]. It would be interesting to further investigate how PARylation-mediated ubiquitination impacts DNA damage signaling and repair processes, particularly when fast kinetics of protein recruitment and dissociation are needed to execute chromatin-based processes.

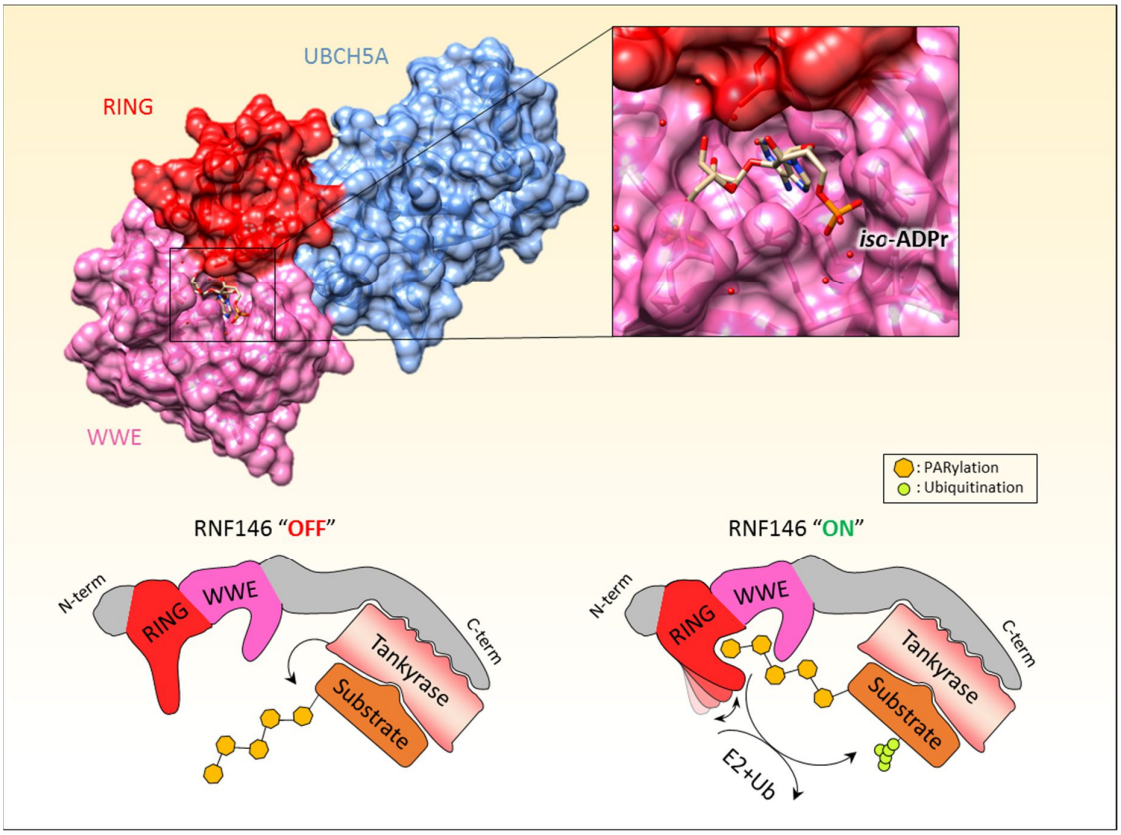

Figure 7 : The mechanism of PARylation-triggered ubiquitination.

(Top) The crystal structure of RNF146 WWE/RING domains associated with the UBCH5A E2 conjugating enzyme showing a binding pocket for *iso*-ADPr within the ((RING-WWE) domains) WWE domain and with additional contact with the RING domain (PDB: 4QPL). (Bottom) PARylation of a target protein by the Tankyrase enzymes interacting with RNF146 is bound by the WWE domain of the latter. This binding triggers an allosteric conformational change within the RING domain of RNF146 switching its E3 ubiquitin ligase activity from an "OFF" to an "ON" state, leading to efficient recruitment of E2 ubiquitinating enzyme and ubiquitination of the PARylated target protein.

10. Protein hydroxylation-associated ubiquitination

Protein hydroxylation on proline residues was observed several decades ago and initially linked to the maturation of secreted proteins such as collagen [232, 233], but since the discovery of the link between protein stability and hydroxylation states, studies on this PTM significantly shifted toward cell signaling processes [234-236]. An eminent example is provided by the hydroxylation-mediated degradation of the hypoxia-inducible factor (HIF1α) transcription factor. HIF1α is normally activated under hypoxia stress conditions, which lead to the activation

of hypoxia-inducible genes. However, under normal physiological conditions, HIF-1α is targeted to ubiquitination by the von Hippel-Lindau ubiquitin E3 ligase complex (pVHL). pVHL acts in a multi-subunit protein complex called VCB including Cul2, Elongin B, Elongin C and Rbx1 [237, 238]. The protein responsible of HIF-1α hydroxylation was originally identified as HIF-1α prolyl-hydroxylase (HIF-PH) but further investigations have shown that this factor corresponds to the *Egg Laying defective Nine* family proteins (EGLN) also known as prolyl-hydroxylase-domain proteins (PHDs) [234, 239, 240]. The hydroxylation of HIF-1α on its conserved proline res dues (P402 or P564) creates binding site for pVHL **(Figure 8A)** [234]. The molecular basis of pVHL-HIF1α-interaction was rapidly established, and it was revealed that pVHL forms a conserved hydroxyproline binding pocket involving well-arranged hydrogen bonds for selective binding of hydroxylated prolyl residues of HIF1α [237] **(Figure 8B)**. Indeed, the HIF1α N-terminal segment containing P564 inserted into a hydrophobic core region within the β domain of pVHL where van der walls contacts are made between HIF1α P564 and pVHL W88, Y98 and W117. The hydroxylated P564 inserts even further by forming hydrogen bounds with pVHL H115 and S111. The binding of pVHL is highly specific to hydroxylated prolines on HIF-1α as a non-hydroxylated peptide couldn't form a stable complex with pVHL indicating the tight regulation of HIF-1α degradation by hydroxylation. Additional interaction specificity is provided through hydrogen bounds involving multiple HIF1α backbone residues and pVHL side-chain groups. These interactions limits HIF1α backbone flexibility allowing tighter binding between pVHL and hydroxylated HIF1α. pVHL cancer mutations occurring in the binding interface with the hydroxylated proline peptide of HIF-1α have been reported, further supporting the involvement of pVHL in regulating HIF-1α function [238].

The regulation of HIF-1α stability by hydroxylation appears to be more complex *in vivo*. For instance, HIF-1α prolyl-hydroxylation by the PHDs could be assisted by third party proteins such as the Osteosarcoma Amplified 9 (OS-9) protein which binds HIF-1α and PHD2 or PHD3 and is required for HIF-1α hydroxylation and degradation [241]. Regulation of HIF-1α stability also involve SUMOylation which interfere with its degradation [242]. During hypoxia, active deSUMOylation of HIF-1α by SENP1 occurs independently of proline hydroxylation and leads to HIF-1α stabilization, suggesting a cooperation between SUMOylation and hydroxylation in promoting ubiquitination and degradation of HIF-1α by pVHL [242]. However, it was proposed that pVHL targets SUMOylated HIF-1α in a hydroxylation-independent manner, suggesting additional mechanisms of interaction between pVHL and HIF-1α. Another layer of complexity

is provided by SIRT2, a NAD(+)-dependent protein deacetylase, which destabilizes HIF-1α under hypoxia conditions by removing the acetyl group from K709 residue of HIF-1α. The deacetylation of HIF-1α promotes the binding of PHD2 and prolyl-hydroxylation with the subsequent ubiquitination of HIF-1α [243]. Interestingly, HIF-2α, a paralogue of HIF-1α with almost 50% of shared amino acid composition, is also a transcription factor that might have overlapping and distinct sets of target genes [244]. HIF-2α is also regulated through hydroxylation and SUMOylation with related mechanisms [244, 245]. However, the E3 ubiquitin ligase RNF4 is responsible for targeting SUMOylated HIF-2α for proteasomal degradation underlining the complexity of signaling networks that converge on HIF-1α and HIF-2α [245].

Even though HIF-α proteins were the first studied cases of linkage between proline hydroxylation to ubiquitin-mediated proteasomal degradation, other proteins seems to be modulated via similar mechanisms. The prolyl-4-hydroxylase PHD1 hydroxylates a proline residue on the centrosomal protein Cep192 allowing recognition and ubiquitination by the SCF^{Skp2} Complex (through binding of the F box protein Skp2 to hydroxylated Cep192) and downstream proteasomal degradation [246]. Cep192 was shown to be crucial for centrosomal processes including proper centriole duplication and centrosome maturation during interphase. Thus, Cep192 hydroxylation provides a direct link between oxygen sensing and cell cycle progression, through modulation of its protein levels. Despite hydroxylation by PHD1, Cep192 is not ubiquitinated through pVHL like HIF-1α suggesting a diversity of mechanisms in hydroxylation-induced ubiquitination.

In conclusion, the target list of proteins harboring proline hydroxylation is likely larger than anticipated, and recent proteomics studies suggest that oxygen sensing could potentially be a major determinant in the regulation of many cellular proteins [247]. However, very few ubiquitin ligase complexes have been associated to proline hydroxylation degrons such as VHL and SCF^{Skp2}. It would be interesting to investigate potential roles of other E3 ligase complexes and determine whether an “universal” reader for protein hydroxylation exists. Moreover, protein hydroxylation can regulate protein stability by interfering with the deubiquitination reaction. For instance, hydroxylation of the transcription factor FOXO3a promotes its accumulation by inhibiting interaction with the DUB USP9X [248], highlighting the complexity of crosstalks between these two PTMs.

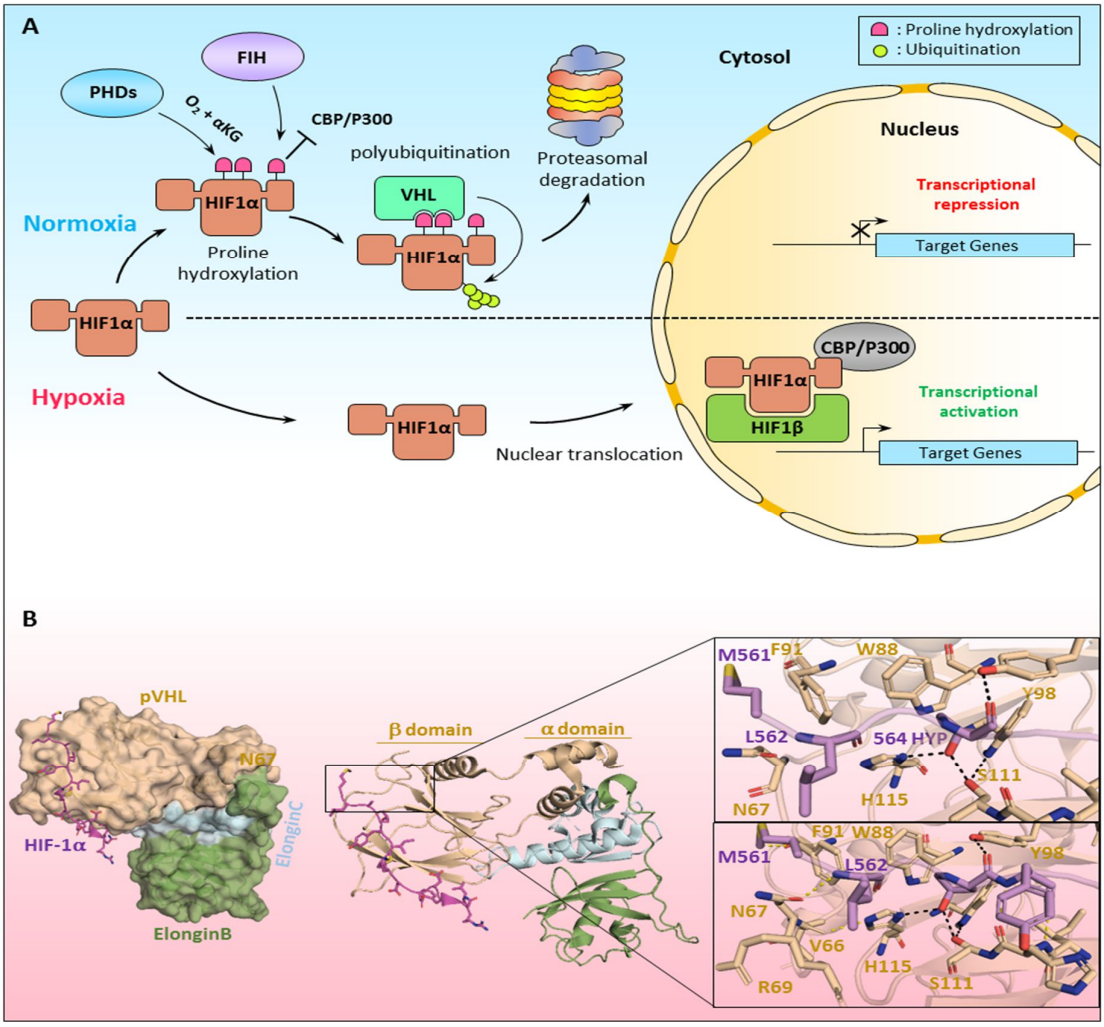

Figure 8 : Oxygen-sensing dependent ubiquitination regulating the function of the hypoxia-induced factor-1 (HIF1α).

A) During hypoxia conditions, the HIF1α factor is translocated to the nucleus where it dimerizes with HIF1β and activates the transcription of hypoxia induced response genes in presence of CBP/P300. However, during normal conditions (normoxia) and in presence of αKG, HIF1α is rapidly targeted by different proline hydroxylating enzymes such as the prolyl-hydroxylase-domain proteins (PHDs) and the factor inhibitor HIF (FIH). While hydroxylation by FIH on the c-terminal end of HIF1α block its interaction with CBP/P300 and thus downstream transcriptional repression, hydroxylation by the PHD enzymes generate a binding site for the von-Hippel-Lindau (VHL) ubiquitin ligase complex. This induces polyubiquitination and proteasomal degradation of HIF1α. **B)** Structural description of the recognition of hydroxylated HIF1α (HYP 564) by pVHL E3 ligase complex (PDB: 1LM8). Left panel, surface representation of the pVHL/ElonginB/ElonginC/HIF1α co-structure showing the binding of

HIF1α peptide with pVHL subunit. Right panel, zoom in of the HIF1α/pVHL β domain. HYP 564 inserts into a β domain hydrophobic core region (top view). Additional contacts are made between HIF1α backbone residues and pVHL side chain group (bottom view). The hydrogen bounds between amino acids are shown by the dash lines.

11. N-end rule and C-end rule pathways of protein degradation

In addition to classical PTMs, other unconventional modifications have been known for several decades as associated with proteolysis. One category of these PTMs is the conjugation of specific amino acids, such as arginine (Arg), at the N-terminal end of proteins, which was initially found to have a destabilizing effect on modified proteins [249]. It was later found that protein Nt-arginylation defines a distinct class of protein modification-inducing degradation, which is part of a general mechanism of protein degradation termed the N-end rule pathway [250-256]. The N-end rule pathway relies on the recognition of a destabilizing amino acid by specific E3 ubiquitin ligases, called N-recognins, which ubiquitinate the target protein (or nascent peptide in the case of co-translational modification) leading to the proteasomal degradation in most cases [254, 255]. In eukaryotes, three major N-end rule pathway branches have been described including Nt-arginylation, Nt-acetylation and the most recently discovered ubiquitination-associated with Nt-Proline [252-257]. Nt-arginylation is known to occur on destabilizing N-terminal Asp, Glu residues and oxidized Cys residues which fall into a Type 1 class of Nt-degron along with unmodified Arg, His and Lys residues. The second class includes the hydrophobic amino acids Ile and Leu and the aromatic amino acids such as Phe, Trp and Tyr [255]. The Type 1 and Type 2 Nt-degrons are known to be bound by the UBR-box domain of the N-recognins E3 ligase family members, which are responsible for substrate ubiquitination and proteolysis [258, 259]. The Nt-arginylation on Asp, Glu and oxidized-Cys residues is promoted by a unique enzyme called the arginyltransferase ATE1 which catalyzes the transfer of the arginine residue from arginyl-tRNA to acceptor amino acid residue on target proteins in an ATP-independent manner [260, 261]. While the exact function of the N-end rule pathway remains only partially elucidated, it was recently proposed that, depending on the availability of the end-point degradation system, Nt-arginylated cleavage fragments could be either degraded by the UPS system or autophagy [262]. Indeed, Nt-arginylated substrates could be bound by the ZZ-type zinc finger (ZZ domain) of the p62 autophagy adaptor and this event can induce autophagy of target proteins [263-266]. Structural analysis revealed the ability of the ZZ domain to use a mechanism of recognition, different from classic N-recognins, to bind both

type 1 and type 2 Nt-degrons [265, 266]. ZZ domain binding to Nt-degrons is strongly enhanced by the oligomerization of p62 in a pH-dependent manner which concurs with the mechanism by which this factor promotes autophagy of cellular targets [265]. It will be interesting to define the signaling pathways associated with changes in cellular contexts including metabolic states and stress conditions that can shift the degradation of Nt-arginylated proteins towards the UPS or autophagy.

The other major and frequent branch of N-end rule pathway is Nt-acetylation (either on Nt-Met or second residue after Nt-Met removal) [255, 256]. Nt-acetylation is carried by several Nt-acetyltransferases including NatA, NatB, NatC, NatD, NatE and NatF classified according to their target specificity even though some of them could overlap in function and targets [267, 268]. In yeast, Nt-acetylation has been linked to proteasomal degradation of several target proteins such as the APC/C complex component Hcn1 and the Conserved Oligomeric Golgi subunit Cog1 [253, 269]. Interestingly, it has been proposed that the degradation-promoting function of Nt-acetylation could be blocked by other interacting proteins or quick proper folding of the target protein in order to prevent the recognition of Nt-acetylated residue by Nt-recognins [269]. Indeed, in mammals, the same mechanism of what is now known as "conditional degrons" has been described for the protein G regulator, RGS2 which is targeted for Nt-acetylation and ubiquitination by TEB4 ER-associated ubiquitin ligase for subsequent degradation. This results in increased $G\alpha_q$ protein activation leading, in turn, to increased PLCβ and ERK1/2 signaling. In contrast, RGS2 is stabilized through interaction with $G\alpha_q$, establishing a regulatory loop for protein G signaling [270]. Whether additional factors could shift RSG2 between the free and assembled forms, thus regulating the extent of Gαq signaling, remains an interesting line of inquiry. Of note, Nt-acetylation has also been reported to direct protein interactions with the immediate effect of stimulating protein function rather than degradation [271-275]. For instance, Nt-acetylation of the E2-ubiquitin conjugating Ubc12 directs its interaction with a hydrophobic pocket of Dcn1 E3-ligase which promote, along with the Rbx RING E3, Neddylation of Cullin 1 [271]. These findings altogether indicate an intricate relationship between Nt-acetylation and protein homeostasis and suggest that N-terminal acetylation might be an important platform of regulation more prevalent than previously appreciated. Consistent with this assumption, it has been proposed that Nt-acetylation could serve as metabolic sensing mechanism that links acetyl-CoA availability and metabolic state of the cells to signaling events [276]. Clearly, the extent by which N-terminal acetylation might

dynamically regulate multi-protein complex assembly, stoichiometry and function would remain an area of active investigation.

Underlining the importance of protein termini in protein quality control, an additional mechanism of proteolysis involving C-terminal degrons was recently discovered [277, 278]. Similar to N-terminal degron of the N-end rule pathway, the C-end rule pathway (also termed DesCEND) is based on the recognition of specific amino acids, notably Gly residue at the C-terminal end of target proteins [277, 278]. While part of the N-end rule pathway relies on PTMs to promote ubiquitination of the target protein, the C-end rule pathway seems to only require recognition of specific "codes" of C-terminal amino acids within the last few residues within the target protein [277, 278]. For instance, the degrons might be generated following limited proteolysis of substrates. The Cullin-RING E3 ubiquitin ligase complexes seem to be the main drivers of the C-end rule pathway with specifically CRL2 and CRL4 directed-ubiquitination using interchangeable substrate recognition modules [277, 278]. Protein stability assay screens using a peptide library representing the human proteome revealed the degron specificity for each of Cullin E3-adapter proteins [277, 278]. For example, CRL2 substrate recognition adaptors KLHDC2, KLHDC3, and KLHDC10 require a Gly residue at the end of the protein, however, FEM1A, FEM1B, and FEM1C target C-terminal Arg residue [277, 278]. APPBP2 adapter protein targets proteins ending with an RxxG motifs for ubiquitination by CRL2, while DCAF12 and TRPC4AP adaptors recognize EE-endings and Arg at -3 position respectively for CRL4 ubiquitination [277, 278]. There are also additional degron signals as part of the C-end rule pathway targeting Ala containing C-termini probably involving non-CRL E3 ligases [278]. Moreover, the authors made an interesting observation following an analysis of the C-termini composition of proteomes for multiple eukaryotic species showing that Gly is less likely to be coded at this position [278]. This led to the hypothesis of avoidance of Gly residue at the C-terminal end to globally protect the gene products from ubiquitination [278]. Despite being at its early stages, the C-end rule pathway provides a novel paradigm of regulation of protein homeostasis that might be deeply involved in coordinating the function of the proteome. Clearly more studies are required to shed light on the mechanisms of this pathway and the upstream signaling that regulate substrate recognition including the coordination with limited proteolysis and the involvement of other PTMs.

12. Interplay between S-nitrosylation and ubiquitination

S-nitrosylation is another abundant PTM consisting of covalently linking a nitric oxide group (a.k.a. nitroso group or NO) to cysteine residues on target proteins resulting in the formation of S-nitrosothiols (SNOs) [229]. Recent studies indicated that a significant proportion of the human proteome, with more than 2,000 sites, is modified by S-nitrosylation under normal conditions [279]. The enzymatic catalysis of S-nitrosylation remains largely elusive, although recent evidence indicated that the *E. Coli* hybrid cluster protein Hcp catalyzes protein S-nitrosylation [280]. This reaction can also be promoted by enzymes including superoxide dismutase (SOD) and GSNO-reductase [281]. Recently, it was found that an inducible heterotrimeric complex containing inducible NOS (iNOS), S100A8 and S100A9 factors is responsible for a transnitrosylase activity that ensure site specific S-nitrosylation of target proteins [282]. The S100A8 and S100A9 proteins play an important role in complex assembly and in directing and coordinating the transfer of NO from iNOS to specific substrates that possess the I/L-X-C-X2-D/E motif. Since most UPS enzymes involve a cysteine in their catalytic sites, a cross talk between ubiquitination and S-nitrosylation seems to be eminent. Indeed, multiple components of the UPS are regulated by S-nitrosylation [283-286]. Several studies revealed that S-nitrosylation promote substrate ubiquitination and degradation [287-291]. For instance, initial observations indicated that S-nitrosylation of iron regulatory protein 2 (IRP2), which binds iron-responsive elements found in mRNAs, induces its ubiquitination and proteasomal degradation [287]. Loss or depletion of the tumor suppressor PARK2 induces mitochondria-associated metabolic defects leading to S-nitrosylation and subsequent ubiquitination of PTEN, leading in turn to activation of the Akt pathway and cellular proliferation [288]. In this setting, S-nitrosylation-mediated ubiquitination plays an important role in promoting tumorigenesis. On the other hand, S-nitrosylation could also block ubiquitination. This is the case of Bcl-2 whose S-nitrosylation protect this cell survival promoting factor from ubiquitination and proteasomal degradation [289, 290], and this regulation might partly underlie cancer cell resistance to chemotherapy.

Overall, S-nitrosylation has emerged as an important PTM with elaborate connections with other classical modifications. It will be interesting to identify, at the structural level, how S-nitrosylation promote or inhibit substrate ubiquitination and whether the ubiquitin ligases or their co-factors could act as “readers” of S-nitrosylated residues. At the functional level, and taking into account the increasingly growing list of proteins modified by NO, it is perhaps safe

to assume that a lot remains to be known on how S-nitrosylation-mediated signaling uses ubiquitination to regulate biological processes.

13. Concluding remarks

Protein ubiquitination is a major PTM involved in many aspects of protein fate decision including localization, function and stability of most known proteins in eukaryotes. The large number of effectors in the ubiquitin signaling system, including more than 600 E3 ligases and 100 DUBs and the corresponding overwhelming number of proteins targeted for ubiquitination, suggest the existence of multiple layers of regulatory mechanisms that extensively involve a wide-spectrum of PTMs. Indeed, decades of research efforts have led to the uncovering of many complex mechanisms underlying the interplay between ubiquitination and other PTMs. Different PTMs were found to promote or inhibit substrate ubiquitination in response to signaling pathways induced by intrinsic processes or environmental changes. On the functional level, the general understanding of these PTM crosstalks and relationships has revealed unexpected connections between signaling pathways and cellular processes and has also improved our knowledge of disease conditions and this will certainly help in elaborating novel diagnosis tools and therapeutic strategies targeting critical signaling nodes.

14. RÉFÉRENCES

1. Pickart, C.M. and M.J. Eddins, *Ubiquitin: structures, functions, mechanisms.* Biochim Biophys Acta, 2004. **1695**(1-3): p. 55-72.
2. Haglund, K. and I. Dikic, *Ubiquitylation and cell signaling.* The EMBO Journal, 2005. **24**(19): p. 3353-3359.
3. Hochstrasser, M., *Origin and function of ubiquitin-like proteins.* Nature, 2009. **458**(7237): p. 422-9.
4. Komander, D. and M. Rape, *The ubiquitin code.* Annu Rev Biochem, 2012. **81**: p. 203-29.
5. Swatek, K.N. and D. Komander, *Ubiquitin modifications.* Cell Res, 2016. **26**(4): p. 399-422.
6. Oh, E., D. Akopian, and M. Rape, *Principles of Ubiquitin-Dependent Signaling.* Annu Rev Cell Dev Biol, 2018. **34**: p. 137-162.
7. Zheng, N. and N. Shabek, *Ubiquitin Ligases: Structure, Function, and Regulation.* Annu Rev Biochem, 2017. **86**: p. 129-157.
8. Olsen, S.K. and C.D. Lima, *Structure of a ubiquitin E1-E2 complex: insights to E1-E2 thioester transfer.* Molecular cell, 2013. **49**(5): p. 884-896.
9. Ciechanover, A. and R. Ben-Saadon, *N-terminal ubiquitination: more protein substrates join in.* Trends Cell Biol, 2004. **14**(3): p. 103-6.
10. van Wijk, S.J.L., et al., *A comprehensive framework of E2–RING E3 interactions of the human ubiquitin–proteasome system.* Molecular Systems Biology, 2009. **5**: p. 295-295.
11. Li, W., et al., *Genome-wide and functional annotation of human E3 ubiquitin ligases identifies MULAN, a mitochondrial E3 that regulates the organelle's dynamics and signaling.* PLoS One, 2008. **3**(1): p. e1487.
12. Stewart, M.D., et al., *E2 enzymes: more than just middle men.* Cell Res, 2016. **26**(4): p. 423-40.
13. Ye, Y. and M. Rape, *Building ubiquitin chains: E2 enzymes at work.* Nat Rev Mol Cell Biol, 2009. **10**(11): p. 755-64.
14. Rotin, D. and S. Kumar, *Physiological functions of the HECT family of ubiquitin ligases.* Nat Rev Mol Cell Biol, 2009. **10**(6): p. 398-409.
15. Xu, P., et al., *Quantitative proteomics reveals the function of unconventional ubiquitin chains in proteasomal degradation.* Cell, 2009. **137**(1): p. 133-145.
16. Kwon, Y.T. and A. Ciechanover, *The Ubiquitin Code in the Ubiquitin-Proteasome System and Autophagy.* Trends Biochem Sci, 2017. **42**(11): p. 873-886.
17. Komander, D., M.J. Clague, and S. Urbe, *Breaking the chains: structure and function of the deubiquitinases.* Nat Rev Mol Cell Biol, 2009. **10**(8): p. 550-63.
18. Clague, M.J., S. Urbe, and D. Komander, *Breaking the chains: deubiquitylating enzyme specificity begets function.* Nat Rev Mol Cell Biol, 2019.
19. Kwasna, D., et al., *Discovery and Characterization of ZUFSP/ZUP1, a Distinct Deubiquitinase Class Important for Genome Stability.* Mol Cell, 2018. **70**(1): p. 150-164 e6.

20. Abdul Rehman, S.A., et al., *MINDY-1 Is a Member of an Evolutionarily Conserved and Structurally Distinct New Family of Deubiquitinating Enzymes.* Mol Cell, 2016. **63**(1): p. 146-55.

21. Lee, M.J., et al., *Trimming of ubiquitin chains by proteasome-associated deubiquitinating enzymes.* Mol Cell Proteomics, 2011. **10**(5): p. R110 003871.

22. Mevissen, T.E.T. and D. Komander, *Mechanisms of Deubiquitinase Specificity and Regulation.* Annu Rev Biochem, 2017. **86**: p. 159-192.

23. Grabbe, C., K. Husnjak, and I. Dikic, *The spatial and temporal organization of ubiquitin networks.* Nat Rev Mol Cell Biol, 2011. **12**(5): p. 295-307.

24. Nguyen, L.K., *Dynamics of ubiquitin-mediated signalling: insights from mathematical modelling and experimental studies.* Brief Bioinform, 2016. **17**(3): p. 479-93.

25. Kruse, J.P. and W. Gu, *SnapShot: p53 posttranslational modifications.* Cell, 2008. **133**(5): p. 930-30 e1.

26. Duda, D.M., et al., *Structural regulation of cullin-RING ubiquitin ligase complexes.* Curr Opin Struct Biol, 2011. **21**(2): p. 257-64.

27. Huang, O.W. and A.G. Cochran, *Regulation of deubiquitinase proteolytic activity.* Curr Opin Struct Biol, 2013. **23**(6): p. 806-11.

28. Sahtoe, D.D. and T.K. Sixma, *Layers of DUB regulation.* Trends Biochem Sci, 2015. **40**(8): p. 456-67.

29. Sluimer, J. and B. Distel, *Regulating the human HECT E3 ligases.* Cell Mol Life Sci, 2018. **75**(17): p. 3121-3141.

30. Welchman, R.L., C. Gordon, and R.J. Mayer, *Ubiquitin and ubiquitin-like proteins as multifunctional signals.* Nat Rev Mol Cell Biol, 2005. **6**(8): p. 599-609.

31. Bayer, P., et al., *Structure determination of the small ubiquitin-related modifier SUMO-1.* J Mol Biol, 1998. **280**(2): p. 275-86.

32. Zuin, A., M. Isasa, and B. Crosas, *Ubiquitin signaling: extreme conservation as a source of diversity.* Cells, 2014. **3**(3): p. 690-701.

33. Rodriguez, M.S., C. Dargemont, and R.T. Hay, *SUMO-1 conjugation in vivo requires both a consensus modification motif and nuclear targeting.* J Biol Chem, 2001. **276**(16): p. 12654-9.

34. Gareau, J.R. and C.D. Lima, *The SUMO pathway: emerging mechanisms that shape specificity, conjugation and recognition.* Nature reviews. Molecular cell biology, 2010. **11**(12): p. 861-871.

35. Seeler, J.S. and A. Dejean, *SUMO and the robustness of cancer.* Nat Rev Cancer, 2017. **17**(3): p. 184-197.

36. Flotho, A. and F. Melchior, *Sumoylation: a regulatory protein modification in health and disease.* Annu Rev Biochem, 2013. **82**: p. 357-85.

37. Hay, R.T., *SUMO: a history of modification.* Mol Cell, 2005. **18**(1): p. 1-12.

38. Müller, S., et al., *Sumo, ubiquitin's mysterious cousin.* Nat Rev Mol Cell Biol, 2001. **2**(3): p. 202-213.

39. Chen, Z., et al., *Signal-induced site-specific phosphorylation targets I kappa B alpha to the ubiquitin-proteasome pathway.* Genes Dev, 1995. **9**(13): p. 1586-97.

40. Scherer, D.C., et al., *Signal-induced degradation of I kappa B alpha requires site-specific ubiquitination.* Proc Natl Acad Sci U S A, 1995. **92**(24): p. 11259-63.

41. Alkalay, I., et al., *Stimulation-dependent I kappa B alpha phosphorylation marks the NF-kappa B inhibitor for degradation via the ubiquitin-proteasome pathway.* Proc Natl Acad Sci U S A, 1995. **92**(23): p. 10599-603.

42. Desterro, J.M., M.S. Rodriguez, and R.T. Hay, *SUMO-1 modification of IkappaBalpha inhibits NF-kappaB activation.* Mol Cell, 1998. **2**(2): p. 233-9.

43. Mulero, M.C., et al., *Chromatin-bound IkappaBalpha regulates a subset of polycomb target genes in differentiation and cancer.* Cancer Cell, 2013. **24**(2): p. 151-66.

44. Aillet, F., et al., *Heterologous SUMO-2/3-ubiquitin chains optimize IkappaBalpha degradation and NF-kappaB activity.* PLoS One, 2012. **7**(12): p. e51672.

45. Lee, M.H., et al., *NF-kappaB induction of the SUMO protease SENP2: A negative feedback loop to attenuate cell survival response to genotoxic stress.* Mol Cell, 2011. **43**(2): p. 180-91.

46. Tatham, M.H., et al., *RNF4 is a poly-SUMO-specific E3 ubiquitin ligase required for arsenic-induced PML degradation.* Nat Cell Biol, 2008. **10**(5): p. 538-46.

47. Lallemand-Breitenbach, V., et al., *Arsenic degrades PML or PML-RARalpha through a SUMO-triggered RNF4/ubiquitin-mediated pathway.* Nat Cell Biol, 2008. **10**(5): p. 547-55.

48. Rojas-Fernandez, A., et al., *SUMO chain-induced dimerization activates RNF4.* Mol Cell, 2014. **53**(6): p. 880-92.

49. Plechanovova, A., et al., *Mechanism of ubiquitylation by dimeric RING ligase RNF4.* Nat Struct Mol Biol, 2011. **18**(9): p. 1052-9.

50. Guo, L., et al., *A cellular system that degrades misfolded proteins and protects against neurodegeneration.* Mol Cell, 2014. **55**(1): p. 15-30.

51. Sriramachandran, A.M., et al., *Arkadia/RNF111 is a SUMO-targeted ubiquitin ligase with preference for substrates marked with SUMO1-capped SUMO2/3 chain.* Nat Commun, 2019. **10**(1): p. 3678.

52. Luo, K., et al., *Sumoylation of MDC1 is important for proper DNA damage response.* EMBO J, 2012. **31**(13): p. 3008-19.

53. Pfeiffer, A., et al., *Ataxin-3 consolidates the MDC1-dependent DNA double-strand break response by counteracting the SUMO-targeted ubiquitin ligase RNF4.* EMBO J, 2017. **36**(8): p. 1066-1083.

54. Garvin, A.J., et al., *The deSUMOylase SENP2 coordinates homologous recombination and nonhomologous end joining by independent mechanisms.* Genes Dev, 2019. **33**(5-6): p. 333-347.

55. Kamitani, T., et al., *Characterization of NEDD8, a developmentally down-regulated ubiquitin-like protein.* J Biol Chem, 1997. **272**(45): p. 28557-62.

56. Ohh, M., et al., *An intact NEDD8 pathway is required for Cullin-dependent ubiquitylation in mammalian cells.* EMBO Rep, 2002. **3**(2): p. 177-82.

57. Sakata, E., et al., *Direct interactions between NEDD8 and ubiquitin E2 conjugating enzymes upregulate cullin-based E3 ligase activity.* Nat Struct Mol Biol, 2007. **14**(2): p. 167-8.

58. Liu, J., et al., *NEDD8 modification of CUL1 dissociates p120(CAND1), an inhibitor of CUL1-SKP1 binding and SCF ligases.* Mol Cell, 2002. **10**(6): p. 1511-8.

59. Zuo, W., et al., *c-Cbl-mediated neddylation antagonizes ubiquitination and degradation of the TGF-beta type II receptor.* Mol Cell, 2013. **49**(3): p. 499-510.

60. Di Guglielmo, G.M., et al., *Distinct endocytic pathways regulate TGF-beta receptor signalling and turnover.* Nat Cell Biol, 2003. **5**(5): p. 410-21.

61. Lee, G.W., et al., *The E3 ligase C-CBL inhibits cancer cell migration by neddylating the proto-oncogene c-Src.* Oncogene, 2018.

62. Burgers, P.M., *Polymerase dynamics at the eukaryotic DNA replication fork.* J Biol Chem, 2009. **284**(7): p. 4041-5.

63. Hoege, C., et al., *RAD6-dependent DNA repair is linked to modification of PCNA by ubiquitin and SUMO.* Nature, 2002. **419**(6903): p. 135-41.

64. Stelter, P. and H.D. Ulrich, *Control of spontaneous and damage-induced mutagenesis by SUMO and ubiquitin conjugation.* Nature, 2003. **425**(6954): p. 188-91.

65. Haracska, L., et al., *Opposing effects of ubiquitin conjugation and SUMO modification of PCNA on replicational bypass of DNA lesions in Saccharomyces cerevisiae.* Mol Cell Biol, 2004. **24**(10): p. 4267-74.

66. Pfander, B., et al., *SUMO-modified PCNA recruits Srs2 to prevent recombination during S phase.* Nature, 2005. **436**(7049): p. 428-33.

67. Papouli, E., et al., *Crosstalk between SUMO and ubiquitin on PCNA is mediated by recruitment of the helicase Srs2p.* Mol Cell, 2005. **19**(1): p. 123-33.

68. Armstrong, A.A., F. Mohideen, and C.D. Lima, *Recognition of SUMO-modified PCNA requires tandem receptor motifs in Srs2.* Nature, 2012. **483**(7387): p. 59-63.

69. Gali, H., et al., *Role of SUMO modification of human PCNA at stalled replication fork.* Nucleic Acids Res, 2012. **40**(13): p. 6049-59.

70. Mohiuddin, M., et al., *SUMOylation of PCNA by PIAS1 and PIAS4 promotes template switch in the chicken and human B cell lines.* Proc Natl Acad Sci U S A, 2018. **115**(50): p. 12793-12798.

71. Kannouche, P.L., J. Wing, and A.R. Lehmann, *Interaction of human DNA polymerase eta with monoubiquitinated PCNA: a possible mechanism for the polymerase switch in response to DNA damage.* Mol Cell, 2004. **14**(4): p. 491-500.

72. Acharya, N., et al., *Roles of PCNA-binding and ubiquitin-binding domains in human DNA polymerase eta in translesion DNA synthesis.* Proc Natl Acad Sci U S A, 2008. **105**(46): p. 17724-9.

73. Sale, J.E., A.R. Lehmann, and R. Woodgate, *Y-family DNA polymerases and their role in tolerance of cellular DNA damage.* Nat Rev Mol Cell Biol, 2012. **13**(3): p. 141-52.

74. Chiu, R.K., et al., *Lysine 63-polyubiquitination guards against translesion synthesis-induced mutations.* PLoS Genet, 2006. **2**(7): p. e116.

75. Branzei, D., F. Vanoli, and M. Foiani, *SUMOylation regulates Rad18-mediated template switch.* Nature, 2008. **456**(7224): p. 915-20.

76. Weston, R., H. Peeters, and D. Ahel, *ZRANB3 is a structure-specific ATP-dependent endonuclease involved in replication stress response.* Genes Dev, 2012. **26**(14): p. 1558-72.

77. Ciccia, A., et al., *Polyubiquitinated PCNA recruits the ZRANB3 translocase to maintain genomic integrity after replication stress.* Mol Cell, 2012. **47**(3): p. 396-409.

78. Vujanovic, M., et al., *Replication Fork Slowing and Reversal upon DNA Damage Require PCNA Polyubiquitination and ZRANB3 DNA Translocase Activity.* Mol Cell, 2017. **67**(5): p. 882-890 e5.

79. Masuda, Y., et al., *Regulation of HLTF-mediated PCNA polyubiquitination by RFC and PCNA monoubiquitination levels determines choice of damage tolerance pathway.* Nucleic Acids Res, 2018. **46**(21): p. 11340-11356.

80. Huang, T.T., et al., *Regulation of monoubiquitinated PCNA by DUB autocleavage.* Nat Cell Biol, 2006. **8**(4): p. 339-47.

81. Gallego-Sanchez, A., et al., *Reversal of PCNA ubiquitylation by Ubp10 in Saccharomyces cerevisiae.* PLoS Genet, 2012. **8**(7): p. e1002826.

82. Alvarez, V., et al., *PCNA Deubiquitylases Control DNA Damage Bypass at Replication Forks.* Cell Rep, 2019. **29**(5): p. 1323-1335 e5.

83. Guan, J., S. Yu, and X. Zheng, *NEDDylation antagonizes ubiquitination of proliferating cell nuclear antigen and regulates the recruitment of polymerase eta in response to oxidative DNA damage.* Protein Cell, 2018. **9**(4): p. 365-379.

84. Park, J.M., et al., *Modification of PCNA by ISG15 plays a crucial role in termination of error-prone translesion DNA synthesis.* Mol Cell, 2014. **54**(4): p. 626-38.

85. Ortega, J., et al., *Phosphorylation of PCNA by EGFR inhibits mismatch repair and promotes misincorporation during DNA synthesis.* Proc Natl Acad Sci U S A, 2015. **112**(18): p. 5667-72.

86. Wang, S.C., et al., *Tyrosine phosphorylation controls PCNA function through protein stability.* Nat Cell Biol, 2006. **8**(12): p. 1359-68.

87. Billon, P., et al., *Acetylation of PCNA Sliding Surface by Eco1 Promotes Genome Stability through Homologous Recombination.* Mol Cell, 2017. **65**(1): p. 78-90.

88. Kumar, D. and S. Saha, *HAT3-mediated acetylation of PCNA precedes PCNA monoubiquitination following exposure to UV radiation in Leishmania donovani.* Nucleic Acids Res, 2015. **43**(11): p. 5423-41.

89. A, P., et al., *EZH2 promotes DNA replication by stabilizing interaction of POLdelta and PCNA via methylation-mediated PCNA trimerization.* Epigenetics Chromatin, 2018. **11**(1): p. 44.

90. Manning, G., et al., *The protein kinase complement of the human genome.* Science, 2002. **298**(5600): p. 1912-34.

91. Alonso, A., et al., *Protein tyrosine phosphatases in the human genome.* Cell, 2004. **117**(6): p. 699-711.

92. Sacco, F., et al., *The human phosphatase interactome: An intricate family portrait.* FEBS Lett, 2012. **586**(17): p. 2732-9.

93. Needham, E.J., et al., *Illuminating the dark phosphoproteome.* Sci Signal, 2019. **12**(565).

94. Swaney, D.L., et al., *Global analysis of phosphorylation and ubiquitylation cross-talk in protein degradation.* Nat Methods, 2013. **10**(7): p. 676-82.

95. Bai, C., et al., *SKP1 connects cell cycle regulators to the ubiquitin proteolysis machinery through a novel motif, the F-box.* Cell, 1996. **86**(2): p. 263-74.

96. Sheaff, R.J., et al., *Cyclin E-CDK2 is a regulator of p27Kip1.* Genes Dev, 1997. **11**(11): p. 1464-78.

97. Martin, A., et al., *Cdk2 is dispensable for cell cycle inhibition and tumor suppression mediated by p27(Kip1) and p21(Cip1).* Cancer Cell, 2005. **7**(6): p. 591-8.

98. Tsvetkov, L.M., et al., *p27(Kip1) ubiquitination and degradation is regulated by the SCF(Skp2) complex through phosphorylated Thr187 in p27.* Curr Biol, 1999. **9**(12): p. 661-4.

99. Carrano, A.C., et al., *SKP2 is required for ubiquitin-mediated degradation of the CDK inhibitor p27.* Nat Cell Biol, 1999. **1**(4): p. 193-9.

100. Ganoth, D., et al., *The cell-cycle regulatory protein Cks1 is required for SCF(Skp2)-mediated ubiquitinylation of p27.* Nat Cell Biol, 2001. **3**(3): p. 321-4.

101. Hao, B., et al., *Structural basis of the Cks1-dependent recognition of p27(Kip1) by the SCF(Skp2) ubiquitin ligase.* Mol Cell, 2005. **20**(1): p. 9-19.

102. Chu, I., et al., *p27 phosphorylation by Src regulates inhibition of cyclin E-Cdk2.* Cell, 2007. **128**(2): p. 281-94.

103. Rath, S.L. and S. Senapati, *Mechanism of p27 Unfolding for CDK2 Reactivation.* Sci Rep, 2016. **6**: p. 26450.

104. Huntwork-Rodriguez, S., et al., *JNK-mediated phosphorylation of DLK suppresses its ubiquitination to promote neuronal apoptosis.* J Cell Biol, 2013. **202**(5): p. 747-63.

105. Symington, L.S. and J. Gautier, *Double-strand break end resection and repair pathway choice.* Annu Rev Genet, 2011. **45**: p. 247-71.

106. Zimmermann, M. and T. de Lange, *53BP1: pro choice in DNA repair.* Trends Cell Biol, 2014. **24**(2): p. 108-17.

107. Ceccaldi, R., B. Rondinelli, and A.D. D'Andrea, *Repair Pathway Choices and Consequences at the Double-Strand Break.* Trends Cell Biol, 2016. **26**(1): p. 52-64.

108. Orthwein, A., et al., *A mechanism for the suppression of homologous recombination in G1 cells.* Nature, 2015. **528**(7582): p. 422-6.

109. Lu, H., et al., *Cell cycle-dependent phosphorylation regulates RECQL4 pathway choice and ubiquitination in DNA double-strand break repair.* Nat Commun, 2017. **8**(1): p. 2039.

110. Moldovan, G.L. and A.D. D'Andrea, *How the fanconi anemia pathway guards the genome.* Annu Rev Genet, 2009. **43**: p. 223-49.

111. Niraj, J., A. Farkkila, and A.D. D'Andrea, *The Fanconi Anemia Pathway in Cancer.* Annu Rev Cancer Biol, 2019. **3**: p. 457-478.

112. Ceccaldi, R., P. Sarangi, and A.D. D'Andrea, *The Fanconi anaemia pathway: new players and new functions.* Nat Rev Mol Cell Biol, 2016. **17**(6): p. 337-49.

113. Ishiai, M., et al., *FANCI phosphorylation functions as a molecular switch to turn on the Fanconi anemia pathway.* Nat Struct Mol Biol, 2008. **15**(11): p. 1138-46.

114. Shigechi, T., et al., *ATR-ATRIP kinase complex triggers activation of the Fanconi anemia DNA repair pathway.* Cancer Res, 2012. **72**(5): p. 1149-56.

115. Sareen, A., et al., *Fanconi anemia proteins FANCD2 and FANCI exhibit different DNA damage responses during S-phase.* Nucleic Acids Res, 2012. **40**(17): p. 8425-39.

116. Cheung, R.S., et al., *Ubiquitination-Linked Phosphorylation of the FANCI S/TQ Cluster Contributes to Activation of the Fanconi Anemia I/D2 Complex.* Cell Rep, 2017. **19**(12): p. 2432-2440.

117. Verdin, E. and M. Ott, *50 years of protein acetylation: from gene regulation to epigenetics, metabolism and beyond.* Nat Rev Mol Cell Biol, 2015. **16**(4): p. 258-64.

118. Narita, T., B.T. Weinert, and C. Choudhary, *Functions and mechanisms of non-histone protein acetylation.* Nat Rev Mol Cell Biol, 2019. **20**(3): p. 156-174.

119. Drazic, A., et al., *The world of protein acetylation.* Biochim Biophys Acta, 2016. **1864**(10): p. 1372-401.

120. Lee, D.Y., et al., *A positive role for histone acetylation in transcription factor access to nucleosomal DNA.* Cell, 1993. **72**(1): p. 73-84.

121. Li, M., et al., *Acetylation of p53 inhibits its ubiquitination by Mdm2.* J Biol Chem, 2002. **277**(52): p. 50607-11.

122. Ito, A., et al., *MDM2-HDAC1-mediated deacetylation of p53 is required for its degradation.* Embo j, 2002. **21**(22): p. 6236-45.

123. Ikura, T., et al., *DNA damage-dependent acetylation and ubiquitination of H2AX enhances chromatin dynamics.* Mol Cell Biol, 2007. **27**(20): p. 7028-40.

124. Du, Z., et al., *DNMT1 stability is regulated by proteins coordinating deubiquitination and acetylation-driven ubiquitination.* Sci Signal, 2010. **3**(146): p. ra80.

125. Cheng, J., et al., *Molecular mechanism for USP7-mediated DNMT1 stabilization by acetylation.* Nat Commun, 2015. **6**: p. 7023.

126. Jiang, W., et al., *Acetylation regulates gluconeogenesis by promoting PEPCK1 degradation via recruiting the UBR5 ubiquitin ligase.* Mol Cell, 2011. **43**(1): p. 33-44.

127. Ambler, R.P. and M.W. Rees, *Epsilon-N-Methyl-lysine in bacterial flagellar protein.* Nature, 1959. **184**: p. 56-7.

128. Murray, K., *The Occurrence of Epsilon-N-Methyl Lysine in Histones.* Biochemistry, 1964. **3**: p. 10-5.

129. Boriack-Sjodin, P.A. and K.K. Swinger, *Protein Methyltransferases: A Distinct, Diverse, and Dynamic Family of Enzymes.* Biochemistry, 2016. **55**(11): p. 1557-69.

130. Cheng, X., R.E. Collins, and X. Zhang, *Structural and sequence motifs of protein (histone) methylation enzymes.* Annu Rev Biophys Biomol Struct, 2005. **34**: p. 267-94.

131. Nishiyama, A., et al., *Uhrf1-dependent H3K23 ubiquitylation couples maintenance DNA methylation and replication.* Nature, 2013. **502**(7470): p. 249-53.

132. Arita, K., et al., *Recognition of modification status on a histone H3 tail by linked histone reader modules of the epigenetic regulator UHRF1.* Proc Natl Acad Sci U S A, 2012. **109**(32): p. 12950-5.

133. Rothbart, S.B., et al., *Association of UHRF1 with methylated H3K9 directs the maintenance of DNA methylation.* Nat Struct Mol Biol, 2012. **19**(11): p. 1155-60.

134. Rothbart, S.B., et al., *Multivalent histone engagement by the linked tandem Tudor and PHD domains of UHRF1 is required for the epigenetic inheritance of DNA methylation.* Genes Dev, 2013. **27**(11): p. 1288-98.

135. Harrison, J.S., et al., *Hemi-methylated DNA regulates DNA methylation inheritance through allosteric activation of H3 ubiquitylation by UHRF1.* Elife, 2016. **5**.

136. DaRosa, P.A., et al., *A Bifunctional Role for the UHRF1 UBL Domain in the Control of Hemi-methylated DNA-Dependent Histone Ubiquitylation.* Mol Cell, 2018. **72**(4): p. 753-765 e6.

137. Biggar, K.K. and S.S. Li, *Non-histone protein methylation as a regulator of cellular signalling and function.* Nat Rev Mol Cell Biol, 2015. **16**(1): p. 5-17.

138. Lee, J.M., et al., *EZH2 generates a methyl degron that is recognized by the DCAF1/DDB1/CUL4 E3 ubiquitin ligase complex.* Mol Cell, 2012. **48**(4): p. 572-86.

139. He, Y.J., et al., *DDB1 functions as a linker to recruit receptor WD40 proteins to CUL4-ROC1 ubiquitin ligases.* Genes Dev, 2006. **20**(21): p. 2949-54.

140. He, A., et al., *PRC2 directly methylates GATA4 and represses its transcriptional activity.* Genes Dev, 2012. **26**(1): p. 37-42.

141. Kim, E., et al., *Phosphorylation of EZH2 activates STAT3 signaling via STAT3 methylation and promotes tumorigenicity of glioblastoma stem-like cells.* Cancer Cell, 2013. **23**(6): p. 839-52.

142. Chuikov, S., et al., *Regulation of p53 activity through lysine methylation.* Nature, 2004. **432**(7015): p. 353-60.

143. Huang, J., et al., *Repression of p53 activity by Smyd2-mediated methylation.* Nature, 2006. **444**(7119): p. 629-32.

144. Shi, X., et al., *Modulation of p53 function by SET8-mediated methylation at lysine 382.* Mol Cell, 2007. **27**(4): p. 636-46.

145. Huang, J., et al., *p53 is regulated by the lysine demethylase LSD1.* Nature, 2007. **449**(7158): p. 105-8.

146. Fei, Q., et al., *Histone methyltransferase SETDB1 regulates liver cancer cell growth through methylation of p53.* Nat Commun, 2015. **6**: p. 8651.

147. Cui, G., et al., *PHF20 is an effector protein of p53 double lysine methylation that stabilizes and activates p53.* Nat Struct Mol Biol, 2012. **19**(9): p. 916-24.

148. Johmura, Y., et al., *SCF(Fbxo22)-KDM4A targets methylated p53 for degradation and regulates senescence.* Nat Commun, 2016. **7**: p. 10574.

149. Tan, M.K., H.J. Lim, and J.W. Harper, *SCF(FBXO22) regulates histone H3 lysine 9 and 36 methylation levels by targeting histone demethylase KDM4A for ubiquitin-mediated proteasomal degradation.* Mol Cell Biol, 2011. **31**(18): p. 3687-99.

150. Fang, L., et al., *A methylation-phosphorylation switch determines Sox2 stability and function in ESC maintenance or differentiation.* Mol Cell, 2014. **55**(4): p. 537-51.

151. Wang, G., et al., *SETDB1-mediated methylation of Akt promotes its K63-linked ubiquitination and activation leading to tumorigenesis.* Nat Cell Biol, 2019. **21**(2): p. 214-225.

152. Bedford, M.T. and S.G. Clarke, *Protein arginine methylation in mammals: who, what, and why.* Mol Cell, 2009. **33**(1): p. 1-13.

153. Hu, D., et al., *Interplay between arginine methylation and ubiquitylation regulates KLF4-mediated genome stability and carcinogenesis.* Nat Commun, 2015. **6**: p. 8419.

154. Hart, G.W., et al., *Cross talk between O-GlcNAcylation and phosphorylation: roles in signaling, transcription, and chronic disease.* Annu Rev Biochem, 2011. **80**: p. 825-58.

155. Hanover, J.A., M.W. Krause, and D.C. Love, *Bittersweet memories: linking metabolism to epigenetics through O-GlcNAcylation.* Nat Rev Mol Cell Biol, 2012. **13**(5): p. 312-21.

156. Dorfman, A., et al., *The biosynthesis of hyaluronic acid by group A Streptococcus. IV. Role of glucosone as an intermediate in the synthesis of glucosamine.* J Biol Chem, 1955. **216**(2): p. 549-52.

157. Marshall, S., V. Bacote, and R.R. Traxinger, *Discovery of a metabolic pathway mediating glucose-induced desensitization of the glucose transport system. Role of hexosamine biosynthesis in the induction of insulin resistance.* J Biol Chem, 1991. **266**(8): p. 4706-12.

158. Yang, W.H., et al., *Modification of p53 with O-linked N-acetylglucosamine regulates p53 activity and stability.* Nat Cell Biol, 2006. **8**(10): p. 1074-83.

159. Shieh, S.Y., Y. Taya, and C. Prives, *DNA damage-inducible phosphorylation of p53 at N-terminal sites including a novel site, Ser20, requires tetramerization.* EMBO J, 1999. **18**(7): p. 1815-23.

160. Shieh, S.Y., et al., *The human homologs of checkpoint kinases Chk1 and Cds1 (Chk2) phosphorylate p53 at multiple DNA damage-inducible sites.* Genes Dev, 2000. **14**(3): p. 289-300.

161. Sakaguchi, K., et al., *Damage-mediated phosphorylation of human p53 threonine 18 through a cascade mediated by a casein 1-like kinase. Effect on Mdm2 binding.* J Biol Chem, 2000. **275**(13): p. 9278-83.

162. Bech-Otschir, D., et al., *COP9 signalosome-specific phosphorylation targets p53 to degradation by the ubiquitin system.* EMBO J, 2001. **20**(7): p. 1630-9.

163. Mohawk, J.A., C.B. Green, and J.S. Takahashi, *Central and peripheral circadian clocks in mammals.* Annu Rev Neurosci, 2012. **35**: p. 445-62.

164. Lowrey, P.L. and J.S. Takahashi, *Genetics of circadian rhythms in Mammalian model organisms.* Adv Genet, 2011. **74**: p. 175-230.

165. Li, M.D., et al., *O-GlcNAc signaling entrains the circadian clock by inhibiting BMAL1/CLOCK ubiquitination.* Cell Metab, 2013. **17**(2): p. 303-10.

166. Huang, N., et al., *Crystal structure of the heterodimeric CLOCK:BMAL1 transcriptional activator complex.* Science, 2012. **337**(6091): p. 189-94.

167. Udeshi, N.D., et al., *Refined preparation and use of anti-diglycine remnant (K-epsilon-GG) antibody enables routine quantification of 10,000s of ubiquitination sites in single proteomics experiments.* Mol Cell Proteomics, 2013. **12**(3): p. 825-31.

168. Lee, J.M., et al., *The epithelial-mesenchymal transition: new insights in signaling, development, and disease.* J Cell Biol, 2006. **172**(7): p. 973-81.

169. Xu, Y., et al., *Role of CK1 in GSK3beta-mediated phosphorylation and degradation of snail.* Oncogene, 2010. **29**(21): p. 3124-33.

170. Zhou, B.P., et al., *Dual regulation of Snail by GSK-3beta-mediated phosphorylation in control of epithelial-mesenchymal transition.* Nat Cell Biol, 2004. **6**(10): p. 931-40.

171. Park, S.Y., et al., *Snail1 is stabilized by O-GlcNAc modification in hyperglycaemic condition.* EMBO J, 2010. **29**(22): p. 3787-96.

172. Ma, X., et al., *Poleta O-GlcNAcylation governs genome integrity during translesion DNA synthesis.* Nat Commun, 2017. **8**(1): p. 1941.

173. Fujiki, R., et al., *GlcNAcylation of histone H2B facilitates its monoubiquitination.* Nature, 2011. **480**(7378): p. 557-60.

174. Gagnon, J., et al., *Undetectable histone O-GlcNAcylation in mammalian cells.* Epigenetics, 2015. **10**(8): p. 677-91.

175. Stevenson, J., E.Y. Huang, and J.A. Olzmann, *Endoplasmic Reticulum-Associated Degradation and Lipid Homeostasis.* Annu Rev Nutr, 2016. **36**: p. 511-42.

176. Xu, C. and D.T. Ng, *Glycosylation-directed quality control of protein folding.* Nat Rev Mol Cell Biol, 2015. **16**(12): p. 742-52.

177. Ruggiano, A., O. Foresti, and P. Carvalho, *Quality control: ER-associated degradation: protein quality control and beyond.* J Cell Biol, 2014. **204**(6): p. 869-79.

178. Olzmann, J.A., R.R. Kopito, and J.C. Christianson, *The mammalian endoplasmic reticulum-associated degradation system.* Cold Spring Harb Perspect Biol, 2013. **5**(9).

179. McCracken, A.A. and J.L. Brodsky, *Assembly of ER-associated protein degradation in vitro: dependence on cytosol, calnexin, and ATP.* J Cell Biol, 1996. **132**(3): p. 291-8.

180. Finger, A., M. Knop, and D.H. Wolf, *Analysis of two mutated vacuolar proteins reveals a degradation pathway in the endoplasmic reticulum or a related compartment of yeast.* Eur J Biochem, 1993. **218**(2): p. 565-74.

181. Sommer, T. and S. Jentsch, *A protein translocation defect linked to ubiquitin conjugation at the endoplasmic reticulum.* Nature, 1993. **365**(6442): p. 176-9.

182. Jensen, T.J., et al., *Multiple proteolytic systems, including the proteasome, contribute to CFTR processing.* Cell, 1995. **83**(1): p. 129-35.

183. Ward, C.L., S. Omura, and R.R. Kopito, *Degradation of CFTR by the ubiquitin-proteasome pathway.* Cell, 1995. **83**(1): p. 121-7.

184. Carvalho, P., V. Goder, and T.A. Rapoport, *Distinct ubiquitin-ligase complexes define convergent pathways for the degradation of ER proteins.* Cell, 2006. **126**(2): p. 361-73.

185. Vashist, S. and D.T. Ng, *Misfolded proteins are sorted by a sequential checkpoint mechanism of ER quality control.* J Cell Biol, 2004. **165**(1): p. 41-52.

186. Stein, A., et al., *Key steps in ERAD of luminal ER proteins reconstituted with purified components.* Cell, 2014. **158**(6): p. 1375-88.

187. Habeck, G., et al., *The yeast ERAD-C ubiquitin ligase Doa10 recognizes an intramembrane degron.* J Cell Biol, 2015. **209**(2): p. 261-73.

188. Braakman, I. and D.N. Hebert, *Protein folding in the endoplasmic reticulum.* Cold Spring Harb Perspect Biol, 2013. **5**(5): p. a013201.

189. Clerc, S., et al., *Htm1 protein generates the N-glycan signal for glycoprotein degradation in the endoplasmic reticulum.* J Cell Biol, 2009. **184**(1): p. 159-72.

190. Jakob, C.A., et al., *Degradation of misfolded endoplasmic reticulum glycoproteins in Saccharomyces cerevisiae is determined by a specific oligosaccharide structure.* J Cell Biol, 1998. **142**(5): p. 1223-33.

191. Szathmary, R., et al., *Yos9 protein is essential for degradation of misfolded glycoproteins and may function as lectin in ERAD.* Mol Cell, 2005. **19**(6): p. 765-75.

192. Kim, W., E.D. Spear, and D.T. Ng, *Yos9p detects and targets misfolded glycoproteins for ER-associated degradation.* Mol Cell, 2005. **19**(6): p. 753-64.

193. Xie, W., et al., *Intrinsic conformational determinants signal protein misfolding to the Hrd1/Htm1 endoplasmic reticulum-associated degradation system.* Mol Biol Cell, 2009. **20**(14): p. 3317-29.

194. Schoebel, S., et al., *Cryo-EM structure of the protein-conducting ERAD channel Hrd1 in complex with Hrd3.* Nature, 2017. **548**(7667): p. 352-355.

195. Gauss, R., et al., *A complex of Pdi1p and the mannosidase Htm1p initiates clearance of unfolded glycoproteins from the endoplasmic reticulum.* Mol Cell, 2011. **42**(6): p. 782-93.

196. Liu, Y.C., D.G. Fujimori, and J.S. Weissman, *Htm1p-Pdi1p is a folding-sensitive mannosidase that marks N-glycoproteins for ER-associated protein degradation.* Proc Natl Acad Sci U S A, 2016. **113**(28): p. E4015-24.

197. Ye, Y., H.H. Meyer, and T.A. Rapoport, *The AAA ATPase Cdc48/p97 and its partners transport proteins from the ER into the cytosol.* Nature, 2001. **414**(6864): p. 652-6.

198. Ye, Y., H.H. Meyer, and T.A. Rapoport, *Function of the p97-Ufd1-Npl4 complex in retrotranslocation from the ER to the cytosol: dual recognition of nonubiquitinated polypeptide segments and polyubiquitin chains.* J Cell Biol, 2003. **162**(1): p. 71-84.

199. Ye, Y., et al., *A membrane protein complex mediates retro-translocation from the ER lumen into the cytosol.* Nature, 2004. **429**(6994): p. 841-7.

200. Yoshida, Y., et al., *Glycoprotein-specific ubiquitin ligases recognize N-glycans in unfolded substrates.* EMBO Rep, 2005. **6**(3): p. 239-44.

201. Ilyin, G.P., et al., *A new subfamily of structurally related human F-box proteins.* Gene, 2002. **296**(1-2): p. 11-20.

202. Yoshida, Y., et al., *E3 ubiquitin ligase that recognizes sugar chains.* Nature, 2002. **418**(6896): p. 438-42.

203. Yoshida, Y., et al., *Fbs2 is a new member of the E3 ubiquitin ligase family that recognizes sugar chains.* J Biol Chem, 2003. **278**(44): p. 43877-84.

204. Mizushima, T., et al., *Structural basis of sugar-recognizing ubiquitin ligase.* Nat Struct Mol Biol, 2004. **11**(4): p. 365-70.

205. Mizushima, T., et al., *Structural basis for the selection of glycosylated substrates by SCF(Fbs1) ubiquitin ligase.* Proc Natl Acad Sci U S A, 2007. **104**(14): p. 5777-81.

206. Chambon, P., J.D. Weill, and P. Mandel, *Nicotinamide mononucleotide activation of new DNA-dependent polyadenylic acid synthesizing nuclear enzyme.* Biochem Biophys Res Commun, 1963. **11**: p. 39-43.

207. Ziegler, M., *New functions of a long-known molecule. Emerging roles of NAD in cellular signaling.* Eur J Biochem, 2000. **267**(6): p. 1550-64.

208. Berger, F., M.H. Ramirez-Hernandez, and M. Ziegler, *The new life of a centenarian: signalling functions of NAD(P).* Trends Biochem Sci, 2004. **29**(3): p. 111-8.

209. Gupte, R., Z. Liu, and W.L. Kraus, *PARPs and ADP-ribosylation: recent advances linking molecular functions to biological outcomes.* Genes Dev, 2017. **31**(2): p. 101-126.

210. Hassa, P.O. and M.O. Hottiger, *The diverse biological roles of mammalian PARPS, a small but powerful family of poly-ADP-ribose polymerases.* Front Biosci, 2008. **13**: p. 3046-82.

211. Krishnakumar, R. and W.L. Kraus, *The PARP side of the nucleus: molecular actions, physiological outcomes, and clinical targets.* Mol Cell, 2010. **39**(1): p. 8-24.

212. Alemasova, E.E. and O.I. Lavrik, *Poly(ADP-ribosyl)ation by PARP1: reaction mechanism and regulatory proteins.* Nucleic Acids Res, 2019.

213. Kraus, W.L., *Transcriptional control by PARP-1: chromatin modulation, enhancer-binding, coregulation, and insulation.* Curr Opin Cell Biol, 2008. **20**(3): p. 294-302.

214. Kraus, W.L. and J.T. Lis, *PARP goes transcription.* Cell, 2003. **113**(6): p. 677-83.

215. Liu, C., et al., *The role of poly ADP-ribosylation in the first wave of DNA damage response.* Nucleic Acids Res, 2017. **45**(14): p. 8129-8141.

216. Gagne, J.P., et al., *Proteome-wide identification of poly(ADP-ribose) binding proteins and poly(ADP-ribose)-associated protein complexes.* Nucleic Acids Res, 2008. **36**(22): p. 6959-76.

217. Aravind, L., *The WWE domain: a common interaction module in protein ubiquitination and ADP ribosylation.* Trends Biochem Sci, 2001. **26**(5): p. 273-5.

218. Ahel, I., et al., *Poly(ADP-ribose)-binding zinc finger motifs in DNA repair/checkpoint proteins.* Nature, 2008. **451**(7174): p. 81-5.

219. Karras, G.I., et al., *The macro domain is an ADP-ribose binding module.* EMBO J, 2005. **24**(11): p. 1911-20.

220. Wang, Z., et al., *Recognition of the iso-ADP-ribose moiety in poly(ADP-ribose) by WWE domains suggests a general mechanism for poly(ADP-ribosyl)ation-dependent ubiquitination.* Genes Dev, 2012. **26**(3): p. 235-40.

221. Kang, H.C., et al., *Iduna is a poly(ADP-ribose) (PAR)-dependent E3 ubiquitin ligase that regulates DNA damage.* Proc Natl Acad Sci U S A, 2011. **108**(34): p. 14103-8.

222. Yan, Q., et al., *BAL1 and its partner E3 ligase, BBAP, link Poly(ADP-ribose) activation, ubiquitylation, and double-strand DNA repair independent of ATM, MDC1, and RNF8.* Mol Cell Biol, 2013. **33**(4): p. 845-57.

223. Li, M. and X. Yu, *Function of BRCA1 in the DNA damage response is mediated by ADP-ribosylation.* Cancer Cell, 2013. **23**(5): p. 693-704.

224. Huang, S.M., et al., *Tankyrase inhibition stabilizes axin and antagonizes Wnt signalling.* Nature, 2009. **461**(7264): p. 614-20.

225. DaRosa, P.A., et al., *Allosteric activation of the RNF146 ubiquitin ligase by a poly(ADP-ribosyl)ation signal.* Nature, 2015. **517**(7533): p. 223-6.

226. Logan, C.Y. and R. Nusse, *The Wnt signaling pathway in development and disease.* Annu Rev Cell Dev Biol, 2004. **20**: p. 781-810.

227. Lee, E., et al., *The roles of APC and Axin derived from experimental and theoretical analysis of the Wnt pathway.* PLoS Biol, 2003. **1**(1): p. E10.

228. Zhang, Y., et al., *RNF146 is a poly(ADP-ribose)-directed E3 ligase that regulates axin degradation and Wnt signalling.* Nat Cell Biol, 2011. **13**(5): p. 623-9.

229. Oberoi, J., et al., *Structural basis of poly(ADP-ribose) recognition by the multizinc binding domain of checkpoint with forkhead-associated and RING Domains (CHFR).* J Biol Chem, 2010. **285**(50): p. 39348-58.

230. Kashima, L., et al., *CHFR protein regulates mitotic checkpoint by targeting PARP-1 protein for ubiquitination and degradation.* J Biol Chem, 2012. **287**(16): p. 12975-84.

231. Liu, C., et al., *CHFR is important for the first wave of ubiquitination at DNA damage sites.* Nucleic Acids Res, 2013. **41**(3): p. 1698-710.

232. Kivirikko, K.I., R. Myllyla, and T. Pihlajaniemi, *Protein hydroxylation: prolyl 4-hydroxylase, an enzyme with four cosubstrates and a multifunctional subunit.* FASEB J, 1989. **3**(5): p. 1609-17.

233. Kivirikko, K.I. and J. Myllyharju, *Prolyl 4-hydroxylases and their protein disulfide isomerase subunit.* Matrix Biol, 1998. **16**(7): p. 357-68.

234. Jaakkola, P., et al., *Targeting of HIF-alpha to the von Hippel-Lindau ubiquitylation complex by O2-regulated prolyl hydroxylation.* Science, 2001. **292**(5516): p. 468-72.

235. Ivan, M., et al., *HIFalpha targeted for VHL-mediated destruction by proline hydroxylation: implications for O2 sensing.* Science, 2001. **292**(5516): p. 464-8.

236. Yu, F., et al., *HIF-1alpha binding to VHL is regulated by stimulus-sensitive proline hydroxylation.* Proc Natl Acad Sci U S A, 2001. **98**(17): p. 9630-5.

237. Hon, W.C., et al., *Structural basis for the recognition of hydroxyproline in HIF-1 alpha by pVHL.* Nature, 2002. **417**(6892): p. 975-8.

238. Min, J.H., et al., *Structure of an HIF-1alpha -pVHL complex: hydroxyproline recognition in signaling.* Science, 2002. **296**(5574): p. 1886-9.

239. Epstein, A.C., et al., *C. elegans EGL-9 and mammalian homologs define a family of dioxygenases that regulate HIF by prolyl hydroxylation.* Cell, 2001. **107**(1): p. 43-54.

240. Bruick, R.K. and S.L. McKnight, *A conserved family of prolyl-4-hydroxylases that modify HIF.* Science, 2001. **294**(5545): p. 1337-40.

241. Baek, J.H., et al., *OS-9 interacts with hypoxia-inducible factor 1alpha and prolyl hydroxylases to promote oxygen-dependent degradation of HIF-1alpha.* Mol Cell, 2005. **17**(4): p. 503-12.

242. Cheng, J., et al., *SUMO-specific protease 1 is essential for stabilization of HIF1alpha during hypoxia.* Cell, 2007. **131**(3): p. 584-95.

243. Seo, K.S., et al., *SIRT2 regulates tumour hypoxia response by promoting HIF-1alpha hydroxylation.* Oncogene, 2015. **34**(11): p. 1354-62.

244. Dengler, V.L., M. Galbraith, and J.M. Espinosa, *Transcriptional regulation by hypoxia inducible factors.* Crit Rev Biochem Mol Biol, 2014. **49**(1): p. 1-15.

245. van Hagen, M., et al., *RNF4 and VHL regulate the proteasomal degradation of SUMO-conjugated Hypoxia-Inducible Factor-2alpha.* Nucleic Acids Res, 2010. **38**(6): p. 1922-31.

246. Moser, S.C., et al., *PHD1 links cell-cycle progression to oxygen sensing through hydroxylation of the centrosomal protein Cep192.* Dev Cell, 2013. **26**(4): p. 381-92.

247. Zhou, T., et al., *Proteomic analysis reveals diverse proline hydroxylation-mediated oxygen-sensing cellular pathways in cancer cells.* Oncotarget, 2016. **7**(48): p. 79154-79169.

248. Zheng, X., et al., *Prolyl hydroxylation by EglN2 destabilizes FOXO3a by blocking its interaction with the USP9x deubiquitinase.* Genes Dev, 2014. **28**(13): p. 1429-44.

249. Soffer, R.L., *Enzymatic modification of proteins. 4. Arginylation of bovine thyroglobulin.* J Biol Chem, 1971. **246**(5): p. 1481-4.

250. Hershko, A., et al., *Role of the alpha-amino group of protein in ubiquitin-mediated protein breakdown.* Proc Natl Acad Sci U S A, 1984. **81**(22): p. 7021-5.

251. Ferber, S. and A. Ciechanover, *Role of arginine-tRNA in protein degradation by the ubiquitin pathway.* Nature, 1987. **326**(6115): p. 808-11.

252. Mayer, A., et al., *Degradation of proteins with acetylated amino termini by the ubiquitin system.* Science, 1989. **244**(4911): p. 1480-3.

253. Hwang, C.S., A. Shemorry, and A. Varshavsky, *N-terminal acetylation of cellular proteins creates specific degradation signals.* Science, 2010. **327**(5968): p. 973-7.

254. Sriram, S.M., B.Y. Kim, and Y.T. Kwon, *The N-end rule pathway: emerging functions and molecular principles of substrate recognition.* Nat Rev Mol Cell Biol, 2011. **12**(11): p. 735-47.

255. Tasaki, T., et al., *The N-end rule pathway.* Annu Rev Biochem, 2012. **81**: p. 261-89.

256. Nguyen, K.T., et al., *Control of protein degradation by N-terminal acetylation and the N-end rule pathway.* Exp Mol Med, 2018. **50**(7): p. 91.

257. Chen, S.J., et al., *An N-end rule pathway that recognizes proline and destroys gluconeogenic enzymes.* Science, 2017. **355**(6323).

258. Tasaki, T., et al., *The substrate recognition domains of the N-end rule pathway.* J Biol Chem, 2009. **284**(3): p. 1884-95.

259. Roman-Hernandez, G., et al., *Molecular basis of substrate selection by the N-end rule adaptor protein ClpS.* Proc Natl Acad Sci U S A, 2009. **106**(22): p. 8888-93.

260. Hu, R.G., et al., *Arginyltransferase, its specificity, putative substrates, bidirectional promoter, and splicing-derived isoforms.* J Biol Chem, 2006. **281**(43): p. 32559-73.

261. Wang, J., et al., *Arginyltransferase is an ATP-independent self-regulating enzyme that forms distinct functional complexes in vivo.* Chem Biol, 2011. **18**(1): p. 121-30.

262. Yoo, Y.D., et al., *N-terminal arginylation generates a bimodal degron that modulates autophagic proteolysis.* Proc Natl Acad Sci U S A, 2018. **115**(12): p. E2716-E2724.

263. Cha-Molstad, H., et al., *p62/SQSTM1/Sequestosome-1 is an N-recognin of the N-end rule pathway which modulates autophagosome biogenesis.* Nat Commun, 2017. **8**(1): p. 102.

264. Cha-Molstad, H., et al., *Amino-terminal arginylation targets endoplasmic reticulum chaperone BiP for autophagy through p62 binding.* Nat Cell Biol, 2015. **17**(7): p. 917-29.

265. Kwon, D.H., et al., *Insights into degradation mechanism of N-end rule substrates by p62/SQSTM1 autophagy adapter.* Nat Commun, 2018. **9**(1): p. 3291.

266. Zhang, Y., et al., *ZZ-dependent regulation of p62/SQSTM1 in autophagy.* Nat Commun, 2018. **9**(1): p. 4373.

267. Aksnes, H., K. Hole, and T. Arnesen, *Molecular, cellular, and physiological significance of N-terminal acetylation.* Int Rev Cell Mol Biol, 2015. **316**: p. 267-305.

268. Aksnes, H., et al., *First Things First: Vital Protein Marks by N-Terminal Acetyltransferases.* Trends Biochem Sci, 2016. **41**(9): p. 746-760.

269. Shemorry, A., C.S. Hwang, and A. Varshavsky, *Control of protein quality and stoichiometries by N-terminal acetylation and the N-end rule pathway.* Mol Cell, 2013. **50**(4): p. 540-51.

270. Park, S.E., et al., *Control of mammalian G protein signaling by N-terminal acetylation and the N-end rule pathway.* Science, 2015. **347**(6227): p. 1249-1252.

271. Scott, D.C., et al., *N-terminal acetylation acts as an avidity enhancer within an interconnected multiprotein complex.* Science, 2011. **334**(6056): p. 674-8.

272. Scott, D.C., et al., *Blocking an N-terminal acetylation-dependent protein interaction inhibits an E3 ligase.* Nat Chem Biol, 2017. **13**(8): p. 850-857.

273. Holmes, W.M., et al., *Loss of amino-terminal acetylation suppresses a prion phenotype by modulating global protein folding.* Nat Commun, 2014. **5**: p. 4383.

274. Yang, D., et al., *Nalpha-acetylated Sir3 stabilizes the conformation of a nucleosome-binding loop in the BAH domain.* Nat Struct Mol Biol, 2013. **20**(9): p. 1116-8.

275. Arnaudo, N., et al., *The N-terminal acetylation of Sir3 stabilizes its binding to the nucleosome core particle.* Nat Struct Mol Biol, 2013. **20**(9): p. 1119-21.

276. Yi, C.H., et al., *Metabolic regulation of protein N-alpha-acetylation by Bcl-xL promotes cell survival.* Cell, 2011. **146**(4): p. 607-20.

277. Lin, H.C., et al., *C-Terminal End-Directed Protein Elimination by CRL2 Ubiquitin Ligases.* Mol Cell, 2018. **70**(4): p. 602-613 e3.

278. Koren, I., et al., *The Eukaryotic Proteome Is Shaped by E3 Ubiquitin Ligases Targeting C-Terminal Degrons.* Cell, 2018. **173**(7): p. 1622-1635 e14.

279. Mnatsakanyan, R., et al., *Proteome-wide detection of S-nitrosylation targets and motifs using bioorthogonal cleavable-linker-based enrichment and switch technique.* Nat Commun, 2019. **10**(1): p. 2195.

280. Seth, D., et al., *A Multiplex Enzymatic Machinery for Cellular Protein S-nitrosylation.* Mol Cell, 2018. **69**(3): p. 451-464 e6.

281. Hess, D.T., et al., *Protein S-nitrosylation: purview and parameters.* Nat Rev Mol Cell Biol, 2005. **6**(2): p. 150-66.

282. Jia, J., et al., *Target-selective protein S-nitrosylation by sequence motif recognition.* Cell, 2014. **159**(3): p. 623-34.

283. Chung, K.K., et al., *S-nitrosylation of parkin regulates ubiquitination and compromises parkin's protective function.* Science, 2004. **304**(5675): p. 1328-31.

284. Iglesias, M.J., et al., *Regulation of SCF(TIR1/AFBs) E3 ligase assembly by S-nitrosylation of Arabidopsis SKP1-like1 impacts on auxin signaling.* Redox Biol, 2018. **18**: p. 200-210.

285. Kumar, R., et al., *S-nitrosylation of UCHL1 induces its structural instability and promotes alpha-synuclein aggregation.* Sci Rep, 2017. **7**: p. 44558.

286. Amal, H., et al., *S-nitrosylation of E3 ubiquitin-protein ligase RNF213 alters non-canonical Wnt/Ca+2 signaling in the P301S mouse model of tauopathy.* Transl Psychiatry, 2019. **9**(1): p. 44.

287. Kim, S., S.S. Wing, and P. Ponka, *S-nitrosylation of IRP2 regulates its stability via the ubiquitin-proteasome pathway.* Mol Cell Biol, 2004. **24**(1): p. 330-7.

288. Gupta, A., et al., *PARK2 Depletion Connects Energy and Oxidative Stress to PI3K/Akt Activation via PTEN S-Nitrosylation.* Mol Cell, 2017. **65**(6): p. 999-1013 e7.

289. Azad, N., et al., *S-nitrosylation of Bcl-2 inhibits its ubiquitin-proteasomal degradation. A novel antiapoptotic mechanism that suppresses apoptosis.* J Biol Chem, 2006. **281**(45): p. 34124-34.

290. Chanvorachote, P., et al., *Nitric oxide regulates cell sensitivity to cisplatin-induced apoptosis through S-nitrosylation and inhibition of Bcl-2 ubiquitination.* Cancer Res, 2006. **66**(12): p. 6353-60.

291. Zhang, P., et al., *S-nitrosylation-dependent proteasomal degradation restrains Cdk5 activity to regulate hippocampal synaptic strength.* Nat Commun, 2015. **6**: p. 8665.